



**HAL**  
open science

# Removal of micropollutants with activated sludge : proposition of a new kinetic model and special focus on hydrodynamic reactor configuration and local mixing

Rana Hatoum

► **To cite this version:**

Rana Hatoum. Removal of micropollutants with activated sludge : proposition of a new kinetic model and special focus on hydrodynamic reactor configuration and local mixing. Chemical and Process Engineering. Université de Lorraine, 2019. English. NNT : 2019LORR0331 . tel-02880680

**HAL Id: tel-02880680**

**<https://hal.univ-lorraine.fr/tel-02880680>**

Submitted on 3 Apr 2023

**HAL** is a multi-disciplinary open access archive for the deposit and dissemination of scientific research documents, whether they are published or not. The documents may come from teaching and research institutions in France or abroad, or from public or private research centers.

L'archive ouverte pluridisciplinaire **HAL**, est destinée au dépôt et à la diffusion de documents scientifiques de niveau recherche, publiés ou non, émanant des établissements d'enseignement et de recherche français ou étrangers, des laboratoires publics ou privés.



## AVERTISSEMENT

Ce document est le fruit d'un long travail approuvé par le jury de soutenance et mis à disposition de l'ensemble de la communauté universitaire élargie.

Il est soumis à la propriété intellectuelle de l'auteur. Ceci implique une obligation de citation et de référencement lors de l'utilisation de ce document.

D'autre part, toute contrefaçon, plagiat, reproduction illicite encourt une poursuite pénale.

Contact : [ddoc-theses-contact@univ-lorraine.fr](mailto:ddoc-theses-contact@univ-lorraine.fr)

## LIENS

Code de la Propriété Intellectuelle. articles L 122. 4

Code de la Propriété Intellectuelle. articles L 335.2- L 335.10

[http://www.cfcopies.com/V2/leg/leg\\_droi.php](http://www.cfcopies.com/V2/leg/leg_droi.php)

<http://www.culture.gouv.fr/culture/infos-pratiques/droits/protection.htm>



## Doctoral School SIMPPÉ

Science and Engineering, Resources, Processes, Products and Environment

A thesis submitted for the title of

## Doctor of the University of Lorraine

*Specialty: Génie des Procédés, des Produits et des Molécules*

Presented and defended on December 13, 2019 by

**Rana HATOUM**

---

### REMOVAL OF MICROPOLLUTANTS WITH ACTIVATED SLUDGE: PROPOSITION OF A NEW KINETIC MODEL AND SPECIAL FOCUS ON HYDRODYNAMIC REACTOR CONFIGURATION AND LOCAL MIXING

---

#### Jury

<b>Joachim HANSEN</b>	<i>University of Luxembourg</i>	Reviewer
<b>Ingmar NOPENS</b>	<i>University of Ghent</i>	Reviewer
<b>Harald HORN</b>	<i>Karlsruhe Institute of Technology</i>	Examiner
<b>Stéphanie OGNIER</b>	<i>University of Pierre and Marie-Curie</i>	Examiner
<b>Olivier POTIER</b>	<i>University of Lorraine</i>	Director (France)
<b>Joumana TOUFAILY</b>	<i>Lebanese University</i>	Co-Director (Lebanon)
<b>Ewa BOROWSKA</b>	<i>Karlsruhe Institute of Technology</i>	Invited
<b>Cécile LEMAITRE</b>	<i>University of Lorraine</i>	Invited
<b>Tayssir HAMIEH</b>	<i>Lebanese University</i>	Invited
<b>Thibault ROQUES-CARMES</b>	<i>University of Lorraine</i>	Invited



إلى القريب في القلوب، الغريب في الأرواح

لن تنضج ثماري إلا في حينها

...

في الموسم الموعود

...

في انتظار لقائك

...



*This thesis  
is dedicated  
to*

**Dear parents Mohamad and Leila,**

An inexhaustible source of tenderness, patience and perseverance. Your prayers and blessings have been helpful to me throughout my life. I present you this work as a fruit of all your efforts and sacrifices. On this day I hope I realized one of your dreams. May Allah protect you and grant you health, long life and happiness. I ask ALLAH every single moment to bless you with sincere faith, good health, security and peace.

**Dear Husband Wissam,**

My superhero, my friend and my partner! You are always my greatest support and strongest motivation. Your love gave me confidence and stability. Since I knew you, you never stopped giving of yourself in countless ways. I thank God who crossed my path with your soft heart, your wise spirit and your friendly character. No words could express my gratitude, my love and my respect. Without your presence it will not be beautiful like this. Over and over again, I will choose to spend eternal life with you.

**Dear sisters Lama and Roula,**

You have been at my side during all the stages of this work. No dedication can express the depth of the feelings of love and attachment I feel towards you. My sisters, you are the real meaning of peace of mind. I cannot breathe without you by my side. Lama you are always the queen, the fighter and the cutest mom ever. Roula, an angel like I cannot find anywhere else. You are the smile, the beats and the soft smell of my life. I always ask ALLAH to bless you with sincere faith, good health, success, peace and joy.

My nephews Abdullah and Muhamad, I cannot wait to see you grow and achieve your goals. I will be always by your side. I don't want to miss any moments with you. I am sure that you will treat nice your future siblings. I love you forever and for always.



**Dear auntie Happo, grandma Khadija and mother-in-law Kamilia,**

You are the real symbol of blameless love and giving. I am here because of your pure prayers. May God bless you with longevity, peace and joy because you deserve. I love you deeper than my heart can comprehend.

**Dear future child (ren),**

I can't wait to announce that moment for your dad and your grand-parents. I asked God to see you, hold you, kiss you, hug you, and touch you. I would like to feel your presence with us here, on this Earth. Your dad and I would be your guide to follow in the footsteps of Ahl-beit-Mohamad (a. s.) beside Sayyed Hassan Nsrallah.

**Dear Friends,**

I want to express my gratitude to the friends whom I shared with them this path: Ewa, Rouwayda, Ali, Amira, Fatima, and Rana. Every one of you represents a separate special graved experience for me. We really shared different moments together. I dedicate this research for you and to my friends in Lebanon who encourage and support me: Hala (lawzi), Abou jaafar, Diaa, Cheich Mohamad, Badder, Fafi Mawsoule, Hiba pluie, Salam, Houssein and Rania. Even not mentioning the names, I can't forget all other friends in my life who touch my heart.



# *Acknowledgement*

I would like to express my thanks to Mr. Ingmar NOPENS and Mr. Joachim HANSEN for giving me the honor to be the reviewers of this thesis. I also would like to thank the members of the jury Mrs. Stéphanie OGNIER, Mr. Harald HORN, Mrs. Cécile LEMAITRE, Mrs. Ewa BOROWSKA, Mr. Tayssir HAMIEH and Mr. Thibault ROQUES-CARMES for their remarks and notes.

My great gratitude to Mr. Harald HORN for welcoming me in your laboratory EBI in Karlsruhe, helping me in planning and organisation of experiments and increasing my knowledge in the technical part by your beneficial remarks and suggestions to operate the biological reactors for waste water treatment.

I would like to express my big thanks to my supervisor, Mr. Olivier POTIER for the help, encouragement and trust you gave me through our work together. Thanks to Mr. Thibault ROQUES-CARMES for the support and effective discussions you provided. Thank you both for the care you were always showing for me.

A special thanks to my Lebanese co-supervisor Mrs. Joumana TOUFAILY and Mr. Tayssir HAMIEH for providing me this chance for pursuing our high research study and having a trust in my abilities to achieve our goal successfully.

Special appreciation to Mrs. Ewa BOROWSKA for the beneficial and effective knowledge you shared with me, for your availability to provide me with any help and encouraged me in many situations. I would like to express my gratitude to Mrs. Cécile LEMAITRE for the help you provided me to carry on modelling. Thanks also to Mr. Reichert ULRICH for your help in sampling even in cold weather. Thanks to Mr. Rafael PESCHKE and Mr. Reinhart AHLRICHS for your help to advance the analyses.

I can't forget my LRGP and EBI lab mates. I was touched by the kindness and sympathy with which you welcomed me. My deep gratitude for the considerable attention you have given me.

# Table of content

Motivation and aim of the project.....	1
Chapter I. State of the art of micropollutant's removal modelling in activated sludge systems..	9
I.1.Introduction.....	10
I.2.Problematic of the micropollutant removal in conventional wastewater treatment plant .....	13
I.2.1.Micropollutants and Environment.....	13
I.2.1.1.Sources of micropollutants (MPs) .....	13
I.2.1.2.Occurrence of micropollutants in wastewater and their regulations .....	15
I.2.1.3.Categories of micropollutants .....	21
I.2.1.3.1.Focus on Pharmaceuticals and Personal Care Products (PPCPs) and industrial chemicals ..	21
I.2.1.3.2.Impacts of MPs on environment and living beings .....	22
I.2.2.Removal of micropollutants in wastewater treatment plant .....	23
I.2.2.1. Water treatment.....	23
I.2.2.2.Biological treatment process in secondary system.....	25
I.2.2.2.1.Attached and suspended growth systems .....	25
I.2.2.2.2.Optimization of some parameters to improve the removal performances.....	27
I.2.2.3.Micropollutants removal in conventional activated sludge systems .....	28
I.2.2.3.1.Biological/physical-chemical properties and removal efficiencies of PPCPs.....	28
I.2.2.3.2.Conventional activated sludge (CAS) vs. membrane bioreactor treatment (MBR) .....	33
I.2.2.3.3.Advanced technologies in wastewater treatment.....	34
I.2.2.4. Effect of operational parameters and biomass concentration on the removal of pharmaceuticals.....	34
I.3.Modelling of micropollutant removal in biological wastewater systems.....	38
I.3.1.State of the art.....	38
I.3.2.Mechanisms of micropollutants fate and modelling concepts.....	40
I.3.2.1.Volatilization.....	42
I.3.2.2.Sorption of lipophilic compounds onto suspended sludge .....	43

I.3.2.3. Biodegradation/Biotransformation .....	46
I.4. Hydrodynamics .....	52
I.4.1. Different hydrodynamics approaches .....	52
I.4.2. Systemic modelling approach .....	55
I.4.3. Impact of hydrodynamic reactor configuration on MPs removal .....	58
I.5. Conclusion of chapter I and objectives of the thesis .....	59
I.6. References of chapter I .....	60

Chapter II. Biological experiments- Effect of SRT, HRT and biomass concentration on elimination of micropollutants with activated sludge.....	79
II.1. Introduction .....	80
II.2. Materials and Methods .....	85
II.2.1. Wastewater system and sampling site .....	85
II.2.2. Selection of micropollutants.....	86
II.2.2.1. Sorption tests on the wall of the reactor .....	86
II.2.2.2. Physico-chemical properties of investigated micropollutants.....	87
II.2.2.3. Chemical and reagents.....	85
II.2.3. Sequencing Batch Reactors .....	90
II.2.3.1. Design of the SBRs .....	90
II.2.3.2. Operation of the SBRs.....	93
II.2.3.3. Sludge inoculum.....	95
II.2.3.4. Synthetic wastewater.....	95
II.2.3.5. Adjustment of SRT.....	96
II.2.3.6. $k_{La}$ measurement and estimation.....	96
II.2.4. Kinetics of micropollutants' removal in SBR .....	99
II.2.5. Apparent-first-order kinetics estimation .....	100
II.2.6. Nitrification capacity (NC).....	101
II.2.7. Analytical methods.....	101
II.2.7.1. Quantification of MPs by LC-MS/MS .....	101
II.2.7.2. Measurement of basic chemical parameters of wastewater .....	102
II.3. Results and discussion.....	102
II.3.1. Sorption on wall's reactor .....	102

II.3.2.Effect of SRT on MPs' elimination in activated sludge.....	104
II.3.3.Influence of HRT on MPs' elimination in activated sludge.....	111
II.3.4.Overall synthesis of the impact of SRT and HRT .....	118
II.3.4.1.MPs removal efficiency.....	118
II.3.4.2.Global effect of SRT and HRT.....	119
II.3.5.Effect of biomass concentration on MPs' elimination in activated sludge .....	120
II.4.Conclusion of chapter II .....	126
II.5.References of chapter II .....	127

Chapter III. New kinetics law of micropollutants removal in activated sludge: non-linear influence of biomass concentration..... 135

III.1 Introduction .....	136
III.2.In-depth analysis of kinetics results at various biomass concentration .....	138
III.3.The power law kinetics .....	140
III.3.1.Determination of n coefficient.....	140
III.3.2.Determination of the new kinetic constants $k_{MPs}$ .....	142
III.3.3.Discussion on the effect of external transport on MPs' kinetics.....	143
III.3.3.1.Effect of non-ideal mixing .....	144
III.3.3.2.Effect of solids concentration of activated sludge on the rheological behavior .....	145
III.3.4.MPs diffusion limitation interflocs .....	146
III.4.Conclusion of chapter III .....	149
III.5.References of chapter III.....	149

Chapter IV. Simulation of the micropollutants removal in batch and continuous systems..... 155

IV.1.Introduction.....	157
IV.2.Modelling of activated sludge biological treatment .....	158
IV.2.1.State variables and biological phenomena of ASM1 .....	158
IV.2.2.ASM1 model description.....	160
IV.2.3.Relations between ASM1 model & usual experimental analyses and some ASM1 limitations.....	165
IV.3.Kinetics of MPs removal .....	167
IV.4. Sequencing Batch Reactor simulations .....	168
IV.4.1.Numerical resolution.....	170

IV.4.2.Parameter optimization of ASM1 model .....	171
IV.4.3.Predictive accuracy of simulation: statistical calculation .....	176
IV.4.4.Simulation of Mps removal .....	178
IV.4.4.1.Simulation of the apparent-first-order kinetics .....	178
IV.4.4.2.Modelling of series 2 with the power law kinetics .....	183
IV.4.4.3.Predictions by applying power law kinetics .....	187
IV.4.4.4.Partial conclusion.....	190
IV.5.Extrapolation to continuous system.....	191
IV.5.1.Validation by comparison with Benchmark Simulation Model no.1 (BSM1) .....	191
IV.5.1.1.Material balance in the cascade .....	192
IV.5.1.2.Material balance in the clarifier .....	194
IV.5.1.3.Benchmark parameters .....	196
IV.5.1.4.Comparison with the Benchmark results .....	198
IV.5.2.Cascade of an arbitrary number of CSTR operated with power law kinetics.....	201
IV.5.3.Cascade of 5 reactors tested with wide range of inlet $C_{MPS}$ .....	206
IV.6.Estimation of fundamental dimensions of the continuous reactor configuration .....	210
IV.6.1.Reactor modelling .....	210
IV.6.2.Proper design of biological reactor .....	212
IV.7.Conclusion of chapter IV .....	215
IV.8.References of chapter IV .....	216
V.Conclusions and perspectives .....	220
V.1.General conclusion.....	220
V.2.Perspectives.....	223
List of Figures .....	225
List of Tables .....	228
Supplementary Information .....	230
Abstract&Résumé .....	285



## Notation

### Abbreviations and acronyms

ABR	Anaerobic baffled reactor
ABs	Antibiotics
ADM	Axial dispersion model
APHA	American Public Health Association
AOPs	Advanced oxidation processes
ASM	Activated sludge model
BNR	Biological nutrient removal
BOD	Biological oxygen demand
BOD <sub>5</sub>	Biochemical Oxygen Demand over five days
BSAP	Baltic Sea Action Plan
BSM	Benchmark Simulation Model
BZT	Benzotriazole
CAF	Caffeine
CAS	Conventional activated sludge
CBZ	Carbamazepine
CFA	Clofibric acid
CFD	Computational fluid dynamics
COD	Chemical oxygen demand
CRE	Chemical Reaction Engineering
CSTR	Continuous stirred tank reactor
DCF	Diclofenac
DCM	Dissolved and colloidal matter
DO	Dissolved oxygen
EA	Environment Agency
EC	European Commission
ECs	Emerging Contaminants
EDCs	Endocrine disruptor compounds
EEA	European Environment Agency
EQS	Environmental Quality Standards
EMs	Emerging micropollutants
ERY	Erythromycin
ETSS	Effluent suspended solids
EU	European Union
HPLC	High-performance liquid chromatography
HRT	Hydraulic Retention Time
IC	Ionic chromatography
KPF	Ketoprofen
MBR	Membrane bioreactors
MF	Membrane filtration
MLSS	Mixed liquor suspended solids
MPs	Micropollutants
MRM	Multi-reaction monitoring
LC-MS/MS	Liquid chromatography coupled with tandem-mass spectrometer

N/A	Not applicable
ND	Not detected
NSAIDs	Non-steroidal anti-inflammatory drugs
NTK	Kjeldal nitrogen
PAH	Polycyclic aromatic hydrocarbons
PE	Population equivalents
PhAC	Pharmaceuticals Active Compounds
PFR	Plug Flow Reactor
PLC	Programmable logic controller
PPCPs	Pharmaceutical and personal care products
RBD	River Basin District
RBMPs	River Basin Management Plans
RE	Removal efficiency
ROX	Roxithromycin
rpm	Rotation per minute
RTD	Residence time distribution
RSD	Relative Standard Deviation
SBR	Sequencing batch reactor
SCADA	Supervisory control and data acquisition
SMX	Sulfamethoxazole
SRT	Sludge Retention Time
SWBs	Surface Water Bodies
SW	Surface water
SWW	Synthetic wastewater
TSM	Tanks in series model
TN	Total nitrogen
TOC	Total organic carbon
UPBTs	Ubiquitous, persistent, bioaccumulative and toxic
UHPLC	Ultra-high-performance liquid chromatography
UF	Ultrafiltration
UN	United Nations
UASB	Upflow Anaerobic Sludge Blanket
UV	Ultraviolet radiation
VER	Volumetric exchange ratio
WHO	World health organization
WFD	Water Framework Directive
WWTP	Wastewater treatment plant

### Latin letters

a	Specific interface surface area
$C_0$	Initial concentration of micropollutants
$C_{BOC}$	Non-soluble concentration at the bottom of the clarifier
$C_e$	Inlet concentration to the cascade of the reactors
$C_{eff}$	Effluent concentration of clear water at the outlet of the upper part of the clarifier

$C_L$	Mixed liquor concentration
$C_m$	Mass loading rate
$C_{MPs}$	Dissolved micropollutant concentration
$coef$	Ratio of the flowrate at the overflow of the clarifier to the total flowrate entering the clarifier
$CO_2$	Carbon dioxide
$C_{out}$	Concentration in the upper part of the clarifier
$C_S$	Sludge concentration at the outlet of the bottom part of the clarifier
$C_{tot}$	Total substrate concentration in water
$C_{TSS}$	Total Suspended Solids concentration
$X_{TSS}$	Volatile suspended solids concentration
$d$	Days
$D$	Axial dispersion coefficient
$D_m$	Molecular diffusion coefficient
$F_{in,i,j}$	Inward flux
$F_{out,i,j}$	Outward flux
$H$	Water depth
$H/H'$	Henry's law constant
$h$	Hours
$i$	Compound
$j$	Reactor of the cascade
$J_i$	Number of CSTR used in the Benchmark
$J_{cal}$	Number of CSTR to sizing
$jc$	Cell of the clarifier
$j_{max}$	Maximum number of reactors
$k$	Pseudo-first order kinetic constant
$k'$	Apparent-first order kinetic constant
$k_2$	Rate constant of the pseudo-second order sorption
$k_{biol}$	Biodegradation kinetic constant
$K_d$	Sludge adsorption coefficient
$k_{Des}$	Desorption rate coefficient
$K_I$	Inhibition constant
$k_G$	Gaz side transfer mass coefficient
$k_{MPs}$	Power law removal rate constant
$k_L$	Liquid side transfer mass coefficient
$k_{La_{surf}}$	Surface transfer coefficient
$k_O$	Semi-saturation in oxygen
$k_{sor}$	Sorption rate coefficient
$K_{ow}$	Octanol-water partition coefficient
$M$	Node before the clarifier inlet
$M_{MPs}$	Molecular weight of micropollutants
$M_{sol}$	Solvent molecular weight
$M_w$	Molecular weight
$n$	Order of the reaction
$N$	Node before the inlet of the cascade reactors

$N_2$	Nitrogen gaz
$n_B$	Number of the interconnected cells on the bottom of the clarifier
NC	Nitrification capacity
$N-NH_4^+$	Ammonium concentration as nitrogen
$N-NO_2^-$	Nitrite concentration as nitrogen
$N-NO_3^-$	Nitrate concentration as nitrogen
$NO_2$ -DCF	Nitro diclofenac
$n_T$	Number of the interconnected cells of the top of the clarifier
Pe	Peclet number
$P-PO_4^{3-}$	Phosphate concentration as phosphorus
pKa	Acid dissociation constant
$q$	Growth substrate availability
Q	Flow rate
$Q_{BOC}$	Bottom of the clarifier flow rate
$q_{C,Axf}$	Maximum specific cometabolic substrate biotransformation rate in anoxic condition
$q_{C,Ox}$	Maximum specific cometabolic substrate biotransformation rate in aerobic condition
$Q_e$	Inlet flow rate
$Q_{eff}$	Effluent flow rate
$Q_G$	Gaz flow rate
$Q_{IC}$	Inlet clarifier flow rate
$Q_L$	Recycled liquid mixer flow rate
$Q_{out}$	Clarifier upper outlet
$Q_S$	Sludge recycling flow rate
$Q_{tot}$	Total flow rate
$Q_w$	Sludge withdrawal flow rate
L	Length of the reactor
$L_{cal}$	Calculated length of new the reactor design
$r_{i,m}$	Net production of compound $i$ due to chemical reactions
$r_{MPs}$	Removal rate of micropollutants
$S_h$	Horizontal serction
$S_O$	Dissolved oxygen concentration
$S_{O,sat}$	Dissolved oxygen concentration in water at saturation
$u$	Average longitudinal velocity
$V_B$	Volume of the lower part of the clarifier
$V_j$	Volume of the reactor in the cascade
$V_{jc}$	Volume of each elementary reactor of both parts of the clarifier
$V_T$	Volume of the upper part of the clarifier
W	Width of the reactor
$W_i$	Initial width of the reactor
$W_{cal}$	Calculated width for a new reactor design
$W_d$	Air diffuser width
$X_{MPs}$	Sorbed micropollutant concentration on the sludge phase
Y	Conversion rate

[y]	Vector of concentrations
[dydt]	Vector of derivatives of the concentrations

### Composition of synthetic wastewater

NH <sub>4</sub> HCO <sub>3</sub>	Ammonium bicarbonate
H <sub>3</sub> BO <sub>4</sub>	Boric acid
CaCl <sub>2</sub> .2H <sub>2</sub> O	Calcium chloride dihydrate
CoCl <sub>2</sub> .6H <sub>2</sub> O	Cobaltous chloride hexahydrate
CuSO <sub>4</sub> .5H <sub>2</sub> O	Copper sulfate pentahydrate
C <sub>10</sub> H <sub>6</sub> N <sub>2</sub> O <sub>8</sub>	4-(2,4-dinitrophenoxy)-4-oxobut-2-enoic acid
FeSO <sub>4</sub> .7H <sub>2</sub> O	Ferrous sulfate heptahydrate
MgSO <sub>4</sub> .7H <sub>2</sub> O	Magnesium sulfate heptahydrate
MnCl <sub>2</sub> .4H <sub>2</sub> O	Manganese (II) chloride tetrahydrate
NiCl <sub>2</sub> .6H <sub>2</sub> O	Nickel (II) chloride hexahydrate
KH <sub>2</sub> PO <sub>4</sub>	Potassium dihydrogenphosphate
NaMoO <sub>4</sub> .2H <sub>2</sub> O	Sodium molybdate dehydrate
CH <sub>3</sub> COONa	Sodium acetate
NaSeO <sub>4</sub> .10H <sub>2</sub> O	Sodium selenite
ZnSO <sub>4</sub> .7H <sub>2</sub> O	Zinc sulfate heptahydrate

### Greek letters

$\alpha$	Association parameter
$\beta$	Ratio of C <sub>VSS</sub> to C <sub>TSS</sub>
$\mu$	Growth rate
$\mu_{\max}$	Maximum growth rate
$\Delta x$	Thickness of section
$\tau$	Hydraulic retention time
$\propto$	Proportional
$\eta$	Viscosity of the solvent
$\rho$	Density of the solvent
$\rho_u$	Biological reaction kinetics
$\gamma$	Ratio of experimental k <sub>L</sub> a in clear water and simulated k <sub>L</sub> a in bulk liquid
$\Omega$	Vertical section

## Parameters of ASM1 model

$b_A$	Coefficient of mortality of autotrophic biomass
$b_H$	Coefficient of mortality of heterotrophic biomass
$f_p$	Inert COD fraction generated by dead biomass
$i_{XB}$	Fraction of nitrogen assimilated by heterotrophic biomass
$i_{XP}$	Nitrogen fraction assimilated by inert biomass
$k_a$	Ammonification Rate Constant
$k_h$	Hydrolysis rate constant
$K_{NH}$	Coefficient of half-saturation of ammoniacal nitrogen
$K_{NO}$	Nitrates-nitrite half-saturation coefficient
$K_{O,A}$	Dissolved oxygen half-saturation constant for autotrophic biomass
$K_X$	Semi-saturation constant of the proportion of substrate to be hydrolyzed with respect to the heterotrophic biomass
$K_{O,H}$	Dissolved oxygen half-saturation coefficient for heterotrophic biomass
$K_S$	Rapidly biodegradable substrate half-saturation coefficient
$\eta_g$	Comparative efficacy of anoxic growth versus aerobic growth
$\eta_h$	Effectiveness of the anoxic pathway compared to the aerobic pathway
$X_{B,H}$	Heterotrophic biomass
$X_{B,A}$	Autotrophic biomass
$X_P$	Inert biomass
$S_S$	Carbon substrate rapidly biodegradable
$X_S$	Carbon substrate slowly biodegradable
$S_{NO}$	Nitrates and nitrites
$S_{NH}$	Ammonium and ammonia
$S_{ND}$	Organic nitrogen substrate rapidly biodegradable
$X_{ND}$	Organic nitrogen substrate slowly biodegradable
$S_I$	Carbon and nitrogen substrate soluble and non- biodegradable
$X_I$	Carbon and nitrogen substrate non-soluble and non- biodegradable
$S_O$	Dissolved oxygen
$Y_A$	Conversion rate of the substrate into autotrophic biomass
$Y_H$	Conversion rate of the substrate into heterotrophic biomass
$\mu_H$	Maximum growth rate of heterotrophic biomass
$\mu_A$	Maximum growth rate of autotrophic biomass

# **Résumé Du Rapport En Français**

L'eau est une ressource naturelle renouvelable impliquée dans de nombreux aspects de la vie humaine. Des majeurs problèmes auxquels l'humanité est confrontée au XXI<sup>e</sup> siècle sont liés à la détérioration de l'eau par divers polluants provenant de diverses sources. Celles-ci peuvent être industrielles, provenir de l'agriculture intensive, du transport, des déchets domestiques, des produits de santé, des déchets urbains, de la pollution aérienne soluble dans l'eau, etc. Au cours des dernières décennies, une attention croissante a été portée à la présence d'un large groupe de polluants organiques présents dans les effluents provenant de diverses sources à des gammes de concentrations de l'ordre du  $\text{ng L}^{-1}$  et  $\mu\text{g L}^{-1}$ . Cette nouvelle classe de polluants est appelée micropolluants (MPs). Ces substances incluent notamment les composés pharmaceutiques, les produits de soins cosmétiques, et les produits chimiques industriels et hospitaliers. La grande majorité de ces composés est considérée comme dangereuses mêmes lorsque ces composés sont présents à l'état de traces: cancérogènes, perturbateur endocriniens, etc. Les procédés de traitement dans les stations d'épuration (STEP) ne permettent pas d'éliminer toute la pollution présente dans les effluents et de nombreux micropolluants demeurent présents dans les eaux en sortie des stations. En outre, le rejet de ces polluants pose également des problèmes pour le fonctionnement de l'écosystème.

Il devient donc nécessaire de développer des procédés de façon à éliminer, à un coût acceptable, les traces de mélanges micropolluants les plus indésirables tout en préservant l'écosystème. Il s'agit notamment de l'adsorption, de la technologie des membranes, des processus d'oxydation avancés (AOP), y compris plusieurs méthodes d'oxydation, et des traitements biologiques. Néanmoins, les méthodes AOP présentent plusieurs inconvénients, notamment des coûts élevés et un risque de génération de produits de transformation toxiques ou d'oxydants restants (par exemple le peroxyde d'hydrogène) qui peuvent endommager les micro-organismes. Par ailleurs, les bioprocédés ont encore plusieurs limites. Par exemple, ils ne peuvent transformer que des composés biodégradables et, par conséquent, ne sont pas en mesure d'éliminer les contaminants biologiquement persistants. Par conséquent, les processus biologiques aérobies actuellement utilisés pour traiter ces composés pharmaceutiquement actifs ne sont pas satisfaisants en termes d'efficacité. Cela est dû par exemple au transfert de ces polluants vers la phase gazeuse, à leur adsorption et à leur persistance dans les phases solides, ou à un temps de contact insuffisant avec la biomasse. Malgré cela, le traitement



biologique des eaux usées reste la première solution utilisée depuis de nombreuses années. Les traitements conventionnels à boues activées sont considérés comme rentables - en termes de coûts d'exploitation. Le principe des traitements biologiques repose sur les capacités métaboliques des bactéries, des champignons, des algues ou des plantes afin d'oxyder ou de réduire les composés organiques et inorganiques. Les processus qui se produisent dans la nature sont intensifiés en garantissant des conditions appropriées telles que la concentration en oxygène, le pH, l'accès aux nutriments, etc. Ils sont généralement mis en œuvre dans des réacteurs biologiques, avec un équipement d'aération et d'agitation adéquat.

Les mécanismes d'élimination des MPs dans une station d'épuration à boues activées classiques dépendent des propriétés physico-chimiques de chaque composé telles que la solubilité, la volatilité et la sensibilité à la photodégradation ainsi que la biodégradabilité des produits pharmaceutiques. L'efficacité de l'élimination des micropolluants par traitement biologique a déjà été étudiée auparavant. De plus, ces efficacités sont potentiellement influencées par les paramètres opérationnels des stations d'épuration, souvent utilisés dans les procédés conventionnels, tels que l'âge des boues (SRT), le temps de passage (HRT), les concentrations de biomasse représentées par la concentration de solides en suspension totaux ( $C_{TSS}$ ), le pH et la température. Les conditions de fonctionnement HRT et SRT offrent une grande flexibilité de fonctionnement aux réacteurs biologiques. Il est important de noter que l'influence de ces paramètres sur les cinétiques d'élimination des MPs n'est pas déjà clairement comprise dans la littérature. La très grande majorité des travaux ont été conduits à des faibles concentrations en biomasse i.e.  $3 \text{ g L}^{-1}$ . Dans des autres études, les HRT et SRT sont relativement élevés i.e. entre 6 h et 12 h et supérieur à 5 jours, respectivement. Seulement quelques études travaillent à des SRT très élevés supérieurs à 20 jours.

Il apparaît donc très intéressant de conduire une étude systémique sur l'effet de ces paramètres afin d'améliorer l'élimination des polluants biologiquement persistants. Ce travail a été réalisé en coopération entre LRGP-CNRS Université de Lorraine à Nancy, France et Engler-Bunte-Institut de l'Institut de Technologie de Karlsruhe (EBI-KIT) à Karlsruhe, Allemagne et plus particulièrement via une collaboration avec Monsieur Harald Horn et Madame Ewa Borowska. Au début de cette étude, le groupe de micropolluants choisi représente une famille chimique rencontrée dans un grand nombre d'effluents domestiques, hospitaliers et les effluents classiques

de la station d'épuration ainsi qu'un degré de biodégradabilité différent dans le réacteur. Il est important de mentionner le fait que la dégradation de micropollutants à ces très faibles niveaux de concentration ( $1 \mu\text{g L}^{-1}$ ) est représentative des niveaux de concentrations en micropollutant émergents rencontrés dans les stations d'épurations.

Ce travail de thèse est donc divisé en deux grandes parties (Figure 1):

1) Dans un premier temps, il a été nécessaire de déterminer les constantes de vitesse cinétique d'élimination dans le processus de boues activées. Dans ce contexte, l'étude à l'échelle du laboratoire a été appliquée à des réacteurs discontinus en séquençage (SBR). Pour cela, le changement de concentration des MPs lors du traitement biologique a été suivi en phase aqueuse. L'élimination des MPs a été évaluée par la détermination des constantes de vitesse cinétique selon la forme la plus populaire du modèle cinétique, à savoir le modèle apparent du premier ordre.

2) Dans une deuxième partie, nous avons développé un programme numérique comprenant une cinétique réelle déterminée à EBI-KIT pour la simulation de l'élimination des MPs en testant l'effet des conditions de fonctionnement telles que le mélange et les configurations hydrodynamiques du réacteur biologique. Dans une étape intermédiaire une étude approfondie de la cinétique liée aux résultats expérimentaux a été effectuée au LRGP-CNRS. Un nouveau modèle cinétique d'élimination des MPs effectué à diverses concentrations de biomasse a été élaboré. Par la suite, l'objectif était de simuler un réacteur de traitement biologique continu typique couplé à différentes cinétiques d'élimination des MPs et ainsi de tester la nouvelle cinétique afin de prédire l'effet de la conception du réacteur et de proposer une meilleure configuration du réacteur pour améliorer l'élimination des MPs.

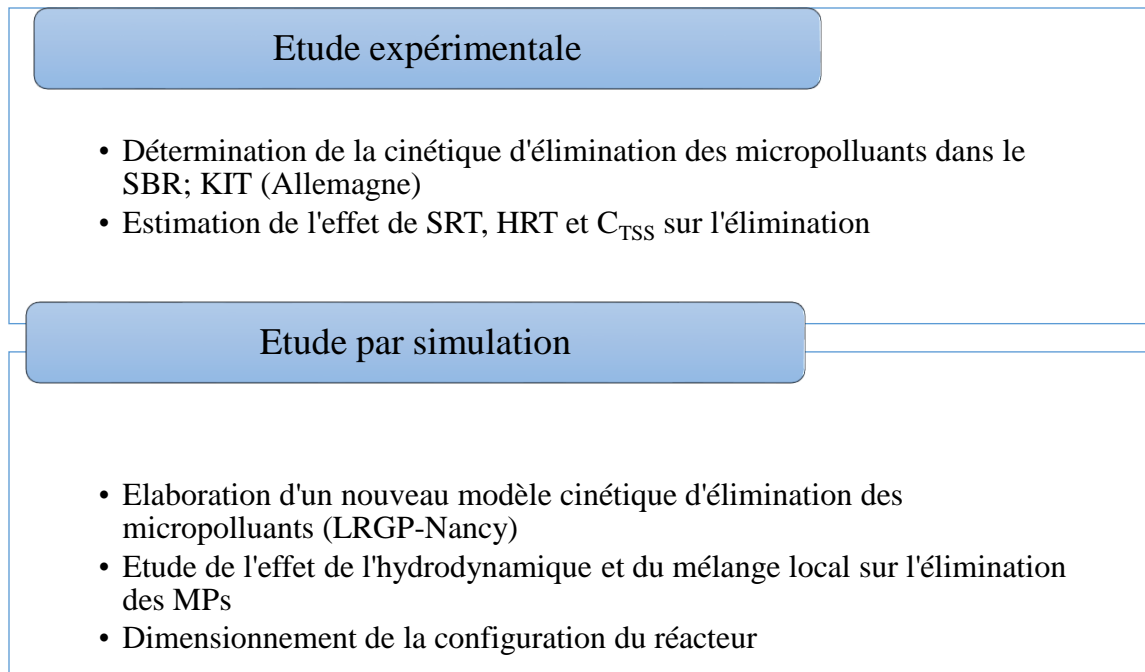


Figure 1. Résumé des étapes de la thèse.

Ce travail se situe donc à la rencontre de la cinétique chimique, la génie des procédés, le traitement de l'eau, et la simulation numérique ceci dans le cadre d'une collaboration internationale entre la France, l'Allemagne et le Liban. Ceci constitue une des originalités de ce travail de thèse.

La première partie de ce travail a pour objectif d'estimer si l'élimination des MPs dans les boues activées peut être attribuée à la manipulation de la SRT et de la HRT, et donc liée aux paramètres du processus de traitement. D'autres expériences ont été effectuées dans des SBR à l'échelle du laboratoire variant en concentration de solides en suspension totaux ( $C_{TSS}$ ) pour étudier le rôle de la concentration de biomasse dans l'élimination des MPs et l'applicabilité de l'approche cinétique du pseudo-premier ordre pour la description des phénomènes d'élimination. Sept contaminants émergents couvrent un large spectre de biodégradabilité, allant de composés hautement biodégradables à des composés assez persistants. Ainsi, la caféine (CAF), le sulfaméthoxazole (SMX), le benzotriazole (BZT), la roxithromycine (ROX), l'érythromycine (ERY), le diclofenac (DCF) et la carbamazépine (CBZ) ont été sélectionnés comme molécules modèles. Durant une période de 6 mois, sept configurations expérimentales ont été appliquées au séquençage des réacteurs discontinus (SBR). La configuration expérimentale de tous les SBR était identique. Les SBR fonctionnaient sur une base de remplissage et d'étirage avec des cycles consécutifs

comprenant les phases suivantes: remplissage, réaction (phase aérobie), décantation de la biomasse et enfin tirage du surnageant clarifié. Les SBR ne différaient que par le SRT et le taux de charge organique de l'influent comme le montre le Tableau 1. Les SBR-3 j et 10 j ont été testés avec trois durées différentes de HRT (4, 8 et 12 h), tandis que le SBR-20 j a été testé uniquement avec un HRT de 4 h. Chaque expérience cinétique des combinaisons SRT et HRT a été dupliquée 3 fois (nombre de répétitions = 3). Plus tard, le SBR-10 j a également été utilisé pour mesurer l'effet de la concentration de biomasse. Les concentrations de TSS suivantes ont été testées - 3, 5 et 8 g<sub>TSS</sub> L<sup>-1</sup> et également répétées 3 fois par condition expérimentale. Au début de l'expérience cinétique, les réacteurs inoculés avec des boues activées et alimentés par des eaux synthétiques, ont été dopés directement avec une solution de mélange de MPs de concentration 1 µg L<sup>-1</sup> et des échantillons ont été prélevés à des moments fixes pendant la phase d'aération de toutes les configurations testées. La quantification de l'élimination des différents MPs dans la phase aqueuse a été effectuée par analyse LC-MS/MS.

Le taux d'élimination des micropolluants est généralement considéré comme directement proportionnel aux concentrations de micropolluants et de biomasse. En conséquence, la réaction doit suivre une cinétique de second ordre (Eq.1). Cependant, cette loi cinétique a été appelée approche de pseudo-premier ordre dans des études récentes car la biomasse n'est pas considérée comme un facteur limitant. Dans la littérature, des fluctuations relativement faibles du C<sub>TSS</sub> sont souvent supposées et, par conséquent, un effet négligeable également sur le processus de traitement, ce qui conduit à une cinétique apparente de premier ordre (Eq.2). Cette approche est appliquée dans la présente étude. La constante de vitesse d'élimination apparente du premier ordre, exprimée en k'(h<sup>-1</sup>), a été dérivée de l'ajustement de la solution analytique d'Eq. (2) aux données mesurées de chacune des configurations expérimentales et aucune normalisation à la concentration de biomasse n'a été appliquée

$$r_{MPs} = -k C_{TSS} C_{MPs} \quad (1)$$

$$r_{MPs} = -k' C_{MPs} \quad \text{with } k' = k C_{TSS} \quad (2)$$

où  $r_{MPs}$  est le taux d'élimination (µg L<sup>-1</sup> h<sup>-1</sup>),  $k$  est la constante du taux d'élimination (L g<sup>-1</sup> h<sup>-1</sup>),  $C_{MPs}$  est la concentration de micropolluants dissous au temps  $t$  (µg L<sup>-1</sup>),  $t$  est le temps (h),  $C_{TSS}$  est la concentration totale de biomasse (g L<sup>-1</sup>),  $k'$  est la constante de vitesse d'élimination apparente du premier ordre (h<sup>-1</sup>) sans normalisation au  $C_{TSS}$ .

Tableau 1. Opération des réacteurs discontinus en séquençage à différents SRT au cours des expériences cinétiques.

		Expériences cinétiques		
		SBR- 3 j	SBR- 10 j	SBR- 20 j
Source de boues activées		Après un traitement secondaire de la station d'épuration de Bruchsal, Allemagne		Filtres à lit biologiques de la station d'épuration de Neureut, Allemagne
Alimentation des eaux usées synthétiques		$1.2 \text{ g}_{\text{DCO}} \text{ g}_{\text{TSS}}^{-1} \text{ j}^{-1}$ $0.08 \text{ g}_{\text{N}} \text{ g}_{\text{TSS}}^{-1} \text{ j}^{-1}$	$0.5 \text{ g}_{\text{DCO}} \text{ g}_{\text{TSS}}^{-1} \text{ j}^{-1}$ $0.08 \text{ g}_{\text{N}} \text{ g}_{\text{TSS}}^{-1} \text{ j}^{-1}$	$0.1 \text{ g}_{\text{DCO}} \text{ g}_{\text{TSS}}^{-1} \text{ j}^{-1}$ $0.08 \text{ g}_{\text{N}} \text{ g}_{\text{TSS}}^{-1} \text{ j}^{-1}$
HRT		4 h, 8 h et 12 h		4 h

Les résultats majeurs de cette étude sont les suivants:

- 1- Les constantes de vitesse d'élimination ont été affectées par le HRT et le SRT. L'amélioration du SRT a augmenté l'élimination de tous les MPs à l'exception de la roxithromycine et de l'érythromycine comme le montre la Figure 2. L'application d'un HRT plus élevé a également amélioré leur élimination, comme on pouvait s'y attendre à partir des constantes de vitesse d'élimination mesurées. Pour les composés persistants, une très faible efficacité d'élimination dans tous les combinaisons testés ( $\geq 10\%$ ) a été rapportée; Le HRT a montré un impact mineur et le SRT n'a présenté un léger effet que s'il était très long (par exemple, diclofénac SRT 20 j, 25%).

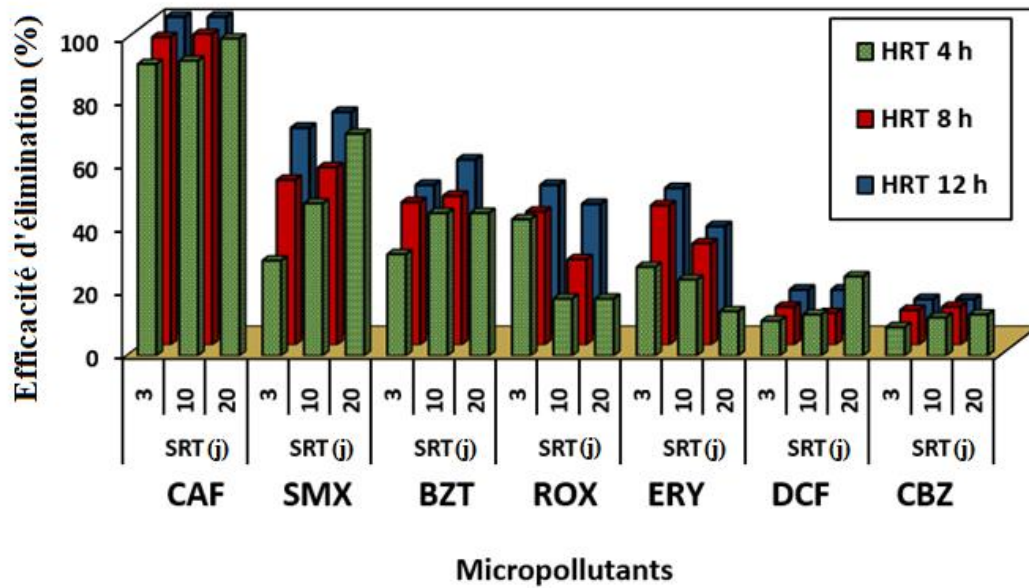


Figure 2. Élimination (%) des MPs sélectionnés dans les SBR - 3, 10 et 20 j sur trois HRT 4, 8 et 12 h différents.  $C_{TSS} \sim 3 \text{ gTSS L}^{-1}$  et  $C_{MPs} \sim 1 \mu\text{g L}^{-1}$ .

2- Plus intéressant, les résultats comme on peut le voir sur la Figure 3 ont indiqué que logiquement l'augmentation de la concentration de biomasse de 3 à 5  $\text{gTSS L}^{-1}$  augmentait significativement le taux d'élimination des composés hautement et modérément dégradables (caféine, sulfaméthoxazole, benzotriazole, érythromycine, roxithromycine). Inversement, une nouvelle augmentation à 8  $\text{gTSS L}^{-1}$  n'a produit qu'un effet modéré inattendu. En supposant une cinétique linéaire, l'évolution de  $k'$  en fonction du  $C_{TSS}$  devrait donner une droite passant par l'origine avec une pente correspondant à  $k$ . Cependant, nos résultats ont mis en évidence que l'augmentation n'est pas linéaire et, par conséquent,  $k$  n'est pas constant. La constante apparente  $k'$  augmente avec la  $C_{TSS}$  mais avec une évolution inférieure à celle qui serait attendue si elle était directement proportionnelle au  $C_{TSS}$  (Eq.2). En termes de variation de  $k'$  ( $\Delta k'$ ), les  $k'$  attendus de tous les MPs sont plus grands que les  $k'$  mesurés expérimentalement. Cela signifie qu'une augmentation de  $C_{TSS}$  améliore l'élimination, mais la cinétique n'est pas proportionnelle à  $C_{TSS}$  (Figure 3).

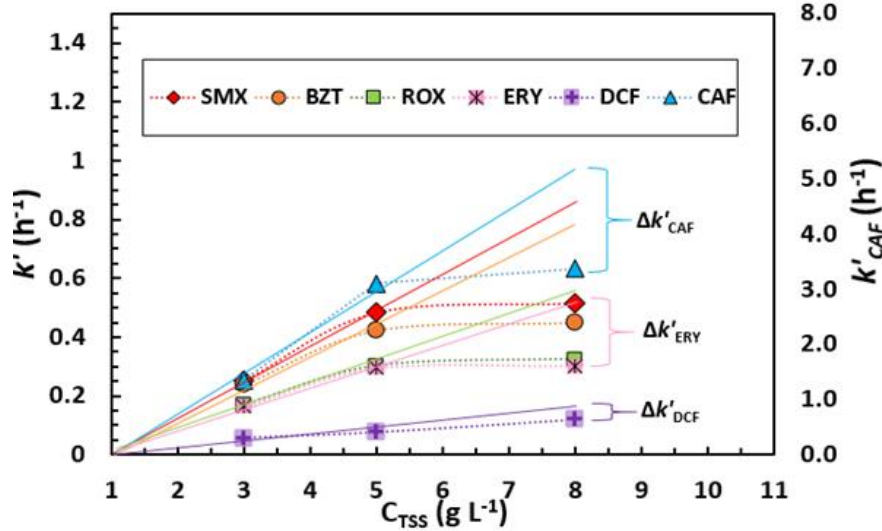


Figure 3. Effet du  $C_{TSS}$  (g L<sup>-1</sup>) sur la constante de vitesse d'élimination apparente du premier ordre  $k'$  (h<sup>-1</sup>) pour CAF, SMX, BZT, ROX, ERY et DCF. Les constantes apparentes  $k'$  de SMX, BZT, ROX, ERY et DCF et  $k'$  de CAF sont montrées respectivement sur le côté gauche et le côté droit du graphique. Les lignes continues représentaient l'approche pseudo-premier ordre linéaire attendue (calculée à partir des trois premiers  $C_{TSS}$  de 0, 3 et 5 g L<sup>-1</sup>).

La deuxième partie de ce travail de thèse a pour objectif de (a) simuler un réacteur de traitement biologique continu typique couplé à différentes cinétiques d'élimination des MPs, (b) prédire l'effet de la conception du réacteur et (c) proposer une meilleure configuration du réacteur pour améliorer l'élimination des MPs.

Les résultats de la première partie ont mis en évidence que la cinétique habituelle, qui considère que le taux est proportionnel à la concentration de biomasse n'est valable que pour des concentrations de biomasse faibles et modérées. Cet effet inattendu nous a poussé à développer une corrélation pour expliquer la dépendance du taux cinétique d'élimination des MPs à la concentration de biomasse élevée à la puissance de  $n$  inférieure à 1 et d'environ 0,5 (Eq.3).

$$r_{MPs} = -k_{MPs} C_{MPs} (C_{TSS})^n \quad (3)$$

La cinétique de la loi de puissance permet une détermination simple des valeurs de vitesse d'élimination intrinsèque  $k_{MPs}$ , en se concentrant sur certains phénomènes physiques. En

structurant les facteurs influençant les taux d'élimination en paramètres d'advection et de diffusion, l'importance des conditions de mélange, qui sont représentées par l'ordre de la réaction  $n$  sur la concentration de biomasse a été mise en évidence.

D'une part, si des problèmes de mélange se produisent, les cinétiques classiques telles que le premier ordre ou le premier ordre apparent sont inadéquates. D'autre part, une concentration élevée de biomasse augmente la surface active de la biomasse mais également l'augmentation de la viscosité conduit à la création de gros agrégats de floes et de zone liquide stagnante comme le montre la Figure 4. Par la suite, les MPs doivent diffuser dans l'eau stagnante entre les agrégats des floes et à l'intérieur des floes pour atteindre les bactéries où ils peuvent être éliminés.

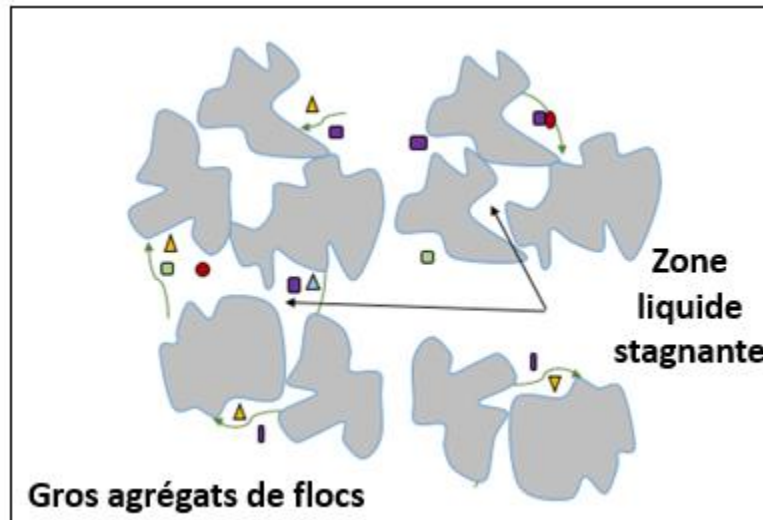


Figure 4. Limites physiques de transport et de diffusion des MPs à une concentration élevée de biomasse.

Cependant, aucun coefficient de diffusion des MPs étudiés dans la base de données chimiques, nous avons donc suivi une méthode inspirée de l'équation de diffusion d'Einstein. En fait plus précis que l'équation d'Einstein, des modèles tels que Wilke-Chang et Tyn-Calus permettent d'obtenir une bonne approximation de la valeur réelle du coefficient de diffusion du composant dans les systèmes en phase liquide à partir de la masse moléculaire. Un résultat intéressant est que le réarrangement de l'équation de Wilke-Chang en fonction de la masse moléculaire des MPs ( $M_{MPs}$ ) révèle une dépendance fonctionnelle de la forme  $D_m = f(1/M_{MPs}^{0,6})$ . L'équation complète est:



$$D_m = \frac{7.4 \cdot 10^{-8} T \alpha^{0.5} M_{sol}^{0.5} \rho^{0.6}}{\eta M_{MPs}^{0.6}} \quad (4)$$

où T est la température absolue,  $M_{MPs}$  est la masse moléculaire des MPs,  $M_{sol}$  est la masse moléculaire du solvant,  $\eta$  est la viscosité du solvant,  $\rho$  est la densité du solvant et  $\alpha$  est le paramètre d'association qui est supposé être 2,3 pour l'eau.

Nous avons tracé  $n$  vs. de  $1/M_{MPs}^{0.6}$  (Figure 5).

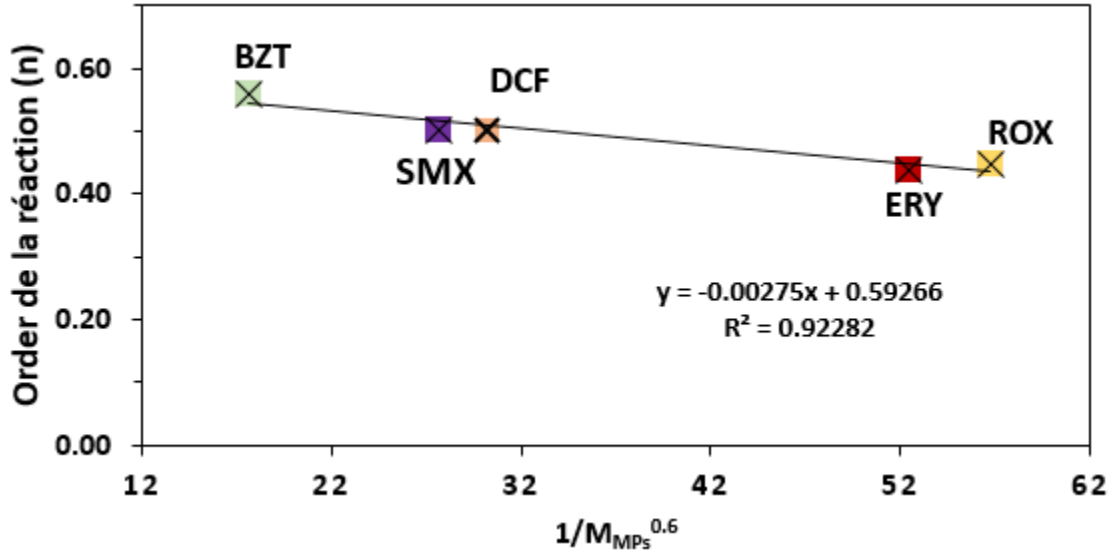


Figure 5. Tracé de l'ordre de la réaction  $n$  pour les cinq micropolluants étudiés SMX, BZT, ROX, ERY et DCF en fonction de  $1/M_{MPs}^{0.6}$ .

Un des résultats majeurs de cette étude est le très bon ajustement obtenu comme le montre la Figure 5. Ceci montre qu'il existe une relation entre le coefficient  $n$  et les phénomènes de diffusion. Le coefficient de corrélation ( $R^2$ ) pour un ajustement linéaire avec le modèle respectif était de 0,92. Cela indique que la diminution de l'ordre de la réaction est attribuée à l'augmentation de la masse moléculaire du MP. Ensuite, l'expression de  $n$  peut être réécrite comme:

$$n = k_1 M_{MPs}^{-0.6} + k_2 \quad (5)$$

Remplacer l'équation. (5) dans l'Eq. (3), la nouvelle vitesse de réaction prend la forme de l'équation suivante:

$$r_{MPs} = -k_{MPs} C_{MPs} C_{TSS}^{\left(\frac{k_1}{M_{MPs}^{0.6}} + k_2\right)} \quad (6)$$

avec

$$k_1 = -0.00275 \text{ (mol}^{0.6} \text{ g}^{-0.6}\text{)} \text{ and } k_2 = 0.593.$$

De point de vue simulation, il nous a paru fondamental de tester numériquement la biocinétique des boues activées représentées par l'ASM1 couplée au modèle cinétique d'élimination des micropolluants. Nous avons donc subi une simulation préliminaire afin de reproduire l'évolution temporelle expérimentale des variables d'état ASM1 (macropolluants et biomasse) mesurées. Dans une deuxième étape, la cinétique d'élimination des micropolluants a été ajoutée au modèle ASM1. Deux modèles cinétiques ont été considérés, le modèle classique du premier ordre apparent et une cinétique de loi de puissance, afin de (i) vérifier les résultats expérimentaux et (ii) prédire l'effet du mélange local pour une large gamme de concentrations de biomasse sur l'élimination des MPs. Les évolutions des concentrations entre le début et la fin de la réaction ont été évaluées. Des simulations ont été effectuées à l'aide du logiciel Matlab pour représenter les conditions du système fermé de deux série d'expériences. La première série a été réalisée à différents SRT et HRT mais en maintenant la concentration de biomasse presque constante autour de  $3 \text{ g}_{\text{TSS}} \text{ L}^{-1}$ . La deuxième série de simulations a été réalisée à SRT de 10 jours et HRT de 4 heures à différentes concentrations de biomasse de 3, 5 et  $8 \text{ g}_{\text{TSS}} \text{ L}^{-1}$ .

Les résultats des simulations avec deux cinétiques différentes d'élimination des MPs dans des systèmes fermés ont montré que le premier ordre apparent correspond bien aux expériences effectuées à divers SRT et HRT avec  $C_{\text{TSS}}$  autour de  $3 \text{ g}_{\text{TSS}} \text{ L}^{-1}$  (Figure 6).

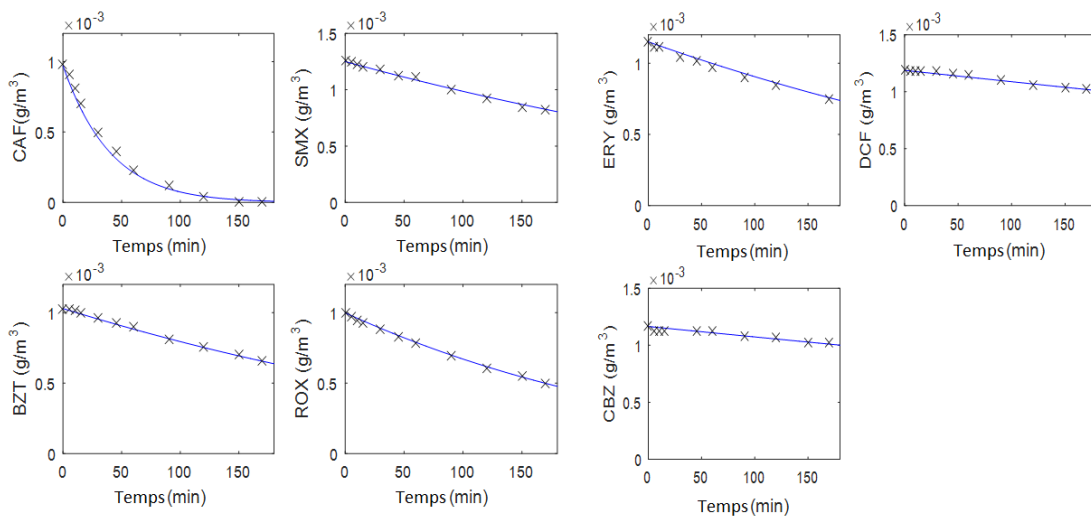


Figure 6. Profils simulés et expérimentaux des concentrations de MPs en appliquant l'approche de premier ordre apparent à un exemple de la série 1 des SBR opéré à  $C_{TSS}$  de  $3 \text{ g L}^{-1}$ . Les croix se réfèrent aux données expérimentales et la ligne bleue se réfère aux résultats simulés.

Cependant, la cinétique apparente de premier ordre échoue pour les autres concentrations de biomasse de la série 2 des expériences (Figures 7a, 7b).

(a)

(b)

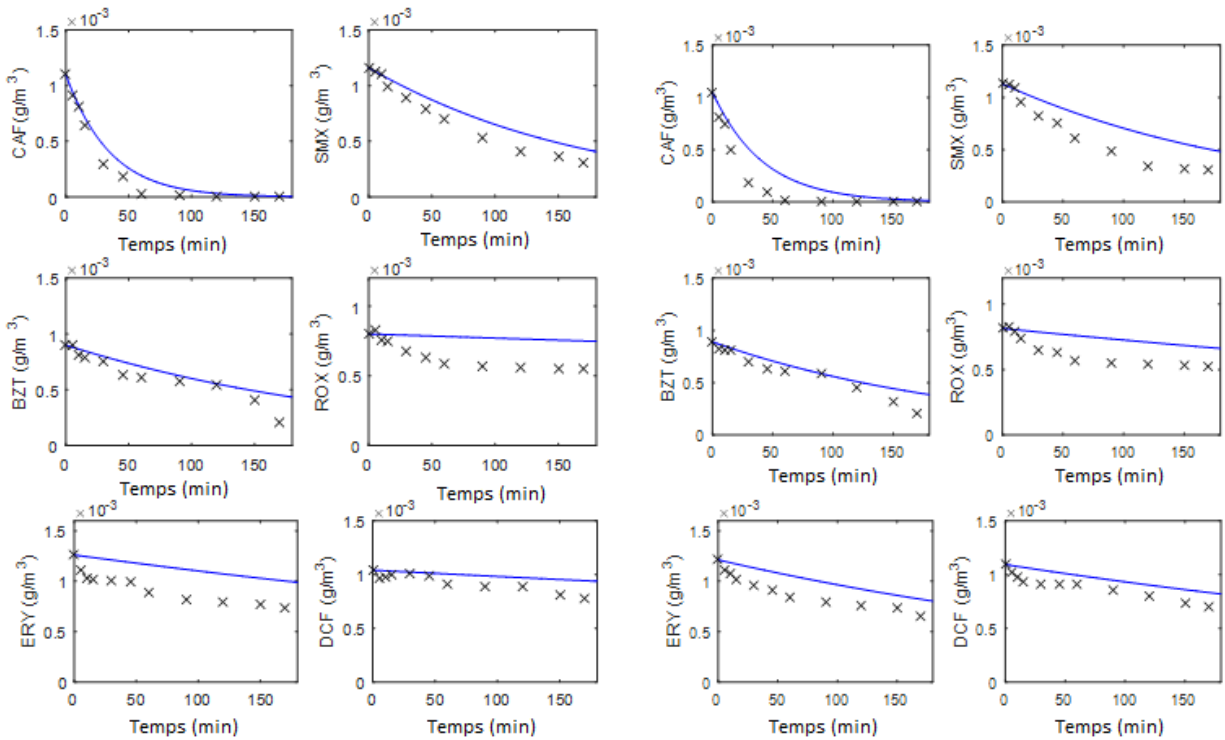


Figure 7. Profils simulés et expérimentaux des concentrations de MPs en appliquant l'approche de premier ordre apparent à la série 2 des expériences opérés à  $C_{TSS}$  de  $5 \text{ g L}^{-1}$  (a) et  $8 \text{ g L}^{-1}$  (b).

Alternativement, la cinétique de la loi de puissance a été testée et comparée aux profils de concentration expérimentaux. Cette nouvelle cinétique réussit à prédire l'élimination de tous les MPs étudiés à tous les  $C_{TSS}$  testés (Figure 8).

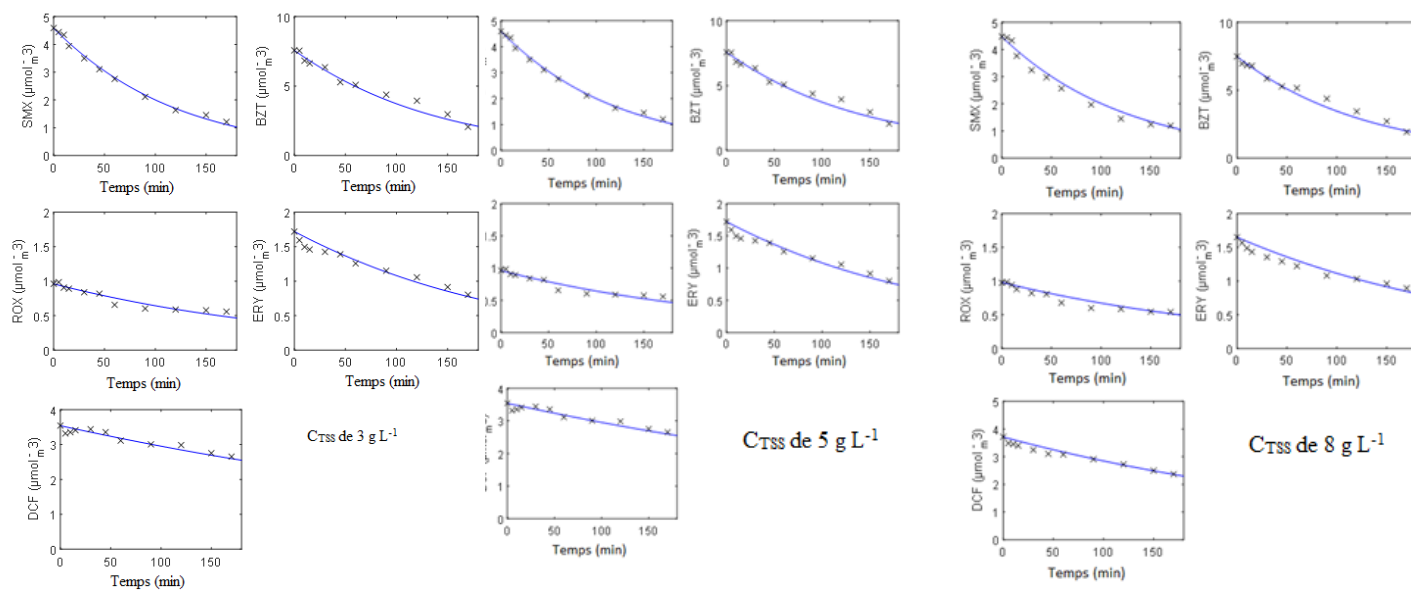


Figure 8. Profils simulés et expérimentaux des concentrations de MP en appliquant l'approche de la loi de puissance au SBR exploité à SRT de 10 j et HRT de 4 h testé à  $C_{TSS}$  de  $3 \text{ g L}^{-1}$ ,  $5 \text{ g L}^{-1}$  et  $8 \text{ g L}^{-1}$ .

Nous avons également pu simuler l'élimination des MPs pour différentes valeurs du mélange local représenté par  $n$  et différentes valeurs de concentration de biomasse. Un exemple de résultats affichés sous forme des contours dans la Figure 9 a montré que dans des conditions favorables ( $n$  élevé,  $C_{TSS}$  élevé), une élimination très élevée de tous les MPs se produit dans les 3 premières heures de la réaction. Inversement, pour des conditions défavorables ( $n$  faible,  $C_{TSS}$  faible), moins de 50% d'élimination des différents types de MPs ont été atteints. Si nous affichons les valeurs expérimentales, sachant que le résultat  $n$  de BZT est 0,56, il semble évident que nous ne sommes pas dans les zones de forte élimination. Si nous avons augmenté la quantité de biomasse, nous avons pu améliorer la qualité de l'agitation et nous déplacer vers la droite mais ce n'était pas le cas.

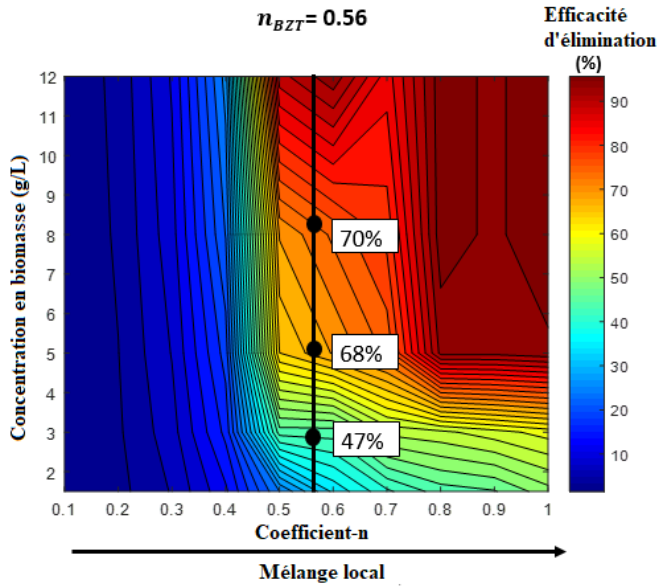


Figure 9. Contours de l'efficacité d'élimination (%) du BZT en fonction de la concentration de la biomasse des boues et du coefficient  $n$ . La couleur rouge signifie l'efficacité d'élimination la plus élevée de chaque MP. La ligne noire et les pourcentages sur chaque figure correspondent à la valeur expérimentale  $n$  et à l'efficacité d'élimination de chaque MP à 3, 5 et 8  $g_{TSS} L^{-1}$ , respectivement.

Par la suite, on a extrapolée la nouvelle cinétique appropriée sur un système continu en testant différentes conditions hydrodynamiques telles que le mélange local et les configurations de réacteurs afin d'améliorer l'élimination des contaminants des plans d'eau. Pour cela, la station d'épuration modèle testée est identique à celle utilisée dans le Benchmark avec un nombre plus élevé des réacteurs parfaitement agités (J) jusqu'à 100 avec un volume total constant et en gardant le même rapport d'aérobies de 3/5ème (Figure 10). Nous avons donc effectué un nouveau code de simulation, les évolutions des concentrations entre l'entrée et la sortie des systèmes ont été réalisées.

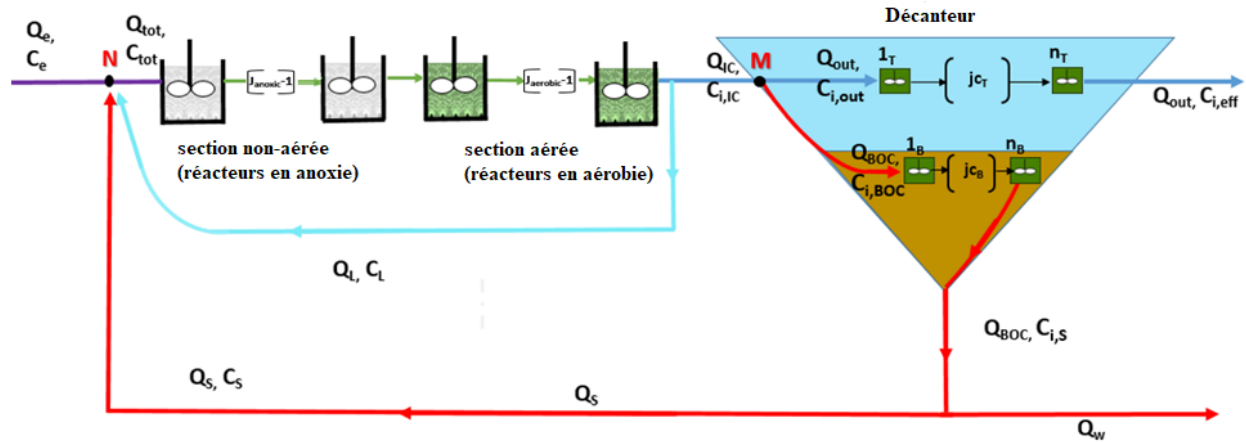


Figure 10. Schéma de la station d'épuration de Benchmark.

Différentes configurations ont été testées. L'augmentation du nombre de réacteurs aérobie jusqu'à 60 ainsi que l'application d'un bon mélange local augmentent considérablement l'élimination de tous les MPs étudiés. Dans le cas de SMX par exemple, le petit nombre de réacteurs de la cascade avec une faible valeur de  $n$  qui traduisent respectivement une mauvaise hydrodynamique locale et globale, l'élimination est faible autour de 20% (Figure 11). Du point de vue du micromélange, si  $n$  est faible, il est inutile d'augmenter le nombre de réacteurs. En revanche, dans les meilleures conditions extrêmes d'hydrodynamique à un  $n$  élevé qui tend vers un réacteur à piston, 90% de l'élimination est atteinte. Ce résultat montre que le SMX considéré comme moyennement biodégradable est plutôt bien éliminé si l'on trouve les configurations pratiques avec les conditions de mélange locales adéquates. Des comportements similaires sont présentés pour le BZT, ROX, ERY et DCF mais avec des efficacités d'élimination différentes.

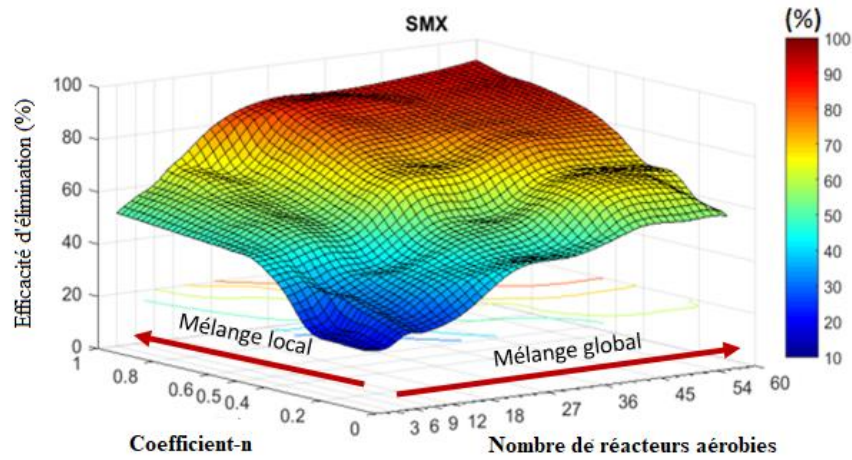


Figure 11. Tracé 3D représentant l'efficacité d'élimination (%) de SMX en fonction de l'ordre de la réaction  $n$  (variant de 0,1 à 1) et en fonction du nombre de réacteurs aérobies (de 3 à 60). La couleur rouge signifie l'efficacité d'élimination la plus élevée.

Dans une dernière partie, il nous a paru aussi fondamental de concevoir des réacteurs à canaux aérés, dont l'hydrodynamique correspond à différentes cascades de RPA. Nous commencerons d'abord par un réacteur à canal aéré correspondant à celui du Benchmark: volume de  $3600 \text{ m}^3$ . Nous avons essayé d'estimer sa géométrie pour correspondre à 3 RPA. Sur la base de l'équivalence entre le réacteur à écoulement piston à dispersion axiale et les réservoirs en modèles de série établis par Villiermaux 1982 et la corrélation donnant la dispersion axiale  $D$  proposée par Potier 2005 et Le Moullec 2008, le nombre de cellules ( $J$ ) a été calculé. Ensuite, nous changerons ses proportions de forme pour s'adapter à un nombre correspondant plus élevé de RPA. Le volume total, la surface horizontale et la profondeur restent constants pour toutes les configurations. Le résultat majeur de cette étude est l'équation (7) qui relie le nombre initial de RPA utilisé dans le Benchmark ( $J_i$ ) et le nombre de RPA ( $J_{cal}$ ) à calculer.

$$J_{cal} = 1 + \frac{(J_i - 1) W_i^{5/2} (H + W_{cal}) \sqrt{((W L) + W_i^2)}}{W_{cal}^{5/2} (H + W_i) \sqrt{((W L) + W_{cal}^2)}} \quad (7)$$

Enfin, pour atteindre le nombre maximum de réacteurs testé pour  $J_{cal} = 60$ , une largeur de 2,0 m et donc une longueur de 255 m pour la même surface horizontale sont nécessaires (Figure 12).

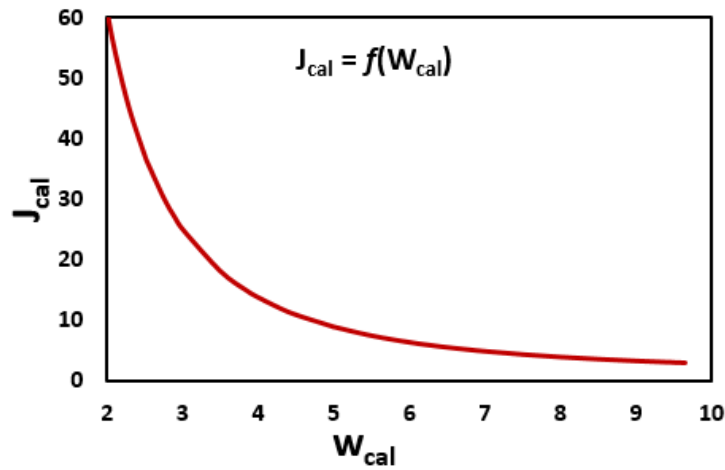


Figure 12. Nombre de RPA ( $J_{cal}$ ) correspondant à la largeur du réacteur ( $W_{cal}$ ).  $J_{cal}$  a été calculé pour la gamme du  $W_{cal}$  initial jusqu'à 9,65 m ( $J_i = 3$ ,  $W_i = 9,65$  m et surface horizontale de 514,3 m<sup>2</sup>).

En respectant le même volume et la même surface du réacteur et par rapport au réacteur initial, la largeur est divisée par environ 5 alors que la longueur a été multipliée par environ 5. Afin d'éviter les problèmes de construction et de gagner de l'espace, il est possible de construire le nouveau réacteur avec 5 chicanes comme le montre la Figure 13.

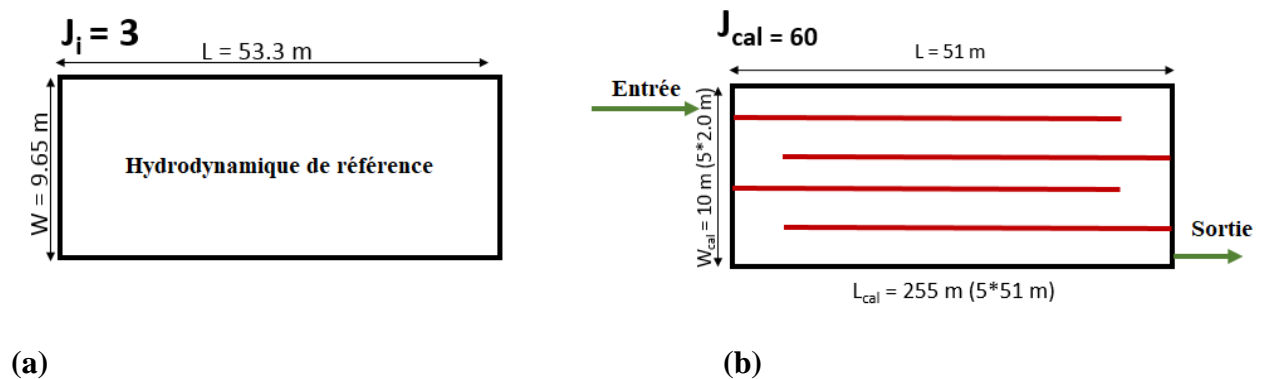


Figure 13. Représentations schématiques du (a) réacteur avec  $J = 3$  (géométrie initiale) et (b) de la nouvelle géométrie avec 5 chicanes pour le plus haut  $J = 60$  avec entrée et sortie sur les côtés opposés.



## **Motivation and aim of the project**

As natural resource, water is a real wealth, precious, fragile and limited, which must be managed sustainably and coherently. The complete water cycle is an essential part of the long-term management of water resources, requiring the protection of surface waters from persistent polluting compounds, the latter being difficult to remove and/or toxic. At the European level, 52 % of water is consumed by industry, 34 % by agriculture and 14 % for domestic use (FAO UN, 2002). It appears that during these various uses, the water becomes often polluted. Its discharge into the natural environment, in the form of more or less polluted effluents, can produce alterations of vital functions (= acute toxicity) of living beings, or even death caused by exposures (over a short period of time) to high doses of a toxic substance. They can also lead to alterations of the physiological functions (growth, reproduction) caused by exposures (in the long term) to low doses of a toxic substance. Over the last decades, increasing attention has been focused on the presence of micropollutants in the aquatic environment and in wastewater treatment plants (Bramard et al. 2016). Micropollutants (MPs) are pollutants that can have an effect on the environment and living beings even at low concentrations. They are often present in the aquatic environment at very low concentrations (range of  $\text{ng L}^{-1}$ -  $\mu\text{g L}^{-1}$ ) compared to other pollutants ( $\text{mg L}^{-1}$ ). The sources of micropollutants are of very diversified origin: domestic (pharmaceutical compounds, detergents), industrial (e.g. chemicals used in the products manufacturing or for cleaning), hospital (e.g. pharmaceutical compounds), urban (e.g. polycyclic aromatic hydrocarbon PAHs and metals from road traffic emissions or atmospheric deposition from building heating that in the form of runoffs reach soils or roofs), and agricultural (e.g. pesticides). The micropollutants released by cities and industries reach the WWTP via the segregated or unitary wastewater collection networks. The performance of micropollutant removal by WWTP is not negligible although they are not dimensioned with the aim of treating this type of substance (except recently for Switzerland). However, some substances are quantified in treated wastewater at significant concentrations ( $> 100 \text{ ng L}^{-1}$ ) (Miège et al. 2009; Coquery et al. 2011). This is attributed to both their "high" concentrations in the raw inlet wastewater and their weak elimination due to their properties (hydrophobicity, low biodegradability, etc.). The releases of WWTP thus represent one of the

sources of entry of micropollutants into the environment (Stumpf et al. 1999; Heberer 2002) and the presence of these compounds in effluents from sewage treatment plants has been reported in several studies (Hamid and Eskicioglu 2012; Tran and Gin 2017; Blum et al. 2018). Several treatment methods are considered for the removal of these microcontaminants from wastewater and drinking water as well, often as post-treatment. These include adsorption, membrane technology, advanced oxidation processes (AOPs) including several oxidation methods, and biological treatments (Giannakis et al. 2015; Ribeiro et al. 2019). Biological treatment processes use the metabolic abilities of bacteria, fungi, algae or plants in order to oxidize or reduce organic and inorganic compounds (Bhatia et al. 2017; Khandare and Govindwar 2015). The processes that occur in nature are intensified by ensuring appropriate conditions such as the oxygen concentration, pH, access to nutrients, etc. They are generally implemented in biological reactors, with adequate aeration and agitation equipment. The biodegradation methods in conventional treatments with activated sludge are the mainly used and most widespread in France (Verlicchi et al. 2012). They are considered as cost effective – in terms of operation costs (Punzi et al. 2015; Khandare and Govindwar 2015). However, bioprocesses have several limitations. For instance, they are able to transform only biodegradable compounds (Ganzenko et al. 2014) and, thus, are not able to eliminate the biologically persistent contaminants (Castiglioni et al. 2006). Therefore, the aerobic biological processes currently employed to treat these pharmaceutically active compounds are unsatisfactory in terms of efficiency. This is due to for instance the transfer of these pollutants to the gas phase, their adsorption and persistence in the solid phases, or an insufficient contact time with biomass. For these reasons, AOPs have been developed in several studies due to the overall high degradation efficiency of these methods (Paździor et al. 2018; Prieto-Rodríguez et al. 2013). Nevertheless, AOPs methods have several drawbacks including high costs, and risk of generation of toxic transformation products, or remaining oxidants (e.g. hydrogen peroxide) which may cause damage to microorganisms (Punzi et al. 2015; Ledakowicz et al. 2001). Matafonova and Batoev (2018) showed recently that practical implementation of AOPs is still limited at lab scale and more estimation of energy requirements are required.

The biological wastewater treatment remains the first solution that has been used for many years. One of the economical solutions suggested in this study is to investigate the effect of operational parameters of biological treatment, often employed in conventional processes, in order to improve the conversion of the biologically persistent pollutants (Majewsky et al. 2011; Falås et

al. 2016). The WWTP operating conditions such as hydraulic retention time (HRT) and sludge retention time (SRT) offer a great flexibility of operation to the biological reactors. It is important to note that the influence of these parameters is not already clearly understood (Pomiès et al. 2013). Membrane bioreactors are generally operated at high sludge ages and at large biomass concentrations represented by the total suspended solids ( $C_{TSS}$ ), allowing the intensification of biological processes. The supplementary operating condition of high  $C_{TSS}$  can also promote the removal of contaminants with particular characteristics, such as those with low bio-degradability and at low concentration (Sipma et al. 2010; Lejeune and Choubert 2019). Hydrodynamics is another field to explore; long reactor could help to improve removal rates (Joss et al. 2006; Villermeaux, 1982).

This thesis project aims to evaluate the effect of these parameters on the removal efficiency of some selected micropollutants. This work was undertaken in cooperation between LRGP-CNRS University of Lorraine in Nancy, France and Engler-Bunte-Institut of the Karlsruhe Institute of Technology (EBI-KIT) in Karlsruhe, Germany. Experiments were performed in EBI-KIT in order to determine removal kinetic rate constants, and investigate the effects of SRT, HRT and  $C_{TSS}$ . It was followed by a period of time in LRGP-CNRS to work on kinetics modelling and simulation. At the beginning of the study a group of micropollutants that represent various characteristics was selected. The micropollutants had to meet the following criteria:

- Represent a chemical family encountered in a large number of domestic and hospital effluents as well as in the conventional WWTP effluents.
- Have different properties which lead to their different biodegradability distribution in the reactor.
- Be able to be handled and measured satisfactorily.

Thus, caffeine, sulfamethoxazole, benzotriazole, roxithromycin, erythromycin, diclofenac and carbamazepine were selected as model molecules.

In this context, the laboratory scale study is presented in chapter II. For this, the change of MPs' concentration during biological treatment was monitored in aqueous phase. The removal of MPs was assessed by the determination of kinetic rate constants according to the most popular form of kinetic model, namely the apparent first-order model.

Chapter III is dedicated to an in-depth study of kinetics related to the results of previous chapter.

Chapter IV presents a model including real kinetics determined at EBI-KIT used for the simulation of MPs' removal in the activated sludge process by testing the effect of operating conditions such as mixing and hydrodynamic configurations of biological reactor. A new kinetics model of MPs removal performed at various biomass concentration was investigated in chapter III. Subsequently, the purpose was to simulate a typical continuous biological treatment reactor coupled with different MPs removal kinetics and thus to test the new kinetics in order to predict the effect of the reactor design and propose better reactor configuration to improve MPs removal.

## **References**

- Bhatia, D., Sharma, N.R., Singh, J., Kanwar, R.S., 2017. Biological methods for textile dye removal from wastewater: A review. *Critical Reviews in Environmental Science and Technology*, 47, 1836–76.
- Bramard, M., 2016. Monitoring micropollutants in French aquatic environments: Recent advances. [http://www.eaufrance.fr/IMG/pdf/campex\\_201603\\_EN.pdf](http://www.eaufrance.fr/IMG/pdf/campex_201603_EN.pdf).
- Blum, K.M., Andersson, P.L., Ahrens, L., Wiberg, K., Haglund, P., 2018. Persistence, mobility and bioavailability of Emerging Organic Contaminants discharged from sewage treatment plants. *Science of The Total Environment*, 612, 1532–42.
- Brusseau, M.L., Artiola, J.F., 2019. Chemical contaminants. In *Environmental and Pollution Science*, 175–90. Elsevier.
- Castiglioni, S., Bagnati, R., Fanelli, R., Pomati, F., Calamari, D., Zuccato, E., 2006. Removal of pharmaceuticals in sewage treatment plants in Italy. *Environmental Science & Technology* 40, 357–63.
- Coquery, M., Pomies, M., Martin-Ruel, S., Budzinski, H., Miège, C., Esperanza, M., Soulier, C., Choubert, J.M., 2011. Mesurer les micropolluants dans les eaux usées brutes et traitées: protocoles et résultats pour l'analyse des concentrations et des Flux. *Techniques Sciences Méthodes*, no. 1/2, 25–43.
- Fairbairn, D.J., Karpuzcu, M. E., Arnold, W.A., Barber, B.L, Kaufenberg, E.F., Koskinen, W.C., Novak, P.J., Rice, P.J. Swackhamer, and D.L., 2016. Sources and transport of contaminants

- of emerging concern: a two-year study of occurrence and spatiotemporal variation in a mixed land use watershed. *Science of The Total Environment*, 551–552, 605–13.
- FAO UN (Food and Agriculture Organization of the United Nations), 2002. *Produire plus avec moins d'eau*; 26 pg; Y3918/F; (<http://www.fao.org/docrep/005/Y3918F/y3918f03.htm>).
- Falås, P., Wick, A., Castronovo, S., Habermacher, J., Ternes, T.A., Joss, A., 2016. Tracing the limits of organic micropollutant removal in biological wastewater treatment. *Water Research*, 95, 240–49.
- Giannakis, S., Gamarra Vives, F.A., Grandjean, D., Magnet, A., De Alencastro, L.F., Pulgarin, C. 2015 Effect of advanced oxidation processes on the micropollutants and the effluent organic matter contained in municipal wastewater previously treated by three different secondary methods. *Water Research*, 84, 295-306.
- Hamid, H., Eskicioglu, C., 2012. Fate of estrogenic hormones in wastewater and sludge treatment: a review of properties and analytical detection techniques in sludge matrix. *Water Research*, 46, 5813–33.
- Heberer, T., 2002. Occurrence, fate, and removal of pharmaceutical residues in the aquatic environment: a review of recent research data. *Toxicology Letters*, 131, 5–17.
- Khandare, R.V., Govindwar, Sanjay P., 2015. Phytoremediation of textile dyes and effluents: current scenario and future prospects. *Biotechnology Advances*, 33, 1697–1714.
- Lado Ribeiro, A.R., Moreira, N.F.F., Puma, G.L., Silva, A.M.T. 2019 Impact of water matrix on the removal of micropollutants by advanced oxidation technologies. *Chemical Engineering Journal*, 363, 155-173.
- Ledakowicz, S., Monika Solecka, and Renata Zylla. 2001. Biodegradation, decolourisation and detoxification of textile wastewater enhanced by advanced oxidation processes. *Journal of Biotechnology*, 89, 175–84.
- Lejeune, A., Choubert, J.M., 2019. Modelling of micropollutant removal in full-scale membrane bioreactors: calibration and operations to limit the emissions. *Bioprocess and Biosystems Engineering*.
- Majewsky, M., Gallé, T., Yargeau, V., Fischer K., 2011. Active heterotrophic biomass and sludge retention time (SRT) as determining factors for biodegradation kinetics of pharmaceuticals in activated sludge. *Bioresource Technology*, 102, 7415–21.

- Matafonova, G., Batoev, V., 2018. Recent advances in application of UV light-emitting diodes for degrading organic pollutants in water through advanced oxidation processes: a review. *Water Research*, 132, 177–89.
- Miège, C., Choubert, J.M., Ribeiro, L., Eusèbe, M., Coquery, M., 2009. Fate of pharmaceuticals and personal care products in wastewater treatment plants – Conception of a database and first results. *Environmental Pollution*, 157, 1721–26.
- Paździor, K., Bilińska, L., Ledakowicz, S., 2018. A review of the existing and emerging technologies in the combination of AOPs and biological processes in industrial textile wastewater treatment. *Chemical Engineering Journal*, 12, 1285-1317.
- Pomiès, M., Choubert, J.M., Wisniewski, C., Coquery, M., 2013. Modelling of micropollutant removal in biological wastewater treatments: a review. *Science of The Total Environment*, 443, 733–48.
- Prieto-Rodríguez, L., Oller, I., Klammerth, N., Agüera, A., Rodríguez, E.M., Malato, S., 2013. Application of solar AOPs and ozonation for elimination of micropollutants in municipal wastewater treatment plant effluents. *Water Research*, 47, 1521–28.
- Punzi, M., Nilsson, F., Anbalagan, A., Svensson, B.M., Jönsson, K., Mattiasson, B., Jonstrup, M., 2015. Combined anaerobic–ozonation process for treatment of textile wastewater: removal of acute toxicity and mutagenicity. *Journal of Hazardous Materials*, 292, 52–60.
- Sipma, J., Osuna, B., Collado, N., Monclús, H., Ferrero, G., Comas, J., Rodriguez-Roda, I., 2010. Comparison of removal of pharmaceuticals in MBR and activated sludge systems. *Desalination* 250, 653–59.
- Stumpf, M., Ternes, T.A., Wilken, R.D., Rodrigues, S.V., Baumann, W., 1999. Polar drug residues in sewage and natural waters in the state of Rio de Janeiro, Brazil. *Science of the Total Environment*, 225, 135–141.
- Tran, N.H., Gin, K.Y.H., 2017. Occurrence and removal of pharmaceuticals, hormones, personal careproducts, and endocrine disrupters in a full-scale water reclamation plant. *Science of The Total Environment*, 599–600, 1503–16.
- Verlicchi, P., Al Aukidy, M., Zambello, E., 2012. Occurrence of pharmaceutical compounds in urban wastewater: removal, mass load and environmental risk after a secondary treatment—a review. *Science of The Total Environment*, 429, 123–55.



**Chapter I. State of the art of micropollutant's removal  
modelling in activated sludge systems**



*By proposing a description of the biological treatment in wastewater treatment plant (WWTP), the parameters associated with its monitoring as well as study of the micropollutants' (MPs) removal modelling, this chapter aims to define the framework for this work and provide the knowledge needed to understand it.*

*The first part elaborated on the assessment of European waters by highlighting the surface water state as well as the impact of some pressures including pollution on it.*

*Then, in a second main part, after a short discussion of the water pollution sources, the occurrence of micropollutants (MPs) in wastewaters, their categories and impacts on the environment, are investigated. Indeed, scientific researchers have tried throughout the two last decades to improve the removal of this pollution and counteract its harmful effects by different means of suitable treatment.*

*In terms of water treatment to remove organic contaminants, biological treatment is the technique of choice and in particular, the conventional process activated sludge is used the most. The effectiveness of these treatment processes as well as the expensive implementation of new advanced processes for water have attracted considerable attention from professionals to modify existing biological treatment. In addition, an estimation of micropollutants removal efficiency in conventional systems based on their physical-chemical properties was performed. This is continued with the evaluation of the effect of some adapted operational parameters to MPs removal improvement.*

*In the third main part, we exposed the MPs modelling in WWTPs which has become an integral part of WWTP design and operation. Various mechanisms of removal are described in order to assess and regulate MP emission into the environment. Finally, the hydrodynamic of the biological reactor which affect the MPs removal, were also investigated.*

## **I.1. Introduction**

Water is a renewable natural resource involved in many aspects of human life. Many of the major problems that humanity is facing in the twenty-first century are related to water quantity and/or water quality issues (UN, 2009). In terms of quantity, the saline waters of the oceans account for 97.6 % of the hydrosphere, leaving only 2.4 % of freshwater. The 86.3 % of these freshwaters are almost solidly blocked in the polar ice caps, snowfields and glaciers, and 11.7-29.9 % form groundwater (at 1 km depth), with only 0.26-2 % surface water in rivers, lakes, soil moisture, atmospheric moisture and biomass water (Hanslmeier 2010; Li and Qian 2018). Globally, rainfall pattern has changed because of rise in temperature as a result of climatic changes. As a result, water demand and availability of freshwater resources are affecting at local, regional and global levels. In addition, increased population growth, resulting urbanization, consequent industrialization, competing demands for water and altered socio-economic conditions have put additional pressure on the water supply.

In terms of quality, EU's water policy aims to ensure a good status in all bodies of surface water and groundwater for both people's needs and environment. In general, good status means that water shows only a slight change under undisturbed conditions. Achieving good status involves meeting certain standards for the ecology, chemistry and quantity of waters. The ecological status is an assessment of the functioning of surface water ecosystems based on biological quality elements such as phytoplankton, fauna and fish and supported by physico-chemical parameters, e.g. nutrients, transparency, and salinity. EU Member States have reported that 80 % of surface water bodies are rivers, 16 % are lakes and 4 % are coastal and transitional waters (EEA, 2018). The ecological status shows the influence of pressures (e.g. pollution and climate change) on water quality. On European scale, around 40 % of the surface water bodies are in good or high ecological status, with lakes and coastal waters having better status than rivers and transitional waters, while 60 % did not (EEA, 2018). As can be shown in Figure I.1, the northern countries, particularly the northern Scandinavian region and Scotland, as well as Estonia, Slovakia and several River Basin Districts (RBDs) in the Mediterranean region have a high proportion of water bodies in high or good ecological status.

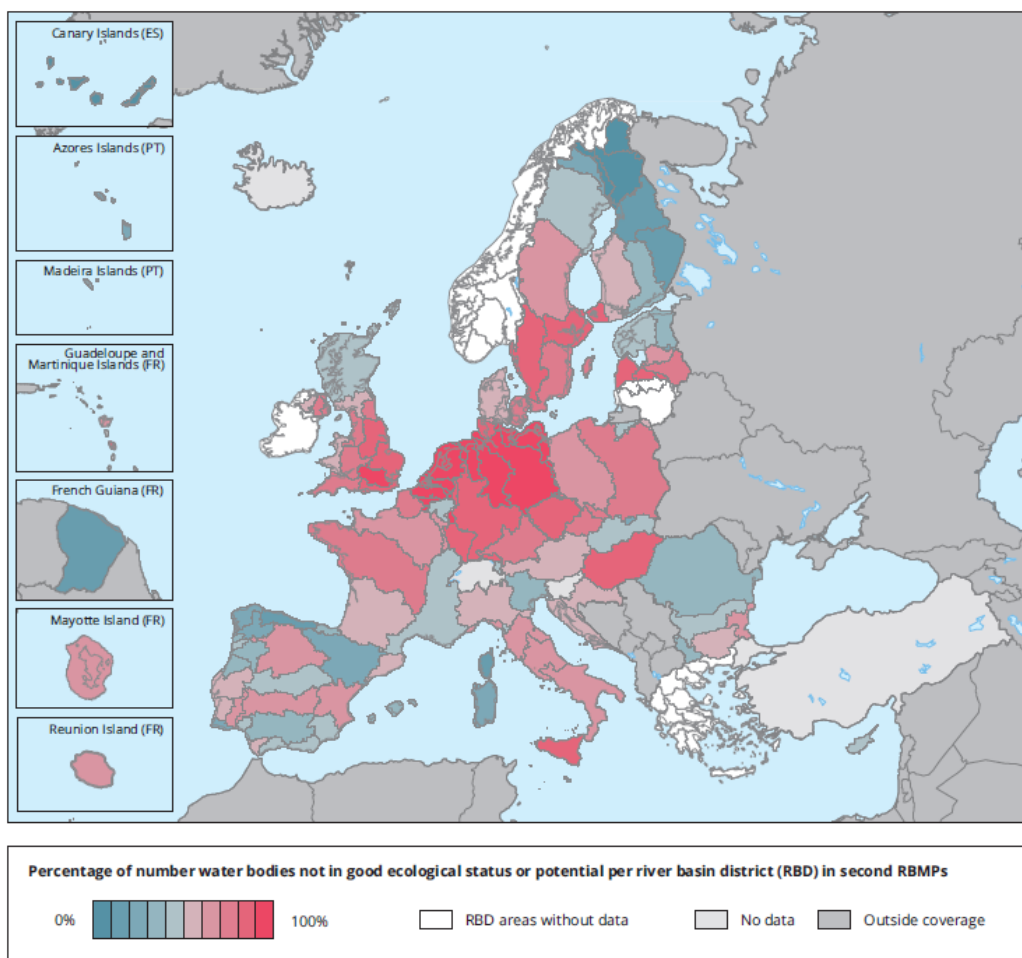


**Figure I. 1.** Map showing the percentage of water bodies in Europe's River Basin District (RBD) that are not in good ecological status: second River Basin Management Plans (RBMPs) (EEA, 2018).

In contrast, many of the central European RBDs have the highest proportion of water bodies that are not in good ecological status (up to 99 %). In addition, for surface waters, good chemical status is defined by no concentrations of hazardous substances exceed the relevant environmental quality standards (EQS) established in the Directive 2008/105/EC (EU, 2008). The report of EEA (2018) showed in Figure I.2a that the widespread presence of such substances, identified in (EU, 2013) as ubiquitous, persistent, bioaccumulative and toxic (uPBTs) pollutants, leads to significant failure to achieve good chemical status (46 %) followed by a notable decrease of good chemical status to 38 % compared to 81% without the presence of uPBTs, while a status of 16 % is unknown. Moreover, to meet the aim of good chemical status, for groundwater, hazardous substances should be prevented from entering groundwater, and the entry of other pollutants (e.g. nitrates, pesticides)

should be limited. Recent member States' reports in the second River Basin Management Plans (RBMPs) showed that 74 % of EU groundwater bodies (by area) are in good chemical status and 25 % have poor chemical status, with 1 % of unknown status (Figure I.2b; EEA, 2018).

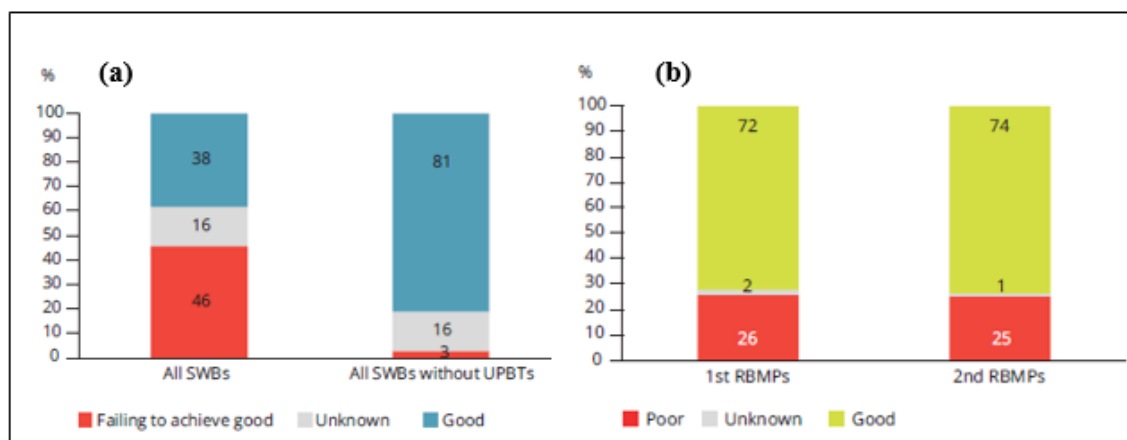


**Figure I. 2.** Chemical status of (a) surface water bodies (SWBs), with and without ubiquitous, persistent, bioaccumulative and toxic (uPBTs) pollutants and (b) groundwater bodies, by area, reported in first and second River Basin Management Plans (RBMPs) (EEA Report No 7/2018 2018).

Brusseu and Artiola (2019) related that statistics to the influence of chemical pressures on the water systems. The significant pressures on water bodies are from a variety of sources including, industry, food production, health developments, agriculture, transport, waste disposal, household purposes and discharges that are not connected to sewage treatment plants (Amiri et al. 2019; Evans et al. 2019; Schwarzenbach et al. 2005). It is a well-known fact that the main objective of a wastewater treatment plant (WWTP) is the reduction of pollutants according to the legal requirements (carbon, nitrogen and phosphorus) and the second is to obtain a good quality of water reuse of treated municipal or industrial water effluents to minimize the disturbances of the discharge of organic/inorganic contaminants in the environment (Esplugas et al. 2007). However, many studies showed that the WWTP itself are not efficiently and specifically designed to eliminate such contaminants (EEA, 2018; Laquaz et al. 2018). Beside the deep scientific investigations of various water contaminants such as microbial pollutants, heavy metals, nutrients and other pollutants, recent studies reported on the presence of a wide group of contaminants

originating from diverse sources including WWTPs (Rodriguez-Narvaez et al. 2017) named as micropollutants. Because of their persistence, some organic micropollutants could be toxic and bioaccumulate with potential significant impacts on human health and ecosystems (Grandclément et al. 2017).

The purpose of this chapter is to present the current state of art concerning the occurrence of several contaminants detected in WWTPs, their possible removal mechanisms and modelling concepts with activated sludge, the effect of the operational parameters on their removal and finally the impact of the reactor configuration in order to improve the removal of such contaminants before discharging into surface water.

## **I.2. Problematic of the micropollutant removal in conventional wastewater treatment plant**

### I.2.1. Micropollutants and Environment

#### I.2.1.1. Sources of micropollutants (MPs)

Micropollutants are bioactive and persistent contaminants that cannot be fully eliminated with traditional wastewater treatment methods and that are not completely biodegradable (Luo et al. 2014). Most of them are enough to disturb natural balance, causing a potential danger towards environment (Al Aukidy et al. 2012; Blair et al. 2013). For some, they are still considered as emerging micropollutants (EMs; Richardson and Kimura 2017) since they are not specifically associated with any regulation to date (Tran and Gin 2017) or in process of regularization. Water is used in three main sectors: agriculture (including animal husbandry), industry and domestic use (Figure I.3). These anthropogenic activities make water contaminated by many compounds (mineral and organic) and in many ways (directly or by transfer from other natural environments) (Yu et al. 2007) .

In order to improve productivity in agriculture, fertilizers and pesticides are used intensively. Large quantities of agrochemicals, nutrients, organic matter, drug residues, sediments, saline drainage inducing salinization and alkalization, microplastics and pathogens are discharged into surface water. Industrialized animal breeding also requires the use of veterinary drugs. The water used for irrigation and fish farming, as well as urinary and fecal waste of animal origin, will subsequently run off into surface water (Barbosa et al. 2016), or can also pass by direct leaching into ground water which may contaminate the drinking water as well (Feng et al. 2013).

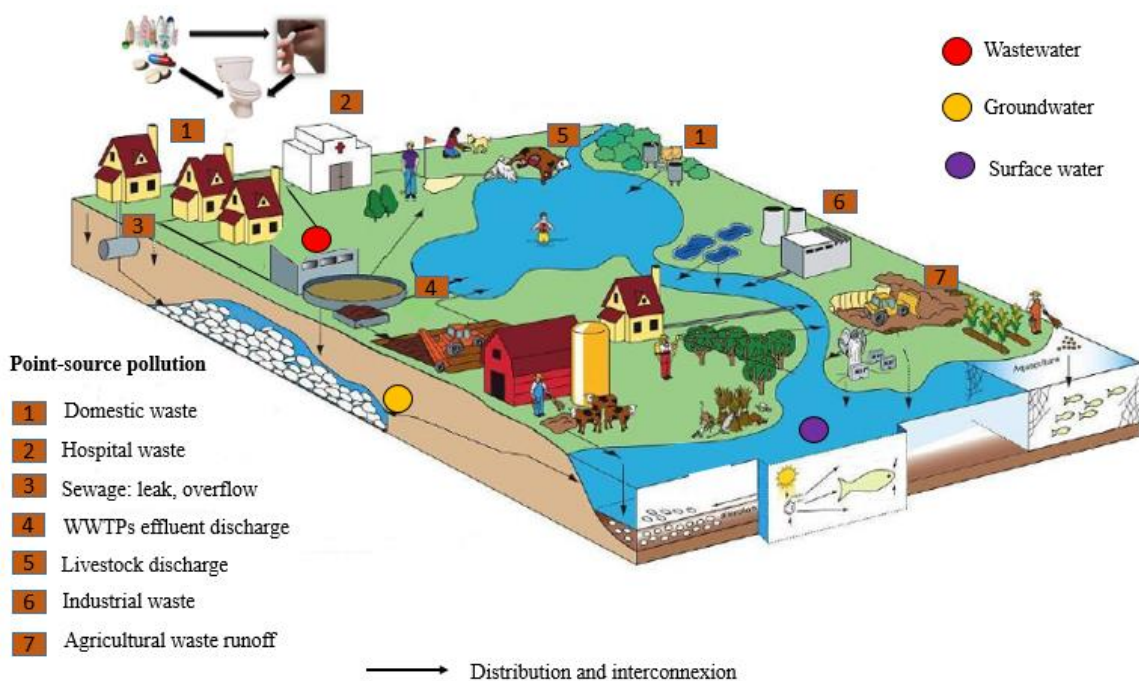


**Figure I. 3.** Sources and possible pathways of water pollution into the environment (adapted from Daughton (2006)).

In industry, air pollution induced by the release of toxic gases into the atmosphere is easily transferable to surface water through precipitation; it is the well-known phenomenon of "acid rain" that affects fauna and flora in lakes, public health and other enclosed water bodies (Gwenzi et al. 2015). Also, industrial wastewater from landfill leachate from improper disposal of used, improper or expired items find their way into surface water (Walker et al. 2019). Moreover, the leakage of different micropollutants from industrial waste systems, find their way into surface water and ground water as well. For example, stationery mills, dairy products, textile dyes, drugs, fertilizers and pesticides are viewed with concern.

The domestic use of water to drink, wash, cook, clean and dispose of human waste results in the formation of municipal wastewater. Organic matter in these waters includes food waste, detergents, personal care products, medications and excreted metabolites. The effluents from hospitals that usually come into these same waters are particularly loaded with pharmaceutical substances (Richardson and Postigo 2015; Quesada et al. 2019).

To solve the problem of the limited availability of water, the purification of contaminated water for possible reuse seems to be the only solution. For decades, wastewater treatment plants have been the solution adopted in many developed countries (mainly in Europe and North America). As can be seen in Figure I.3, even though the WWTPs act as primary barriers against the diffusion of pollutants to the environment, the effluents discharge is one of the pathways for the introduction of micropollutants to the aquatic environment.

#### I.2.1.2. Occurrence of micropollutants in wastewater and their regulations

In recent years, the scientific researches on micropollutants occurrence in the environment have been increasing, reflecting this worldwide issue of increasing environmental concern (Ratola et al. 2012). Several review papers reported the occurrence of a wide variety of emerging micropollutants in different types of waters, including wastewater (Miège et al. 2009; Verlicchi et al., 2012), surface water (Luo et al. 2014), groundwater (Lapworth et al. 2012; Luo et al. 2014), and drinking water (Utrilla et al. 2013; Luo et al. 2014). Among all aforementioned types of waters, wastewater is the most exhaustively reviewed. The occurrence of various MPs in both influent and effluent, collected from recent studies (from 2008–to date), are summarized in Table I.1. It is easy to see in the table a significant spatial and temporal variations in micropollutant's concentration in WWTP. This difference can be attributed to the water consumption (per person and per day), the habits of the population, the metabolism of the population (excretion rate), the size, the efficacy of WWTPs, and the physico-chemical properties of micropollutants (Petrovic et al. 2009; Jelic et al. 2012) (see section I.2.2.3.1 for more details).

At present, standards and valid discharge guidelines limits are not yet being done for most micropollutants (Luo et al. 2014). However, in some countries, few regulations of a small group of micropollutants have been published (Barbosa et al. 2016). In the year 2000, an initial list of 33 priority substances was also identified within the EU Water Framework Directive (WFD) 2000/60/EC to be used as a control measure for the next 20 years (Directive 2000). In 2007, some substances/groups were identified as future emerging priority candidates such as diclofenac, iopamidol, musks and carbamazepine. At the same time, ibuprofen, clofibrac acid, triclosan, phthalates and bisphenol were added to the previous list (Fairbairn et al. 2016). Always in terms of protection of human health and aquatic environment, the European Union 2013/39/EU

(Directive, 2013) was concerned to the study of the treatment processes for a group of 45 pharmaceuticals (Barbosa et al. 2016). Also, Baltic Sea Action Plan (BSAP) and the EU's Baltic Sea strategy have led to a greater focus on problems with the load of pharmaceuticals to the in land water bodies and the marine environment in the Baltic Sea (Marine Framework directive 2008/56/EG, Water Framework directive (WFD) 2000/60/EEG, and the WFD daughter directive 2008/105/EG). Moreover, the EU has identified a number of priority substances on the EU pollutants priority watch list (European Commission, 2016).



**Table I. 1.** The concentrations and removals of several micropollutants present in the WWTPs of different countries.

Group	Selected compound	Country	Influent ( $\mu\text{g L}^{-1}$ )	Effluent ( $\mu\text{g L}^{-1}$ )	Removal efficiency (%)	References
Pharmaceutical Antibiotic	Sulfapyridine	Switzerland; UK	0.06 – 1.5		-29 – 20	Gobel et al. 2007; Kasprzyk-Hordern et al. 2009
	N <sup>4</sup> -acetyl sulfamethoxazole	Switzerland	8.5 – 1.6	1.27 – 0.24	9 – 21	Gobel et al. 2007
	Trimethoprim	Switzerland; UK	0.21 – 0.44	0.19 – 0.41	-13 – 31	Gobel et al. 2007; Kasprzyk-Hordern et al. 2009
	Azithromycin	Switzerland	0.09 – 0.38	0.08 – 0.34	10 – 33	Gobel et al. 2007
	Clarithromycin	Switzerland; Germany	0.33 – 0.6	0.26 – 0.48	11 – 14	Gobel et al. 2007; Sahar et al. 2011; Ternes et al. 2003
Anti-inflammatory/analgesics	Paracetamol	UK	68 – 482	18 – 24	73.5 – 95*	Kasprzyk-Hordern et al. 2009
	Salicylic acid	Greece; Spain	0.58 – 63.7	ND – 0.50	89.6 – 100	Gracia-Lor et al. 2012; Kasprzyk-Hordern et al. 2009; Stamatis et al. 2010; Santos et al. 2009
	Mefenamic acid	Korea; Spain ; UK	<0.017 – 0.32	<0.005 – 1.03	< 0 – 70.2	Behera et al. 2011; Gracia-Lor et al. 2012; Kasprzyk-Hordern et al. 2009; Santos et al. 2009
	Codeine	Germany; UK	0.12 – 0.16	0.022 – 0.025	81.6 – 84.3*	Wick et al. 2009; Kasprzyk-Hordern et al. 2009

(Continued on next page)

Table I. 1. Continued

Group	Selected compound	Country	Influent ( $\mu\text{g L}^{-1}$ )	Effluent ( $\mu\text{g L}^{-1}$ )	Removal efficiency (%)	References
Anti-inflammatory/ analgesics	Ibuprofen	UK; Korea; Greece; Sweden; Spain	<0.003 – 603	ND –55	70 – 100	Kasprzyk-Hordern et al. 2009; Behera et al. 2011; Zorita et al. 2009; Radjenovic et al. 2009; Gracia-Lor et al. 2012
	Ketoprofen	UK; Korea; Spain	<0.019 – 1.27	< 0.005 – 0.39	0 – 70*	Kasprzyk-Hordern et al. 2009; Behera et al. 2011; Gracia-Lor et al. 2012; Zorita et al. 2009; Radjenovic et al. 2009
	Naproxen	Spain; Sweden	0.002 – 52.9	0.13 – 0.67	64 – 98.7*	Radjenovic et al. 2009; Singer et al. 2010; Gracia-Lor et al. 2012; Santos et al. 2009
	Gabapentin	UK	10.6 – 25	1.78 – 3.51	83.2 – 85.9*	Kasprzyk-Hordern et al. 2009
	Primidone	Germany	0.23 – 0.42	0.14 – 0.25	39.1 – 40.4*	Wick et al. 2009
Lipid regulator	Clofibrate	Spain; Korea; EU-wide; UK	0 – 0.7	0.33	52.8	Behera et al. 2011; Gracia-Lor et al. 2012; Loos et al. 2013; Santos et al. 2009
	Bezafibrate	Spain; Korea; UK	0.05 – 1.9	0.03 – 0.67	10 – 64.7*	Behera et al. 2011; Gracia-Lor et al. 2012

(Continued on next page)

Group	Selected compound	Country	Influent ( $\mu\text{g L}^{-1}$ )	Effluent ( $\mu\text{g L}^{-1}$ )	Removal efficiency (%)	References
PCP** Hormones	Estriol	China; Korea	0.125 – 0.80	ND	100	Behera et al. 2011; Nie et al. 2012
	Estrone	France; Germany; Italy; Korea	0.01 – 0.26	<0.001 – 0.09	72.8 – 90.8*	Janex-Habibi et al. 2009; Nie et al. 2012; Zorita et al. 2009
	Estradiol	France; Germany; Italy; Korea	0.002 – 0.05	0.001 – 0.007	92.6 – 100	Janex-Habibi et al. 2009; Nie et al. 2012; Zorita et al. 2009
Industrial chemicals	Bisphenol-A	Austria; UK	0.013 – 2.3	0.026 – 1.53	<0 – 33.4	Clara et al. 2005b; Kasprzyk-Hordern et al. 2009
Antiseptics	Triclosan	Spain; UK; Greece; Korea; France; USA	0.03 – 23.9	0.01 – 6.88	71.3 – 99.2	Santos et al. 2009; Behera et al. 2011; Kumar et al. 2010; Yu and Chu 2009
	Galaxolide	Germany; Switzerland; Austria	0.6 – 3.1	0.45 – 1.15	25 – 62.9*	Janex-Habibi et al. 2009
Pesticide	Diuron	EU-wide	0.03 – 1.96	0.002 – 2.53	26.7 – 71.9	Loos et al. 2013
Industrial chemicals	4-Tolyltriazole	Germany	1.3	1.2	11	Weiss et al. 2006
	5-Tolyltriazole	Germany	2.1	2.2	-6	Weiss et al. 2006

Table I. 1. Continued

ND: not detected. \* When the removal efficiency was not mentioned in the research, it was calculated using the following equation, removal efficiency (%) = (Influent– Effluent) / Influent × 100. \*\* Personal care product.

Due to the various chemical nature as well as the large number of emerging contaminants (ECs), the Environment Agency (EA) of England and Wales proposed a classification system in order to identify substances with great potential to pose a risk to the aquatic environment. Moreover, regulatory agencies as European Commission and scientific community is working on covering a larger groups, 46 of toxic micropollutants to set their regulatory limits as well as to study their detrimental effects and new treatment processes (Luo et al. 2014; Barbosa et al. 2016).

#### I.2.1.3. Categories of micropollutants

In general, emerging micropollutants can be grouped into six major categories specifically pharmaceuticals active compounds (PhAC), personal care products (PCPs), endocrine disruptor compounds (EDCs) including hormones (Rodriguez-Narvaez et al. 2017; Luo et al. 2014), surfactants, industrial compounds (Ribeiro et al. 2015), and pesticides (Luo et al. 2014). This classification into categories and groups is based on their application or chemical structure. It also illustrates the diversity of use of compounds considered as emerging contaminants. Pharmaceuticals and personal care products, two main categories of emerging contaminants are often combined in one category called Pharmaceuticals and Personal Care Products (PPCPs).

##### *I.2.1.3.1. Focus on Pharmaceuticals and Personal Care Products (PPCPs) and industrial chemicals*

Over the last twenty years, the PPCPs constitute a highly heterogeneous group of compounds of quite diverse chemical properties and structures. However, the structural formula of these compounds shows in most cases a non-polar hydrocarbon backbone with a polar functional group which is most often oxygenated or nitrogenous. Detection of pharmaceuticals in aquatic environment at high concentrations is strongly impacted by the pharmaceutical industry waste, hospital and domestic waste, as well as animal waste that eventually reach natural waters (Utrilla et al. 2013). This important category of ECs includes about 3000 different compounds such as stimulant, anti-inflammatory drugs, antibiotics, beta blockers, antidiabetics, antiseptics, antidepressants, lipid regulators, 49 anti-epileptics, antimicrobials, contraceptives and impotence

drugs (Tijani et al. 2013). Concerning stimulants, i.e. caffeine was used as a cardiostimulant till the end of 19th century (van Wijhe, 2002). In modern medicine, caffeine is used as an adjuvant to the analgesic actions of aspirin and paracetamol. Antibiotics can be categorized by their following structures: sulfonamides, fluoroquinolones, nitroimidazoles, penicillins, cephalosporins, tetracyclines and macrolides (Jelic et al. 2012). In particular, the release of antibiotics into the environment can cause the appearance of resistant bacterial strains (Potier et al. 2014). In contrast to pharmaceuticals, benzotriazoles are found more frequently in industrial than domestic wastewater. Benzotriazoles are complexing agents that are widely used as anticorrosives or detergents. The two most common forms, benzotriazole (1H-benzotriazole) and tolyltriazole (a mixture of 4- and 5-methyl-1H-benzotriazole), are soluble in water, resistant to biodegradation, and only partially eliminated in wastewater treatment (Richardson 2008; Weiss and Reemtsma 2005). In addition, the chemicals that compose personal care products including skin care products, cosmetics, perfumes, preservatives, and UV filters, also number in the thousands. Unlike pharmaceuticals, they are designed for external usage and enter easily the environment without passing through the human body. Due to their intensive use, their presence in the aquatic environment and their potential impacts on wildlife and humans, residues of PhACs pose a significant environmental problem (Mutiyar et al. 2018).

#### *1.2.1.3.2. Impacts of MPs on environment and living beings*

In the last few years, the potential impacts of MPs, even at concentrations as low as  $\text{ng L}^{-1}$  in different environmental compartments (K'oreje et al. 2018; Huang et al. 2018; Liu et al. 2018), have raised a great concern that is currently a major axis of scientific research. Esplugas et al (2007) proved that the effect of these contaminants does not depend only on their concentrations in the environment. It depends also on many other factors such as exposition time, persistence, bioaccumulation and the mechanisms of eliminations and biotransformation. Several studies reported that the simultaneous presence of micropollutants recalcitrant compounds as complex mixtures and their long-term exposition lead to constant but imperceptible effects that can accumulate gradually resulting in irreversible effects on wildlife and human being as well (Barbosa et al. 2016). Toxicological studies have shown that PPCPs might can cause direct toxicity towards the ecosystem associated with a number of negative effects such as effects on the hormonal control

of development in aquatic organisms, disruption of endocrine systems (Esplugas et al. 2007), and antibiotic resistance of microorganisms (Pruden et al. 2006). Moreover, the toxic potency of some residuals that inhibit microbial metabolism completely or partially in the case of antibiotics or antiseptics, can also disrupt the biological treatment process by damaging microorganisms in activated sludge. Concerning human beings, their exposure to EDCs could be through dermal absorption or contaminated media such as water, food, air, and soil (Tijani et al. 2013). The major concern is related to foetuses and newborn babies due to their higher sensitivity (Barbosa et al. 2016). Finally, the relevance of micropollutants to a surface water ecosystem also depends on the sensitivity of the ecosystem and the input of specific compounds or groups of compounds in the system, both in terms of concentration and duration between inputs. This makes the question of micropollutants also a location-specific issue.

## I.2.2. Removal of micropollutants in wastewater treatment plant

### I.2.2.1. Water treatment

In general, organic and inorganic pollutants derived from hospitals wastewater, industry, anthropogenic activities, drug manufacturing and agriculture enter WWTPs. Figure I.4 presents the basic steps of water treatment processes taking place inside a WWTP.

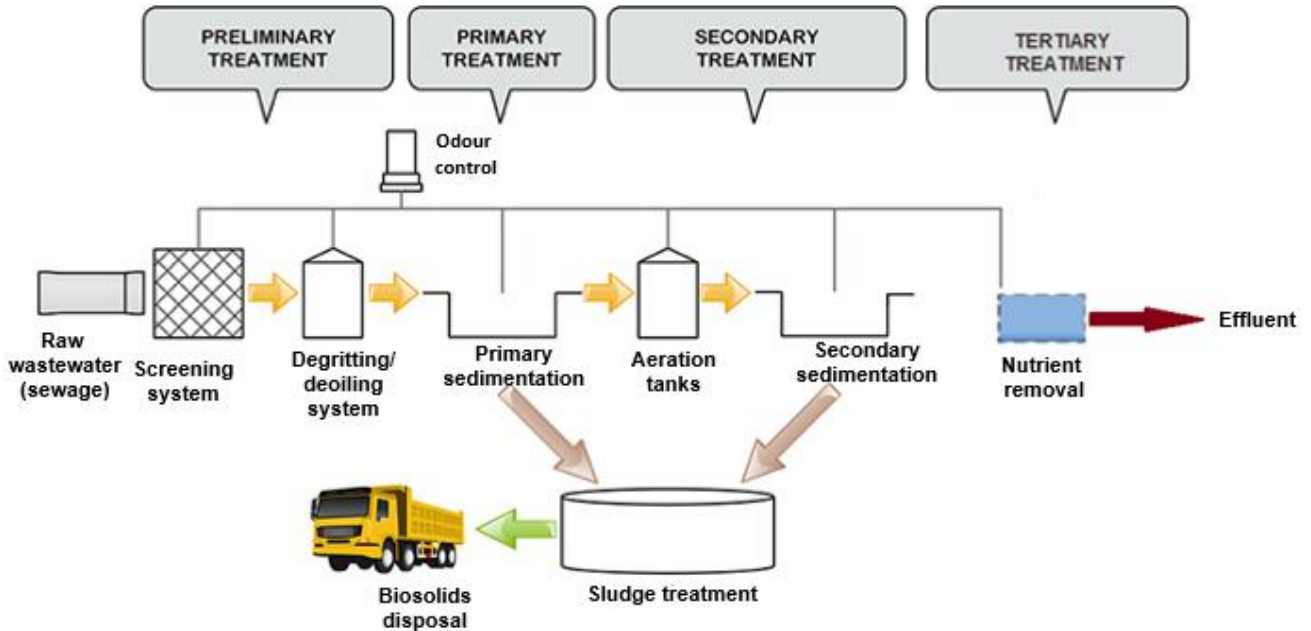


**Figure I. 4.** Basic steps of wastewater treatment process (adapted from Gandiglio et al. (2017)).

The removal processes in a conventional wastewater treatment plant start by the pretreatment that eliminates a large part of the suspended solids by grit removal and sand by decantation channel. A following physical primary treatment removes a part of colloidal and suspended solids through primary clarifier. Later on, a secondary treatment is applied that is based on attached or suspended growth systems for removal by biodegradation of easily biodegradable dissolved organics or residual solid. The sludge from both primary and secondary clarifiers after being separated from the water goes through the sludge treatment process. This treatment is based on a common employed technologies as filtration, sedimentation, centrifugation and sometimes on anaerobic digestion, aerobic digestion composting and incineration in order to reduce the amount of organic matter and microorganisms in the sludge prior to biosolids disposal (Das et al. 2017). Tertiary treatment is an optional system in order to remove nutrients but can also include processes to eliminate other pollutants. Finally, the WWTP effluent is discharged into a receiving water body. Unfortunately, due to the fact that current conventional WWTPs are equipped to remove biodegradable pollution (carbon, nitrogen, phosphorus) and the microorganisms are not efficient to metabolize micropollutants as source of carbon at low concentrations (Daughton and Ternes



1999; Tijani et al. 2013), these compounds persist in the treatment effluents of WWTPs and are released into receiving water systems (Esplugas et al. 2007).

#### I.2.2.2. Biological treatment process in secondary system

The biological treatment of wastewater is essentially based on the activity of bacteria. It has for main objective the removal of the soluble compounds of organic origin to make water acceptable by the natural environment in terms of organic, nitrogen, phosphorus and particulate pollution. The principle of this treatment is to put in contact a diversified group of microorganisms (bacteria, fungi, protozoa, etc.) with the organic matter to be removed from wastewater. These bacteria consume the pollution for its own development.

##### *I.2.2.2.1. Attached and suspended growth systems*

There are mainly two families of biological processes for water treatment wastewater: fixed-film or attached growth processes (biological disks, bacterial bed and rotating biological contactors) and free culture or suspended growth processes (activated sludge and membrane biological reactors) (Duchene, 2005). Below two fixed cultures and one free culture are characterized in detail:

- Biological disks: the biomass fixed on rotating disks within the mixture to be treated is very sensitive to climatic conditions such as leaching of the biofilm by rain. This system is characterized by low operating costs and high efficiency at low loading charge.
- Bacterial or granular bed: this technique allows the degradation of organic matter by organisms naturally present in wastewater (aerobic and anaerobic bacteria) and microscopic algae. This system is characterized by low operating costs and does not require clarifier.
- Activated sludge system: is the most commonly applied biological wastewater treatment technology. It is called two-phase treatment since biomass and the wastewater in a reactor are in contact. The process is followed by a separation of solids from the purified liquid phase by decantation. Ardern and Lockett (1914) noticed that the presence of oxygen increases the bacterial activity and so, the natural degradation of organic matters. Comparable to a self-cleaning process present in the natural environment, the active biomass was called activated sludge. The basic diagram of biological treatment with activated sludge is presented in Figure I.5. This process is

composed of two main tanks: a biological reactor and a clarifier connected by a return activated sludge loop.

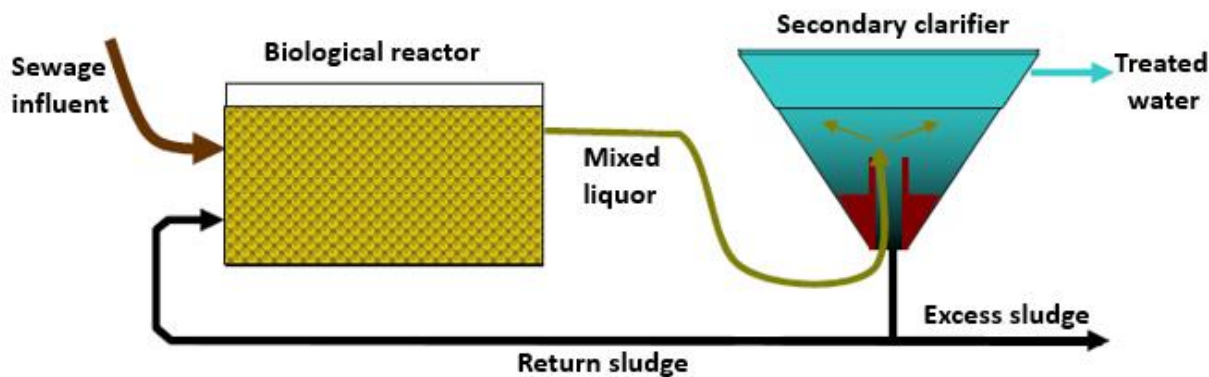


*Figure I. 5. Schematic of basic diagram of biological treatment with activated sludge (Duchene, 2005).*

The different containers as well as the unit operation are described below in details (see Figure I.5).

**Biological reactor.** It contains a mixture of a solid phase (micro-organisms, mineral matter, and debris organic) and a liquid phase containing dissolved matter. The microorganisms transform the organic biodegradable pollutions into inorganic compounds such as  $\text{CO}_2$ ,  $\text{NO}_3^-$ , and  $\text{NO}_2^-$ . Two types of organic pollution are generally encountered: macropollution (carbon, nitrogen and phosphorus) in concentration range of several hundreds of  $\text{mg L}^{-1}$ , and the micropollution reaching concentrations range of  $\text{ng L}^{-1}$   $\mu\text{g L}^{-1}$ . To eliminate the organic matter, only an aerobic zone is necessary (Figure 1.6a). However, in the case of an influent charged with nitrogen matter, two separates aerobic and anoxic phases have to be applied to eliminate this type of contaminants. In the majority of cases, an anoxic tank is placed upstream of the aerobic tank for denitrification process. The removal of oxidized nitrogen pollutants is due to the recycling of mixed liquor from the aerobic to the anoxic zone (Figure I.6b).

**Secondary clarifier.** At the reactor outlet, the mixed liquor composed of flocculated sludge starts to separate from water purified which is ready to be rejected in a natural environment. They are separated within the clarifier which has a phase separation function and a thickening function in order to bring back the most possible concentration of sludge into the biological reactor.

**Return sludge.** To maintain a constant biomass concentration in the reactor, a portion of the clarifier sludge is recycled to the reactor. Besides recycling rate, an excess sludge should be extracted in order to control the sludge age.

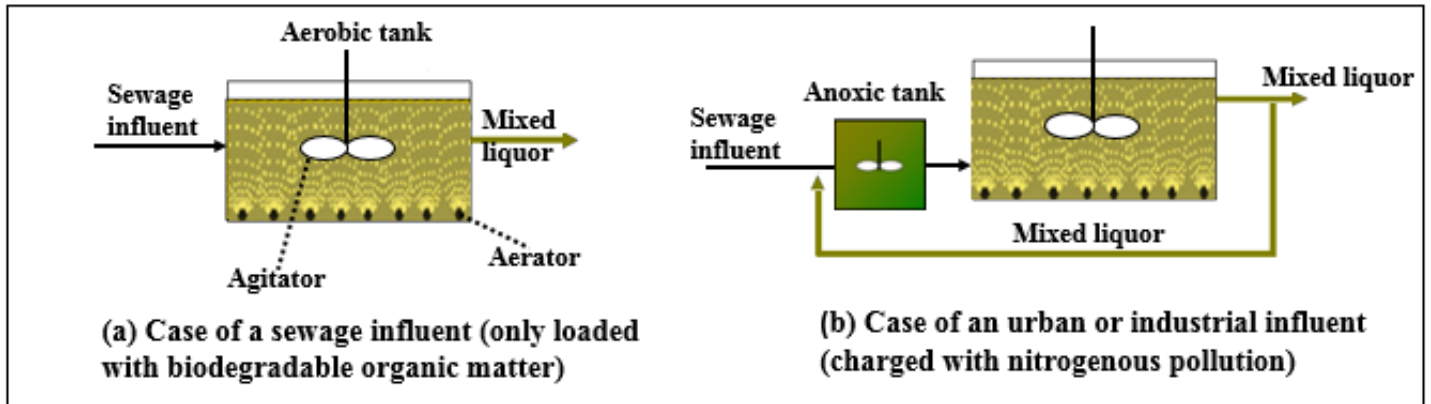


**Figure I. 6.** Reactor configuration according to the composition of the influent (adapted from Lee et al. (2017)).

#### 1.2.2.2. Optimization of some parameters to improve the removal performances

In order to estimate micropollutant emissions to receiving waters, the removal performance of WWTPs is usually assessed by the determination of biodegradation rates at lab-scale (Vieno et al., 2007; Wick et al., 2009). This estimation approach relies essentially on different operating characteristics which are defined below. They will be useful in the following chapters (II and IV).

- The massic loading rate-  $C_m$  ( $\text{kg}_{\text{BOD}_5} \text{kg}_{\text{TSS}}^{-1} \text{d}^{-1}$ ) is attributed to the loading of sludge in the reactor and corresponds to the relationship between the volumetric charge and the biomass concentration expressed by the Total Suspended Solids concentration ( $C_{\text{TSS}}$ ) in the reactor of volume  $V$  ( $\text{m}^3$ ) (Eq. I-1):

$$C_m = \frac{Q_0 \text{BOD}_5}{V C_{\text{TSS}}} \quad (\text{I-1})$$

The hydraulic retention time (HRT) represents the time required for a drop of liquid to pass through the reactor. This hydraulic characteristic of the reactor is an easily accessible parameter since it can be calculated from flow through and tank volumes using Eq. (I-2).

$$HRT = \frac{V}{Q} \quad (I-2)$$

where  $Q$  is the sum of flow rates through the reactor (inflow, recycling, addition of nutrients, etc.) ( $m^3 d^{-1}$ ).

- The sludge age (SRT)

The sludge age characterizes the mean residence time of the micro-organisms in a reactor. It represents the ratio between the mass of sludge present in the bioreactor and the extraction flow rate of sludge (Henze 2008). It can be estimated using the Eq. (I-3):

$$SRT = \frac{C_{TSS} V}{C_{TSS_{eff}} Q_{eff} + C_{TSS_w} Q_w} \quad (I-3)$$

where  $C_{TSS}$  is the Total Suspended Solids concentration in the reactor ( $g_{TSS} L^{-1}$ );  $C_{TSS_{eff}}$  is the Total Suspended Solids concentration in the effluent ( $g_{TSS} L^{-1}$ );  $Q_{eff}$  is the effluent flow rate ( $L d^{-1}$ );  $C_{TSS_w}$  is the Total Suspended Solids concentration of the withdrawn sludge ( $g_{TSS} L^{-1}$ ) and  $Q_w$  is the sludge withdrawal ( $L d^{-1}$ ).

### I.2.2.3. Micropollutants removal in conventional activated sludge systems

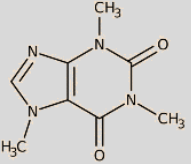
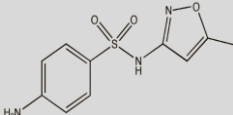
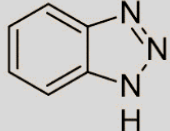
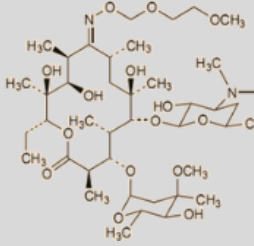
#### I.2.2.3.1. *Biological/physical-chemical properties and removal efficiencies of PPCPs*

The variation in removal efficiencies of PPCPs in WWTPs depends on (i) the degradability of the compounds, (ii) the treatment process employed and (iii) notably their physico-chemical properties such as solubility, octanol-water partition coefficient  $K_{ow}$ , and Henry's constant (Barbosa et al. 2016; Das et al. 2017). Chemical structure and some physico-chemical properties of micropollutants investigated in this work (see chapter II), were compiled in Table I.2.

The most important physico-chemical property that influence the fate of a compound during wastewater treatment is its hydrophilic/hydrophobic character. The hydrophilic compounds can remain in dissolved form in the aqueous phase of the effluent of the treatment plant, while the hydrophobic substances have the tendency to adsorb to bio-solids. Thus, these two types of compounds can reach the environment either via WWTP effluents that will be released into a

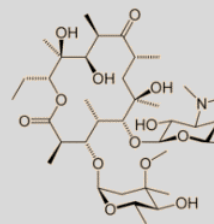
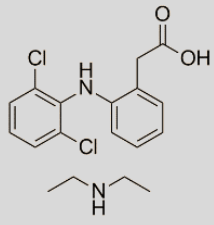
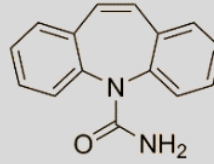
receiving surface water or with bio-solids that will be discharged into agricultural land. This connection of pharmaceuticals with bio-solids occurs due to the hydrophobic interaction of aliphatic and aromatic group, to lipid molecules of sludge or to cell membrane of microorganisms and due to electrostatic interaction of a positively charged compound to negatively charged microbes and sludge. It means sorption depends on the values of  $\log K_{ow}$  (octanol-water coefficient),  $K_d$  (sludge adsorption coefficient) and  $pK_a$  (acid dissociation constant). Compounds with high  $\log K_{ow} > 5$  and high molecular weight tend to absorb stronger than the compounds with low  $\log K_{ow} < 2.5$  (Clara et al. 2004). Sorption of most of the pharmaceutical compounds on sludge is insignificant due to their low  $K_d$  values. Ternes et al. (2004) reported that compounds with  $K_d$  values  $< 500 \text{ L kg}_{TSS}^{-1}$  will be removed by  $< 10\%$  only via sorption and the overall removal can be evaluated by comparing the influent and effluent concentrations with no information about the intermediate steps (Joss et al. 2005). From Table I.2, it is clear that sorption is a minor removal pathway for most of the pharmaceuticals. Cirja et al. (2008) reported that depending on the  $pK_a$  value, a pharmaceutical can exist in various protonation states due to pH variation, which results in changing hydrophobicity at different pH values (see sections I.2.2.4 and I.3.2.2 for more details).

Table I. 2. Physical-chemical properties and chemical structure of the target compounds which are studied in this thesis.

PPCPs	Abbreviation	Molecular weight (g mol <sup>-1</sup> )	pKa	Log <i>K<sub>ow</sub></i>	<i>K<sub>d</sub></i> (L kgSS <sup>-1</sup> )	Solubility (g L <sup>-1</sup> ) in water	Henry's constant (atm·m <sup>3</sup> mol <sup>-1</sup> )	Chemical structure
Caffeine	CAF	194.1	14.0 <sup>a</sup>	-0.07 <sup>b</sup>	-	11	1.90 10 <sup>-19</sup>	
Sulfametoxazole	SMX	253.2	7.1 <sup>c</sup>	0.48 <sup>c</sup>	200-400 <sup>c</sup>	0.459	6.42 10 <sup>-13</sup>	
Benzotriazole	BZT	119.1	8.2-8.8 <sup>e</sup>	1.23 <sup>d</sup>	220 (±9) <sup>e</sup>	19	-	
Roxithromycin	ROX	837.0	9.2 <sup>c</sup>	2.1-2.8 <sup>c</sup>	200-400 <sup>c</sup>	18.87	7.8 10 <sup>-23</sup>	

(Continued on next page)

Table I. 2. Continued

PPCPs	Abbreviation	Molecular weight (g mol <sup>-1</sup> )	pKa	Log <i>K<sub>ow</sub></i>	<i>K<sub>d</sub></i> (L kgSS <sup>-1</sup> )	Solubility (g L <sup>-1</sup> ) in water	Henry's constant (atm·m <sup>3</sup> mol <sup>-1</sup> )	Chemical structure
<b>Erythromycin</b>	ERY	733.9	8.8 <sup>c</sup>	2.48 <sup>c</sup>	160 <sup>c</sup>	0.459	2.22 10 <sup>-27</sup>	
<b>Diclofenac</b>	DCF	296.1	4.5 <sup>a,c</sup>	4.02 <sup>c</sup>	16 <sup>c</sup>	477 10 <sup>-5</sup>	4.73 10 <sup>-12</sup>	
<b>Carbamazepine</b>	CBZ	236.2	13.9 <sup>a,c</sup>	2.45 <sup>c</sup>	0.1 <sup>c</sup>	0.152	1.08 10 <sup>-10</sup>	

–: Data not available. <sup>a</sup>Ejhed et al. 2018; <sup>b</sup>Majewsky et al. 2011a; <sup>c</sup>Sipma et al. 2010; <sup>d</sup>Vasiliadou et al. 2014; <sup>e</sup>Weiss et al. 2006

- **Removal efficiencies**

Pharmaceuticals load in the wastewater produced by medical services has become source of concern because pharmaceuticals are continuously used in hospitals and health clinics (Azuma et al. 2016; Verlicchi et al. 2015, 2017). Alygizakis et al (2016) and López-Serna et al. (2013) studied the detection of pharmaceutical compounds together with their metabolites in conventional WWTP and river water receiving its effluent. Ternes (1998) noted that their removal occurs due to a combination of biodegradation and sorption pathways. Verlicchi et al. (2012) showed that conventional activated sludge systems give rise to a wide range of removal efficiencies regarding PPCPs. Among the PPCPs and some of their human metabolites, carbamazepine, ciprofloxacin, sulfamethoxazole and penicillin V are poorly removed from influent, whereas estrone, ibuprofen and naproxen are well removed (> 90 %) (Radjenovic et al. 2009; Blair et al. 2015). Carballa et al. (2004) found that the removal efficiency during the primary treatment of the 8 pharmaceuticals in municipal WWTPs was in the range of 20–50 %. However, their removal efficiency was found to be better in the activated sludge process which was varied from 30 to 70 %. Joss et al. (2004) revealed that the diclofenac removal rate is low and it is in a range of 10 and 50 %. This is attributed to a chlorine atom in their structure, which contribute to its persistence in the effluent of the WWTP. As far as the removal mechanism is concerned, there is still debate about the occurrence of biological degradation and adsorption. The study of Samaras et al. (2013) showed that biodegradation was the major removal mechanism for pharmaceutical pollutants in WWTP. However, Jelic et al. (2011) showed that the removal of 21 pharmaceutical compounds was due to the adsorption of the pharmaceuticals to the sludge. According to some authors, co-metabolic biodegradation could play a major role in the removal mechanism of micropollutants during activated sludge treatment of municipal wastewater, since the micropollutants concentrations could be too low to serve as a direct growth substrate (Xue et al. 2010). In an aerated tank the nitrification takes place and leads to the oxidation of ammonia to nitrates due to the presence of nitrifying microorganisms, which could co-metabolize the micropollutants and, thus, improve their removal from WWTPs (Margot et al. 2016). Vieno et al. (2007) assumed that the higher concentrations of carbamazepine in effluent are most likely due to enzymatic cleavage of the glucuronic conjugate of carbamazepine and release of the parent compound in the treatment plant. Gobel et al. (2007) reported a negative elimination for erythromycin and roxithromycin resulting



from an observed increase of loads from inflow to outflow of the respective treatment step. Since, the presence of conjugated metabolites is unlikely it has been hypothesized that these macrolides can be enclosed in fecal particles and then, be released to the liquid during biological treatment.

#### *1.2.2.3.2. Conventional activated sludge (CAS) vs. membrane bioreactor treatment (MBR)*

Membrane bioreactors have been evaluated in order to improve the efficiencies of removal of many types of trace organic pollutants. MBR technology combines biodegradation by activated sludge followed by a solid–liquid separation using membrane filtration (MF), usually using microfiltration or ultrafiltration. Regarding the removal of micropollutants in WWTPs, no real difference was found between CAS and MBR (Cirja et al. 2008). Although they noted that the removal rates differed from one compound to another. This can probably be attributed to the different physico-chemical properties of each pharmaceutical. Kimura et al. (2005) reported that the removal efficiency of ibuprofen and diclofenac were similar when using the both techniques. On the contrary, most of the studies pointed at higher removals in MBRs due to high SRT and biomass concentration, which contribute greater to biodegradation efficiency than CAS. Generally, CAS are operated at 1–5 g L<sup>-1</sup> of mixed liquor suspended solids (MLSS), while in MBR this concentration is much higher, ranging from 8 to ≥ 25 g L<sup>-1</sup> (Galil et al. 2003). The Table I.3 compares the removal efficiency and removal mechanism of some compounds in CAS and MBR processes. Enhanced xenobiotic removal in MBR could be achieved by the use of supporting medium which facilitate the biofilm growth and improve the micropollutant retention. Smaller flocs (10-100 μm in MBRs against 100-500 μm in CAS systems), higher specific floc surface (ten times higher in MBRs than in CAS system), and the presence of some free-living bacteria in MBRs could enhance mass transfer kinetics, and, thereby, removal efficiencies with this process. Kimura et al. (2005) showed that pharmaceuticals with a complex chemical structure, such as ketoprofen and naproxen, were not eliminated in a CAS treatment process, but could be eliminated by MBR. Snyder et al. (2007) showed that the concentrations of caffeine, sulfamethoxazole, acetaminophen, and carbamazepine, decreased in MBRs with removal efficiencies varying between 99.1 % (sulfamethoxazole) and 99.9 % (acetaminophen). In contrary, Radjenovic et al. (2009) reported that similar removal of carbamazepine was recorded by both techniques as well as slightly higher

removal efficiency of sulfamethoxazole by the MBR technology (80 %) compared to that removal by the CAS (75 %). Another study of Kim et al. (2014), presented in Table I.3, showed the same trend for carbamazepine removal which remained non-degraded by both MBR and CAS by less than 30 %. Furthermore, the study conducted by Behera et al. (2011) represented higher removal of diclofenac by the CAS (50 %) than by the MBR (32 %) as shown in Table I.3.

**Table I. 3.** Comparison of the average removal efficiency of a pharmaceuticals in conventional activated sludge process and in MBR and their removal mechanisms (Tiwari et al. 2017).

Compound	%Removal MBR	%Removal CAS	Biodegradation%	Sorption	References
Ibuprofen	99	99	90 – 100	<5	Samaras et al. 2013; Joss et al. 2006
Naproxen	94	95	55 – 85	<5	Jelic et al. 2011
Diclofenac	32	50	5 – 45	<5	Behera et al. 2011
Ketoprofen	99	50	70	0	Jelic et al. 2011
Sulfamethoxazole	81	52	50 – 90	0	Behera et al. 2011
Carbamazepine	28	<25	<40	<5	Kim et al. 2014
Mefenamic acid	63	36	55 – 58	<30	Jelic et al. 2011; Sipma et al. 2010

Moreover, in the case of highly degradable compounds, an important degradation has been observed with trace concentrations: 40 ng L<sup>-1</sup> for caffeine, 1000 ng L<sup>-1</sup> for metformin, and 90 ng L<sup>-1</sup> for acetaminophen (Blair et al. 2015), whereas, the results using MBRs did not show any significant improvements (Hai et al. 2010).

#### 1.2.2.3.3. Advanced technologies in wastewater treatment

Despite the possible ecological risk, the spread of antibacterial resistance and the threat to drinking water quality no legal limits have been established for wastewater treatment. The aforementioned removal efficiencies of WWTPs showed that pharmaceuticals are from hardly to well biodegraded,

depending on the substance. Hence, upgrading of existing WWTPs and implementing new technologies seem to be an alternative solution for enhanced MPs' removal before they enter the aquatic environment (Sudhakaran et al. 2013). These non-conventional technologies are mostly categorized into physical methods (adsorption and membrane filtration) and the advanced oxidation processes (AOPs). Adsorption on activated carbon is the widespread process adapted for sophisticated MPs' removal at low concentrations before their discharge (Alsaiee et al. 2016). As far as AOPs are concerned, the main techniques are characterized by the presence of oxidants such as hydrogen peroxide and ozone, and the use of UV light radiation. The performance of AOPs in the degradation of MPs is similarly and relatively high for all the studies (Tijani et al. 2013; Rodriguez-Narvaez et al. 2017). Being quite effective, all previous new concepts in treatment have been proven to have several disadvantages. For example, advanced adsorption does not perfectly remove micropollutants at low concentrations in water (Rodriguez-Narvaez et al. 2017). AOPs are generally expensive because of the oxidation intermediates formed during treatment by increasing energy consumption. Moreover, their high operation costs limit their use also (Grassi et al. 2013). Based on the above-mentioned restrictions, modifying existing biological treatment and identify the critical parameters affecting the removal of problematic substances of MPs during wastewater treatments seems an interesting low-cost alternative to conventional physical and chemical processes.

#### I.2.2.4. Effect of operational parameters and biomass concentration on the removal of pharmaceuticals

Physico-chemical properties such as solubility, volatility and susceptibility to photodegradation as well as the biodegradability of pharmaceuticals control the fate and removal efficiency of these micropollutants. Moreover, these efficiencies are potentially influenced by the WWTP operational parameters such as sludge retention time (SRT), hydraulic retention time (HRT),  $C_{TSS}$ , pH, and temperature.

SRT is a key operating parameter for suspended growth systems allowing the selection of a desired microbial population. A critical SRT value for the SRT at 10 °C amounting to approximately 10 days, allows an estimation of outlet concentrations and the nitrification process along biological wastewater treatment systems (Kreuzinger et al. 2004). Polesel et al. (2016) reported that the

activated sludge systems for COD removal ( $SRT \leq 5$  d) consist of single-stage aeration, whereas, biological nutrient removal (BNR) requires higher SRTs ( $\geq 8-10$  d) for the growth of nitrifying bacteria.

Additionally, SRT was hypothesized to influence pharmaceuticals removal capacity by suspended and attached biomass. Clara et al. (2005a) proposed a minimum value of 10-15 days and low effluent concentrations can be achieved in WWTPs operated at SRTs higher than 10 days. This trend is particularly true for the biodegradation of hormones, bezafibrate, and ibuprofen. If a WWTP performed with SRT below this critical value, effluent concentrations of micropollutants are expected to be in the range of influent concentrations. High SRT increases metabolic capabilities (e.g., mixed substrate growth) or microbial diversity e.g., enrichment of slowly growing autotrophic bacteria such as nitrifiers. The latest can also excrete enzymes that can possibly decompose some low degradable compounds with aromatic rings (Cirja et al. 2008). A high SRT combined with low organic load (low substrate/biomass ratio) also seems to favor biodegradation of antibiotics (Gobel et al. 2007). Lesjean et al. (2005) reported an increase removal of pharmaceutical compounds with the longer SRT of 26 days, whereas decreased removal with shorter SRT of 8 days. For a SRT of 15 days, the degradation of ketoprofen (KPF) and clofibrac acid (CFA) was about 83 % and 50 %, respectively, whereas, their removal efficiencies achieved 99 % and 82 % for a SRT of 65 days (Grandclément et al. 2017). Although, SRT has been reported as critical for pharmaceutical biodegradation, the effect of SRT for some authors does not become clear since no direct correlations between SRT and removal rates of pharmaceuticals can be found (Zhang et al. 2014). Falås et al. (2016) confirm this idea, observing no systematic relation between the SRT and the rate constants of more than 20 micropollutants with SRTs ranging from 25 to 80 days. Increasing the SRT over 30 days does not seem to improve the removal for most pharmaceuticals (Suarez et al. 2008). An explanation could be that biodegradation of micropollutants is most likely performed in a co-metabolic manner. The low concentrations of micropollutants do not likely support growth for specific microorganisms and, thus, the SRT is relevant for an efficient biodegradation of the primary substrate. On the contrary, several studies showed that the removal by sorption was only important at short SRTs (i.e. 3 days) than at higher SRTs. There are two reasons to expect that sorption in bioreactors with low SRTs will play a more important role than for bioreactors with high SRTs: (i) at low SRT the slow growing specific degraders will be washed out from the reactor system. Consequently, biodegradation is stopped

and the concentration level in the bioreactor increases, which leads to an increased sorption and (ii) a higher mass-flow of wasted biomass will contribute to an increased removal of pollutants in the sorbed phase (Jacobsen 1993; Mannina et al. 2018).

Besides SRT, a relation between HRT and biodegradation efficiency of pharmaceuticals could be expected as this defines the contact time between the pollutant and the microorganisms. The role of HRT has been highlighted by Joss et al. (2005) and Maurer et al. (2007). Although a longer HRT implies prolonged contact between wastewater and sludge and would be expected to have a positive effect on the removal of micropollutants, this has not been shown in any full-scale test of different types of WWTPs (Ejhed et al. 2018). Vieno et al. (2007) also noticed that the relationship between HRT and biodegradation rates was not straightforward for all investigated compounds, sampled in different WWTPs in Finland, with an SRT ranging from 2 to 20 days. They found that a decrease of the HRT diminishes the removal of atenolol. However, the effect was not so evident for sotalol. Contrarily, Weiss and Reemtsma (2008) found no significant effects on removal of some organic contaminants when increasing HRT from 7 to 14 h in MBR systems.

In terms of abiotic factors, Tadkaew et al. (2010) reported that the degradation of ionizable pharmaceuticals, such as ibuprofen and sulfamethoxazole, greatly depend on pH. However, the removal of non-ionizable compounds like carbamazepine is independent of pH. Cirja et al. (2008) showed that pH can affect the hydrophobicity and thus the sorption of ionizable compounds. Urase and Kikuta (2005), suggested that at a decrease of pH, lead to a better removal of various acidic pharmaceuticals electrically neutral solutes in the acidic condition. This is attributed to their high hydrophobic properties (high  $\text{LogK}_{ow}$ ) that results in higher elimination.

Depending on pH, the acid-base nature of the compound as well as the anionic or cationic forms affect the sorption process. The potential of sorption of acidic compounds (positively charged) increases for pH values higher than that of their pKa (Jones et al. 2005). Additionally, the basic compounds (negatively charged) pass more easily in octanol for pH values lower than that of their pKa, while the neutral compounds have a partition coefficient independent of the pH value (Figure I.7).

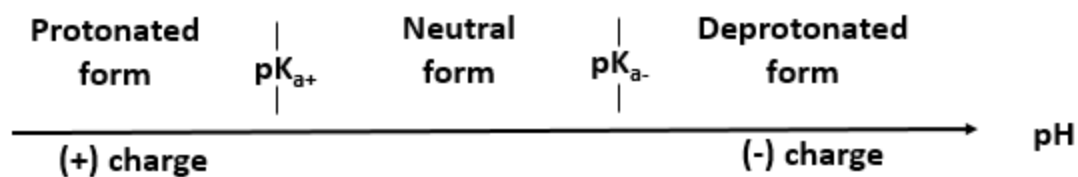


**Figure I. 7.** Schematic of the relation between pH and charge forms partition in aqueous phase.

Regarding the temperature, Joss et al. (2004) reported that it has an effect on biodegradation rates of micropollutants, but no clear effects can be drawn from the literature. Gobel et al. (2007) found no difference in pharmaceutical removal based on defined temperatures, whereas, Vieno et al. (2005) did find that temperature was responsible for variations in removal.

Beside these operational parameters, the increase of  $C_{TSS}$  raised the number of reactive sites available for the sorption phenomenon (Zhao et al. 2008). Lu et al. (2018) suggested that an increased amount of degradation bacteria is one reason for higher removal efficiencies at higher TSS concentration, i.e MBRs. Aminot et al (2018) also showed an overall increase in the biodegradation rate was measured for increasing concentrations of biomass concentrations. This tendency has been attributed to the additional bacteria brought with increasing  $C_{TSS}$  and the promoted biochemical processes involved. Regarding kinetics, the pseudo-first order expressions (see section I.3.2.3. for more details) take into account mixed liquor suspended solids (MLSS) and so differentiates between, for example, an activated sludge reactor (high MLSS) and an aerated lagoon (low MLSS).

### **I.3. Modelling of micropollutant removal in biological wastewater systems**

#### **I.3.1. State of the art**

Starting from 1950, wastewater treatment plants have been broadly studied and, more particularly, the activated sludge biological reactors, because of the different species of bacteria residing in the sludge drive the treatment cycle. To technically facilitate this procedure the residence time of the bacteria in the treatment plant is increased and their oxygen consumption is supplied by injecting pressurised air. Early examples of multimedia models ("Mackay models") were established to predict the distribution of organic contaminants in different media (air, water, soil, sediments) of

an ideal environment section (the "Unit World"; Mackay, 1979), under steady state conditions. Subsequently, the development of mathematical models that can predict the fate of MPs in WWTPs started in the 1980s, after the publication of Mackay 1979. To increase the understanding of the process, concentration-based models whether state-state or dynamic were used for fate predictions in laboratory-scale systems (Polosel et al. 2016). On one hand, in steady-state concentration-based models, analytical solutions, derived from mass balance equations, are used to predict MPs concentrations and removal efficiencies in full-scale WWTP. Steady-state generic WWTP models have been developed and applied for: (i) scenario simulations in an ideal WWTP (Byrns, 2001); (ii) model validation with measured data, following model implementation of actual design parameters from the WWTPs investigated (Cowan et al. 1993). In both cases, limited data was required in terms of model input (chemical properties, collected from literature or estimated via experiments) and of full-scale measurements (assuming steady-state WWTP operation). On other hand, dynamic fate models are sets of ordinary differential equations, describing specific process rates and overall mass balances in the systems studied. Models were calibrated to data obtained in batch (Urase and Kikuta 2005) or continuous flow experiments (Fernandez-Fontaina et al. 2014). It is important to note that the dynamic models were also applied for fate predictions in selected pilot- and full-scale WWTPs, mostly focusing on secondary treatment. Dynamic models developed, e.g., SimpleTreat (Struijs et al. 1991), WWTREAT (Cowan et al. 1993), Water9 (USEPA 1994) and TOXCHEM (Melcer et al. 1994) were calibrated to continuous pilot-scale monitoring data. These models were often developed as extension of Activated Sludge Models, thus providing a simultaneous description of conventional pollutant and MPs removal processes during wastewater treatment. The ASM1 was well received in order to describe microbial growth/mortality and substrate degradation kinetics. Monod's formulation appears in the mass balance equations of ASM1 which has the advantage of its simplicity and relatively accurate representativeness. The models have grown more complex over the years, from ASM1, including nitrogen removal processes, to ASM2, including biological phosphorus removal processes (Gujer et al. 1995) and to ASM3 including internal storage compounds, which have an important role in the metabolism of the organisms (Gujer et al. 1999). Advanced extensions of the ASM3 model to consider nitrification and denitrification phenomena have also been reported (Cruz et al. 2012). However, as many number of wastewater processes rely on low substrate concentrations, a deep understanding of constants, e.g. the affinity constant  $K_s$ , is mandatory.

Arnaldos et al. (2015) showed in his paper that different physical phenomena such as advective and diffusional transports affect obviously the value of  $K_s$ . Additionally, it has been shown that the observed  $K_s$  for some substrates will reflect transport or biological limitations more than others; but no differentiation of the appropriate model of each substrate was supposed due to the biological complexity of the system.

Related to activated sludge models, ASM-X models were created for xenobiotic organic compounds by Plosz et al. (2010). Also, Joss et al. (2006) showed that the existing biological wastewater treatment processes can remove a broad array of pharmaceuticals to a certain extent (Suarez et al. 2010; Plosz et al. 2013). More recently, full-scale dynamic models have been employed in integrated dynamic modelling tools (Vezzaro et al. 2014), simulating MPs fate at catchment scale and describing fate and transport in sewer systems, WWTPs and recipients. Generic WWTP layouts were considered using, e.g., Benchmark Simulation Model No. 1 (e.g., BSM1; Alex et al., 2008). To date, application of integrated models in WWTP catchments has been limited to realistic scenario simulations. The MP fate models currently being developed differ in the number and definition of state variables and processes. Pomiès et al. (2013) showed that the number of different micropollutant models (18) is high compared to that of macropollutant models often represented by the ASM. One of the key issues is the question of the "optimum complexity" of process models, i.e., the simplest model structure that allows solving the problem to be addressed. Although most categories of MPs have been modelled before, ( Lee et al. 1998; Byrns 2001; Dionisi et al. 2008) showed that volatile organic carbons, surfactants and priority metals (cadmium, lead and nickel) have been the most studied over the last 30 years. Polycyclic aromatic hydrocarbons (PAH), bisphenol A and some pesticides such as dieldrin, lindane, are referenced in a few models (Lee et al. 1998; Byrns 2001; Urase and Kikuta 2005; Lindblom et al. 2009). More recently, models for pharmaceutical and personal care products have appeared in the literature (Urase and Kikuta 2005; Plosz et al. 2012). Fate processes as well as process rates and relevant parameters related to aforementioned models are described in the following sections.

### I.3.2. Mechanisms of micropollutants fate and modelling concepts

The mechanisms of MPs' removal in a standard WWTP play a role according to the treatment step and the properties of each compound. It started by sorption onto solids and sedimentation during



preliminary and primary treatment. However, their removal capacity in these steps is noted to be low (Zorita et al. 2009). The overall removal of MPs can be attributed to the photolysis, hydrolysis, volatilization to air phase, sorption on (i) suspended particulates, (ii) secondary sludge and (iii) on activated carbon (post-treatment), and biological transformation called biodegradation in secondary treatment. Figure I.8 shows a schematic representation of the underlying mechanisms influencing MP removal in biological reactor. The volatilization, the sorption/desorption on the activated sludge and the biodegradation are characterized by the relevant parameters: Henry constant of the molecule, the  $K_d$  coefficient and the  $k_{biol}$ , respectively. Moreover, the fate of MPs is governed by the solubilisation which is characterised by the  $\log K_{ow}$ . In general, the removal process in the secondary sludge system is characterized by the fast sorption onto the sludge and subsequent slow biodegradation (Zhao et al. 2008), and loss through volatilization is expected to be minimal for most of the pharmaceuticals. Moreover, for the majority of pharmaceutical compounds and pesticides, sorption can be neglected because these compounds are generally hydrophilic (Pomiès et al. 2013).

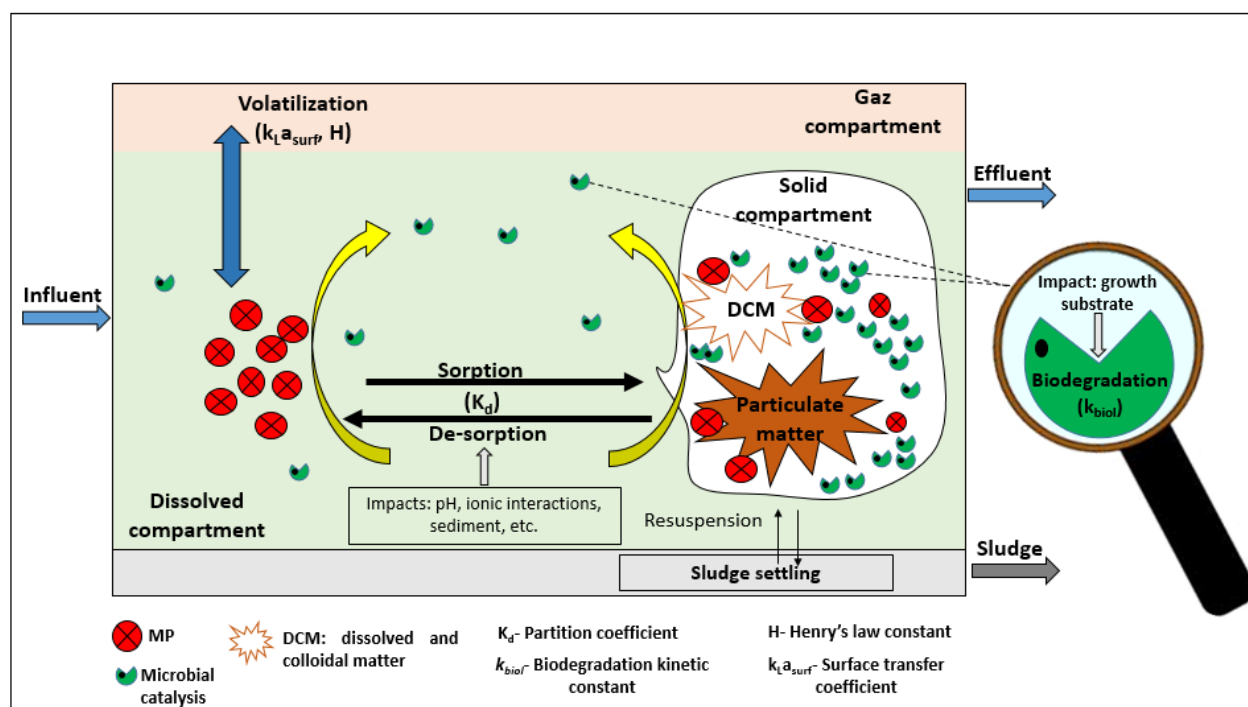


**Figure I. 8.** Scheme of the fate of a micropollutant in a biological reactor: mechanisms occurring between the different compartments (gas, dissolved, solid). Compiled based on studies by (Clouzot et al. 2013; Plosz et al. 2013; Pomiès et al. 2013).

The sorption and biodegradation processes reflect the transfers and reactions that take place in the dissolved phase and the particulate phase. Das et al. (2017) showed that the efficiency of the conventional methods in the removal of micropollutants (PPCPs assessed in this PhD thesis) do not distinguish between sorption and biodegradation. In the following, most important mechanisms and their process rates are described in details in the biological reactor.

- **Modelling fate concepts**

### I.3.2.1. Volatilization

This process depends essentially on the one and only physico-chemical property of the micropollutant, namely the Henry's law constant, and on the operating conditions of the process (i.e. temperature, aeration, atmospheric pressure and mixing). It characterizes the transfer from dissolved to gaseous phase. Most of micropollutants such as PAHs and pesticides are characterized by a very low Henry's constant ( $< 10^{-5} \text{ atm}\cdot\text{m}^3 \text{ mol}^{-1}$ ) (Lee et al. 1998). Byrns (2001) reported that their volatilization at "the surface" of the biological reactor is often not taken into account (Table I.2). The volatilization may also be due to the effect of aeration, this phenomenon is called 'stripping'. However, and according to the authors, these two phenomena are included under the term of volatilization. It can be a relevant process for some MPs in treatment coupled with high aeration rate (e.g., membrane bioreactors). Therefore, Pomiès et al. (2013) modelled this phenomenon with Eq. (I-4) between the atmosphere and the wastewater surface at equilibrium.

$$(\mathbf{r}_{MPs})_{\substack{\text{surface} \\ \text{volatilization}}} = -k_L a C_{MPs}(t) \times \frac{H'}{H' + (k_L/k_G)_{surf}} \quad (\text{I-4})$$

where  $r_{MPs}$  is the removal rate ( $\text{M L}^{-3} \text{ T}^{-1}$ ),  $H'$  is the Henry's law constant ( $\text{m}^3$  of wastewater/ $\text{m}^3$  of air);  $C_{MPs}$  is the dissolved micropollutant concentration ( $\text{M L}^{-3}$ );  $a$  is the specific interface surface area ( $\text{L}^{-1}$ );  $k_L$  is the liquid side transfer mass coefficient ( $\text{L T}^{-1}$ ) and  $k_G$  is the gas side transfer mass coefficient ( $\text{L T}^{-1}$ ).

### I.3.2.2. Sorption of lipophilic compounds onto suspended sludge

Adsorption is the attachment of a molecule to the surface of a solid phase while absorption is the entry of a molecule into a bulk (here the liquid phase). In the case of activated sludge, mainly the lipophilic compounds that undergo these two phenomena once they are in contact with the solid phase in suspension. In the secondary sludge, micropollutants can be adsorbed (i) by electrostatic interactions that occur between the positively charged groups in the MPs and the negatively charged microorganisms or (ii) due to the hydrophobic interactions between the aliphatic and aromatic groups of the micropollutants with the lipophilic cell membrane of the microorganisms. Since in this context it is difficult to study adsorption and absorption separately, we speak of a phenomenon of MP "sorption" and it is quantified by the partitioning or sorption coefficient onto  $C_{TSS}$  ( $g L^{-1}$ ), as total suspended solids concentration. It can be characterized by assuming an equilibrium state between the concentrations of the dissolved micropollutant,  $C_{MPs}$  ( $\mu g-ng L^{-1}$ ), and the solid phase,  $X_{MPs}$  ( $\mu g-ng L^{-1}$ ) and denoted as  $K_d$  as follows:

$$K_d = \frac{X_{MPs}}{C_{TSS} C_{MPs}} \quad (I-5)$$

Equilibrium partitioning can also be characterized with the ratio  $k_{Sor}/k_{Des}$ , where  $k_{Sor}$  and  $k_{Des}$  are the sorption and desorption rate coefficients, respectively (Joss et al. 2006). In this case, Ternes and Joss (2006) showed that sorption and desorption can be assumed to be in close equilibrium if the sorption substance mass flux is about 10 times higher than the biodegradation flux.

Subsequently, many studies showed that can also sorb to dissolved and colloidal matter (DCM) (Barret et al. 2010; Clouzot et al. 2013; Plosz et al. 2013, Figure I.8). However, water quality analysis often consists of filtration through a 0.45  $\mu m$  porous membrane to separate suspended solids from colloidal and soluble matter (APHA 2012). Therefore, the influence of colloids on sorption is not differentiated in most published cases.

In fact, since  $K_d$  parameter is a physico-chemical property of a micropollutant, a unique  $K_d$  value should be assumed for each micropollutant. However, the values of  $K_d$  for the same molecule can be very different according to the impact of type of sludge, ionic interactions and pH. Indeed, (Pomiès et al. 2013) reported that the other interactions than hydrophobic ones (represented by

$\log K_{ow}$ ) play an important role in sorption mechanisms, such as electrostatic interactions, cationic exchanges, cationic bridges. Several MPs, such as most of the PPCPs found in municipal wastewater, are ionic substances, i.e., anionic, cationic or zwitterionic; therefore, their partitioning behavior is affected by pH and ionic interactions (Plosz et al. 2012). One way to account for the impact of pH on partitioning behavior is to use different  $K_d$  values estimated under typical pH conditions prevailing in aerobic and anoxic reactors.  $K_d$  values of some micropollutants in activated sludge published in the literature are gathered in Table I-4.

**Table I. 4.**  $K_d$  values of some pharmaceuticals in activated sludge found in the literature.

Pharmaceutical	$K_d$ (L kgSS <sup>-1</sup> )	Reference
Benzotriazole	220	Vasiliadou et al. 2014
Bezafibrate	87	Abegglen et al. 2009
Carbamazepine	1 <1 135	Ternes et al. 2004; Fernandez-Fontaina et al. 2012; Radjenovic et al. 2009
Caffeine	50	Xue et al. 2010
Clarithromycin	1200 260	Abegglen et al. 2009; Joss et al. 2006
Codeine	14	Wick et al. 2009
Paracetamol	0.4 1160	Joss et al. 2006; Radjenovic et al. 2009
Loratidine	3321	Radjenovic et al. 2009
Diclofenac	151 118 16 32.1 <30	Hyland et al. 2012; Radjenovic et al. 2009; Joss et al. 2006; Fernandez-Fontaina et al. 2012; Ternes et al. 2004; Stevens-Garmon et al. 2011
Naproxen	13–444 16.7 <30 13	Urase and Kikuta 2005; Fernandez-Fontaina et al. 2012; Stevens-Garmon et al. 2011; Joss et al. 2006
Roxithromycin	200-400 158	Sipma et al. 2010; Joss et al. 2005
Sulfametoxazole	77 160–500 11	Radjenovic et al. 2009; Joss et al. 2005
Erythromycin	160	Sipma et al. 2010
Tetracycline	7943	Kim et al. 2005

It appears that a large variability in values of  $K_d$  is noticed especially for some pharmaceuticals such as erythromycin, ibuprofen, naproxen, sulfamethoxazole, diclofenac and carbamazepine. According to Ternes et al. (2004), their removal by sorption is insignificant since their  $K_d$  values were less than  $0.5 \text{ L kgSS}^{-1}$ . Note also that, higher  $K_d$  values up to  $1000 \text{ L kgSS}^{-1}$  were recorded in other studies (Xue et al. 2010; Urase and Kikuta 2005; Fernandez-Fontaina et al. 2012). On the contrary, the high  $K_d$  values for Loratidine, tetracycline (Sipma et al. 2010) reflect that these compounds tend to be strongly sorbed while being hardly biodegradable. We cannot speak about a "real" depollution. It means that the micropollutant has just been transferred from the water to the sludge which must then undergo a suitable posterior treatment. However, fluoroquinolone antibiotics, although their highly hydrophilic properties, are mostly removed from the aqueous phase by sorption to sludge probably through electrostatic interactions (Gobel et al. 2007; Vieno et al. 2007).

#### I.3.2.3. Biodegradation/biotransformation

In addition to previously described physical elimination pathways, the fundamental biochemical phenomenon of biotransformation/biodegradation of many pharmaceuticals contribute significantly to the removal of micropollutants at the end of a secondary treatment (Halling-Sørensen et al. 1998). The term biotransformation is applied if some end products are still organic whereas, a complete biodegradation term is used if the end products are all minerals. Biodegradation is the breakdown of complex, toxic chemical compounds into simpler, less toxic products by the action of the enzymes secreted by the microorganisms (Tiwari et al. 2017). The first discrepancy depends on the discrimination whether (i) growth substrate supports MPs biotransformation as a result of cometabolism; or (ii) strongly limiting substrate availability is beneficial for MPs biotransformation. Various studies show that organic micropollutants are most often degraded by cometabolism in WWTPs, but for some compounds it may exist microorganisms capable of degrading them directly (Pomiès et al. 2013). The presence of growth substrates can affect, i.e. improve or competitively inhibit the cometabolic MP substrate oxidation process (Polosel et al. 2016, Figure I.8). Traditionally, cometabolic biotransformation kinetics is modelled using various approaches (Chang and Alvarez-Cohen 1995) which may often become complex models since large number of kinetic parameters could complicate the modelling effort.

The cometabolic model was assessed in activated sludge WWTP for selected antibiotics (occurring in the  $< 10 \mu\text{g L}^{-1}$  range) and hydrophobic MP removal present at low concentration (Plosz et al. 2013). Some MP models consider biotransformation in both dissolved and sorbed fraction simultaneously (Lee et al. 1998; Byrns 2001; Peev et al. 2004). However, Pomiès et al. (2013) showed that highest number of models (8 of 18 models) considered that only the micropollutant in the dissolved compartment is biodegraded (Figure I.8). Delgadillo-Mirquez et al. (2011) showed that the aqueous fraction can include both the freely dissolved fraction of MPs and the fraction sorbed onto dissolved and colloidal matter.

Moreover, the major difference among all models reviewed is certainly the mathematical description of the rate of biotransformation/biodegradation. The kinetic models usually used to describe the biodegradation of micropollutants are the following. (i) Monod-based kinetic expressions with respect to  $C_{\text{MPs}}$  were considered to describe biotransformation as a growth process for the biomass (Polesel et al. 2016, Eq. I-6). (ii) This can be described using the second order kinetic expression also called pseudo-first order in literature if the  $C_{\text{MPs}}$  is significantly lower than the half-saturation coefficient (Cowan et al. 1993; Helbling et al. 2012; Monteiro and Boxall 2010; Polesel et al. 2016; Zhao et al. 2008, Eq. I-7). Nevertheless, using the assumption of negligible biomass growth (constant  $C_{\text{TSS}}$ ) during batch experiments or continuous operation, the biomass growth and transformation capacity increase linearly with the MPs concentrations. (iii) This can be described using the apparent-first-order biotransformation kinetics (Byrns 2001; Joss et al. 2006; Wick et al. 2009; Xue et al. 2010; Li and Zhang 2011; Zhao et al. 2008; Helbling et al. 2012; Min et al. 2018, Eq. I-8). (iv) Other possible micropollutants removal rate formulations on models describing the biodegradation and/or sorption of only aqueous MPs concentration are presented in Table I.5.

Table I. 5. Different models for biological degradation/and sorption of micropollutants found in the literature.

Kinetic model	Sorption	Biodegradation	Sorption+ biodegradation	Description	References
Second order			$r = \frac{-k_{biol} C_{TSS} C_{tot}}{1 + C_{TSS} K_d}$	In order to account for the instantaneous adjustment of partitioning equilibria via desorption during biodegradation. $C_{tot}$ is the total MPs concentration in water in $\mu\text{g L}^{-1}$	Andersen et al. 2005; Joss et al. 2006
Pseudo-first order/pseudo-second order			$r = -k_{biol} C_{MPs} C_{VSS}$ $r = -k_{biol} C_{MPs} X_{B,H}$	Same kinetics formulated in Eq I-7, but with biomass expressed by the volatile suspended solids concentration $C_{VSS}$ ( $\text{g L}^{-1}$ ) Same kinetics formulated in Eq I-7, but with biomass expressed by the heterotrophic biomass $X_{BH}$ ( $\text{g L}^{-1}$ )	Fernandez-Fontaina et al. 2013; Suarez et al. 2010 Majewsky et al. 2011a; Plosz et al. 2012; Sathyamoorthy et al. 2013
Pseudo-first order	$\log(X_{MPs(e)} - X_{MPs(t)}) = \log X_{MPs(e)} - \frac{k' t}{2.303}$			$X_{MPs}$ (e) and $X_{MPs}$ (t) are the sorbed MPs concentration in the solid phase and at time t, respectively and $k_2$ is the rate constant of the pseudo-second order sorption ( $\text{g mg}^{-1} \text{h}^{-1}$ ).	Al-Othamn al. 2013
Pseudo-second order		$r = k_2 (X_{MPs(e)} - X_{MPs(t)})^2$			



Cometabolic model	$r = - \left( q \frac{S}{S+K_S} \right) \frac{C_{MPs}}{C_{MPs} + K_{C_{MPs}}} C_{TSS}$	Assumption of non-limiting growth substrate availability $q$ ( $L \text{ g}^{-1} \text{ d}^{-1}$ ) defined as maximum MPs utilization rate constant in the presence of growth substrate (S).	Fernandez-Fontaina et al. 2014; Plosz et al. 2012
-	$r_{aerobic} = - [q_{C,Ox} f(S) + k_{biol, Ox} C_{MPs} \frac{S_0}{k_O + S_0}] C_{TSS}$	ASM-X $q_{C,Ox}$ and $q_{C,Axf}$ are the maximum specific cometabolic substrate biotransformation rate in the presence of growth substrate (S) for the MPs dissolved in water in aerobic and anoxic conditions, respectively. $k_O$ is the semi-saturation in oxygen	(Lee et al. 2012; Plosz et al. 2010; Pomiès et al. 2013)
-	$r_{solid} = k_{sor} C_{TSS} C_{MPs} - \frac{k_{sor}}{k_d} X_{MPs}$	$r_{water} = - (k_{biol} C_{VSS} + k_{sor} C_{TSS}) C_{MPs} + \frac{k_{sor}}{k_d} X_{MPs}$	Dynamic model Fernandez-Fontaina et al. 2013
-	$r = -k_{biol} \frac{C_{MPs}}{C_{MPs} + \left( \frac{S + K_I}{K_I} \right)} C_{TSS}$	Competitive inhibition effects on MPs biodegradation $K_I$ ( $\text{mg}_S \text{ L}^{-1}$ ) is defined as inhibition constant	Lee et al. 2012; Plosz et al. 2010; Pomiès et al. 2013

A common assumption used in all models, describing biotransformation in suspended growth systems, is that diffusion into bacterial cells is not a rate limiting process, and MPs concentration in cells equals the concentration in bulk aqueous phase (Schwarzenbach et al. 2003).

- Monod-based kinetics equation considering micropollutant biodegradation as a growing process:

$$\mathbf{r}_{\text{MPs}} = - \frac{\mu_{\text{MPs,max}}}{Y_{\text{CMPs}}} \left( \frac{C_{\text{MPs}}}{K_{\text{CMPs}} + C_{\text{MPs}}} \right) C_{\text{TSS}} \quad (\text{I-6})$$

where  $\mu_{\text{MPs,max}}$ ,  $Y_{\text{CMPs}}$  and  $K_{\text{CMPs}}$  denote the maximum growth rate to the total biomass ( $\text{d}^{-1}$ ), the conversion rate ( $\text{g}_{\text{CTSS}} \text{g}_{\text{MPs}}^{-1}$ ) and the affinity constant ( $\text{mg}_{\text{MPs}} \text{L}^{-1}$ ) for growth on micropollutants.

- Pseudo-first order kinetics equation ( $C_{\text{MPs}} \ll K_{\text{CMPs}}$ ):

$$\mathbf{r}_{\text{MPs}} = -k_{\text{biol}} C_{\text{MPs}} C_{\text{TSS}} \quad (\text{I-7})$$

where  $k_{\text{biol}}$  is the biodegradation kinetic constant in ( $\text{L g}_{\text{TSS}}^{-1} \text{d}^{-1}$ ) and equals  $\frac{\mu_{\text{MPs,max}}}{Y_{\text{CMPs}}} \left( \frac{1}{K_{\text{CMPs}}} \right)$

- Apparent-first order kinetics equation ( $C_{\text{TSS}}$  is constant):

$$\mathbf{r}_{\text{MPs}} = -k' C_{\text{MPs}} \quad (\text{I-8})$$

where  $k'$  is the removal kinetic constant in ( $\text{d}^{-1}$ ) and equals  $k_{\text{biol}} C_{\text{TSS}}$ .

The pseudo-first order kinetics model and the apparent-first order are similar;  $C_{\text{TSS}}$  is considered as a constant and including in  $k'$ . A review of biodegradation rates of some pharmaceuticals  $k_{\text{biol}}$  and  $k'$  found in scientific literature is gathered in Table I.6. Joss et al (2006) showed that three groups of micropollutants can be identified according to their  $k_{\text{biol}}$  biodegradation constant: (i) compounds with  $k_{\text{biol}} < 0.1 \text{ L g}^{-1} \text{ day}^{-1}$  are not removed in significant amounts ( $< 20 \%$ ); (ii) compounds with  $k_{\text{biol}} > 10 \text{ L g}^{-1} \text{ day}^{-1}$  are converted to more than 90 %; and (iii) for compounds with  $0.1 \text{ L g}^{-1} \text{ day}^{-1} < k_{\text{biol}} < 10 \text{ L g}^{-1} \text{ day}^{-1}$ , moderate transformation is expected. However, it remains difficult to assess exactly the contribution of each of the mechanisms mentioned above because of: (i) the great diversity of MPs and their associated physicochemical properties, (ii) the structure

and properties of the biological matrix and (iii) operational conditions such as SRT, HRT and biomass concentration.

**Table I. 6.** Values of biodegradation rates  $k_{biol}$  and  $k'$  of some pharmaceuticals in activated sludge found in the literature.

Pharmaceutical	$k_{biol}$ (L g <sub>TSS</sub> <sup>-1</sup> d <sup>-1</sup> )	Reference	$k'$ (h <sup>-1</sup> )	Reference
Benzotriazole	0.21-0.22	Mazioti et al. 2015	0.026-0.028	Mazioti et al. 2015
Bezafibrate	2.1-3.0	Joss et al. 2006	-	-
Carbamazepine	<0.1	Wick et al. 2009	0.03-0.011	Urase and Kikuta 2005
Caffeine	-	-	0.38	Xue et al. 2010
Clarithromycin	≤0.5	Joss et al. 2006;	-	-
Codeine	4.8	Wick et al. 2009	-	-
Paracetamol	58-80	Joss et al. 2006	-	-
Diclofenac	0.02 1.2 5 ≤0.1	Plosz et al. 2012; Joss et al. 2006	0.052-0.493	Urase and Kikuta 2005
Naproxen	0.2-9 0.5-4.2	Suarez et al. 2010	0.013-0.389	Urase and Kikuta 2005
Ketoprofen	-	-	0.01-0.02 0.028-0.389	Xue et al. 2010; Urase and Kikuta 2005
Naproxen	0.2-9 0.5-4.2	Suarez et al. 2010	0.013-0.389	Urase and Kikuta 2005
Roxithromycin	<0.2 0.2-9	Joss et al. 2006; Suarez et al. 2010	-	-

(Continued on the next page)

Table I. 6. Continued

Pharmaceutical	$k_{biol}$ (L g <sub>TSS</sub> <sup>-1</sup> d <sup>-1</sup> )	Reference	$k'$ (h <sup>-1</sup> )	Reference
Sulfametoxazole	0.3 5.9–7.6	Suarez et al. 2010; Joss et al. 2006	-	-
Erythromycin			0.11	Xue et al. 2010
Tetracycline	0.44	Plosz et al. 2010	-	-

#### I.4. Hydrodynamics

Besides the kinetics aspect studied previously, the reactor modelling also requires the consideration of the hydrodynamics aspect being treated as the transport of the liquids (and possibly gas and solids) in the reactor. Over the last seventy years, the influence of hydrodynamics on reactor yields was shown thanks to the coupling of kinetics and hydrodynamics (Le Moullec et al. 2008; Lesage et al. 2003; Levenspiel 1972; Potier et al. 2005; Rehman 2014, 2017; Villermeaux 1982). In order to model the effect of the hydrodynamic on biological/biochemical reactions, the description of the reactor has a critical importance to obtain representative process dynamics. Development of a hydrodynamical model of a reactor requires careful consideration with respect to the number of phases and their description, the reactor geometry, the spatial resolution of the numerical domain, the conditions applied (i.e. gas and liquid flow rates), in addition to the discretization and solution techniques used to characterize the hydrodynamics. In recent years a whole new perspective to this field of research was provided by modelling the hydrodynamics of WWTPs by the application of different approaches detailed in the following section.

##### I.4.1. Different hydrodynamics approaches

In the second half of the 20<sup>th</sup> century, the systemic approach came from work in cybernetics and formalized by Danckwerts (1953); Dudukovic (2010); Villermaux (1982) and von Bertalanffy (1968). The systemic approach observes and analyzes the problems globally in their entirety

without necessarily trying to understand the functioning of the sub-systems one by one. The reactor is seen through its inputs and outputs and is modeled globally. Afterwards, other processes were added such as thermodynamics, kinetics, transfers of mass and heat. The notion of residence time distribution (RTD, Danckwerts 1953) allowed the development of the systemic modelling of the reactor hydrodynamics. Chemical Reaction Engineering (CRE) was then created by the association of systemic modelling of hydrodynamics, kinetics, etc. One of the limitations of the systemic approach to process engineering lies in the difficulty of linking, in principle, the overall operation of the reactor to its geometrical characteristics, below a certain scale. Thus, to overcome this limitation, researchers and engineers in chemical engineering used the computational fluid dynamics (CFD) method to solve additional physical phenomena (Gresch et al. 2011, Laurent et al. 2015, Nopens et al. 2015). The 2000s have seen the development of CFD with reaction applied to wastewater reactor. Currently, the systemic approach and the CFD are commonly used; each of these two approaches has its advantages and disadvantages; systemic: global, rapid, proven and easy to use in CRE to optimize the reactor design; CFD: precise, long computational time, and not easy to use in global optimization of design but very useful to optimize local process. A third methodology: the compartmental modelling, is in between for each characteristic; it is notably useful to model and design very large processes (Jourdan et al. 2019). The models obtained by this approach allow to combine more comprehensive results than the systemic approach without requiring as much computing time as the CFD approach. Table I-7 summarizes most of the characteristics of the three aforementioned modelling approaches (Le Moullec 2008). However, in this work since we need only global reactor design trend, the systemic approach is taken into consideration.

**Table I. 7.** Summary of the characteristics of different modelling approaches by Le Moullec (2008).

Modelling	Systemic	CFD	Compartmental
Scientific background			
Approach	Based on experimental observations	Based on phenomenological equations	Based on both experimental observations and phenomenological equations
Structure of the model			
Simplicity	Relatively simple	Complex	Relatively simple
Adjustable parameters	Limited in numbers	Equations of transport and the parameters of the models	Some for the model itself, like the CFD for the design of the model structure
Number of sub models	Limited : kinetic, oxygen transfer	Turbulence, bubble shapes, forces, oxygen transfer, etc.	
Preliminary work			
Experimental research	Some tracing experiments needed	Many physicochemical constants to be determined	Same as for CFD
Tool design	Simple algorithm, fast programming	Very complex programming replaced by the handling of the software quite long	Relatively simple algorithm and fast programming
Preparation and calculation time			
Preparation time	Relatively short: experience of tracing and programming (2 to 4 days)	Long: bibliography, tests and validation experiments, adjustment of adjustable parameters (2 months)	Long: same as for CFD + programming time (CFD+4 days)
Calculation time	Very short	Long-very long	Short

(Continued on next page)

Table I.7 Continued

Modelling	Systemic	CFD	Compartmental
Technical and economic analysis			
Use	Optimization, comparison, understanding	Understanding, design, comparison	Design, optimization, comparison
Cost	Low on pilot reactor High on industrial reactor	Relatively high (software + working time)	Same as for CFD, can be reduced with the help of the systemic model

In the field of chemical engineering, the chemical reaction engineering has been well developed in order to study the reactions that produce desired products as well as to optimize the design of the necessary reactors accordingly. The optimization of a plant can be related to economy purpose by using adapted configurations in order to either minimize operating costs or to maximize the conversion rates or, yet again, to occupy less space.

#### I.4.2. Systemic modelling approach

In systemic model, there are a few basic elements (or basic reactors) that can be used alone or in a more or less complex networks (parallel, series, etc...). These elements are mainly the continuously stirred tank reactor (CSTRs), the plug flow reactor (PFR), and the plug flow reactor with axial dispersion. The simplest is the continuously stirred tank reactor (CSTR). It consists of a well-mixed tank with inlet and outlet (Figure I.9a). In the case of continuous operation, the perfect mixing gives rise to a large distribution of the residence time of the elements: some can leave the system quickly (like short circuit), others stay very long (as a result of recirculation), and residence times mainly range from zero to 5 times HRT. Plug Flow Reactor (PFR) is presented in Figure I.9b. Fluid going through a PFR may be modeled as flowing through the reactor as a series of coherent sections (A) for infinite thickness ( $\Delta x$ ). The flow is characterized by the fact that all elements in a straight section progress at the same rate. The residence time is identical for all the elements and the composition changes along the reactor: in this way we obtain a very uniform

treatment of the fluid. A PFR is assumed to be perfectly mixed radially. In an ideal PFR, there is no dispersion of the reactants and products (Levenspiel 1999). In practice, some real reactors can have hydrodynamics close to CSTR, but PFR are impossible; there are only approximation of some very long real reactor.

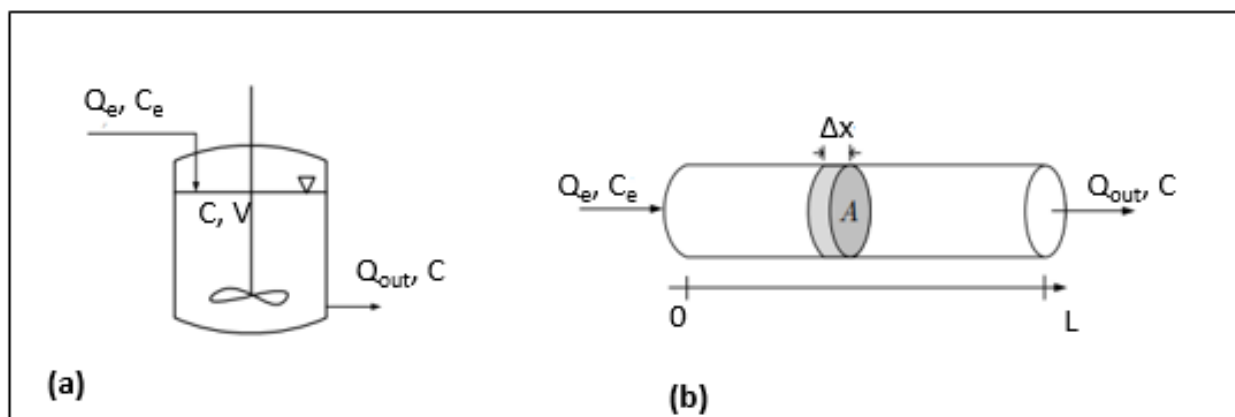


**Figure I. 9.** Scheme of a continuous stirred tank reactor (CSTR) (a) and a plug-flow reactor (PFR) (b) (Levenspiel 1999).

It should be emphasized that generally PFR exhibit better performances than CSTR. It is important to mention that the term ‘better’ means that the volume of a PFR will be smaller than a well-mixed reactor in order to obtain a given conversion rate. In other words, a shorter residence time will be needed if one uses a PFR instead of a CSTR for identical steady-state performance requirements. However, the PFR technology suffers from a number of drawbacks which have been known for a long time and have been extensively studied since the end of the 1950s, in particular in the field of catalytic chemical reactions.

A deviation from the two ideal models can be caused by many factors such as recycling, fluid channeling, creation of dead zones, geometrical changes inside the reactor or by a combination of all these factors (Renuka 2015). A number of investigators have studied the optimal design of continuously stirred tank reactors in series in the last 50 years (De Clercq et al. 1999; Harmand and Dochain 2005, Levenspiel 1972) in order to describe the hydrodynamics in various wastewater treatment units. Others noticed the combination of stirred tank and tubular reactors in most practical industrial situations (Aris 1962). Further complex behaviors of flow were detected by the



presence of anomalies within the reactors, such as dead zones and short circuits, which can reduce the efficiency of these units (Cholette et al. 1960; Dias et al. 2018; Khalekuzzaman et al. 2018). The PFR cannot represent aerated reactors of wastewater treatment plant, even very long ones (Potier et al. 2005). However, another model can be used: the plug flow reactor with axial dispersion (axial dispersion model or ADM). Hydrodynamics of CSTR is characterized by the number of reactors (J). PFR with axial dispersion is characterized by the Peclet number:

$$P_e = \frac{uL}{D} \quad (\text{I-9})$$

where  $u$  is the average longitudinal velocity of the liquid phase inside the reactor ( $\text{m s}^{-1}$ ),  $D$  is the axial dispersion coefficient ( $\text{m}^2 \text{s}^{-1}$ ) and  $L$  is the reactor length (m).

(Potier et al. 2005; Villermieux 1982):

There is similarity between the two models and their RTD curves. There is a relation between  $J$  and  $Pe$

$$P_e \# 2(J - 1) \quad (\text{I-10})$$

The effect of the hydrodynamics on the reaction yields has particular practical as well as theoretical interests in both chemical and biological engineering fields (Levenspiel and Smith 1995). The principle being that some reactors, because of their hydrodynamics, can create concentration gradients. Such gradients locally induce high concentrations, and so, the rate of the reaction will be also increased. This reasoning is true for reaction kinetics of order greater than zero. For example, the conversion rate for first order kinetics, is expressed as a function of the hydraulic retention time (Equations I-11 and I-12). These expressions show that the CSTR is less efficient than the PFR for the same hydraulic retention time.

$$X_{CSTR} = \frac{\tau k}{1 + \tau k} \quad (\text{First order}) \quad (\text{I-11})$$

$$X_{PFR} = 1 - e^{-\tau k} \quad (\text{First order}) \quad (\text{I-12})$$

where  $X_{CSTR}$  is the conversion rate for a perfectly continuous stirred tank reactor and  $X_{PFR}$  is the conversion rate for Plug Flow Reactor,  $k$  is the rate constant and  $\tau$  is the hydraulic retention time.

#### I.4.3. Impact of hydrodynamic reactor configuration on MPs removal

Hydrodynamic performance of a biological reactor is an important design concern since it directly affects the water treatment efficiency. Many models based on basic elements such as CSTR, tubular reactor or closed-loop reactor, mixer and decanter offer simple modelling tools for wastewater treatment plant. Such basic hydrodynamic takes into consideration the number of reactors, the operation in anoxic or in aerobic conditions, and the multiple recycling. Szpyrkowicz (2006) showed that the hydrodynamic conditions such as mixing in the reactor for treatment of industrial wastewater can affect the differential selectivity of the removal of pollutants and this can be used for optimizing the performance of the reactor with respect to a target pollutant. Meister et al. (2017) reported that whilst the original ASM1 was further developed during the past 30 years, a common approximation of the hydraulics based on fully mixed units of reactors connected in series remains as the established concept. Some studies such as of Renuka et al. (2016) showed that the mixing behaviour of an anaerobic baffled reactor (ABR) was intermediate between plug flow and completely mixed and so, improve the treatment performance in terms of chemical oxygen demand removal. Rodriguez-Gomez et al. (2014) showed that the Upflow Anaerobic Sludge Blanket (UASB) reactor viewed as several continuous stirred tank reactors connected in series, is able to well predict the performance of the substrate concentration, biomass concentration, granule size, and height of the sludge bed. However, few studies have been done on the improving of the reactor configurations in order to increase the rate of removal of micropollutants from wastewater treatment plants. Applying this approach, the effect of hydrodynamics on the degradation of micropollutants has been studied through the simulation of the extreme CSTR and PFR cases (Joss et al. 2006). Moreover, Majewsky et al. (2011b) developed a modelling approach to estimate xenobiotic removal efficiencies from monitoring data taking the hydraulic RTD in WWTPs into consideration by using a completely mixed tanks-in-series.

## **I.5. Conclusion of chapter I and objectives of the thesis**

The bibliographic study shows the problematic of wastewater treatment with activated sludge, as well as a description of types of kinetics models of MPs' removal that exist and their modelling concepts. Removal mechanisms are not fully identified and there is a lack of available information on the effect of operational parameters on the MP's removal. The variety of models proposed in the literature to describe MPs' removal in activated sludge indicates that there is presently no consensus between authors, as they use various concepts to model micropollutants' fate in a WWTP. Therefore, the choice of the optimal operation conditions of a WWTP, the appropriate kinetic model of removal as well as the best hydrodynamic configuration(s) seem to be the key points of this study for better MPs' removal.

The major objective of this research is to define the conditions that can enhance MPs' removal and to develop a simulation able to find better hydrodynamic configuration(s) of biological reactor to improve the removal of different classes of MPs present in wastewater. In order to achieve this goal, an experimental approach was used and presented in chapter II to evaluate the removal kinetics for a group of investigated micropollutants taking into account the effect of different operational parameters such as SRT, HRT and biomass concentration. The influence of the biomass concentration on the kinetics of MPs' removal is dedicated to chapter III, with development of a new kinetic model.

Furthermore, the implementation of such kinetic modelling approaches in digital simulation tools dedicated to removal of micropollutants with activated sludge is the key of kinetics-hydrodynamics relation. Thus, we evaluated the extension of the ASM1- MPs integrating the appropriate kinetics to describe removal of some investigated MPs in chapter IV. Numerical predictions were estimated for different hydrodynamics of continuous system in the same chapter. Various cascades of different numbers of CSTRs up to 100 were tested in order to minimize the concentrations of MPs released into the environment. Subsequently, a new reactor hydrodynamic configuration was proposed.

## I.6. References of chapter I

- Abegglen, C., Joss, A. McArdell, C.S., Fink, G. Schlüsener, M.P., Ternes, T.A., Siegrist, H., 2009. The fate of selected micropollutants in a single-house MBR. *Water Research* 43, 2036–46.
- Alex, J., Benedetti, L., Copp, J., Gernaey, K.V., Jeppsson, U., Nopens, I., Pons, M.-N., Rieger, L., Rosen, C., Steyer, J.P., Vanrolleghem, P., Winkler, S., 2008. Benchmark Simulation Model No. 1 (BSM1). *Industrial Electrical Engineering and Automation*. Dept. of Industrial Electrical Engineering and Automation, Lund University.
- AL-Othman, Z.A., Ali, R., Naushad, M., 2012. Hexavalent chromium removal from aqueous medium by activated carbon prepared from peanut shell: adsorption kinetics, equilibrium and thermodynamic studies. *Chemical Engineering Journal* 184, 238–47.
- Al Aukidy, M., Verlicchi, P., Jelic, A., Petrovic M., Barcelò D., 2012. Monitoring release of pharmaceutical compounds: occurrence and environmental risk assessment of two WWTP effluents and their receiving bodies in the Po Valley, Italy. *Science of The Total Environment*, 438, 15–25.
- Isbaiee, A., Smith, B.J., Xiao, L., Ling, Y., Helbling, D.E., Dichtel, W.R., 2016. Rapid removal of organic micropollutants from water by a porous  $\beta$ -Cyclodextrin polymer. *Nature*, 529, 190–94.
- Alygizakis, N.A., Gago-Ferrero, P., Borova, V.L., Pavlidou, A., Hatzianestis, I., Thomaidis, N.S., 2016. Occurrence and spatial distribution of 158 pharmaceuticals, drugs of abuse and related metabolites in offshore seawater.” *Science of The Total Environment*, 541, 1097–1105.
- Aminot, Y., Fuster, Pardon, L.P., Le Menach, K., Budzinski, H., 2018. Suspended solids moderate the degradation and sorption of waste water-derived pharmaceuticals in estuarine waters. *Science of The Total Environment*, 612, 39–48.
- Amiri, S., Mazaheri, M., Samani, J.M.V., 2019. Introducing a general framework for pollution source identification in surface water resources (theory and application). *Journal of Environmental Management*, 248, 109-281.
- Andersen, H.R., Hansen, M., Kjølholt, J., Stuer-Lauridsen, F., Ternes, T., Halling-Sørensen, B., 2005. Assessment of the importance of sorption for steroid estrogens removal during activated sludge treatment. *Chemosphere*, 61, 139–146.

- Ardern, E., Lockett, W.T., 1914. Experiments on the oxidation of sewage without the aid of filters. *Journal of the Society of Chemical Industry*, 33, 523–39.
- Aris, R., 1962. On optimal adiabatic reactors of combined types. *Canadian Journal of Chemical Engineering*, 40, 87–92.
- Arnaldos, M., Amerlinck, Y., Rehman, U., Maere, T., Van Hoey, S., Naessens, W., Nopens, I., 2015. From the affinity constant to the half-saturation index: Understanding conventional modelling concepts in novel wastewater treatment processes. *Water Research*, 70, 458–70.
- Azuma, T., Arima, N., Tsukada, A., Hiram, S., Matsuoka, R., Moriwake, R., Ishiuchi, H., 2016. Detection of pharmaceuticals and phytochemicals together with their metabolites in hospital effluents in Japan, and their contribution to sewage treatment plant influents. *Science of The Total Environment*, 548–549, 189–97.
- Barbosa, O., Moreira, F., Ribeiro, R., Pereira R., and Silva, T., 2016. Occurrence and removal of organic micropollutants: an overview of the watch list of EU Decision 2015/495. *Water Research*, 94, 257–79.
- Barret, M., Carrère, H., Latrille, E., Wisniewski, C, Patureau, D., 2010. Micropollutant and sludge characterization for modelling sorption equilibria. *Environmental Science & Technology*, 44, 1100–1106.
- Behera, K., Kim, H., Oh, J., and Park, H., 2011. Occurrence and removal of antibiotics, hormones and several other pharmaceuticals in wastewater treatment plants of the largest industrial city of Korea. *Science of the Total Environment*, 409, 4351–4360.
- Blair, B., Crago, J., Hedman, C., and Klaper R., 2013. Pharmaceuticals and Personal Care Products found in the great lakes above concentrations of environmental concern. *Chemosphere*, 93, 2116–23.
- Blair, B., Nicolaus, A., Hedman, C., Klaper R., and Grundl, T., 2015. Evaluating the degradation, sorption, and negative mass balances of pharmaceuticals and Personal Care Products during wastewater treatment. *Chemosphere*, 134, 395–401.
- Brusseau, M.L., Artiola, J.F., 2019. Chemical contaminants. *Environmental and Pollution Science*, 175–90.
- Byrns, G., 2001. The fate of xenobiotic organic compounds in wastewater treatment plants. *Water Research*, 35, 2523–2533.

- Carballa, M., Omil, F., Lema, J.M., Llompart, M., García-Jares, C., Rodríguez, I., Gomez, M., and Ternes T., 2004. Behavior of pharmaceuticals, cosmetics and hormones in a sewage treatment plant. *Water Research*, 38, 2918–2926.
- Chang, H-L., Alvarez-Cohen, L., 1995. Model for the cometabolic biodegradation of chlorinated organics. *Environmental Science & Technology*, 29, 2357–67.
- Cholette, A., Blanchet, J., Cloutier, L., 1960. Performance of flow reactors at various levels of mixing. *The Canadian Journal of Chemical Engineering*, 38, 1–18.
- Cirja, M., Ivashechkin, P., Schaffer, A., Corvini, P.F.X., 2008. Factors affecting the removal of organic micropollutants from wastewater in conventional treatment plants (CTP) and membrane bioreactors (MBR). *Reviews in Environmental Science and Bio/Technology*, 7, 61–78.
- Clara, M., Kreuzinger, N., Strenn, B., Gans, O., and Kroiss, H., 2005a. The solids retention time—a suitable design parameter to evaluate the capacity of wastewater treatment plants to remove micropollutants. *Water Research*, 39, 97–106.
- Clara, M., Strenn, B., Gans, O., Martinez, E., Kreuzinger, N., and Kroiss, H., 2005b. Removal of selected pharmaceuticals, fragrances and endocrine disrupting compounds in a membrane bioreactor and conventional wastewater treatment plants. *Water Research*, 39, 4797–4807.
- Clouzot, L., Choubert, J.M., Cloutier, F., Goel, R., Love, N.G., Melcer, H., Ort, C., 2013. Perspectives on modelling micropollutants in wastewater treatment plants. *Water Science and Technology*, 68, 448–61.
- Cowan, C., Larson, R., Feijtel, T., and Rapaport, R., 1993. An improved model for predicting the fate of consumer product chemicals in wastewater treatment plants. *Water Research*, 27, 561–73.
- Cruz, N.M., Hooshier, K., Arellano-Garcia, H., Wozny, G., Lyberatos, G., 2013. Model based optimization of the intermittent aeration profile for SBRs under partial nitrification. *Water Research*, 47, 3399–3410.
- Dankwerts. 1953. Continuous flow systems. *Chemical Engineering Science*, 2,1–13.
- Das, S., Ray, N.M., Wan, J., Khan, A., Chakraborty, T., Ray, M.B., 2017. Micropollutants in wastewater: fate and removal processes. In *physico-chemical wastewater treatment and resource recovery*, edited by Robina Farooq and Zaki Ahmad. InTech.

- Daughton, C G., 2006. Pharmaceuticals in the Environment: overview of significance, concerns, and solution. Invited keynote presentation for pharmaceuticals in the environment, webinar series organized by the EPA national regional science council's PPCPs (<Http://Www.Epa.Gov/Esd/Bios/Daughton/Acs-Extend.Pdf>.)
- Daughton, C.G., Ternes, T., 1999. Pharmaceuticals and personal care products in the environment: agents of subtle change? *Environmental health perspectives*, 107, 907–38.
- De Clercq, B., Coen, F., Vanderhaegen, B., Vanrolleghem, P.A., 1999. Calibrating simple models for mixing and flow propagation in waste water treatment plants. *Water Science and Technology*, 39.
- Delgadillo-Mirquez, L., Lardon, L., Steyer, J.P., Patureau, D., 2011. A new dynamic model for bioavailability and cometabolism of micropollutants during anaerobic digestion. *Water Research*, 45, 4511–21.
- Degremont, 1991. *Water Treatment Handbook*, sixth Ed. Lavoisier, Paris.
- Dionisi, D., Bornoroni, L., Mainelli, S., Majone, M., Pagnanelli, F., Papini, M.P., 2008. Theoretical and experimental Analysis of the Role of Sludge Age on the Removal of Adsorbed Micropollutants in activated sludge processes. *Industrial & Engineering Chemistry Research*, 47, 6775–82.
- Directive, 2000. 2000/60/EC of the European Parliament and of the Council of 23 October 2000. Establishing a framework for community action in the field of water policy. *Off. J. Eur. Commun*, 327, 1-72.
- Directive, 2013. 2013/39/EU of the European Parliament and of the Council of 12 August 2013. Amending Directives 2000/60/EC and 2008/105/EC as regards priority substances in the field of water policy. *Off. J. Eur. Union L226*, 1-17.
- Duchene, P. 2005. Cent Ans de procédés d'épuration des eaux résiduaires. *Techniques, sciences et méthodes*, 11, 35-44.
- EEA Report No 7/2018. 2018. *European Waters - Assessment of status and pressures 2018*. European Environment Agency.
- Ejhed, H., Fång, J., Hansen, K., Graae, L., Rahmberg, M., Magnér, J., Dorgeloh, E., Plaza, G., 2018. The effect of hydraulic retention time in onsite wastewater treatment and removal of pharmaceuticals, hormones and phenolic utility substances. *Science of The Total Environment*, 618, 250–61.

- Esplugas, S., Bila, D., Krause, L., and Dezotti, M., 2007. Ozonation and advanced oxidation technologies to remove endocrine disrupting chemicals (EDCs) and pharmaceuticals and personal Care Products (PPCPs) in water effluents. *Journal of Hazardous Materials*, 149, 631–42.
- EU, 2008, Directive 2008/105/EC of the European Parliament and of the Council of 16 December 2008 on environmental quality standards in the field of water policy, amending and subsequently repealing Council Directives 82/176/EEC, 83/513/EEC, 84/156/ EEC, 84/491/EEC, 86/280/EEC and amending Directive 2000/60/EC of the European Parliament and of the Council
- EU, 2013, Directive 2013/39/EU of the European Parliament and of the Council of 12 August 2013 amending Directives 2000/60/EC and 2008/105/EC as regards priority substances in the field of water policy (OJ L 226, 24.8.2013, p. 1-17).
- Evans, A.E.V., Mateo-Sagasta, J., Qadir, M., Boelee, E., Ippolito, A., 2019. Agricultural water pollution: key knowledge gaps and research needs. *Current Opinion in Environmental Sustainability*, 36, 20–27.
- Fairbairn, D., Karpuzcu, M., Arnold, W., Barber, B., Kaufenberg, E., Koskinen, W., Novak, P., Rice, P., Swackhamer, D., 2016. Sources and transport of contaminants of emerging concern: A two-year study of occurrence and spatiotemporal variation in a mixed land use watershed. *Science of The Total Environment*, 551–552, 605–13.
- Falås, P., Wick, A., Castronovo, S., Habermacher, J., Ternes, T., Joss, A., 2016. Tracing the limits of organic micropollutant removal in biological wastewater treatment. *Water Research*, 95, 240–49.
- Feng, L., van Hullebusch, E.D., Rodrigo, M.A., Esposito, G., Oturan, M.A., 2013. Removal of residual anti-inflammatory and analgesic pharmaceuticals from aqueous systems by electrochemical advanced oxidation processes. A review. *Chemical Engineering Journal*, 228, 944–64.
- Fernandez-Fontaina, E., Carballa, M., Omil, F., Lema, J.M., 2014. Modelling cometabolic biotransformation of organic micropollutants in nitrifying reactors. *Water Research*, 65, 371–83.



- Fernandez-Fontaina, E., Omil, F., Lema, J.M., and Carballa, M., 2012. Influence of nitrifying conditions on the biodegradation and sorption of emerging micropollutants. *Water Research*, 46, 5434–44.
- Fernandez-Fontaina, E., Pinho, I., Carballa, M., Omil, F., Lema, J.M., 2013. Biodegradation kinetic constants and sorption coefficients of micropollutants in membrane bioreactors. *Biodegradation*, 24, 165–77.
- Galil, N.I., Sheindorf, C., Stahl, N., Tenenbaum, A., Levinsky, Y., 2003. Membrane bioreactors for final treatment of wastewater. *Water Science and Technology*, 48, 103–10.
- Gandiglio, M., Lanzini, A., Soto, A., Leone, P., Santarelli, M., 2017. Enhancing the energy efficiency of wastewater treatment plants through co-digestion and fuel cell systems. *Frontiers in Environmental Science*, 5, 70.
- Gobel, A., Mcardell, C., Joss, A., Siegrist, H., and Giger, W., 2007. Fate of sulfonamides, macrolides, and trimethoprim in different wastewater treatment technologies. *Science of The Total Environment*, 372, 361–71.
- Gracia-Lor, E., Sancho, J., Serrano, R., and Hernández, F., 2012. Occurrence and removal of pharmaceuticals in wastewater treatment plants at the Spanish mediterranean area of Valencia. *Chemosphere*, 87, 453–62.
- Grandclément, C., Seyssiecq, I., Piram, A., Wong-Wah-Chung, P., Vanot, G., Nicolas, R., Tiliacos, N., Doumenq, P., 2017. From the conventional biological wastewater treatment to hybrid processes, the evaluation of organic micropollutant removal: A Review. *Water Research*, 111, 297–317.
- Grassi, M., Rizzo, L., Farina, A., 2013. Endocrine disruptors compounds, pharmaceuticals and personal care products in urban wastewater: implications for agricultural reuse and their removal by adsorption process. *Environmental Science and Pollution Research*, 20, 3616–28.
- Gresch, M., Armbruster, M., Braun, D., Gujer, W., 2011. Effects of aeration patterns on the flow field in wastewater aeration tanks. *Water Research*, 45, 810–18.
- Gujer, W., Henze, M., Mino, T., van Loosdrecht, M., 1999. Activated Sludge Model No. 3. *Water Science and Technology*, 39, 1.

- Gujer, W., Henze, M., Mino, T., Matsuo, T., Wentzel, M.C., Marais, G.V.R., 1995. The Activated Sludge Model No. 2: Biological Phosphorus Removal. *Water Science and Technology*, 31 2.
- Gwenzi, W., Dunjana, N., Pisa, C., Tauro, T., Nyamadzawo, G., 2015. Water quality and public health risks associated with roof rainwater harvesting systems for potable supply: review and perspectives. *Sustainability of Water Quality and Ecology*, 6, 107–18.
- Hai, F., Yamamoto, K., Nakajima, F., and Fukushi, K., 2010. Chem In form Abstract: Recalcitrant industrial wastewater treatment by membrane bioreactor (MBR). *ChemInform*, 42, 33.
- Halling-Sørensen, B., Nielsen, S., Lanzky, N., Ingerslev, P.F., Lützhøft, F., Holten, H.C., Jørgensen, S. E., 1998. Occurrence, fate and effects of pharmaceutical substances in the environment-A Review. *Chemosphere*, 36, 357–393.
- Hanslmeier, A., 2010. *Water in the universe. Astrophysics and space science library*, vol. 368. Dordrecht ; New York: Springer.
- Harmand, J., and Dochain, D., 2005. The optimal design of two interconnected (Bio)chemical reactors revisited. *Computers & Chemical Engineering*, 30, 70–82
- Helbling, D.E., Johnson, D.R., Honti, M., Fenner, K., 2012. Micropollutant biotransformation kinetics associate with WWTP process parameters and microbial community characteristics. *Environmental Science & Technology*, 46, 10579–88.
- Henze, M., 2008. *Biological wastewater treatment: principles, modelling and design*. London: IWA Pub.
- Huang, H., Wu, J., Ye, J., Ye, T., Deng, J., Liang, Y., Liu, W., 2018. Occurrence, removal, and environmental risks of pharmaceuticals in wastewater treatment plants in south China.” *Frontiers of Environmental Science & Engineering*, 12, 6.
- Hyland, K., Dickenson, E., Drewes, J., Higgins, C., 2012. Sorption of ionized and neutral emerging trace organic compounds onto activated sludge from different wastewater treatment configurations. *Water Research*, 46, 1958–68.
- Jacobsen, B., 1993. Removal of organic micropollutants in laboratory activated sludge reactors under various operating conditions: sorption. *Water Research*, 27, 1505–10.
- Janex-Habibi, M.L., Huyard, A., Esperanza, M., and Bruchet, A., 2009. Reduction of endocrine disruptor emissions in the environment: The benefit of wastewater treatment. *Water Research*, 43, 1565–76.

- Jelic, Aleksandra, Meritxell Gros, Antoni Ginebreda, Raquel Cespedes-Sánchez, Francesc Ventura, Mira Petrovic, Damia Barcelo., 2011. "Occurrence, Partition and Removal of Pharmaceuticals in Sewage Water and Sludge during Wastewater Treatment." *Water Research*, 45, 1165–1176.
- Jelic, A., Gros, M., Petrović, M., Ginebreda, M., Barceló, D., 2012. Occurrence and elimination of pharmaceuticals during conventional wastewater treatment. *Emerging and Priority Pollutants in Rivers*, 19, 1–23.
- Jones, O., Voulvoulis, N., and Lester, J., 2002. Aquatic environmental assessment of the top 25 english prescription pharmaceuticals. *Water Research*, 36, 5013–22.
- Joss, A., Andersen, H., Ternes, T., Richle, P., and Siegrist, H., 2004. Removal of Estrogens in Municipal wastewater treatment under aerobic and anaerobic conditions: consequences for plant optimization. *Environmental Science & Technology*, 38, 3047–3055.
- Joss, A., Keller, E., Alder, A., Göbel, A., McArdell, C., Ternes, T., Siegrist, H., 2005. Removal of pharmaceuticals and fragrances in biological wastewater treatment. *Water Research*, 39, 3139–52.
- Joss, A., Zabczynski, S., Göbel, A., Hoffmann, B., Löffler, D., McArdell, C., Ternes, T., Thomsen, A., Siegrist, H., 2006. Biological degradation of pharmaceuticals in municipal wastewater treatment: proposing a classification scheme. *Water Research*, 40, 1686–96.
- Karichhof, S. W., David S. B., Trudy A. S., 1979. Sorption of hydrophobic pollutants on natural sediments. *Water Research*, 13, 241-248.
- Kasprzyk-Hordern, B., Dinsdale, R., Guwy, A.J., 2009. The Removal of pharmaceuticals, Personal Care Products, endocrine disruptors and illicit drugs during wastewater treatment and its impact on the quality of receiving waters. *Water Research*, 43, 363–80.
- Kim, M., Guerra P., Shah, A., Parsa, M., Alae, M., Smyth, S.A., 2014. Removal of Pharmaceuticals and Personal Care Products in a membrane bioreactor wastewater treatment plant. *Water Science and Technology*, 69, 2221–2229.
- Kim, S., Eichhorn, P., Jensen, J. N., Weber, A.S., Aga, D. S., 2005. Removal of antibiotics in wastewater: effect of hydraulic and solid retention times on the fate of tetracycline in the activated sludge process. *Environmental Science & Technology*, 39, 5816–23.
- Kimura, K., Hara, H., and Watanabe, Y., 2005. Removal of pharmaceutical compounds by submerged membrane bioreactors (MBRs). *Desalination*, 178, 135–40.

- K'oreje, K.O., Kandie, F.J., Vergeynst, L., Abira, M.A., Van Langenhove, H., Okoth, M., Demeestere, K., 2018. Occurrence, fate and removal of pharmaceuticals, personal care products and pesticides in wastewater stabilization ponds and receiving Rivers in the vzoia basin, Kenya. *Science of The Total Environment*, 637–638, 336–48.
- Kreuzinger, N., Clara, M., Strenn, B., Kroiss, H., 2004. Relevance of the Sludge Retention Time (SRT) as design criteria for wastewater treatment plants for the removal of endocrine disruptors and pharmaceuticals from wastewater. *Water Science and Technology*, 50, 149–156.
- Kumar, K. S., Priya, S. M., Peck, A., Sajwan, K.S., 2010. Mass loadings of triclosan and triclocarbon from four wastewater treatment plants to three rivers and landfill in Savannah, Georgia, USA. *Archives of Environmental Contamination and Toxicology*, 58, 275–85.
- Lapworth, D.J., Baran, N., Stuart, M.E., Ward, R.S., 2012. Emerging organic contaminants in groundwater: A review of sources, fate and occurrence. *Environmental Pollution*, 163, 287–303.
- Laquaz, M., Dagot, C., Bazin, C., Bastide, T., Gaschet, M., Ploy, M.C., Perrodin, Y., 2018. Ecotoxicity and antibiotic resistance of a mixture of hospital and urban sewage in a wastewater treatment plant. *Environmental Science and Pollution Research*, 25, 9243–53.
- Le Moullec, Y., 2008. *Comparison des approches systémique, mécanique des fluides numérique et compartimentale pour la modélisation des réacteurs: application à réacteur canal à boues activées* Institut National Polytechnique de Lorraine.
- Lee, D.G., Zhao, F., Rezenom, Y.H., Russell, D.H., Chu, K.H., 2012. Biodegradation of triclosan by a wastewater microorganism. *Water Research*, 46, 4226–34.
- Lee, K.C., Rittmann, B., Shi, J., McAvoy, D., 1998. Advanced steady-state model for the fate of hydrophobic and volatile compounds in activated sludge. *Water Environment Research*, 70, 1118–31.
- Lesage, N., Spérandio, M., Lafforgue, C., Cockx, A. 2003. Calibration and Application of a 1-D Model for Oxidation Ditches. *Chemical Engineering Research and Design*, 81, 1259–64.
- Lesjean, B., Rosenberger, S., Laabs, C., Jekel, M., Gnirss, R., Amy, G., 2005. Correlation between Membrane Fouling and Soluble/Colloidal Organic Substances in Membrane Bioreactors for Municipal Wastewater Treatment. *Water Sciences and Technology*, 51, 1–8.
- Levenspiel, O., 1972. *Chemical reaction engineering*. Wiley, New York.

- Levenspiel O. 1999. Chemical reaction engineering, 3rd edn. Wiley, New York.
- Levenspiel, O., Smith, W. K., 1995. Notes on the diffusion-type model for the longitudinal Mixing of fluids in flow. *Chemical Engineering Science, frontiers of chemical engineering Science*, 50, 3891–96.
- Li, P., Qian H., 2018. Water resources research to support a sustainable China. *International Journal of Water Resources Development*, 34, 327–36.
- Lindblom, E., Press-Kristensen, K., Vanrolleghem, P.A., Mikkelsen, P.S., Henze, M., 2009. Dynamic experiments with high Bisphenol-A concentrations modelled with an ASM model extended to include a separate XOC degrading microorganism. *Water Research*, 43, 3169–76.
- Liu, J., Dan, X., Lu, G., Shen, J., Wu, D., Yan, Z., 2018. Investigation of pharmaceutically active compounds in an urban receiving water: occurrence, fate and environmental risk assessment. *Ecotoxicology and environmental safety*, 154, 214–20.
- Loos, R., Carvalho, R., António, D., Comero, S., Locoro, G., Tavazzi, S., Paracchini, B., et al. 2013. EU-Wide monitoring survey on emerging polar organic contaminants in wastewater treatment plant effluents. *Water Research*, 47, 6475–87.
- López-Serna, R., Jurado, A., Vázquez-Suñé, E., Carrera, J., Petrović, M., Barceló, D., 2013. Occurrence of 95 pharmaceuticals and transformation products in urban groundwaters underlying the metropolis of Barcelona, Spain. *Environmental Pollution*, 174, 305–15.
- Lu, J., Li, H., Tu, Y., and Yang, Z. 2018. Biodegradation of four selected Parabens with aerobic activated sludge and their transesterification product. *Ecotoxicology and Environmental Safety*, 156, 48–55.
- Luo, Y., Guo, W., Ngo, H., Nghiem, L., Hai, F., Zhang, J., Liang, S., and Wang X., 2014. A review on the occurrence of micropollutants in the aquatic environment and their fate and removal during wastewater treatment. *Science of The Total Environment*, 473–474, 619–41.
- Mackay, D., 1979. Finding fugacity feasible. *Environmental Science & Technology*, 13, 1218–23.
- Majewsky, M., Gallé, T., Bayerle, M., Goel, R., Fischer, K., Vanrolleghem, P.A., 2011b. Xenobiotic removal efficiencies in wastewater treatment plants: residence time distributions as a guiding principle for sampling strategies. *Water Research*, 45, 6152–62.

- Majewsky, M., Gallé, T., Yargeau, V., Fischer, K., 2011a. Active heterotrophic biomass and sludge retention time (SRT) as determining factors for biodegradation kinetics of pharmaceuticals in activated sludge. *Bioresource Technology*, 102, 7415–21.
- Mannina, G., Capodici, M., Cosenza, A., Di Trapani, D., A. Ekama, G., 2018. The effect of the solids and hydraulic retention time on moving bed membrane bioreactor performance. *Journal of Cleaner Production*, 170, 1305–15.
- Margot, J., Lochmatter, S., MBarry, D.A., and Holliger, C., 2016. Role of Ammonia-oxidizing bacteria in micropollutant removal from wastewater with aerobic granular sludge. *Water Sci. Technol.*, 73,564–75.
- Mazioti, A., Stasinakis, A., Gatidou, G., Thomaidis, N., and Andersen, H., 2015. Sorption and biodegradation of selected benzotriazoles and hydroxybenzothiazole in activated sludge and estimation of their fate during wastewater treatment. *Chemosphere*, 131, 117–23.
- Meister, M., Winkler, D., Rezavand, M., Rauch, W., 2017. Integrating hydrodynamics and biokinetics in wastewater treatment modelling by using smoothed particle hydrodynamics. *Computers & Chemical Engineering*, 99, 1–12.
- Melcer, H., Bell, J. P., Thompson, D. J., Yendt, C. M., Kemp, J., Steel, P., 1994. Modelling volatile organic contaminants' fate in wastewater treatment plants. *Journal of Environmental Engineering*, 120, 588–609.
- Miège, C., Choubert, J.M., Ribeiro, L., Eusèbe, M., Coquery, M., 2009. Fate of pharmaceuticals and Personal Care Products in wastewater treatment plants – conception of a database and first results. *Environmental Pollution*, 157, 1721–26.
- Min, X., Li, W., Wei, Z., Spinney, R., Dionysiou, D.D., Seo, Y., Tang, C.J., Li, Q., Xiao, R., 2018. Sorption and biodegradation of pharmaceuticals in aerobic activated sludge system: a combined experimental and theoretical mechanistic study.” *Chemical Engineering Journal*, 342, 211–19.
- Monteiro, S.C., Boxall, A.B.A., 2010. Occurrence and fate of human pharmaceuticals in the environment. In *reviews of Environmental Contamination and Toxicology*, 53–154. Springer.
- Mutiyar, P. K., Gupta, S.K., Mittal, A.K., 2018. Fate of pharmaceutical active compounds (PhACs) from river Yamuna, India: an ecotoxicological risk assessment approach. *Ecotoxicology and Environmental Safety*, 150, 297–304.

- Nie, Y., Qiang, Z., Zhang, H., and Ben, H., 2012. Fate and seasonal variation of endocrine-disrupting chemicals in a sewage treatment plant with A/A/O Process. *Separation and Purification Technology*, 84, 9–15.
- Nopens, I., Laurent, J., Wicklein, E., Ducoste, J.M., Griborio, A., Batstone, D.J., Wicks, J.D., Saunders, S., Potier, O., Ratkovich, N., Karpinska, A. M., Samstag, R.W., 2015. *Computational Fluid Dynamics: an important modelling tool for the water sector*.
- Peev, M., Schönerklee, M., De Wever, H., 2004. Modelling the degradation of low concentration pollutants in membrane bioreactors. *Water Science and Technology*, 50, 209–18.
- Petrovic, M., Radjenovic, J., Postigo, C., Kuster, M., Farre, M., López de Alda, M., and Damià Barceló, D., 2009. Emerging contaminants in waste Waters: Sources and occurrence. *Emerging contaminants from industrial and municipal waste*, 1–35. Springer.
- Plosz, B. G., Benedetti, L., Daigger, G. T., Langford, K. H., Larsen, H. F., Monteith, H., Ort, C., Seth, R., Steyer, J.-P., Vanrolleghem, P. A., 2013. Modelling micropollutant fate in wastewater collection and treatment systems: status and challenges. *Water Science and Technology*, 67, 1–15.
- Plosz, B., Langford, K., and Thomas, K., 2012. An activated sludge modelling framework for xenobiotic trace chemicals (ASM-X): assessment of diclofenac and carbamazepine. *Biotechnology and bioengineering*, 109, 2757–69.
- Plosz, B., Leknes, H., and Thomas, K., 2010. Impacts of competitive inhibition, parent compound formation and partitioning behavior on the removal of antibiotics in municipal wastewater treatment. *Environmental Science & Technology*, 44, 734–42.
- Polesel, F., Andersen, H.R., Trapp, S., Plosz, B.G., 2016. Removal of antibiotics in biological WWTPs—a critical assessment using the activated sludge modelling framework for xenobiotics (ASM-X). *Environmental Science & Technology*, 50, 10316–34.
- Pomiès, M., Choubert, J.-M., Wisniewski, C., Coquery, M., 2013. Modelling of micropollutant removal in biological wastewater treatments: A review. *Science of The Total Environment*, 443, 733–48.
- Potier O., Louvet J.N., Merlin C., Pons, M.N., Dumas, D., Goldstein, W.E. 2014. Effect of antibiotics on biological wastewater treatment processes. *Pharmaceutical accumulation in the environment: prevention, control, health effects, and economic impact*. CRR Press, 117-153.

- Potier, O., Leclerc, J. P., and Pons, M.N., 2005. Influence of geometrical and operational parameters on the axial dispersion in an aerated channel reactor. *Water Research*, 39, 4454–4462.
- P Pruden, A., Pei, R., Storteboom, H., and Carlson. K., 2006. Antibiotic Resistance genes as emerging contaminants: studies in northern Colorado. *Environmental Science & Technology*, 40, 7445–50.
- Quesada, H. B., Baptista, A.T.A., Cusioli, L.F., Seibert, D., Bezerra, C.D.O., Bergamasco, R., 2019. Surface water pollution by pharmaceuticals and an alternative of removal by low-cost adsorbents: a review. *Chemosphere*, 222, 766–80.
- Radjenovic, J., Petrović, M., and Barceló, D., 2009. Fate and distribution of pharmaceuticals in wastewater and sewage sludge of the conventional activated sludge (CAS) and advanced membrane bioreactor (MBR) treatment. *Water Research*, 43, 831–41.
- Ratola, N., Cincinelli, A., Alves, A., and Katsoyiannis, A., 2012. Occurrence of Organic microcontaminants in the wastewater treatment process. A mini review. *Journal of Hazardous Materials*, 239–240, 1–18.
- Renuka, R., Mohan, S.M., Raj, S.A., 2016. Hydrodynamic behaviour and its effects on the treatment performance of panelled anaerobic baffle-cum filter reactor. *International Journal of Environmental Science and Technology*, 13, 307–18.
- Ribeiro, A.R., Nunes, O., Pereira, M., and Silva, A., 2015. An Overview on the advanced oxidation processes applied for the treatment of water pollutants defined in the recently launched directive 2013/39/EU. *Environment International*, 75, 33–51.
- Richardson, S.D. 2008. Environmental mass spectrometry: emerging contaminants and current issues. *Analytical Chemistry*, 80, 4373–4402.
- Richardson, S.D., Kimura, S.Y., 2017. Emerging environmental contaminants: challenges facing our next generation and potential engineering solutions. *Environmental Technology & Innovation*, 8, 40–56.
- Richardson, S.D., Postigo, C., 2015. Safe drinking water? Effect of wastewater inputs and source water impairment and implications for water reuse. In *wastewater reuse and current challenges*. Cham: Springer International Publishing, 44, 155–82.



- Rivera-Utrilla, J., Sánchez-Polo, M., Ferro-García, M.A., Prados-Joya, G., Ocampo-Pérez, R., 2013. Pharmaceuticals as emerging contaminants and their removal from water. A review.” *Chemosphere*, 93, 1268–87.
- Rehman, U., Amerlinck, Y., Arnaldos, M., Nopens, I., 2014. CFD and biokinetic model integration applied to a full scale WWTP. *Proceedings of the Water Environment Federation*, 8, 6894–6905.
- Rehman, U., Audenaert, W., Amerlinck, Y., Arnaldos, M., Nopens, I., 2017. How well-mixed is well mixed? Hydrodynamic-biokinetic model integration in an aerated tank of a full-scale water resource recovery facility. *Water Science Technology*, 76, 1950-1965.
- Rodriguez-Gomez, R., Renman, G., Moreno, L., Liu, L., 2014. A model to describe the performance of the UASB reactor. *Biodegradation*, 25, 239–51.
- Rodriguez-Narvaez, O.M., Peralta-Hernandez, J.M., Goonetilleke, A., Bandala, E.R., 2017. Treatment technologies for emerging contaminants in water: A review. *Chemical Engineering Journal*, 323, 361–80.
- Sahar, E., Ernst, M., Godehardt, M., Hein, A., Herr, J., Kazner, C., Melin, T., 2011. Comparison of two treatments for the removal of selected organic micropollutants and bulk organic matter: conventional activated sludge followed by ultrafiltration versus membrane bioreactor. *Water Science and Technology*, 63, 733–40.
- Samaras, V., Stasinakis, A., Mamais, D., Thomaidis, N., Lekkas, T., 2013. Fate of selected pharmaceuticals and synthetic endocrine disrupting compounds during wastewater treatment and sludge anaerobic digestion. *Journal of Hazardous Materials*, 244,259–267.
- Santos, J.L., Aparicio, I., Callejón, M., and Alonso, E. 2009. Occurrence of pharmaceutically active compounds during 1-Year period in wastewaters from four wastewater treatment plants in seville (Spain). *Journal of Hazardous Materials*, 164, 1509–16.
- Schwarzenbach, R.P., Gschwend, P.M., Imboden, D.M., 2003. *Transformation Processes*. Wiley Online Library.
- Schwarzenbach R. P., 2006. The challenge of micropollutants in aquatic systems. *Science*, 313, 1072-77.
- Schwarzenbach, R.P., Gschwend, P.M., Imboden, D.M., 2005. *Sorption I: general introduction and sorption processes involving organic matter*. Wiley Online Library.

- Singer, H., Jaus, S., Hanke, I., Lück, A., Hollender, J., Alder, A., 2010. Determination of biocides and pesticides by on-Line solid phase extraction coupled with mass spectrometry and their behaviour in Wwastewater and surface water. *Environmental Pollution*, 158, 3054–64.
- Sipma, J., Osuna, B., Collado, N., Monclús, H., Ferrero, G., Comas, J., and Rodriguez-Roda, I. 2010. Comparison of removal of pharmaceuticals in MBR and activated sludge systems. *Desalination*, 250, 653–59.
- Snyder, S., Adham, S., Redding, A., Cannon, F., DeCarolis, J., Oppenheimer, J., Wert, E., Yoon, Y., 2007. Role of membranes and activated carbon in the removal of endocrine disruptors and pharmaceuticals. *Desalination*, 202, 156–81.
- Stamatis, N., Hela, D., Konstantinou. I., 2010. Occurrence and removal of fungicides in municipal sewage treatment plant. *Journal of Hazardous Materials*, 175, 829–35.
- Stevens-Garmon, J., Drewes, J., Khan, S., McDonald, J., Dickenson, E., 2011. Sorption of emerging trace organic compounds onto wastewater sludge solids. *Water Research*, 45, 3417–26.
- Struijs, J., Stoltenkamp, J., van de Meent, D., 1991. A spreadsheet-based box model to predict the fate of xenobiotics in a municipal wastewater treatment plant. *Water Research* 25 (7): 891–900.
- Suarez, S., Carballa, M., Omil, F., Lema, J., 2008. How are Pharmaceutical and Personal Care Products (PPCPs) removed from urban wastewaters? *Environmental Science and Bio/Technology*, 7, 125–38.
- Suarez, S., Lema, J., Omil, F., 2010. Removal of Pharmaceutical and Personal Care Products (PPCPs) under nitrifying and denitrifying conditions. *Water Research*, 44, 3214–3224.
- Sudhakaran, S., Maeng, S.K., Amy, G., 2013. Hybridization of natural systems with advanced treatment processes for organic micropollutant removals: new concepts in multi-barrier treatment. *Chemosphere*, 92, 731–37.
- Szpyrkowicz, L., 2006. Application of electrochemical oxidation for treatment of industrial wastewater — the influence of reactor hydrodynamics on direct and mediated processes.” *Journal of Chemical Technology & Biotechnology*, 81, 1375–83.
- Tadkaew, N., Sivakumar, M., Khan, S., McDonald, J., and Nghiem, L. 2010. Effect of mixed liquor pH on the removal of trace organic contaminants in a membrane bioreactor. *Bioresource Technology*, 101, 1494–1500.

- Tao, S., and Xiaoxia L., 1999. Estimation of organic carbon normalized sorption coefficient ( $K_{oc}$ ) for soils by topological indices and polarity factors. *Chemosphere*, 39, 2019–2034.
- Ternes, T., 1998. Occurrence of drugs in German sewage treatment plants and rivers. *Water Research*, 32, 3245–3260.
- Ternes, T., Joss, A., Siegrist, H., 2004. Peer Reviewed: Scrutinizing Pharmaceuticals and Personal Care Products in Wastewater Treatment. ACS Publications.
- Ternes, T., Stüber, J., Herrmann, N., McDowell, D., Ried, A., Kampmann, M., Teiser, B., 2003. Ozonation: A tool for removal of pharmaceuticals, contrast media and musk fragrances from wastewater. *Water Research*, 37, 1976–82.
- Ternes, T., Joss, A., eds. 2006. Human Pharmaceuticals, Hormones and Fragrances: The Challenge of Micropollutants in Urban Water Management. Reprinted. London: IWA Publ.
- Tijani, J., Fatoba, O., Petrik, L., 2013. A review of pharmaceuticals and Endocrine-Disrupting Compounds: sources, effects, removal, and detections. *Water, Air, & Soil Pollution* 224 (11).
- Tiwari, B., Sellamuthu, B., Ouarda, Y., Drogui, P., Tyagi, R., Buelna, G., 2017. Review on fate and mechanism of removal of pharmaceutical pollutants from wastewater using biological approach. *Bioresource Technology*, 224, 1–12.
- Tran, N.H., Gin, K.Y.H., 2017. Occurrence and removal of pharmaceuticals, hormones, personal care products, and endocrine disrupters in a full-scale water reclamation plant. *Science of The Total Environment*, 599–600, 1503–16.
- UN-Water, eds. 2009. *Water in a Changing World*. 3rd ed. The United Nations World Water Development Report 3. Paris : London: UNESCO Publishing ; Earthscan.
- Urase, T., Kikuta, T., 2005. Separate estimation of adsorption and degradation of pharmaceutical substances and estrogens in the activated sludge process. *Water Research*, 39, 1289–1300.
- Vasiliadou, I.A., Molina, R., Martínez, F., Melero, J.A., 2014. Experimental and modelling study on removal of pharmaceutically active compounds in rotating biological contactors. *Journal of Hazardous Materials*, 274, 473–82.
- Verlicchi, P., Al Aukidy, M., Zambello, E., 2012. Occurrence of pharmaceutical compounds in urban wastewater: Removal, mass load and environmental risk after a secondary treatment—A review. *Science of The Total Environment*, 429, 123–55.

- Verlicchi, P., Al Aukily, M., Zambello, E., 2015. What have we learned from worldwide experiences on the management and treatment of hospital effluent? — An overview and a discussion on perspectives. *Science of The Total Environment*, 514, 467–91.
- Vezzaro, L., Benedetti, L., Gevaert, V., De Keyser, W., Verdonck, F., De Baets, B., Nopens, I., Cloutier, F., Vanrolleghem, P.A., Mikkelsen, P.S., 2014. A model library for dynamic transport and fate of micropollutants in integrated urban wastewater and stormwater systems. *Environmental Modelling & Software*, 53, 98–111.
- Vieno, N., Tuhkanen, T., Kronberg, L., 2007. Elimination of pharmaceuticals in sewage treatment plants in Finland. *Water Research*, 41, 1001–12.
- Vieno, N., Tuhkanen, T., Kronberg, L., 2005. Seasonal variation in the occurrence of pharmaceuticals in effluents from a sewage treatment plant and in the recipient water. *Environmental Science & Technology*, 39, 8220–26.
- Villiermaux, J., 1982. *Ge'nie de la r'eaction chimique conception et fonctionnement des r'eacteurs*. Tec&Doc. Lavoisier, Paris.
- Von Bertalanffy, L., 1968. *General System Theory. Foundations, Development, Applications*. George Braziller, New York. ISBN 0—8076-0453-4.
- Walker, D.B., Baumgartner, D.J., Gerba, C.P., Fitzsimmons, K., 2019. Surface water pollution. In *Environmental and Pollution Science*, 261–92.
- Weiss, S., Jakobs, J., Reemtsma, T., 2006. Discharge of three benzotriazole corrosion inhibitors with municipal wastewater and improvements by membrane bioreactor treatment and ozonation <sup>†</sup>. *Environmental Science & Technology*, 40, 7193–99.
- Weiss, S., Reemtsma, T., 2008. Membrane bioreactors for municipal wastewater treatment – A viable option to reduce the amount of polar pollutants discharged into surface waters. *Water Research*, 42, 3837–47.
- Weiss, S., Reemtsma, T., 2008. Membrane bioreactors for municipal wastewater treatment – A viable option to reduce the amount of polar pollutants discharged into surface waters? *Water Research*, 42, 3837–47.
- Wick, A., Fink, G., Joss, A., Siegrist, H., Ternes, T., 2009. Fate of beta blockers and psycho-active drugs in conventional wastewater treatment. *Water Research*, 43, 1060–74.
- Wijhe, M.V., 2002. The history of caffeine as used in anaesthesia. *International Congress Series*, 1242, 101–3.

- Xue, W., Wu, C., Xiao K., Huang, X., Zhou, H., Tsuno, H., Tanaka, H., 2010. Elimination and fate of selected micro-organic pollutants in a full-scale anaerobic/anoxic/aerobic process combined with membrane bioreactor for municipal wastewater reclamation. *Water Research*, 44, 5999–6010.
- Yu, C.P., and Chu, K.H. 2009. Occurrence of Pharmaceuticals and Personal Care Products along the west prong little pigeon river in east tennessee, USA. *Chemosphere*, 75, 1281–86.
- Yu, Z., Peldszus, S., and Huck, P. 2007. Optimizing gas chromatographic–mass spectrometric analysis of selected pharmaceuticals and Endocrine-Disrupting Substances in water using factorial experimental design. *Journal of Chromatography A*, 1148, 65–77.
- Zhang, D., Gersberg, R., Ng, W.J., Tan, S.K., 2014. Removal of Pharmaceuticals and Personal Care Products in aquatic plant-based systems: A review. *Environmental Pollution*, 184, 620–639.
- Zhao, J., Li, Y., Zhang, C., Zeng, Q., Zhou, Q., 2008. Sorption and degradation of bisphenol A by aerobic activated sludge. *Journal of Hazardous Materials*, 155, 305–11.
- Zorita, S., Mårtensson, L., Mathiasson, L., 2009. Occurrence and removal of pharmaceuticals in a municipal sewage treatment system in the south of Sweden. *Science of The Total Environment*, 407, 2760–70.



**Chapter II. Biological experiments- Effect of SRT,  
HRT and biomass concentration on elimination of  
micropollutants with activated sludge**

*This chapter corresponds to an article published in Water Journal. It follows the structure of this article.*

## Abstract

The study of the effects of sludge retention time (SRT), hydraulic retention time (HRT) and biomass concentration on the elimination of micropollutants in activated sludge is the aim of this chapter. The studied MPs are caffeine, sulfamethoxazole, benzotriazole, erythromycin, roxithromycin, diclofenac and carbamazepine. These seven emerging contaminants cover a wide spectrum of biodegradability from highly biodegradable to quite persistent compounds. Seven experimental setups were applied to sequencing batch reactors (SBRs) which varied in SRT (3 d, 10 d and 20 d) and HRT (4 h, 8 h and 12 h). The effect of biomass concentration was measured for 3, 5 and 8  $\text{g}_{\text{TSS}} \text{L}^{-1}$ . The influence of this latter parameter on the pseudo-first order rate constant was verified. The removal rate constants were affected by both the HRT and SRT. The enhancement of the SRT increased the removal of all the MPs except for roxithromycin and erythromycin. Application of a higher HRT did also improve their removal as could be expected from the measured removal rate constants. More interesting, the results indicated that logically the increase of biomass concentration from 3 to 5  $\text{g}_{\text{TSS}} \text{L}^{-1}$  significantly enhanced the removal rate of the highly and moderately degradable compounds (caffeine, sulfamethoxazole, benzotriazole, erythromycin, roxithromycin). Conversely, a further increase to 8  $\text{g}_{\text{TSS}} \text{L}^{-1}$  produced only an unexpected moderate effect, showing that the rate is not proportional to biomass concentration contrary to what is generally postulated. Therefore, the use of classic kinetic models such as pseudo-first order, first order and global second-order is questionable since they do not cover the entire range of possible boundary conditions in activated sludge systems.

## II.1. Introduction

It is now well admitted that a complete removal of all the micropollutants (MPs) cannot be achieved by wastewater treatment plants (WWTPs). This is due to the design of the wastewater treatment plants, their current operation modes, as well as due to the nature of anthropological contaminants present in the wastewater (Chiavola et al. 2019). Among these micropollutants (MPs), pharmaceuticals and personal care products, food additives, industrial chemicals and



pesticides are of the increasing concern. As a result, they are discharged with the wastewater effluents to aquatic environments. However, despite their low concentrations, they may exhibit various adverse effects. As an example, Bonnefille et al. (2018) reviewed a deformation of the dorsal margin line in mussel shells after exposure at 0.01 to 100  $\mu\text{g L}^{-1}$  of diclofenac for 48 h. Moreover, the presence of antibiotics (ABs) in aquatic environments is often discussed in the context of the spread of antibiotic resistance, which has already been recognized as one of the major threats to human health 20 years ago (WHO). Therefore, an improvement of the existing wastewater treatment methods become essential to maintain the natural balance and minimize the potential risk to ecosystems.

In recent years, an application of advanced treatment as a support to biological treatment with activated sludge (CAS system) received a lot of attention. Among these technological solutions, adsorption on activated carbon (Kårelid et al. 2017) and ozonation (Bourgin et al. 2018) seem to be the most common approaches. However, despite their high efficiency, these methods require additional investments and generate regular costs for the maintenance of the systems. Furthermore, as reported in numerous studies, oxidation methods, such as ozonation, lead to formation of by-products of unknown ecotoxicological effects (Tay and Madehi, 2015). To remove them, additional post-treatment step is required (Knopp et al. 2016).

A cost-efficient alternative would be to modify the existing biological treatment and identify the critical parameters affecting the removal of problematic substances. In theory, the removal during the biological treatment can occur via three pathways: biological degradation, sorption, and volatilization. Due to the physico-chemical properties of MPs, volatilization of these substances is usually neglected as a removal pathway (Kim et al. 2014) but it contributes to releasing volatile MPs in the atmosphere. Sorption on sludge is considered as insignificant for compounds with solid-water distribution coefficients ( $K_d$ ) below 500  $\text{L kgSS}^{-1}$  (Ternes et al. 2004), which is the case for some MPs. The biological degradation appears then as the main removal pathway. To estimate MPs' removal kinetics in activated sludge, usually pseudo-first-order removal rate constants ( $k$ ) were mostly determined in lab-scale tests in which biomass and MPs concentrations are the key parameters.

During the last decades, many studies reported on the MPs removal efficiency of WWTPs during biological treatment (Jiang et al. 2013; Luo et al. 2014). The results pointed out that operating parameters, such as hydraulic retention time (HRT) and sludge retention time (SRT), are important

for MPs (Alvarino et al. 2018; Falås et al. 2012; Majewsky et al. 2011; Vieno and Sillanpää 2014). It has been observed that the biomass composition, i.e. the ratio between autotrophic and heterotrophic microbes, is controlled by the SRT (Vuono et al. 2015). In this context, two important hypotheses are often discussed: (i) sludge with high SRT possesses higher microbial diversity than one with low SRT, and (ii) SRT longer than 10 days, operated at a temperature of 10°C that allows the growth of nitrifying bacteria (Clara et al., 2005a) could enhance the removal of some micropollutants either by direct metabolism or by co-metabolic degradation via enzymatic reactions (Alvarino et al. 2014; Tran et al. 2013). On the contrary, the results of Saikaly et al. (2005) showed a higher microbial diversity in the activated sludge bioreactors operated at SRT of 2 days than operated at SRT of 8 days. Thus, there are still no clear data indicating the optimal parameters and the key microorganisms involved in the biological removal of MPs (Falås et al. (2016). Regarding the effect of SRT and HRT on MPs' removal, differences in the removal efficiencies for some PPCPs have also been reported (Luo et al. 2014). Other recently published studies discussed the different removal efficiency depending on SRT, HRT, feed concentrations and total biomass concentration (Table II.1). For example, Santos et al. (2009) indicated that some compounds are removed in the same degree in four WWTPs operated at different low SRTs (1.5–5.1 days) such as caffeine (44-75 %) and carbamazepine (8-15 %). However, Majewsky et al. (2011) showed the same results for carbamazepine (<10 %) by applying higher SRT up to 54 d and HRT of 58.4 h. Although, SRT has been reported as a critical factor for pharmaceutical biodegradation, the effect of SRT for some authors does not become clear since no systematic relation between SRT and removal rates of organic micropollutants can be found (Falås et al. (2016). A statistical analysis performed by Zhang et al. (2014) showed the existence of significant linear correlation between DCF and CAF removal efficiency and HRT. However, the relation is no longer valid for CBZ.

The main objective of the present study is to investigate the relation between the biomass concentration of activated sludge, the operational parameters - SRT and HRT of biological treatment - and the removal efficiency of selected MPs. Seven compounds were selected based on their occurrence data and varying removal efficiency in WWTPs (Tarpani et al. 2018). According to the literature and our own experience, caffeine (CAF), sulfamethoxazole (SMX), benzotriazole (BZT), roxithromycin (ROX), erythromycin (ERY), diclofenac (DCF) and carbamazepine (CBZ) are used. They range from highly biodegradable to quite persistent MPs (Table II.1). The

degradation experiments were conducted with three lab-scale SBRs to compare the effect of operation conditions. For this purpose, the kinetics of MPs removal was investigated and removal rate constants were determined to estimate whether MPs removal can be attributed to the manipulation of SRT and HRT, and therefore linked to treatment process parameters. Further experiments were performed in lab-scale SBRs varying in concentration of total suspended solids ( $C_{TSS}$ ) to investigate the role of the biomass concentration in MPs removal and applicability of the pseudo-first-order kinetics approach for description of removal phenomena.

**Table II. 1.** Overview of the removal efficiency of some MPs in published studies according to some operational conditions in activated sludge.

HRT / SRT	Feed concentration ( $\mu\text{g L}^{-1}$ )							Removal efficiency (%)							Sludge concentration ( $\text{g}_{\text{TSS}} \text{L}^{-1}$ )
	CAF	SMX	BZT	ROX	ERY	DCF	CBZ	CAF	SMX	BZT	ROX	ERY	DCF	CBZ	
>2-3 / >150d (nitrifying conditions) <sup>a</sup>						$\leq 1$							70 <sup>b</sup>		
12-17h / 1.5-5.1d <sup>c</sup>								44-75						8-15	
16.7h / 6d <sup>d</sup>	1	1				1	1	99	90				20	<10	2.4
58.4h / 54d <sup>d</sup>	1	1				1	1	95	45				10	<10	2.5
15h / 10-12d <sup>e</sup>		0.23-0.57							9		25	2			3
31h / 21-25d <sup>e</sup>		0.23-0.57							60						3
- / 20-40d, >40d <sup>f</sup>							10-40							<20	2g <sub>vss</sub> L <sup>-1</sup>
- / 20-40d, >40d <sup>f</sup>						10-40							<20		2g <sub>vss</sub> L <sup>-1</sup>
- / >40d <sup>f</sup>		10-40							64-70		64-70	64-70			2g <sub>vss</sub> L <sup>-1</sup>
12-20h / 25d <sup>g</sup>		1-5	1-5			1-5	1-5		20-90 <sup>h</sup>				<20 <sup>g</sup>	<20 <sup>g</sup>	
12-20h / 40d <sup>g</sup>		1-5	1-5			1-5	1-5		20-90 <sup>h</sup>				<20 <sup>g</sup>	<20 <sup>g</sup>	4-5.5
12-20h / 80d <sup>g</sup>		1-5	1-5			1-5	1-5		20-90 <sup>h</sup>				<20 <sup>g</sup>	<20 <sup>g</sup>	4-5.5
12h / 3d <sup>i</sup>							0.24							--	
12.5-13.6 / 52-114d <sup>i</sup>							0.32-1.85							--	

<sup>a</sup>Vieno and Sillanpää (2014); <sup>b</sup>Fernandez-Fontaina et al. (2012) ; <sup>c</sup>Santos et al. (2009) ; <sup>d</sup>Majewsky et al. (2011); <sup>e</sup>Gobel et al. (2007) ;

<sup>f</sup>Suárez et al. (2012) ; <sup>g</sup>Falås et al. (2016) ; <sup>h</sup>Joss et al. (2006) ; <sup>i</sup>Hai et al. (2018). / --negligeable.

## **II.2. Materials and Methods**

### II.2.1. Wastewater system and sampling site

Activated sludge were collected from two wastewater treatment plants, the Bruchsal WWTP and the Neureut WWTP, in the city of Karlsruhe in Germany. The samples in Bruchsal WWTP were taken every 3 weeks from the sludge collecting point as shown in Figure II.1. The samples in Neureut were collected once directly after the 'cleaning' procedure of the trickling filter reactor performed once per month. The samples were collected using plastic bottle using a thick long stick that was dropped into the sites to take the sludge samples. Samples were placed in 15 L tank and transported to the laboratory. Bruchsal WWTP treats the municipal wastewater received from 57'750 population equivalents (PE). At the time of sampling, the SRT and HRT were 6 d and 4 h, respectively. Neureut/Karlsruhe WWTP covers the 875'000 PE and it receives a fraction of industrial wastewater mainly from electronic and food industry. The treatment is performed by a combination of activated sludge and trickling filter operated with SRT of 10–20 days. Activated sludge of both plants achieves chemical oxygen demand (COD), nitrogen and total phosphorus removal.



**Figure II. 1.** Sampling sites located in the Bruchsal and Neureut WWTPs. The notation B refers to sludge collecting point in Bruchsal WWTP and N trickling filter reactor in Neureut WWTP.

## II.2.2. Selection of micropollutants

### II.2.2.1. Sorption tests on the wall of the reactor

Sorption experiment tests were performed before the startup of the biological removal experiments with activated sludge in order to (i) choose our investigated micropollutants, (ii) avoid physical adsorption by verifying if the micropollutants adsorb on the wall of the reactor, (iii) compromise between real MPs' concentration in WWTPs and their analytical quantification as well as identify the conditions of samples' conservation (fridge or freezer). At the beginning, one reactor of 10 L filled with only tap water was spiked with standard solutions to the final concentration of  $5 \mu\text{g L}^{-1}$  of a stock solution. This latter was a fresh mix of the following micropollutants: caffeine, benzotriazole, sulfamethoxazole, diclofenac, carbamazepine, erythromycin, roxithromycin, tetracycline and ciprofloxacin. The content was mixed using a stirrer in the reactor and samples (2

x 1 ml) were collected at 0, 3, 6, 24, 48, 72, 96, 120 and 144 h. 100  $\mu\text{L}$  of each sample were transferred into an amber vial containing 900  $\mu\text{L}$  of MilliQ water and preserved at 4  $^{\circ}\text{C}$  until analysis. To verify the effect of freezing on the compounds, one series was kept in the freezer and another in the fridge. Based on the sorption results, the following sections were treated using all mentioned micropollutants apart of tetracycline and ciprofloxacin. Results are presented in section II.3.1.

#### II.2.2.2. *Physico-chemical properties of investigated micropollutants*

The selection of the micropollutants to be studied was based on many criteria such as their usage (pharmaceuticals and personal care products), occurrence in the municipal wastewater, relevance for the environment, various degree of biodegradability to test a large spectrum of conditions and based on the sorption results obtained on the wall of the reactor.

Then, seven compounds detected frequently in wastewater influents in the concentration range of  $\text{ng L}^{-1}$  –  $\mu\text{g L}^{-1}$  were selected (Table II.2). The caffeine (CAF), sulfamethoxazole (SMX), benzotriazole (BZT), roxithromycin (ROX), erythromycin (ERY), diclofenac (DCF) and carbamazepine (CBZ) range from easily biodegradable to persistent MPs. Caffeine is the highly biodegradable compound; SMX, BZT, ROX, and ERY are well known as moderately biodegradable compounds; whereas DCF and CBZ are mostly recognized as not readily biodegradable compounds. The application and the physico-chemical properties of the target MPs were summarized from Table I.2 and displayed in Table II.3.

**Table II. 2.** The concentrations and removals of investigated micropollutants present in the WWTPs of different countries.

Group	Selected compound	Country	Influent ( $\mu\text{g L}^{-1}$ )	Effluent ( $\mu\text{g L}^{-1}$ )	Removal efficiency (%)	References
Stimulant	Caffeine	China; EU-wide; Greek; Korea; Spain; UK	0.22–209	ND–43.50	49.9 – 99.6	Behera et al. 2011; Santos et al. 2009; Singer et al. 2010
Pharmaceutical Antibiotic	Sulfamethoxazole	UK; Switzerland; Spain; Austria	<0.003–0.98	<0.003–1.15	4 – 88.9	Behera et al. 2011; Kasprzyk-Hordern et al. 2009; Santos et al. 2009
Industrial chemical	Benzotriazole	Germany	12	7.7	37	Weiss et al. 2006
Pharmaceutical Antibiotic	Roxithromycin	Switzerland; Hong Kong; Spain; Germany	0.01–0.04	0.008–0.036	3 – 9	Clara et al. 2005b; Gobel et al. 2007; Kreuzinger et al. 2004; Li and Zhang 2011; Sahar et al. 2011
Pharmaceutical Antibiotic	Erythromycin	Switzerland; Hong Kong; UK	0.06–0.19	0.09–0.20	-8 – 4	Gobel et al. 2007; Li and Zhang 2011
Anti-inflammatory/analgesics	Diclofenac	UK; Hong Kong; Greece; Korea; Sweden	0.26–2.57	0.33–1.42	<0 – 81.4	Kasprzyk-Hordern et al. 2009; Kreuzinger et al. 2004; Behera et al. 2011; Gracia-Lor et al. 2012
Anticonvulsant	Carbamazepine	Greece; Korea; Spain; UK; Germany	<0.04–4.1	<0.005–4.7	0 – 62.7	Behera et al. 2011; Kasprzyk-Hordern et al. 2009; Wick et al. 2009



**Table II. 3.** Application and physico-chemical properties of the target micropollutants (industrial chemical and PPCPs).

Compound	Application		Molecular weight (g mol <sup>-1</sup> )	pKa	Log K <sub>ow</sub>	K <sub>d</sub> (L kgSS <sup>-1</sup> )
<b>Caffeine</b>	Stimulant	↑ Biodegradability increase	194.1	14.0 <sup>a</sup>	-0.07 <sup>b</sup>	50 <sup>f</sup>
<b>Sulfametoxazole</b>	Antibiotic		253.2	7.1 <sup>c</sup>	0.48 <sup>c</sup>	200-400 <sup>c</sup>
<b>Benzotriazol</b>	Detergent/ corrosion inhibitor		119.1	8.2-8.8 <sup>e</sup>	1.23 <sup>d</sup>	220 (±9) <sup>e</sup>
<b>Roxithromycin</b>	Antibiotic		837.0	9.2 <sup>c</sup>	2.1-2.8 <sup>c</sup>	200-400 <sup>c</sup>
<b>Erythromycin</b>	Antibiotic		733.9	8.8 <sup>c</sup>	2.48 <sup>c</sup>	160 <sup>c</sup>
<b>Diclofenac</b>	Non-steroidal anti-inflammatory drug		296.1	4.5 <sup>c</sup>	4.02 <sup>c</sup>	16 <sup>c</sup>
<b>Carbamazepine</b>	Anti-epileptic drug		236.2	13.9 <sup>c</sup>	2.45 <sup>c</sup>	0.1 <sup>c</sup>

<sup>a</sup> Ejhed et al. (2018); <sup>b</sup> Majewsky et al. (2011); <sup>c</sup> Sipma et al. (2010); <sup>d</sup> Weiss et al. (2006); <sup>e</sup> Vasiliadou et al. (2014); <sup>f</sup> Xue et al. (2010).

### II.2.2.3. Chemicals and reagents

Benzotriazole (pure), carbamazepine (98 %), diclofenac sodium salt (pure), erythromycin (pure) and roxithromycin (≥ 90 %) were supplied by Sigma Aldrich (Germany). The sulfamethoxazole (99.5 %) was purchased at Dr. Ehrendorfer GmbH (Germany). Caffeine (pure) was obtained from Fluka Analytix (Germany). Benzotriazole-d<sub>4</sub> (pure), caffeine-<sup>13</sup>C<sub>3</sub> (pure), carbamazepine-d<sub>8</sub> (pure), diclofenac-d<sub>4</sub> (pure), erythromycin-d<sub>3</sub>, roxithromycin-d<sub>7</sub>, sulfamethoxazole-d<sub>4</sub> were obtained from Toronto Research Chemicals (Canada). All solvents i.e. acetonitrile, methanol, HPLC water, formic acid were analytical grade (≥ 99 %) and purchased at VWR Chemicals International (Germany). Stock solutions of labelled and non-labelled isotope standards of micropollutants were prepared in methanol (1 g L<sup>-1</sup>, 10 mL) and then, further serial dilution with HPLC grade water to required working concentrations. All standard solutions were stored at -20 °C. Calibration standards were prepared by dilution of the standard solution in HPLC grade water.

### II.2.3. Sequencing Batch Reactors

To evaluate the kinetics of MPs' in activated sludge, three SBRs with a working volume of 10 L were operated at different SRTs (3, 10, and 20 days) (see Figure II.2). The reactor setups and further procedures applied in this study are discussed in detail in Sections II.2.3.1 – 2.3.5 and Table II.4.

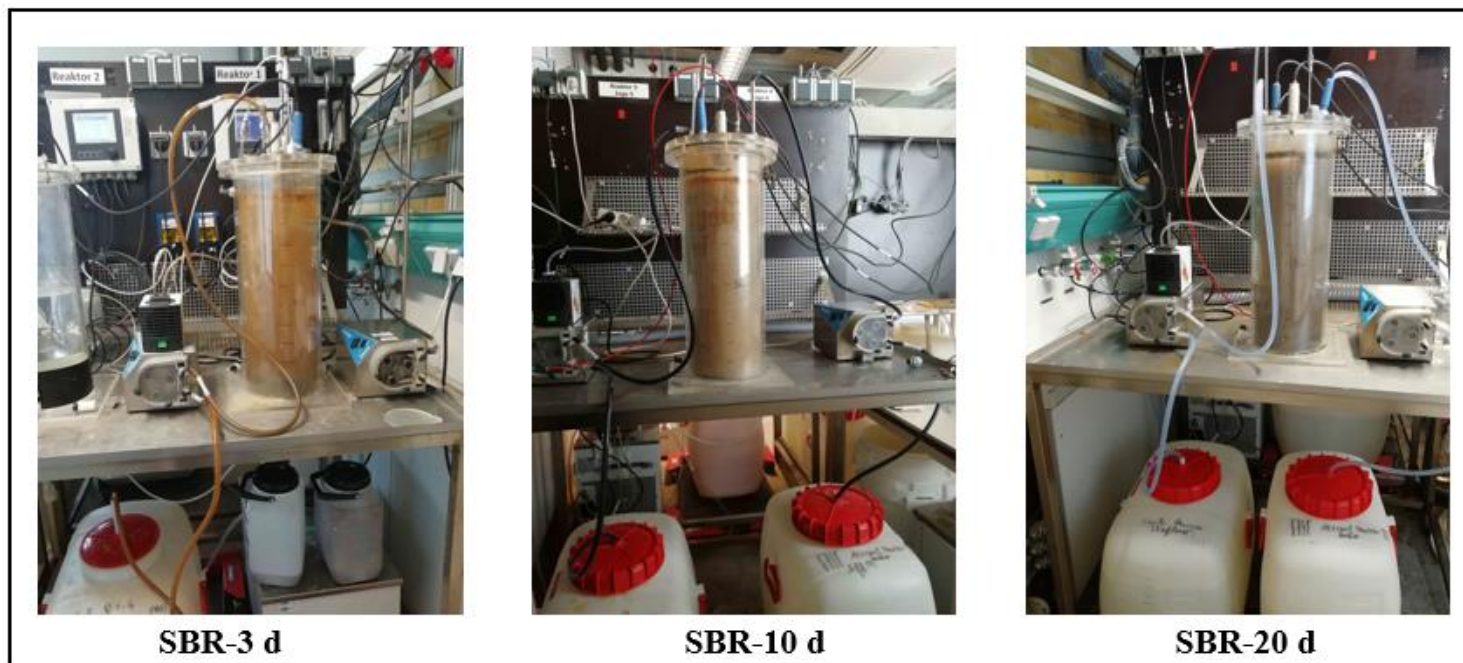


**Figure II. 2.** Photographs of the lab-scale of the Sequencing Batch Reactors (SBR-3 d, SBR-10 d and SBR-20 d).

#### II.2.3.1. Design of the SBRs

The experimental setup of all SBRs was identical. The SBRs differed only in the SRT and the organic load rate of the influent (Table II.4). Influent was pumped into the reactors from separate 100 L wastewater storage tanks. The SBRs were running on a fill-and-draw basis with consecutive cycles including the following phases: filling, reaction (aerobic phase), biomass settling and finally clarified supernatant draw. Filling of synthetic wastewater stopped when 50 % of the column volume was exchanged (Volume Exchange Ratio, VER = 50 %). Air was supplied at a flow rate of  $3 \text{ L min}^{-1}$  through a submerged air mixer which allowed the circulation of the

synthetic wastewater through the settled biomass by pumping the supernatant from the top of the reactors to the bottom. This provided the reactors with oxygenation and guaranteed complete mixing. Air was also introduced continuously, through 3 cm long rectangular diffusers with airflow rates of  $1.5 \text{ L min}^{-1}$ , resulting in saturated oxygen conditions. Both devices were placed 2 cm above the bottom of the SBRs. In all reactors, pH was controlled by a sensor (Orbisint CPS11D Memosens) and it was typically in the range of  $8.1 \pm 0.2$ , at the temperature of  $20 \pm 2^\circ\text{C}$ . Dissolved oxygen (DO) concentration, measured by an oxygen sensor (Oxymax H COS22D), was maintained between 2 and  $6 \text{ mg O}_2 \text{ L}^{-1}$ . A programmable logic controller (PLC) automatically controlled the duration of each phase of cycles, performance of the mixing, air supply, peristaltic pumps and sensors. The PLC was connected to a supervisory control and data acquisition (SCADA) system.

**Table II. 4.** Sequencing Batch Reactor setups operated at different SRTs during kinetics experiments.

		Kinetics experiments		
		SBR- 3 d	SBR- 10 d	SBR- 20 d
Experimental set-up				
	Activated sludge source	After secondary treatment from Bruchsal WWTP, Germany		Trickling filters from Neureut WWTP, Germany
	Synthetic wastewater feed	$1.2 \text{ g}_{\text{COD}} \text{ g}_{\text{TSS}}^{-1} \text{ d}^{-1}$ $0.08 \text{ g}_{\text{N}} \text{ g}_{\text{TSS}}^{-1} \text{ d}^{-1}$	$0.5 \text{ g}_{\text{COD}} \text{ g}_{\text{TSS}}^{-1} \text{ d}^{-1}$ $0.08 \text{ g}_{\text{N}} \text{ g}_{\text{TSS}}^{-1} \text{ d}^{-1}$	$0.1 \text{ g}_{\text{COD}} \text{ g}_{\text{TSS}}^{-1} \text{ d}^{-1}$ $0.08 \text{ g}_{\text{N}} \text{ g}_{\text{TSS}}^{-1} \text{ d}^{-1}$
	HRT	4 h, 8 h and 12 h		5 h

### II.2.3.2. Operation of the SBRs

The settings of SBRs were presented in Table II.5. SBR- 3 d and 10 d were tested with three different duration of HRT (4, 8 and 12 h), whereas SBR-20 d was tested only with HRT of 4 h (Table II.4). Each kinetics experiment of SRT and HRT combinations was duplicated 3 times (number of replicates = 3). It has to be emphasized that here the HRT corresponds to hydraulic retention time applied for the kinetics experiments that were performed in a batch mode. Typical operational HRT for SBRs between kinetics experiments was set to 4 h.

The setups of SRT- 3 d, HRT- 4 h; SRT- 3 d, HRT- 8 h and SRT- 3 d, HRT- 12 h were set at the low-end SRT of a conventional biological wastewater treatment. The operating conditions of the setups of SRT- 10 d, HRT- 4 h and SRT- 10 d, HRT- 8 h are consistent with a conventional activated sludge process (HRT: 4-8 h and SRT: 5-15 d). The conditions of SRT- 10 d, HRT- 8 h and SRT- 20 d, HRT- 4 h are typically similar to those of the activated sludge approach applied with long sludge retention times to remove biodegradable organics (SRT: 10-30 d) (Tchobanoglous et al., 2002).

SBR-10 d was also used for experiments with various biomass concentrations. The following TSS concentrations were tested – 3, 5 and 8  $\text{g}_{\text{TSS}} \text{L}^{-1}$  and also repeated 3 times per experimental condition.

Table II. 5. Operating schedule of SBRs.

	Operating times in each cycle								Treated wastewater (L d <sup>-1</sup> )
	SRT (d)	HRT (h)	Total duration (d)*	Filling (min)	Reaction (min)	Settling (min)	Drawing (min)	# of cycles (d <sup>-1</sup> )	
<b>SBR-3 d</b>	3	4	30	5	170	60	5	6	30
		8	30	5	410	60	5	3	15
		12	30	5	650	60	5	2	10
<b>SBR-10 d</b>	10	4	30	5	170	60	5	6	30
		8	30	5	410	60	5	3	15
		12	30	5	650	60	5	2	10
<b>SBR-20 d</b>	20	4	30	5	170	60	5	6	30

\*: Actual kinetics periods. These periods include transition period between phases.

### II.2.3.3. Sludge inoculum

The activated sludge withdrawn from the previously described WWTPs was inoculated in each column of SBRs. In order to remove potential residues of micropollutants from the withdrawn sludge, the following washing procedure was applied. The biomass was separated from the water phase by centrifugation at 4000 rpm for 10 min, the supernatant was discarded, and the biomass was re-suspended with tap water. The procedure was performed twice. After the second re-suspension, the biomass was used as inoculum for the SBRs. During kinetics experiments the initial biomass concentration in SBRs was  $\sim 3 \text{ g}_{\text{TSS}} \text{ L}^{-1}$ . For kinetic experiments, the biomass concentrations ( $\text{g L}^{-1}$ ), ratio of  $C_{\text{VSS}}$  to  $C_{\text{TSS}}$  ( $\beta$  (%)), the dissolved oxygen ( $\text{mg L}^{-1}$ ), the pH and T ( $^{\circ}\text{C}$ ) were measured and compiled in Table II.6.

**Table II. 6.** Mean values of biomass concentration ( $\pm$  standard error), ratio of  $C_{\text{VSS}}$  to  $C_{\text{TSS}}$  ( $\beta$ ), dissolved oxygen (DO), pH and T ( $^{\circ}\text{C}$ ) in the three SBRs during seven experimental setups.

SRT (d)	3	3	3	10	10	10	20
HRT (h)	4	8	12	4	8	12	4
Biomass concentration ( $\text{g L}^{-1}$ )	3.3 $\pm 0.1$	3.3 $\pm 0.1$	3.2 $\pm 0.1$	3.0 $\pm 0.1$	3.3 $\pm 0.1$	3.1 $\pm 0.1$	3.5 $\pm 0.1$
$\beta$ (%)	70	72	71	79	77	79	81
DO ( $\text{mg L}^{-1}$ )	2.5	2.4	2.2	4.4	4.3	4.2	4.4
pH	8.1	8.1	8	7.5	7.8	7.9	8
T ( $^{\circ}\text{C}$ )	20.1	19	19	18.1	18	18	19.5

### II.2.3.4. Synthetic wastewater

Synthetic wastewater (SWW) containing sodium acetate as a carbon and energy source and ammonium bicarbonate as a nitrogen source was used. Detailed composition of synthetic wastewater was presented in Table II.7.

**Table II. 7.** Composition of the synthetic wastewater and supplementary solutions I and II.

Synthetic wastewater (SWW)	Concentration (mg L <sup>-1</sup> )		
	SWW1 (SBR-3 d)	SWW2 (SBR-10 d)	SWW3 (SBR-20 d)
CH <sub>3</sub> COONa	1200	500	100
NH <sub>4</sub> HCO <sub>3</sub>	75	75	75
KH <sub>2</sub> PO <sub>4</sub>	5	5	5
MgSO <sub>4</sub> .7H <sub>2</sub> O	50	50	50
CaCl <sub>2</sub> .2H <sub>2</sub> O	21	21	21
NaHCO <sub>3</sub>	36	36	36
Supplementary solution I			
C <sub>10</sub> H <sub>6</sub> N <sub>2</sub> O <sub>8</sub>	50	50	5
FeSO <sub>4</sub> .7H <sub>2</sub> O	20	20	2
Supplementary solution II			
C <sub>10</sub> H <sub>6</sub> N <sub>2</sub> O <sub>8</sub>	20	20	20
ZnSO <sub>4</sub> .7H <sub>2</sub> O	0.43	0.43	0.43
CoCl <sub>2</sub> .6H <sub>2</sub> O	0.24	0.24	0.24
MnCl <sub>2</sub> .4H <sub>2</sub> O	1	1	1
CuSO <sub>4</sub> .5H <sub>2</sub> O	0.25	0.25	0.25
NaMoO <sub>4</sub> .2H <sub>2</sub> O	0.22	0.22	0.22
NiCl <sub>2</sub> .6H <sub>2</sub> O	0.19	0.19	0.19
NaSeO <sub>4</sub> .10H <sub>2</sub> O	0.21	0.21	0.21
H <sub>3</sub> BO <sub>4</sub>	0.14	0.14	0.14

#### II.2.3.5. Adjustment of SRT

The target SRTs were maintained manually by adjustment of biomass concentration in SBRs at the end of the aeration period. The volume of sludge withdrawn was calculated according to Henze, 2008 (see Eq.I-3).

#### II.2.3.6. $k_{La}$ measurement and estimation

As the oxygen concentration changed in different SBRs during the experiments in different SBRs-3, 10 and 20 d, it was supposed to measure the  $k_{La}$  in different systems. Moreover, in order to ensure the growth of the biomass in the reactor, it is necessary to have a sufficient dissolved oxygen concentration  $\geq 2 \text{ g}_{\text{O}_2} \text{ m}^{-3}$  (which corresponds to the Flemish WWTP operation practice) for



different setups, and an oxygen transfer denotes  $k_{LA}$  sufficiently high ( $> 3 \text{ h}^{-1}$ ). Therefore, the  $k_{LA}$  was measured without the presence of activated sludge so that to test the operation of the aerators connected to each SBR. The used method for the determination of  $k_{LA}$  was by the deoxygenation with  $\text{N}_2$  and reoxygenation of the reactor in absence of microorganisms. Prior to inoculation of the activated sludge in each of the three SBRs,  $k_{LA}$  was measured in the clear water of each reactor separately at the same airflow of  $2 \text{ L min}^{-1}$ . The procedure was performed according to Finn (1954). The input of atmospheric oxygen via the liquid surface was taken into account in the model used for simulation between different sludge age (SRTs-3 d, 10 d and 20 d) in chapter IV.

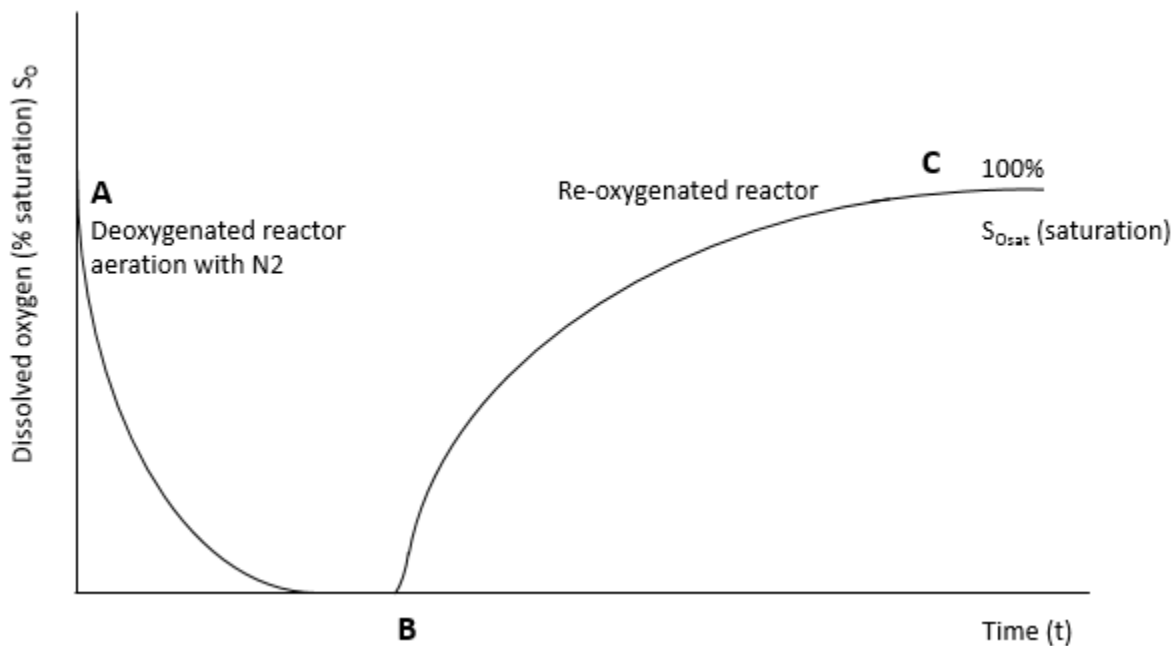


**Figure II. 3.** Method of determination of  $k_{LA}$  by de-oxygenation re-oxygenation, in absence of biomass.

In the absence of microorganisms, the kinetics of the re-oxygenation phase (between B and C on the Figure II.3) obeys the following mass balance equation Eq. (II-1):

$$\frac{dS_o}{dt} = k_L a (S_{O,sat} - S_o) \quad (\text{II-1})$$

where  $S_o$  is the dissolved oxygen concentration in the water supposed perfectly homogenized ( $\text{g L}^{-1}$ ),  $S_{O,sat}$  is the dissolved oxygen concentration ( $\text{g L}^{-1}$ ) in water at saturation with

the gas phase.  $k_L a$  is the product of the coefficient  $k_L$  (global exchange coefficient for  $O_2$  ( $m\ s^{-1}$ ) in the double film theory, on liquid side) and the coefficient "a" (specific exchange area reduced to the volume unit of liquid phase of culture medium, in  $m^2$  per  $m^3$  of culture medium).  $k_L a$  is called volumetric transfer coefficient based on the volume unit of medium in ( $time^{-1}$ ).

By integrating this equation between  $t_0$  and  $t$  and  $S_{O_0}$  and  $S_O$ , the general equation (II-2) is obtained.

$$k_L a (t - t_0) = \ln(S_{O_{sat}} - S_{O_0}) - \ln(S_{O_{sat}} - S_O) \quad (II-2)$$

- a- If at restart of re-oxygenation, point B,  $t = 0$  and  $S_{O_0} = 0$  then we can plot  $\ln(S_{O_{sat}} - S_O)$  vs time and thus, we obtain a slope equal to  $-k_L a$  and the intercept at  $\ln(S_{O_{sat}})$
- b- If at restart of re-oxygenation, point B,  $t = 0$  and  $S_{O_0} \neq 0$  then we can plot  $\ln(S_{O_{sat}} - S_O)$  vs time and thus, we obtain a slope equal to  $-k_L a$  and the intercept at  $\ln(S_{O_{sat}} - S_{O_0})$ .

- **$k_L a$  estimation**

Figure II.4 shows the  $\ln(S_{O_{sat}} - S_O)$  curve versus time and the result of a linear regression on each curve of the different setups. The displayed slopes were 0.1551, 0.1642 and 0.1683 for the SBR-3 d, SBR-10 d and SBR-20 d, respectively. It can be noted that in SBR-20 d of  $k_L a = 10.1\ h^{-1}$ , a slightly greater oxygen transfer was observed compared to that in SBR-10 d ( $k_L a = 9.9\ h^{-1}$ ) and SBR- 3 d ( $k_L a = 9.3\ h^{-1}$ ). Based on these results, we decided to add a second aerator (3 cm long rectangular diffuser) similar for the different setups in order to provide the same aeration conditions. Moreover, the  $k_L a$  results will be useful for the simulation of the batch systems in chapter IV.

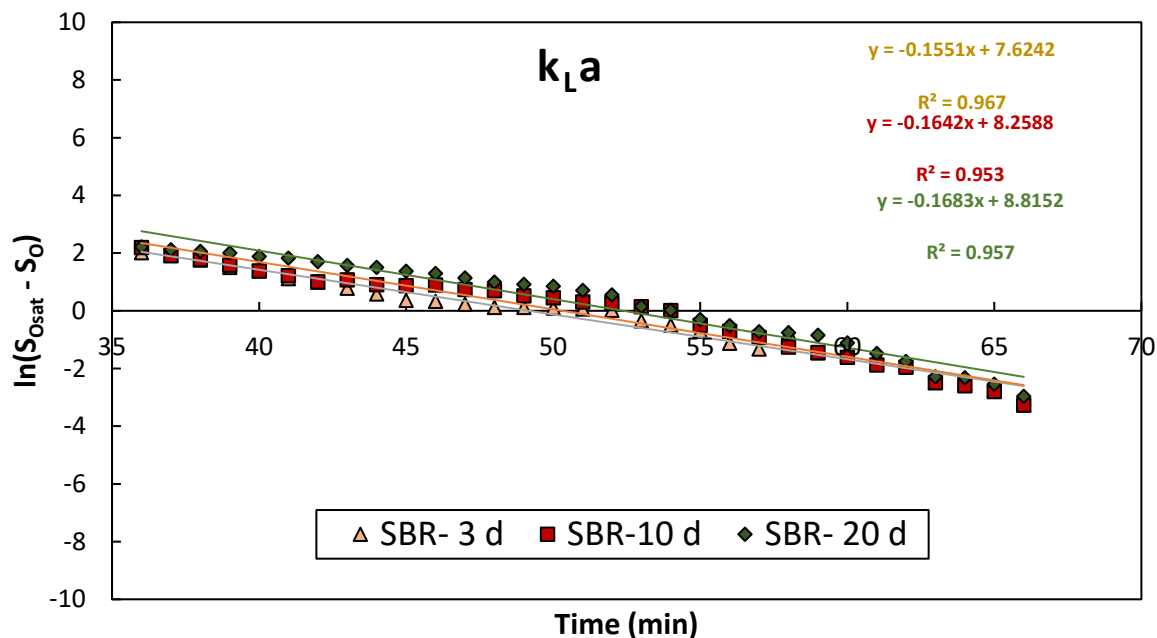


**Figure II. 4.**  $\ln(S_{O_{sat}} - S_O)$  curve versus time for  $k_{La}$  estimation in SBRs-3 d, 10 d and 20d.

#### II.2.4. Kinetics of micropollutants' removal in SBR

Most of the selected compounds are frequently detected in wastewater influents in concentrations from  $\leq 0.1 \mu\text{g L}^{-1}$  -  $10 \mu\text{g L}^{-1}$  (Guerra et al., 2014; Luo et al., 2014; Miège et al., 2009; Santos et al., 2009; Sui et al., 2010; Verlicchi et al., 2012). In order to unify the used approach, we decided to use the concentration of  $1 \mu\text{g L}^{-1}$  for all the compounds, which is in the middle of this range. In Tables II.5, the kinetics experiments were performed in a batch mode with the fixed values of SRT, HRT and  $C_{TSS}$ .

Before each kinetics experiment, microorganisms of activated sludge were fed with synthetic wastewater spiked with MPs mix ( $1 \mu\text{g L}^{-1}$  each) for 7 days, to facilitate their adaptation to anthropogenic contaminants. The complete cycles time between the SBRs acclimatization and the beginning of the first kinetic experiment spanned 35 days. Afterwards, to ensure identical initial concentration of MPs at the beginning of the kinetics experiment, 5 L/cycle of bulk water was replaced by fresh SWW (without MPs) 24 hours before removal study. At the beginning of the kinetics experiment, reactors were spiked directly with a fresh mix solution of MPs of

concentration  $1\mu\text{g L}^{-1}$  and samples were collected at fixed time points during the aeration phase of all tested setups.

### II.2.5. Apparent-first-order kinetics estimation

The rate of micropollutants' removal is usually considered to be directly proportional to both micropollutant and biomass concentrations. As a consequence, the reaction should follow a second-order kinetics (Eq.II-3). However, this kinetic law was called pseudo-first order approach in recent studies since the biomass is not considered as a limiting factor. Generally,  $k_{\text{biol}}$  also called  $k$  ( $\text{L g}_{\text{TSS}}^{-1} \text{h}^{-1}$ ) is defined as an experimental elimination rate constant normalized to  $C_{\text{TSS}}$ . In the literature, relatively small fluctuations of  $C_{\text{TSS}}$  are often assumed and, therefore negligible effect on the treatment process too, which leads to the apparent-first-order kinetics (Eq.II-4). This approach is applied in this present study. The apparent-first-order removal rate constant expressed as  $k'$  ( $\text{h}^{-1}$ ), was derived from the fitting of the analytical solution of Eq. (II-4) to the measured data of each of the seven experimental setups and no normalization to biomass concentration was applied. The analytical solution describing apparent-first order MP's removal evolution with time is given in Eq. (II-5). The actual effect of biomass concentration on kinetics of MPs removal is discussed in Section II.3.5.

$$r_{\text{MPs}} = -k C_{\text{TSS}} C_{\text{MPs}} \quad (\text{II-3})$$

$$r_{\text{MPs}} = -k' C_{\text{MPs}} \quad \text{with } k' = k C_{\text{TSS}} \quad (\text{II-4})$$

$$C_{\text{MPs}}(t) = C_0 e^{-k't} \quad (\text{II-5})$$

where  $r_{\text{MPs}}$  is the removal rate ( $\mu\text{g L}^{-1} \text{h}^{-1}$ ),  $k$  is the removal rate constant ( $\text{L g}^{-1} \text{h}^{-1}$ ),  $C_{\text{MPs}}$  is the dissolved micropollutant concentration at time  $t$  ( $\mu\text{g L}^{-1}$ ),  $t$  is the time (h),  $C_{\text{TSS}}$  is the total biomass concentration ( $\text{g L}^{-1}$ ),  $k'$  is the apparent-first order removal rate constant ( $\text{h}^{-1}$ ) without normalization to  $C_{\text{TSS}}$ , and  $C_0$  is the initial concentration of MPs  $\sim 1 \mu\text{g L}^{-1}$ .

### II.2.6. Nitrification capacity (NC)

The nitrification capacity (NC %) was calculated for each HRT using the nitrate concentrations at the beginning ( $[\text{N-NO}_3^-]_i$ ) and at the end of the cycle ( $[\text{N-NO}_3^-]_f$ ):

$$\text{NC (\%)} = \frac{[\text{N-NO}_3^-]_f - [\text{N-NO}_3^-]_i}{[\text{N-NO}_3^-]_f} \mathbf{100} \quad \text{(II-6)}$$

### II.2.7. Analytical methods

#### II.2.7.1. Quantification of MPs by LC-MS/MS

All samples were filtered through 0.45  $\mu\text{m}$  polyethersulfone syringe filters (PES, Macherrey-Nagel, Germany). 100  $\mu\text{L}$  of each sample were transferred into an amber vial containing 900  $\mu\text{L}$  of MilliQ water and preserved at 4  $^\circ\text{C}$  until analysis (not longer than 12 h). Applied dilution decreased the effect of wastewater matrix that could interfere with the MPs measurement. Analytes were quantified using an Agilent 1290 Infinity II UHPLC system coupled to an Agilent 6470 Triple Quadrupole MS system via an Agilent Jet Stream electrospray ionization source. Separation was performed on an Agilent ZORBAX Eclipse Plus C-18 column (50  $\times$  2.1 mm, 1.8  $\mu\text{m}$  particle size) with a gradient flow of two eluents – ultra pure water [A] and acetonitrile [B] - both acidified with 0.05 % formic acid and a flow rate of 0.3  $\text{mL min}^{-1}$ . The following gradient program was applied (Time [min] / B [%]: 0/5, 4.2/95, 5.6/95, 5.8/5, 8.5/5). To minimize the variation of the compounds ionization during individual runs, samples were spiked with labelled internal standards (listed in section II.2.2.3) before injection for the calculation of the normalized area (i.e., the ratio between the peak area of the analytes of interest and the peak area of the internal standard of the corresponding parent compound). Detection of positive and negative ions was performed in dynamic multi-reaction monitoring (MRM) mode. To maintain high quality of the measurement, the series of measured samples contained also blank samples constituted of ultra-pure water to track possible carry-over. Quality assurance samples containing the 500  $\mu\text{g L}^{-1}$  of individual analytes were also utilized to verify the accurate performance of the device. External calibration was applied in the range of 1-1000  $\text{ng L}^{-1}$ . Measured concentrations of micropollutants were

plotted against the sampling time points including the applied dilution. Settings of the mass spectrometer were collected in Tables II.S1 and II.S2 of the Supplementary Information (SI).

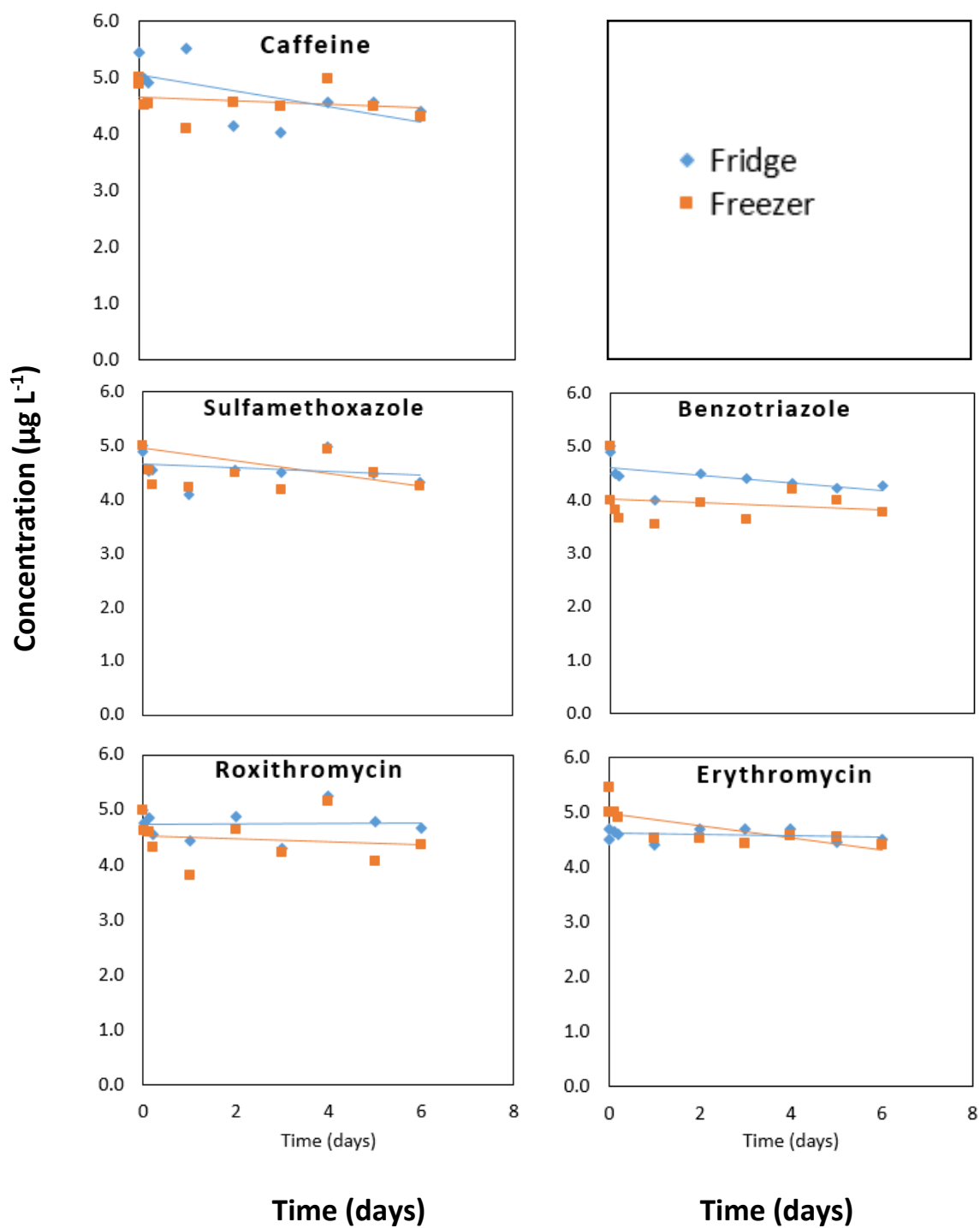
#### II.2.7.2. *Measurement of basic chemical parameters of wastewater*

During the kinetics studies, a volume of 30 mL of sludge mixed with synthetic wastewater was collected hourly for analyses of ammonium ( $\text{N-NH}_4^+$ ), nitrate ( $\text{N-NO}_3^-$ ), and phosphate ( $\text{P-PO}_4^{3-}$ ) concentrations, as well as for the determination of COD. Ammonium concentration was determined using a 881 Compact IC pro – Anion (Metrohm, Switzerland; detection limit of this instrument is  $0.3 \text{ mg}_{\text{N-NH}_4^+} \text{ L}^{-1}$ ). The nitrate and phosphate were quantified by ion chromatography (790 Personal IC, Metrohm, Switzerland; detection limit for nitrate  $0.5 \text{ mg}_{\text{N}} \text{ L}^{-1}$  and for phosphate  $1 \text{ mg}_{\text{P}} \text{ L}^{-1}$ ). Total chemical oxygen demand was measured using cuvette Hach test No. 514 (Hach Lange, Germany). Concentrations of TSS, effluent suspended solids (ETSS) and VSS were measured according to standard methods for the analysis of water and wastewater (APHA et al., 2012).

### II.3. Results and discussion

#### II.3.1. Sorption on wall's reactor

According to the Figure II.5, the removal of the caffeine, benzotriazole, sulfamethoxazole, roxithromycin, erythromycin, diclofenac and carbamazepine concentrations are almost stable, they have not been adsorbed on the wall of the reactor. Oppositely, the tetracycline and ciprofloxacin disappeared rapidly from the beginning of the reaction, it showed successive sorption for a week. Therefore, following the perception of ciprofloxacin and tetracycline, we decided to work on the seven listed above micropollutants. Moreover, no difference was observed between freezing and refrigeration conditions for all tested micropollutants.



(Continued on the next page)

Figure II. 5. Continued

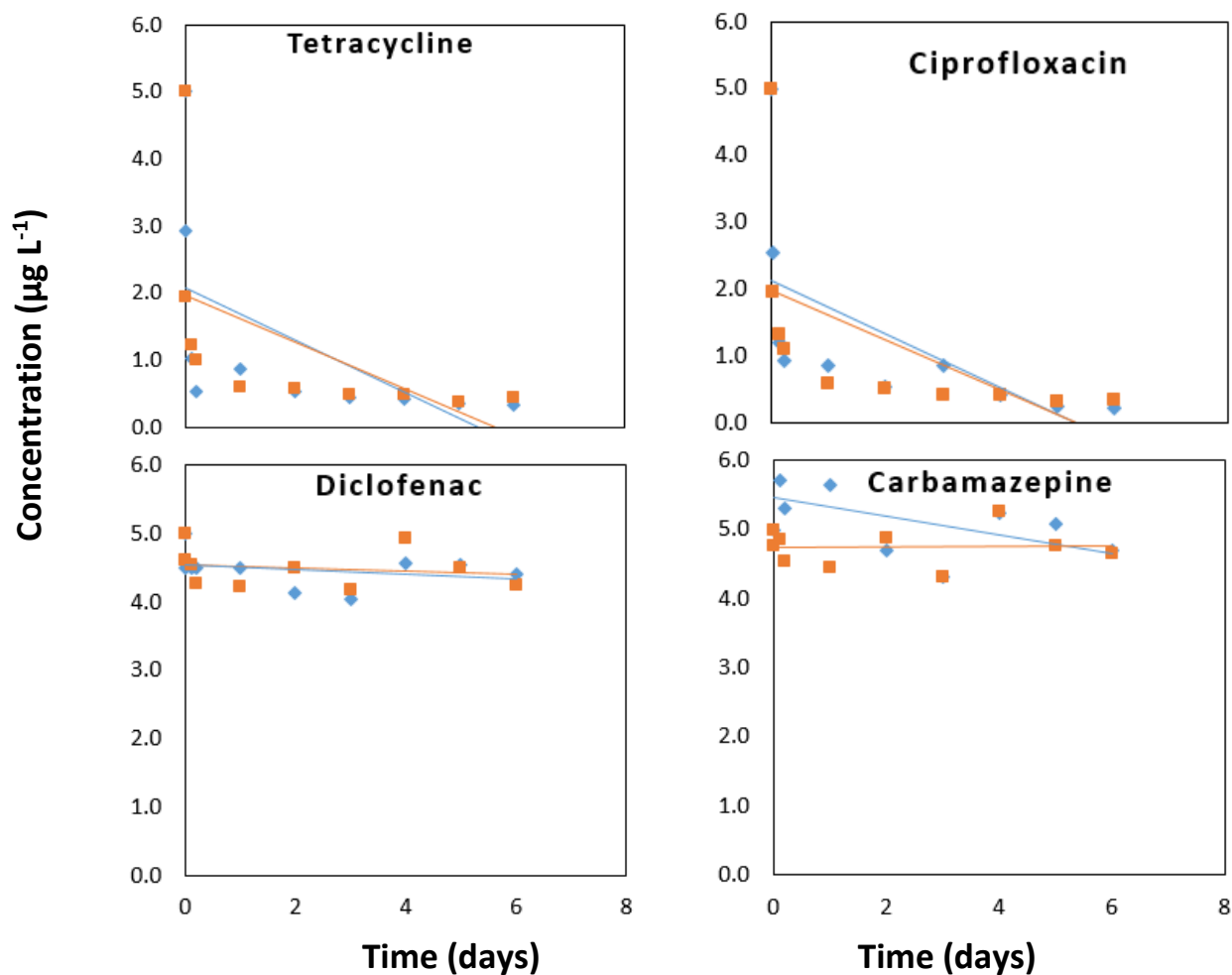


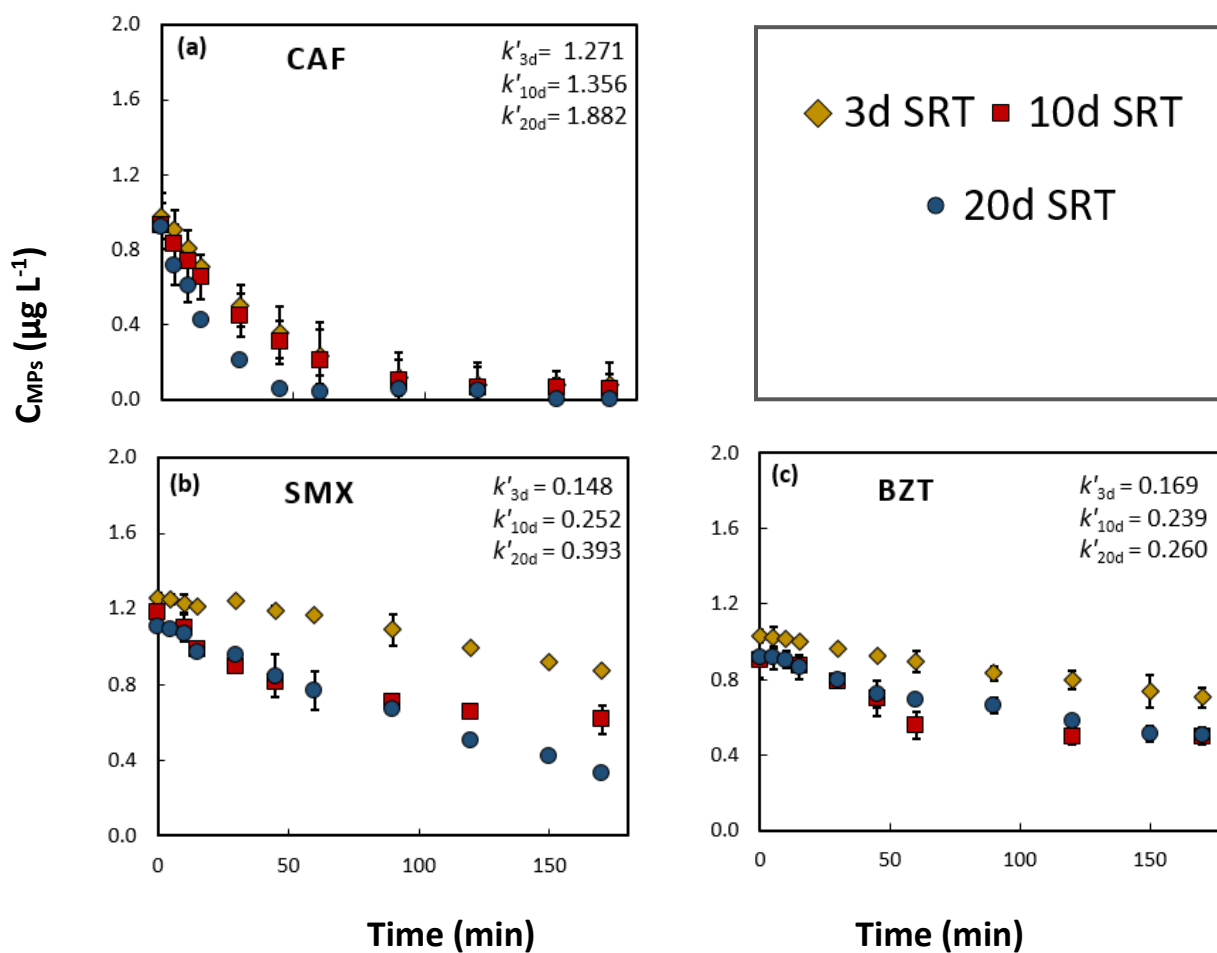
**Figure II. 5.** Sorption results of caffeine, sulfametoxazole, benzotriazole, roxithromycin, erythromycin, tetracycline, ciprofloxacin, diclofenac and carbamazepine on the wall of the reactor at both freeze and fridge conditions.

### II.3.2. Effect of SRT on MPs' elimination in activated sludge

The Figure II.6 displays the elimination profiles of the seven investigated micropollutants belonging to three different categories defined by the biodegradability of MPs. Caffeine is a highly biodegradable compound; sulfamethoxazole appears as a moderately biodegradable compound while diclofenac is a quite persistent compound. The estimated  $k'$  (h<sup>-1</sup>) values were obtained. They are reported in the Figure II.6 and are also collected in Table II.8. For all kinetics experiments,  $k'$  values and changes of  $k'$  are collected in Table II.8.



**Highly biodegradable compound.** As depicted in Figure II.6a and Table II.8, CAF was degraded efficiently in all three reactors. The high  $k'$  values of 1.271 ( $\pm 0.105$ ), 1.356 ( $\pm 0.101$ ) and 1.882 ( $\pm 0.032$ )  $\text{h}^{-1}$  obtained in SBR-3 d, SBR-10 d and SBR-20 d, respectively, indicated that the removal of CAF increased moderately with the SRT (increasing of 48 %). As a consequence, the removal constants  $k'$  by expanding sludge ages from 3 to 20 days was improved by 1.48.



(Continued on next page)

Figure II. 6. Continued

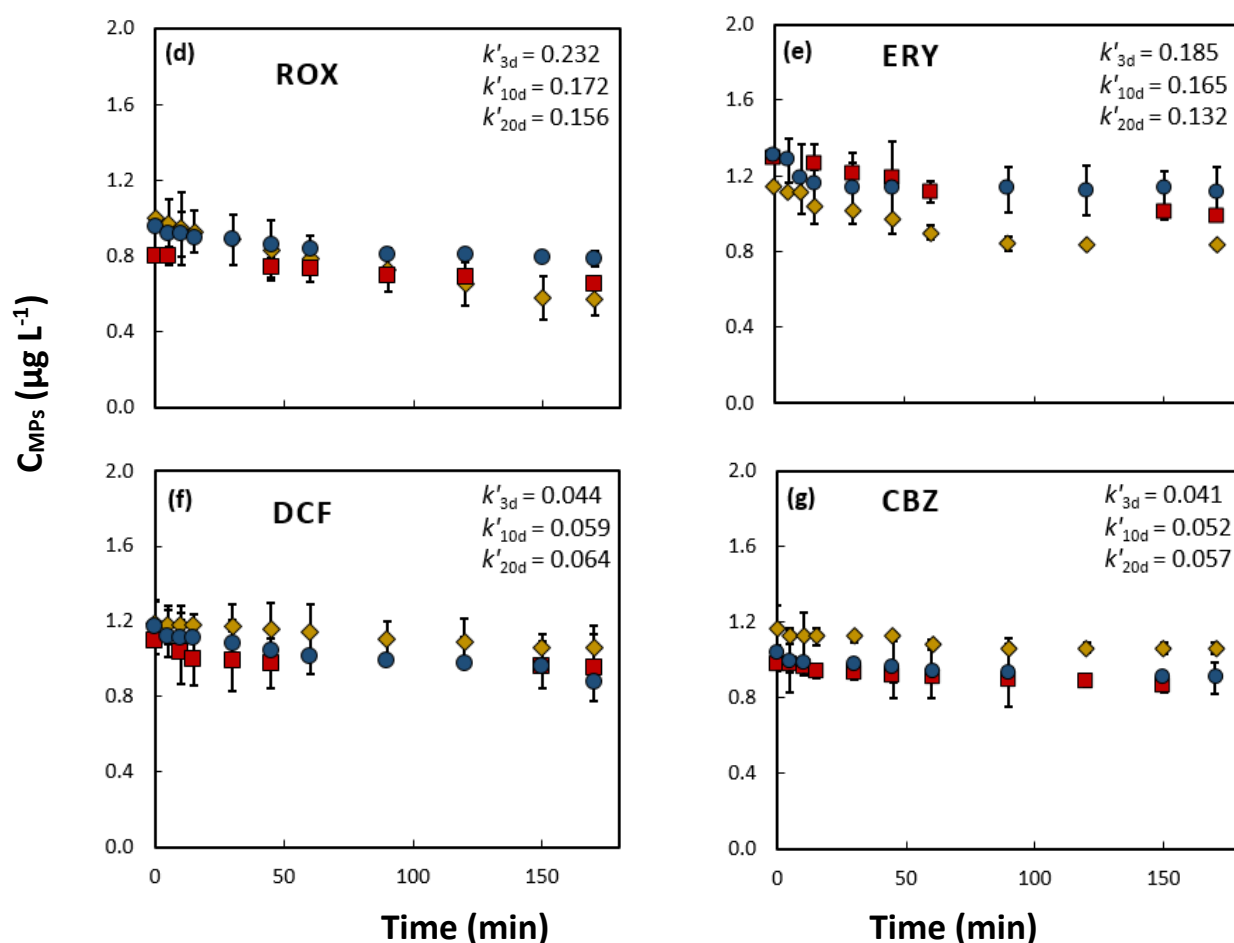


**Figure II. 6.** Removal of (a) CAF, (b) SMX and (c) BZT, (d) ROX, (e) ERY, (f) DCF and (g) CBZ at three different types of sludge age of 3 d, 10 d and 20 d at the HRT of 4 h;  $k'$  is the apparent-first order removal rate constant ( $\text{h}^{-1}$ ); number of replicates = 3; error bars indicate one standard error.

**Moderately biodegradable compounds.** Based on our experimental values of reaction rate constants, sulfamethoxazole can be classified as a moderately biodegradable compound. In SBR-20 d with  $k'_{20d} = 0.393 \pm 0.079 \text{ h}^{-1}$ , an increase of 165 % was observed compared to the removal in SBR-3 d ( $k'_{3d} = 0.148 \pm 0.025 \text{ h}^{-1}$ ). Therefore, the removal rates of SMX were significantly enhanced by the increase of SRT from 3 to 20 d.

**Table II. 8.** Apparent removal rate constant  $k'$  ( $\pm$  standard error) of investigated compounds at different types of sludge age\*, and changes of  $k'$  from: SRT- 3 d to SRT-20 d, 10 d to 20 d and 3 d to 20 d.  $C_{TSS} \sim 3 \text{ g}_{TSS} \text{ L}^{-1}$ .

Effect of SRT on apparent removal rate constant $k'$ ( $\text{h}^{-1}$ )							
HRT- 4 h							
Micropollutants	Degree of biodegradability	SRT- 3 d	SRT- 10 d	SRT- 20 d	Change of $k'$ from SRT-3 d to SRT-10 d	Change of $k'$ from SRT-10 d to SRT-20 d	Change of $k'$ from SRT-3 d to SRT-20 d
CAF	High	$1.271 \pm 0.105$	$1.356 \pm 0.101$	$1.882 \pm 0.032$	Increase by 1.07	Increase by 1.39	Increase by 1.48
SMX	Moderate	$0.148 \pm 0.025$	$0.252 \pm 0.042$	$0.393 \pm 0.079$	Increase by 1.70	Increase by 1.56	Increase by 2.66
BZT	Moderate	$0.169 \pm 0.036$	$0.239 \pm 0.043$	$0.260 \pm 0.039$	Increase by 1.41	Increase by 1.09	Increase by 1.54
ROX	Moderate	$0.232 \pm 0.156$	$0.172 \pm 0.036$	$0.156 \pm 0.024$	Decrease by 1.35	Decrease by 1.10	Decrease by 1.35
ERY	Moderate	$0.185 \pm 0.020$	$0.165 \pm 0.090$	$0.132 \pm 0.123$	Decrease by 1.12	Decrease by 1.25	Decrease by 1.48
DCF	Low	$0.044 \pm 0.121$	$0.059 \pm 0.148$	$0.064 \pm 0.138$	Increase by 1.34	Increase by 1.08	Increase by 1.45
CBZ	Low	$0.041 \pm 0.047$	$0.052 \pm 0.093$	$0.057 \pm 0.094$	Increase by 1.27	Increase by 1.09	Increase by 1.39

\* determined in the SBRs operated at HRT of 4 h

The BZT removal (Table II.8 and Figure II.6c) was also affected by the SRT. The calculated  $k'$  values were equal to  $0.239 \pm 0.043 \text{ h}^{-1}$  and  $0.169 \pm 0.036 \text{ h}^{-1}$ , for SRT-10 d and SRT-3 d, respectively. This corresponded to an increase of 41 %. On the opposite, a slight improvement of 8.8 % was observed between reactors operated from SRT 10 d to 20 d. Thus, these results confirmed the existence of a critical SRT around 10 days below which BZT elimination might be low. The partial removal of BZT has also been reported in studies of full-scale WWTPs (Weiss et al. 2006; Stasinakis et al. 2013).

The removal of both antibiotics ROX and ERY (Figure II.6d and Figure II.6e) exhibited a different behaviour. The removal rate constants decreased for higher SRTs of 10 d and 20 d. In other words, the performance of SBR-3 d with respect to ROX ( $k'_{3d} = 0.232 \pm 0.156 \text{ h}^{-1}$ ) and ERY ( $k'_{3d} = 0.185 \pm 0.020 \text{ h}^{-1}$ ) was found to be larger than in SBR operated at high SRT, i.e. 20 d ( $k'_{20d} = 0.156 \pm 0.024$ ;  $0.132 \pm 0.123 \text{ h}^{-1}$ ). Li and Zhang (2010) showed that the maximum removals recorded for both ROX and ERY was 40-46 % and 15-26 % for SRT < 10 d, respectively. Louvet et al. (2010) showed that the erythromycin toxicity was observed at low concentration of  $4 \mu\text{g L}^{-1}$  which inhibited the growth of fragile biomass and the removal of  $\text{N-NH}_4^+$ , and hence bothered the WWTP efficiency.

**Persistent compounds.** The removal of DCF and CBZ was low in all tested types of activated sludge. In general, the SRT had a minor influence on the removal rate of persistent compounds, which do not exceed the standard error in SBRs-3 d and 10 d, for both compounds (Figures II.6f and II.6g). Moreover, an increase of  $k'$  (1.45 and 1.39) was recorded with increasing the SRT from 3 d to 20 d for DCF and CBZ, respectively. In the case of CBZ, Zhang et al. (2008) did not observe any CBZ removal by CAS even at SRT of 100 days. For DCF, the data provided in the literature were not so consistent. Vieno and Sillanpää (2014) reported that DCF removal was 8–38 % when SRT was 20–48 d, 59 % at SRT of 62 d and 53 % at SRT of 322 d. The low removal efficiency is also in agreement with the work of Joss et al. (2005), in which they reported no enhancement of DCF removal even when extreme duration of SRT (> 60 d) was applied. The authors suggested that DCF persistence in the effluent of the WWTP could be due to a chlorine atom in the structure. Also, formation of nitro diclofenac ( $\text{NO}_2\text{-DCF}$ ) in activated sludge could give false positive results (Vieno and Sillanpää, 2014). Regarding CBZ, its persistence can be

attributed to its physicochemical properties such as molecular structure and hydrophilicity (Cirja et al. 2008; Luo et al. 2015). In general, simple structured compounds, especially without branched/multi-chain groups, are readily degradable (Tadkaew et al. 2011). Moreover, compounds containing an electron withdrawing functional groups (EWG), such as carboxyl, halogens and amides, are resistant to biological treatment. Indeed, CBZ contains amide group that makes it resistant to biodegradation. Therefore, the persistence of DCF and CBZ seem to be independent from the sludge age, and it is more likely due to the individual properties of these compounds.

In general, as suggested by Joss et al. (2006), the enhancement of the micropollutants removal could be explained by the slight changes in biomass physiology and/or biomass quantity between different types of sludge (setups of SRT- 3 d, HRT-4 h; SRT- 10 d, HRT-4 h and SRT- 20 d, HRT- 4 h, Table II.5). Tiwari et al. (2017) reported that population balance of filamentous and floc-framing microorganisms upholds the growth of steady and solid flocs at high SRT. In our study, for SMX, BZT, DCF and CBZ, the increase in  $k'$  is more pronounced from SRT 3 d to SRT 10 d than from SRT 10 d to SRT 20 d (Table II.8).

- **Nitrification capacity (NC) and MP's removal**

Low nitrification capacity of 28 % was achieved in SBR - 3 d (Figure II.7). This can be explained by the slow growth of nitrifying bacteria (Henze et al. 2000). Similarly, the study of Ribeiro et al. (2018) showed that incomplete nitrification occurs at critical SRT of 5 d and limited DO concentration. Higher nitrification capacities of 55 % and 96 % were measured in moderate and high SRTs of 10 d and 20 d, respectively. For CAF, SMX, BZT, DCF and CBZ, nitrification capacities seem correlated to  $k'$  for the various SRTs tested (3 d, 10 d and 20 d). However, the apparent correlation between NC and  $k'$ , should be the consequences of the fact that the biomass diversity increases when the SRT is enhanced. This larger diversity produces the increase of both  $k'$  and the nitrification capacity (Figure II.7).

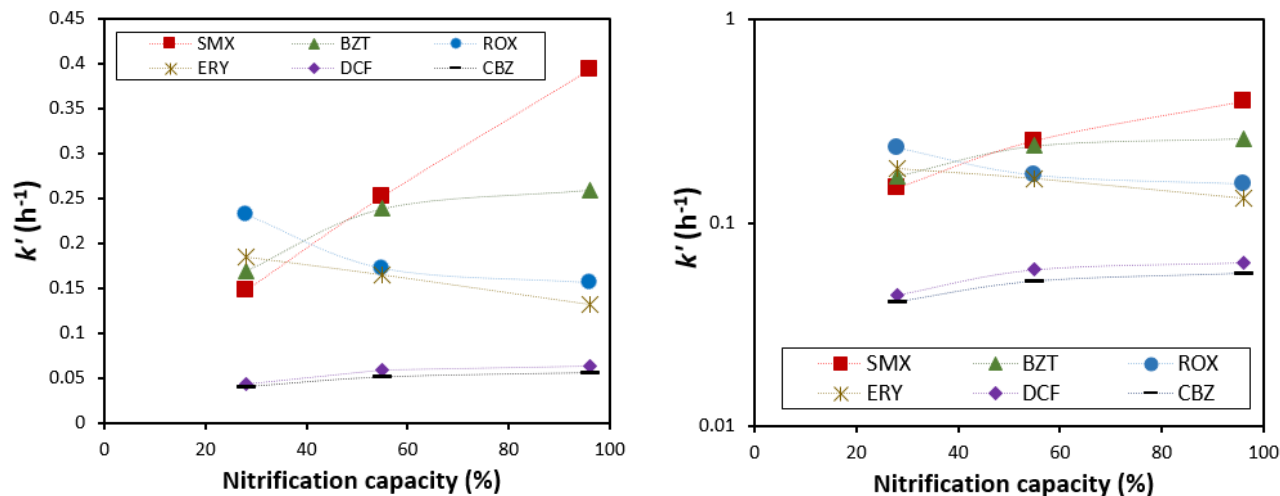


**Figure II. 7.** Linear (on the left side) and logarithmic (on the right side) scales of the correlation between the nitrification capacities (%) and the apparent constants  $k'$  ( $h^{-1}$ ) of SMX, BZT, ROX, ERY, DCF and CBZ estimated at different three different sludge ages (3 d, 10 d and 20 d) at HRT of 4 h. Nitrogen load -  $0.08 g_N g_{TSS}^{-1} d^{-1}$ .

- **Wastewater parameters analysis**

To monitor the general performance of the reactors, standard wastewater parameters were measured in all of the reactors, such as COD, nitrogen and phosphorus at different HRTs (Figure II.8). During the operation periods, all reactors reached effluent COD lower than  $10 mg L^{-1}$  at high HRTs with complete nitrification in SBRs - 10 days and 20 days at low to high HRTs as well.

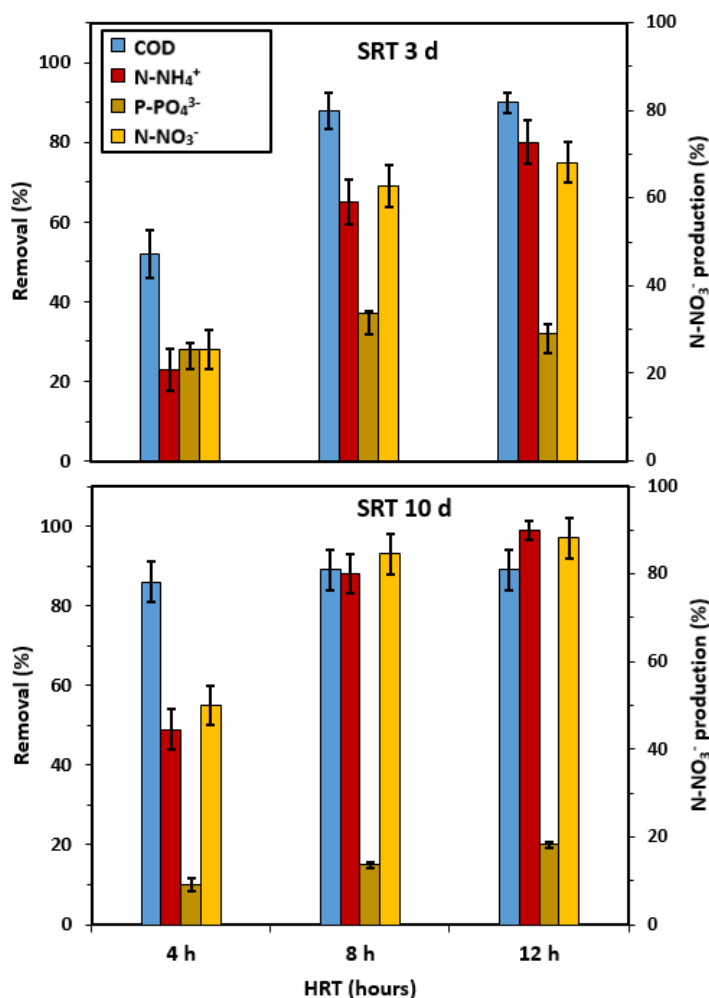


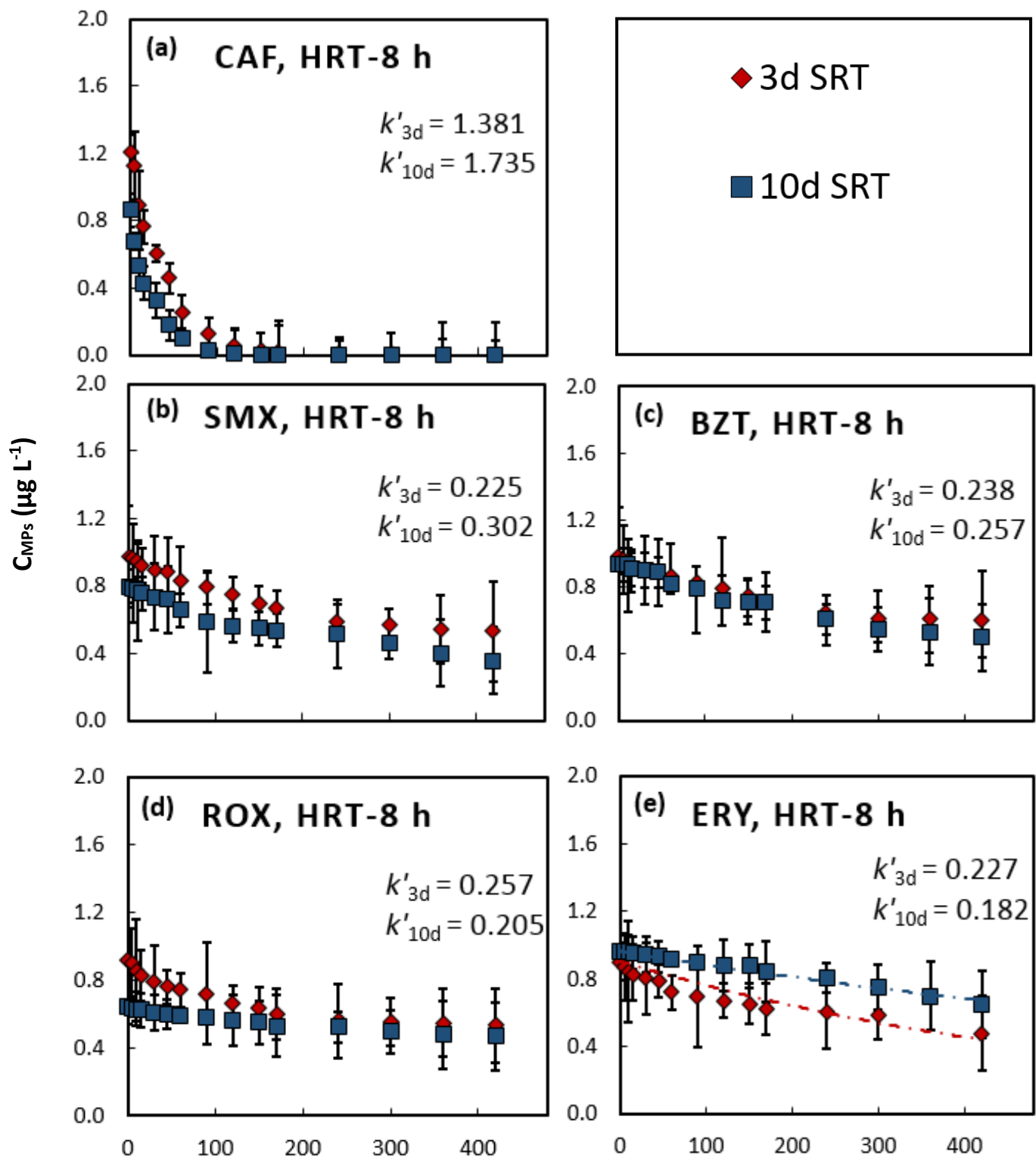
**Figure II. 8.** Removal efficiencies of wastewater parameters (COD, N-NH<sub>4</sub><sup>+</sup> and P-PO<sub>4</sub><sup>3-</sup>) and nitrate-nitrogen production over 4 h, 8 h and 12 h HRT for SRT – 3 d and SRT - 10 d (error bars present standard error).

### II.3.3. Influence of HRT on MPs' elimination in activated sludge

All investigated micropollutants' removal plots at higher HRTs of 8 h and 12 h in both SBRs– 3 d and 10d were presented in Figures II.9 and II.10, respectively. An overview of apparent-first order constants ( $k'$ ) obtained for each MP for various HRT were compiled in the Table II.9. The discussion is based on the comparison of the variation of  $k'$  for HRT from 4 h to 8 h, from 8 h to 12 h, and then from 4 h to 12 h with both sludge ages of 3 d and 10 d, respectively. For all studied compounds, the apparent constants increase with increasing HRT. The highest increase by

2.17 of  $k'$  was observed for SMX with the improvement of HRT from 4 h to 12 h in SBR-3 d. In comparison, in SBR-10 d, the increase of the constant is equal to 1.57. It is important to note that the enhancement of  $k'$  between HRT of 4 h and 8 h is not similar to that estimated between 8 h and 12 h. Therefore, the increase of  $k'$  is not proportional to the increase of HRT for the same sludge age. By calculating the  $k'$  changes between HRT of 8 h and 12 h, the removal of SMX and BZT was multiplied by 1.42 and 1.11, respectively, at the corresponding SRT of 3 d. The change of  $k'$  was multiplied by 1.31 and 1.35 by increasing HRT up to 12 h in SBR operated at SRT 10 d, respectively. In contrast, Li and Zhang (2010) reported a lower  $k'$  value of  $0.0052 \text{ h}^{-1}$  for SMX recorded at SRT of 7 days and HRT of 17 h than that reported in the present study. For both macrolides (ROX and ERY), increasing the HRT from 4 h to 12 h, resulted in an increase of  $k'$  values by 1.39 ( $k'$  at HRT of 4 h =  $0.232 \text{ h}^{-1}$  and  $k'$  at HRT of 12 h =  $0.322 \text{ h}^{-1}$ ) and by 1.42 ( $k'$  at HRT of 4 h =  $0.185 \text{ h}^{-1}$  and  $k'$  at HRT of 12 h =  $0.262 \text{ h}^{-1}$ ) in SBR-3 d for ROX and ERY, respectively. The same trend was observed in SBR operated at 10 d, but with higher increasing by 1.46 for ROX than by 1.34 for ERY, respectively. The low removal of diclofenac and carbamazepine was not significant during the studied HRTs, regardless of the type of sludge (Figures II.9 and II.10).





(Continued on the next page)

Figure II. 9. Continued

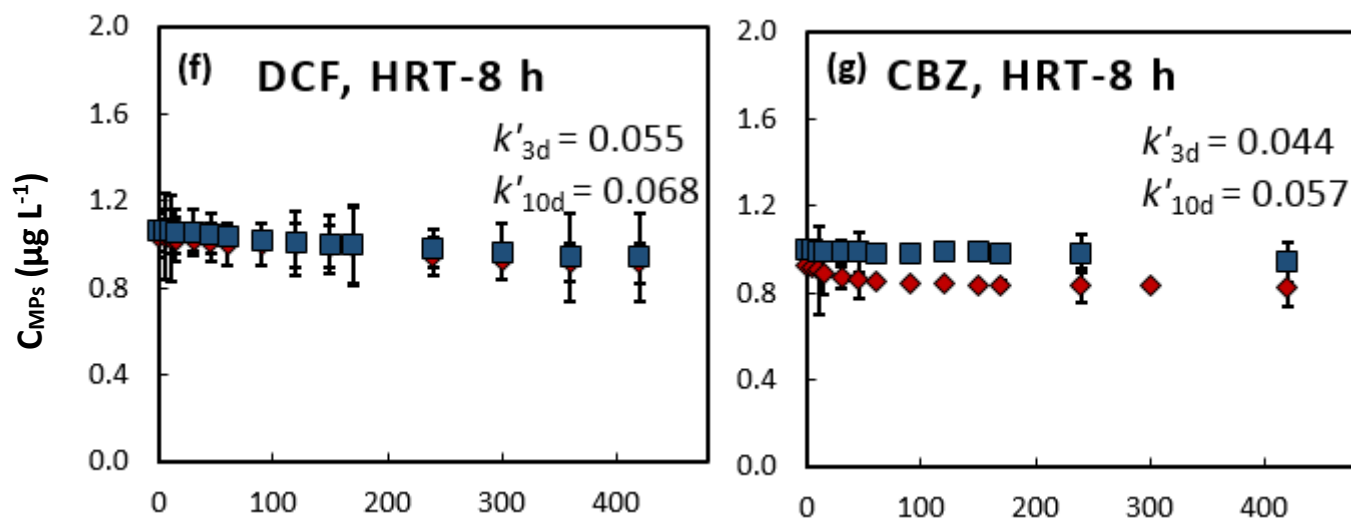
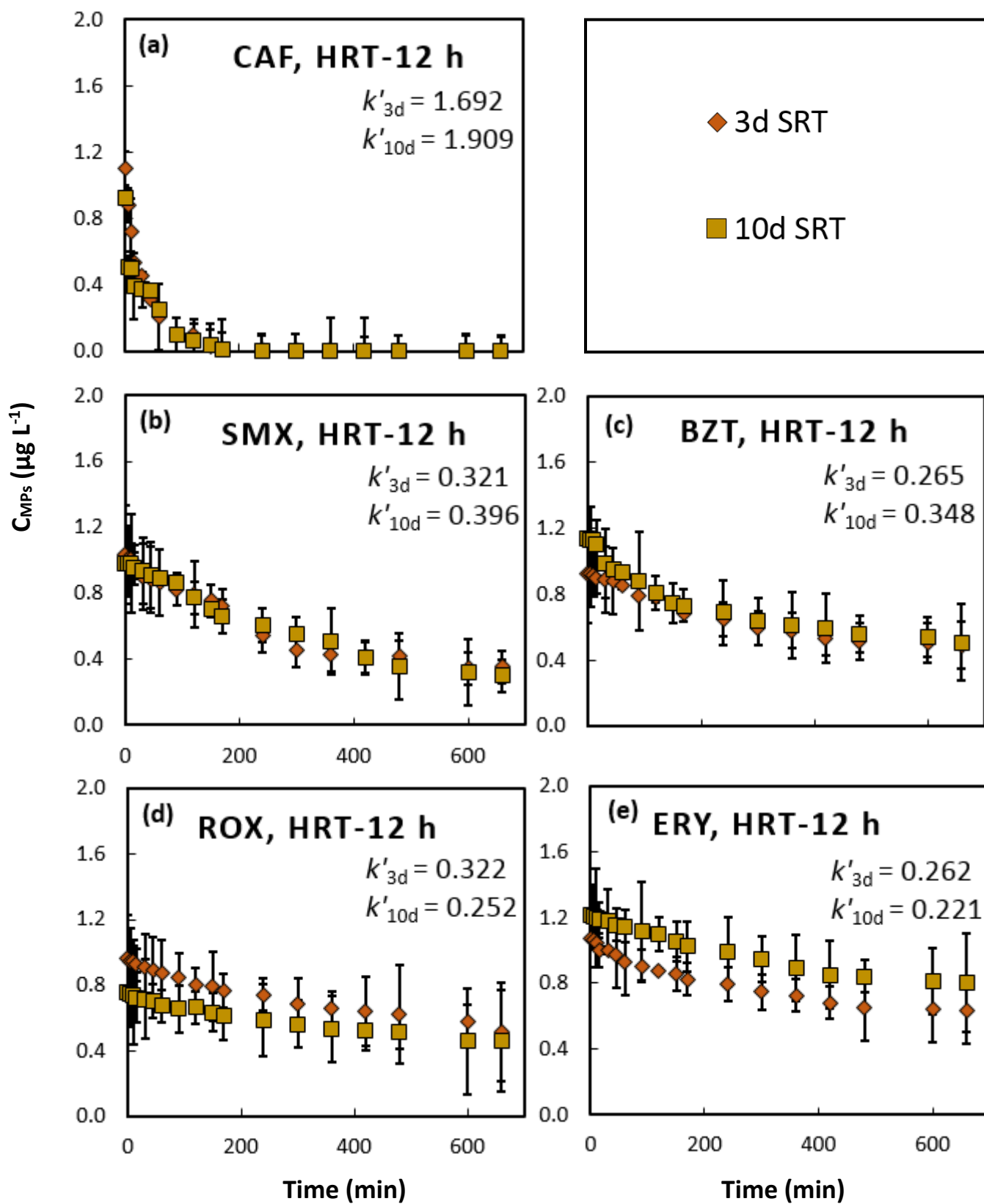


**Figure II. 9.** Removal of (a) CAF, (b) SMX and (c) BZT, (d) ROX and (e) ERY, (f) DCF, (g) CBZ, at both sludge age of 3 d and 10 d at the HRT of 8 h;  $k'$  is the apparent-first order removal rate constant ( $\text{h}^{-1}$ ); number of replicates = 3; error bars indicate one standard error.



(Continued on the next page)

Figure II. 10. Continued

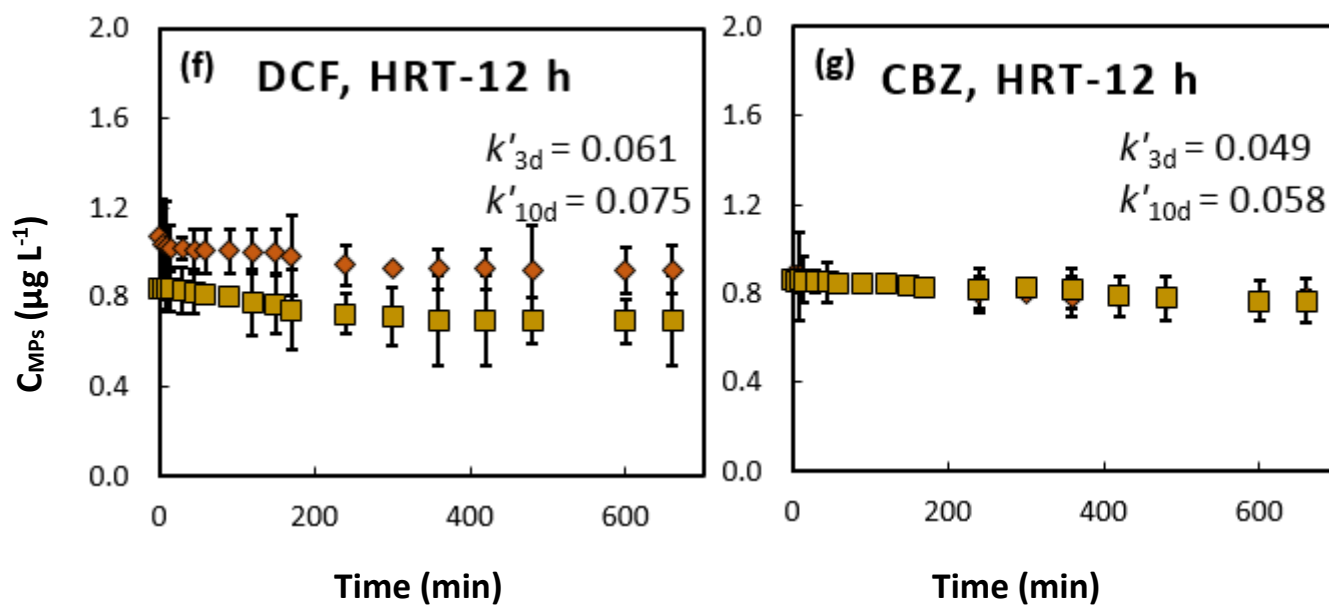


**Figure II. 10.** Removal of (a) CAF, (b) SMX and (c) BZT, (d) ROX, (e) ERY, (f) DCF and (g) CBZ at both sludge age of 3 d and 10 d at the HRT of 12 h;  $k'$  is the apparent-first order removal rate constant ( $\text{h}^{-1}$ ); number of replicates = 3; error bars indicate one standard error.

**Table II. 9.** An overview of calculated apparent-first order rate constants of all investigated MPs at all tested HRT- 4 h, 8 h, and 12 h for both sludge ages of 3 d and 10 d as well as change of  $k'$  from 4 h to 8 h, 8 h to 12 h and 4 h to 12 h.

Effect on HRT on apparent removal rate constant $k'$ (h <sup>-1</sup> )												
MPs	SRT-3 d						SRT- 10 d					
	HRT- 4 h	HRT- 8 h	HRT- 12 h	Change of $k'$ from 4 h to 8 h	Change of $k'$ from 8h to 12 h	Global change of $k'$ from 4 h to 12 h	HRT- 4 h	HRT- 8 h	HRT- 12 h	Change of $k'$ from 4 h to 8 h	Change of $k'$ from 8 h to 12 h	Global change of $k'$ from 4 h to 12 h
CAF	1.271	1.381	1.692	Increase by 1.08	Increase by 1.22	Increase by 1.33	1.356	1.735	1.909	Increase by 1.27	Increase by 1.10	Increase by 1.41
SMX	0.148	0.225	0.321	Increase by 1.52	Increase by 1.42	Increase by 2.17	0.252	0.302	0.396	Increase by 1.20	Increase by 1.31	Increase by 1.57
BZT	0.169	0.238	0.265	Increase by 1.41	Increase by 1.11	Increase by 1.57	0.239	0.257	0.348	Increase by 1.08	Increase by 1.35	Increase by 1.45
ROX	0.232	0.257	0.322	Increase by 1.11	Increase by 1.25	Increase by 1.39	0.172	0.205	0.252	Increase by 1.19	Increase by 1.23	Increase by 1.46
ERY	0.185	0.227	0.262	Increase by 1.23	Increase by 1.15	Increase by 1.42	0.165	0.182	0.221	Increase by 1.10	Increase by 1.21	Increase by 1.34
DCF	0.044	0.055	0.061	Increase by 1.25	Increase by 1.11	Increase by 1.11	0.059	0.068	0.075	Increase by 1.15	Increase by 1.08	Increase by 1.27
CBZ	0.041	0.044	0.049	Increase by 1.07	Increase by 1.11	Increase by 1.19	0.052	0.057	0.058	Increase by 1.09	Increase by 1.02	Increase by 1.12

### II.3.4. Overall synthesis of the impact of SRT and HRT

#### II.3.4.1. *MPs removal efficiency*

The removal efficiency of the micropollutants achieved in SBRs - 3, 10 and 20 d, operated with HRT of 4, 8 and 12 h, are presented in Figure II.11. In both SBRs - 3 and 10 d, the removal of CAF increased by 5 % between HRT of 4 and 8 h, while a slight increase of 2-3 % occurred between 8 and 12 h. Furthermore, the removal of SMX is enhanced from 30 % up to 65 % and from 45 % up to 70 %, in SBR-3 d and SBR-10 d, respectively, with an increase of HRT. Similar data have been reported previously, with the removal of 73 % in the reactors operated at SRT - 10 d and HRT – 12 h (Kang et al. 2018). For BZT, an increase of HRT up to 12 h, resulted in enhanced removal by 15% and 10 % in SBRs - 3 d and 10 d, respectively. Moreover, the effect of HRT on ROX or ERY was noticed in SBR-10 d, since their removal efficiency increased by 23 % and 10 % with HRT increments up to 12 h, respectively. Finally, the lowest removal was observed for DCF and CBZ regardless of the operational parameters of reactors (SRT and HRT). Clara et al. (2005b) reported the relation between DCF removal and HRT of the WWTP. DCF removal of 70 % at high HRT (13 d) was observed, whereas operating system with low HRT (< 1.2 d) gave negligible elimination. This could explain the low removal achieved in this study in which the reactors are operated at the highest HRT of 12 h. During different HRTs, no significant removal of DCF and CBZ was noticed (< 15 %) in SBRs operated at SRT of 3 d and 10 d. Their removal also seems to be enhanced with very high hydraulic retention time that is not applied in wastewater treatment plants.

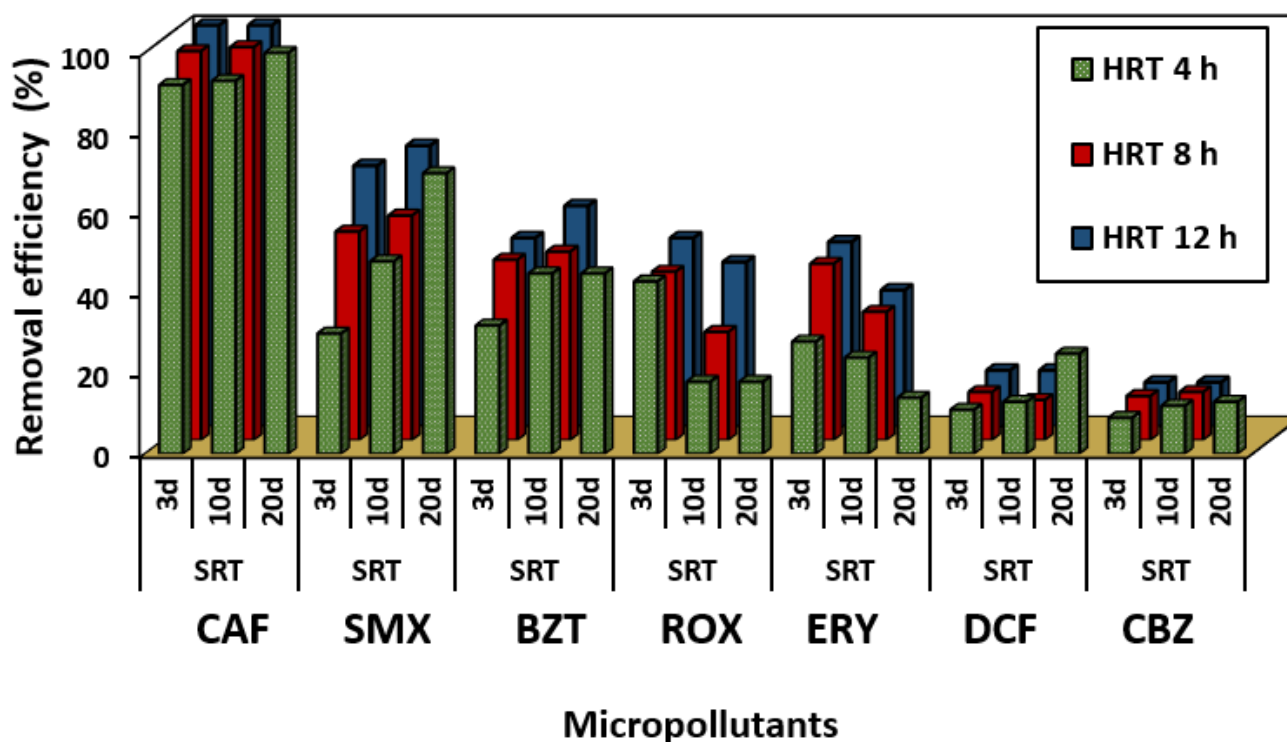


**Figure II. 11.** Removal (%) of selected MPs in SBRs - 3, 10 and 20 d over three different HRT 4, 8 and 12 h.  $C_{TSS} \sim 3 \text{ g}_{TSS} \text{ L}^{-1}$  and  $C_{MPs} \sim 1 \mu\text{g L}^{-1}$ .

#### II.3.4.2. Global effect of SRT and HRT

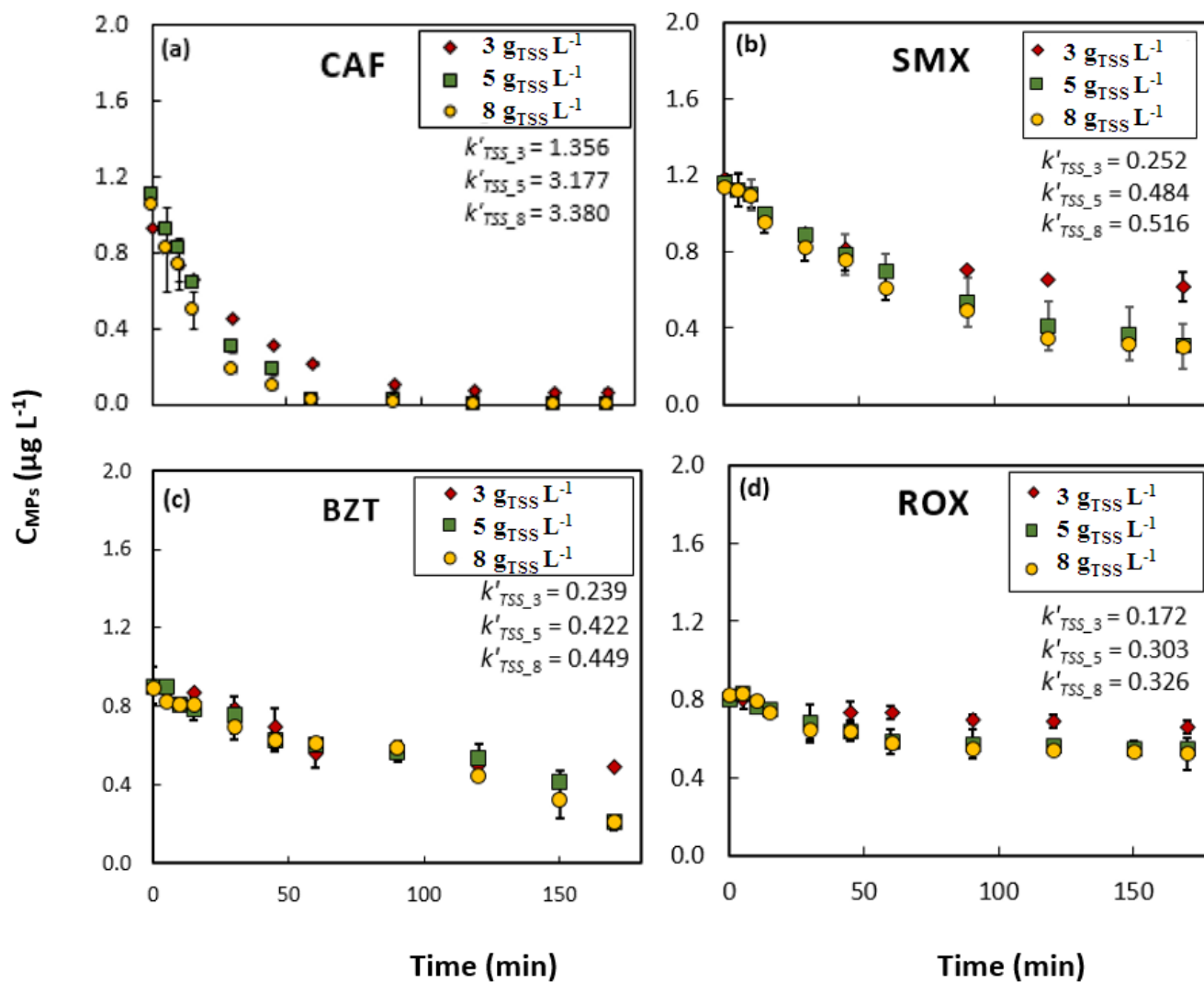
Overall, increasing SRT increases the removal efficiency of all micropollutants except for ROX and ERY. Similarly, increasing of HRT improves the removal efficiency of all studied compounds. On the one hand, increasing of HRT and SRT slightly modify the CAF and CBZ removal. Therefore, highly and non-biodegradable compounds are not sensitive to an increase of HRT or SRT. On the other hand, the moderately biodegradable compounds can be better removed by an increase of HRT and (except for ROX and ERY) by an increase of SRT.

### II.3.5. Effect of biomass concentration on MPs' elimination in activated sludge

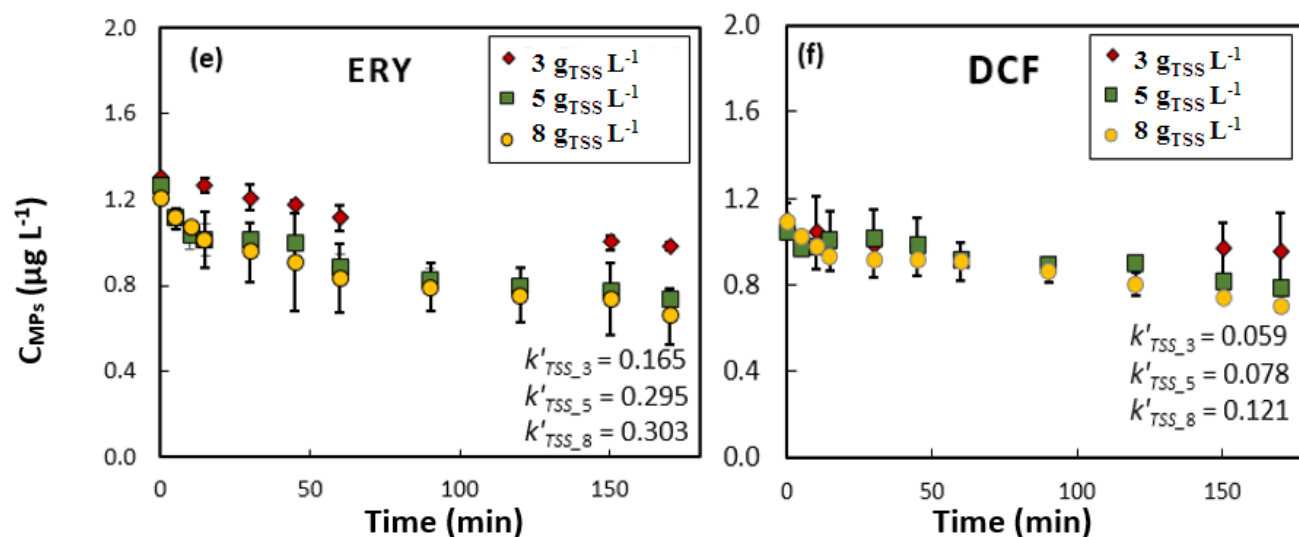
As mentioned before, the pseudo-first-order kinetic approach is the most commonly used for describing MPs' removal in activated sludge. The critical aspect of this approach is the assumption that the relatively small fluctuations of biomass concentration do not have an effect on the treatment process. To verify if the apparent-first order approach is valid, an additional kinetic study was carried out, to compare  $k'$  values in the reactors operated at SRT and HRT of 10 d and 4 h, respectively, with different biomass concentrations. These kinetics experiments were always performed with the same type of sludge (withdrawn from the WWTP 1).

Figure II.12 showed the change of concentration of selected MPs during biological treatment in reactors inoculated with biomass at concentrations of 3, 5 and 8  $\text{g}_{\text{TSS}} \text{L}^{-1}$ . In general, CAF degraded very fast, with a significant difference in removal rate constant between 3 and 5  $\text{g}_{\text{TSS}} \text{L}^{-1}$  ( $k'_{\text{TSS}_3} = 1.356 \pm 0.020$  and  $k'_{\text{TSS}_5} = 3.107 \pm 0.016 \text{ h}^{-1}$ ), but with weak change between 5 and 8  $\text{g}_{\text{TSS}} \text{L}^{-1}$  ( $k'_{\text{TSS}_8} = 3.380 \pm 0.046 \text{ h}^{-1}$ ). Similarly, in the case of SMX, an increase of biomass concentration from 3 to 5  $\text{g}_{\text{TSS}} \text{L}^{-1}$  resulted in substantial improvement of  $k'$  value from  $0.252 \pm 0.042 \text{ h}^{-1}$  to  $0.484 \pm 0.091 \text{ h}^{-1}$ . Conversely, low change in SMX removal apparent constants was observed in reactors with biomass concentration of 5 and 8  $\text{g}_{\text{TSS}} \text{L}^{-1}$  ( $k'_{\text{TSS}_5} = 0.484 \pm 0.098 \text{ h}^{-1}$  and  $k'_{\text{TSS}_8} = 0.516 \pm 0.043 \text{ h}^{-1}$ ). A comparable trend, showing that the biomass concentration below 5  $\text{g}_{\text{TSS}} \text{L}^{-1}$  affected the kinetics was also observed for ROX (Figure II.12d), BZT (Figure II.12c,  $k'_{\text{TSS}_3} = 0.239 \pm 0.043$ ,  $k'_{\text{TSS}_5} = 0.422 \pm 0.041$ ,  $k'_{\text{TSS}_8} = 0.449 \pm 0.037 \text{ h}^{-1}$ ) and ERY (Figure II.12e,  $k'_{\text{TSS}_3} = 0.165 \pm 0.030$ ,  $k'_{\text{TSS}_5} = 0.295 \pm 0.041$ ,  $k'_{\text{TSS}_8} = 0.303 \pm 0.115 \text{ h}^{-1}$ ). However, DCF exhibited a different behaviour (Figure II.12f). An increase of removal rate constant was recorded only in the SBR operated with high biomass concentration, i.e. 8  $\text{g}_{\text{TSS}} \text{L}^{-1}$  ( $k'_{\text{TSS}_8} = 0.121 \pm 0.021 \text{ h}^{-1}$ ).  $k'$  at 3 and 5 ( $k'_{\text{TSS}_3} = 0.059$ ,  $k'_{\text{TSS}_5} = 0.078$ ) remain very low. We can suppose that the rate of DCF is too low for being able to exhibit the same trend as the other MPs.





(Continued on the next page)



**Figure II. 12.** Change of concentration of (a) CAF, (b) SMX, (c) BZT, (d) ROX, (e) ERY and (f) DCF during biological treatment in reactors inoculated with biomass at concentrations of 3, 5 and  $8 \text{ g}_{\text{TSS}} \text{ L}^{-1}$ ;  $k'$  is the apparent-first-order removal rate constant ( $\text{h}^{-1}$ ) operated at SRT-10 d and HRT- 4 h.

To summarize and analyse the results, Figure II.13 shows the relation between the constant  $k'$  determined in the reactors and the biomass concentration. For all presented compounds, i.e. CAF, SMX, BZT, ROX and ERY an evident increase of  $k'$  value was observed with a change of biomass concentration from 3 to  $5 \text{ g}_{\text{TSS}} \text{ L}^{-1}$ . This trend is logical and suggests that the amount of biomass significantly affected the removal kinetics. With the classic kinetics modelling, the expected apparent removal rate constants ( $k'$ ) is directly proportional to  $C_{\text{TSS}}$  (Eq. II-4). However, apart from DCF (very low  $k'$ ), further increase of biomass concentration (from 5 to  $8 \text{ g}_{\text{TSS}} \text{ L}^{-1}$ ) changes only slightly the removal rate. Following the assumption of linear kinetics, the evolution of  $k'$  versus  $C_{\text{TSS}}$  should give a straight line through the origin with a slope corresponding to  $k$ . However, our results highlighted that the increase is not linear and, hence,  $k$  is not constant. The apparent constant  $k'$  increases with  $C_{\text{TSS}}$  but with evolution lower than that it would be expected if it was directly proportional to  $C_{\text{TSS}}$  (Eq.II-4). In other words, an increase of  $C_{\text{TSS}}$  improves the

removal, but the kinetics is not proportional to  $C_{TSS}$ . Henkel et al. (2009) did show that mass-transfer gas/liquid in activated sludge systems is hampered with increasing  $C_{TSS}$ . It can be assumed that the increase of the floc volume at  $8 \text{ g}_{TSS} \text{ L}^{-1}$  reduce the free water and thereby slow down the local mixing and the transport of the MPs around the flocs before entering inside them. In the case of MP removal, the direct dependency of  $r_{MPs}$  on biomass concentration ( $C_{TSS}$ ) will be thereby affected as can be seen from Figure II.13.

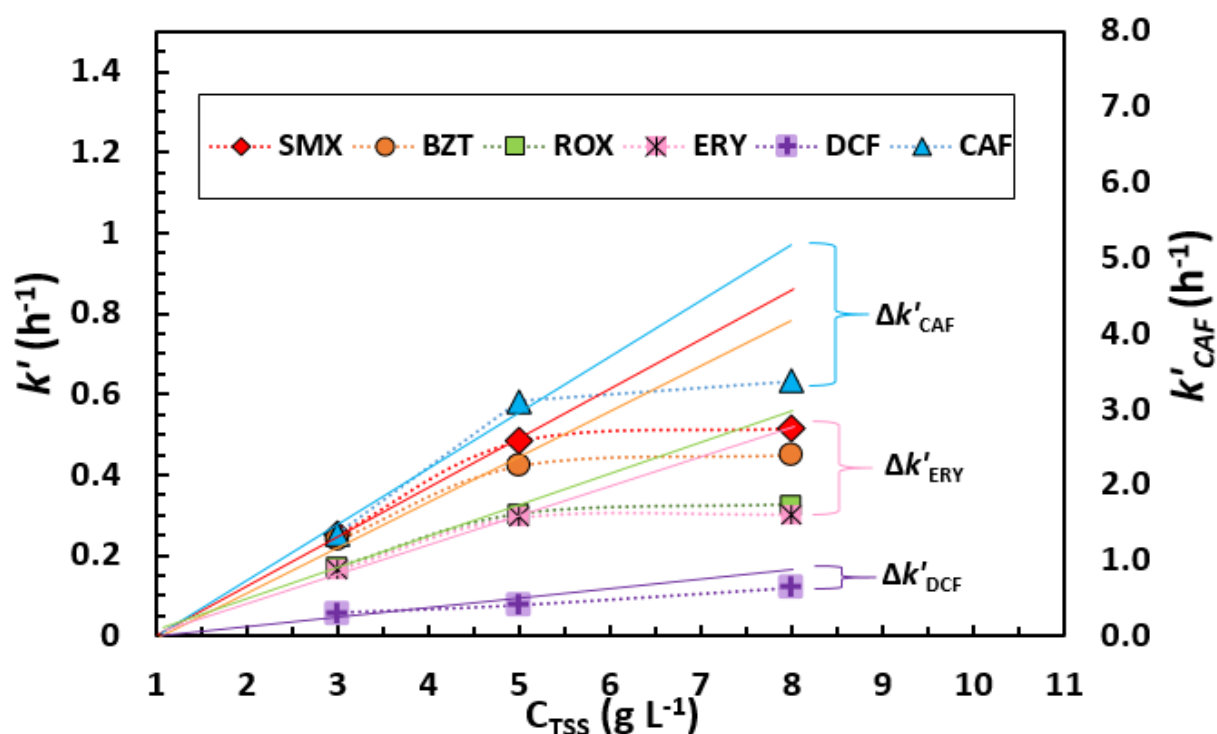


**Figure II. 13.** Effect of the  $C_{TSS}$  ( $\text{g L}^{-1}$ ) on the apparent-first-order removal rate constant  $k'$  ( $\text{h}^{-1}$ ) for CAF, SMX, BZT, ROX, ERY and DCF. The apparent constants  $k'$  of SMX, BZT, ROX, ERY and DCF and  $k'$  of CAF are shown on the left side and the right side of the graph, respectively. Continuous lines represented the linear expected pseudo-first-order approach (calculated from the first three  $C_{TSS}$  of 0, 3 and  $5 \text{ g L}^{-1}$ ).

In order to emphasize the difference between the expected kinetic constants of studied MPs and the experimental  $k'$  recorded at high biomass concentration, an extrapolated parameter was estimated as shown in Figure II.13 at  $C_{\text{TSS}} = 8 \text{ g}_{\text{TSS}} \text{ L}^{-1}$ . The  $k'$  ratio designed by ( $\delta$ ) is defined as:

$$\delta = \frac{k'_{\text{extrapolated}}}{k'_{\text{experimental}}} \quad (\text{II-7})$$

**Table II. 10.** Experimental and expected apparent-first-order rate constants estimated at  $C_{TSS} = 8 \text{ g}_{TSS} L^{-1}$  as well as the experimental and expected  $C_{MPs}$  of SMX, BZT, ROX, ERY and DCF at HRT of 4 h (Time of reaction = 170 min) and their removal efficiency (%).

MPs	$k'_{\text{expected}}$ (h <sup>-1</sup> )	$k'_{\text{experimental}}$ (h <sup>-1</sup> )	$\Delta k'$	%error= $\frac{\Delta k'}{k'_{\text{experimental}}} \times 100$	$\frac{k'_{\text{expected}}}{k'_{\text{experimental}}}$ (Eq. II-7)	Calculated $C_{MPs}$ for $k'_{\text{expected}}$ (Eq. II-5)	Calculated $C_{MPs}$ for $k'_{\text{experimental}}$ (Eq. II-5)	$\frac{C_{MPs_{\text{experimental}}}}{C_{MPs_{\text{expected}}}}$ (Eq. 8)	Removal efficiency (%) of $C_{MPs}$ expected	Removal efficiency (%) of $C_{MPs}$ experimental	Ratio of removal efficiency :  $\frac{\text{Experimental}}{\text{Expected}}$
CAF	5.20	3.38	1.82	54	1.54	0.00000043	0.000072	174	99.99	99.99	1.00
SMX	0.88	0.52	0.36	69	1.71	0.091	0.26	2.81	91.74	76.82	0.84
BZT	0.80	0.45	0.35	78	1.78	0.093	0.25	2.70	89.63	71.98	0.80
ROX	0.55	0.33	0.22	67	1.69	0.17	0.32	1.89	78.95	60.29	0.76
ERY	0.45	0.30	0.15	50	1.49	0.33	0.51	1.52	72.06	57.62	0.80
DCF	0.18	0.12	0.06	50	1.49	0.66	0.77	1.18	39.95	29.02	0.73

However, it appears logical to reason in terms of removal efficiency of each MP at the end of the reaction phase operated at HRT of 4 h ( $t = 2.83$  h) for high  $C_{TSS}$ . Thus,  $C_{MPs}$  were calculated according to Eq. (II-5) for the experimental and the expected  $k'$  (extrapolated). The results are depicted in Table II.10. The ratio of the  $C_{MPs,expected}$  to the  $C_{MPs,experimental}$  designed by ( $\beta$ ) was developed in Eq. (II-8). It represents the ratio between the real remaining MPs concentration ( $C_{MPs,experimental}$ ) and the one that would be expected by extrapolation using the usual kinetics (pseudo-first order approach).

$$\beta = \frac{C_{MPs,experimental}}{C_{MPs,expected}} = \frac{C_0 e^{-t k'_{experimental}}}{C_0 e^{-t k'_{expected}}} = e^{(k'_{expected} - k'_{experimental}) t} \quad (\text{II-8})$$

In order to determine the relation of the  $C_{MPs}$  ratio to the  $k'$  ratio, Eq. (II-8) can be rewritten; it leads to the exponential equation, which takes into consideration the time of the experiment (Eq. (II-9):

$$\beta = e^{k'_{expected} \left( \frac{\delta-1}{\delta} \right) t} \quad (\text{II-9})$$

Therefore, the expected  $k'$  of SMX and BZT for example, were 1.71 and 1.78 times larger than the experimentally measured  $k'$ , respectively. However, because of the time parameter in the exponential relation in (Eq.II-9), the calculated experimental  $C_{MPs}$  ratios are greater by 2.8 and 2.7 after 170 min, respectively. Then, it highlights that  $k'$  ratio and  $C_{MPs}$  ratio changes are not necessary in the same order of magnitude.

#### II.4. Conclusion of chapter II

The systematic study of the operational conditions of the activated sludge process explained the potential effect of each parameter on the MPs removal that represent various degree of biodegradability. The results showed that operational conditions, namely SRT and HRT can influence the MPs removal efficiency to some extent, which depends on the nature of the MPs. Highly biodegradable compounds have in general high removal efficiency, independently from applied conditions. In the case of moderately biodegradable compounds, an increase of SRT caused an improvement of removal efficiency. This aspect was evident at very high SRT for all the compounds except for roxithromycin and erythromycin. Longer HRT also led to higher removal efficiency. However, a complete MPs removal was not achieved in any of the studied

setups. In terms of application, the improvement of removal obtained with a higher HRT should be compared to the cost of a larger reactor. For persistent compounds, very low removal efficiency in all tested scenarios ( $\geq 10\%$ ) was reported; HRT showed minor impact and SRT exhibited a slight effect only if it was very long (e.g. diclofenac SRT 20 d, 25 %). Due to the high-energy demand, such conditions are rarely applied in conventional WWTP's with an activated sludge process. Finally, the increase of biomass concentration from 3 to 5 g<sub>TSS</sub> L<sup>-1</sup> significantly increased the removal of the highly and moderately degradable compounds (caffeine, sulfamethoxazole, benzotriazole, roxithromycin and erythromycin), whereas a further increase to 8 g<sub>TSS</sub> L<sup>-1</sup> had lower effect. The results highlighted that the usual kinetics, which consider that the rate is proportional to the biomass concentration is only valid for low and moderate biomass concentration. This unexpected effect of biomass concentration opens up a new field of research and, particularly, in terms of development of a new kinetic model that can be used for a wide spectrum of biomass concentrations. This will be presented in the following chapter.

## **II.5. References of chapter II**

- Alvarino, T., Lema, J., Omil, F., Suárez, S., 2018. Trends in organic micropollutants removal in secondary treatment of sewage. *Reviews in Environmental Science and Bio/Technology*, 17, 447-69.
- Alvarino, T., Suarez, S., Lema, J.M., Omil, F., 2014. Understanding the removal mechanisms of PPCPs and the influence of main technological parameters in anaerobic UASB and aerobic CAS reactors. *Journal of Hazardous Materials*, 278, 506–513.
- APHA, Awwa, WEF, 2012. Standard methods for the examination of water and wastewater. American Public Health Association (APHA), Washington, DC, USA.
- Behera S.K., Kim W.H., Oh J.E., Park H.S., 2011. Occurrence and removal of antibiotics, hormones and several other pharmaceuticals in wastewater treatment plants of the largest industrial city of Korea. *Science of the Total Environment*, 409, 4351–4360.
- Bonnefille, B., Gomez, E., Courant, F., Escande, A., Fenet, H., 2018. Diclofenac in the marine environment: A review of its occurrence and effects. *Marine Pollution Bulletin*, 131,496–506.

- Bourgin, M., Beck, B., Boehler, M., Borowska, E., Fleiner, J., Salhi, E., Rebekka, T., Ursvon, G., Hansruedi, S., McArdell, C.S., 2018. Evaluation of a full-scale wastewater treatment plant upgraded with ozonation and biological post-treatments: Abatement of micropollutants, formation of transformation products and oxidation by-products. *Water Research*, 129, 486–498.
- Chiavola A., Tedesco P., Rosaria B.M., 2019. Fate of selected drugs in the wastewater treatment plants (WWTPs) for domestic sewage. *Environmental Science and Pollution Research*, 26, 1113-1123.
- Cirja, M., Ivashechkin, P., Schaffer, A., Corvini, F.X., Factors affecting the removal of organic micropollutants from wastewater in conventional treatment plants (CTP) and membrane bioreactors (MBR). *Reviews in Environmental Science Technology*, 7, 61–78.
- Clara, M., Kreuzinger, N., Strenn, B., Gans, O., Kroiss, H., 2005a. The solids retention time—a suitable design parameter to evaluate the capacity of wastewater treatment plants to remove micropollutants. *Water Research*, 39, 97–106.
- Clara, M., Strenn, B., Gans, O., Martinez, E., Kreuzinger, N., Kroiss, H., 2005b. Removal of selected pharmaceuticals, fragrances and endocrine disrupting compounds in a membrane bioreactor and conventional wastewater treatment plants. *Water Research*, 39, 4797–4807.
- Ejhed, H., Fång, J., Hansen, K., Graae, L., Rahmberg, M., Magnér, J., Dorgeloh, E., Plaza, G., 2018. The effect of hydraulic retention time in onsite wastewater treatment and removal of pharmaceuticals, hormones and phenolic utility substances. *Science of The Total Environment*, 618, 250–261.
- Falås, P., Andersen, H.R., Ledin, A., la Cour Jansen, J., 2012. Impact of solid retention time and nitrification capacity on the ability of activated sludge to remove pharmaceuticals. *Environmental Technology*, 33, 865–872.
- Falås, P., Wick, A., Castronovo, S., Habermacher, J., Ternes, T. A., Joss, A. 2016. Tracing the limits of organic micropollutant removal in biological wastewater treatment. *Water Research*, 95, 240–249.
- Fernandez-Fontaina, E., Omil, F., Lema, J.M., Carballa, M., 2012. Influence of nitrifying conditions on the biodegradation and sorption of emerging micropollutants. *Water Research*, 46, 5434–5444.
- Finn, R. K., 1954. Agitation-aeration in the laboratory and in industry. *Bacteriological Reviews* 18, 254-74.



- Gobel, A., Mcardell, C., Joss, A., Siegrist, H., Giger, W., 2007. Fate of sulfonamides, macrolides, and trimethoprim in different wastewater treatment technologies. *Science of The Total Environment*, 372, 361–371.
- Gracia-Lor, E., Sancho, J., Serrano, R., and Hernández, F., 2012. Occurrence and removal of pharmaceuticals in wastewater treatment plants at the Spanish mediterranean area of Valencia. *Chemosphere* 87, 453–62.
- Guerra, P., Kim, M., Shah, A., Alae, M., Smyth, S.A., 2014. Occurrence and fate of antibiotic, analgesic/anti-inflammatory, and antifungal compounds in five wastewater treatment processes. *Science of The Total Environment*, 473–474, 235–243.
- Hai, F., Shufan, Y., Muhammad, A., Vitor, S., Samia, S., Martina, S.S., Jody, G., Zhi-Qiang, X., Kazuo, Y., 2018. Carbamazepine as a possible anthropogenic marker in water: occurrences, toxicological effects, regulations and removal by wastewater treatment technologies. *Water* 10, 107.
- Henkel, J., Lemac, M., Wagner, M., Cornel, P., 2009. Oxygen transfer in membrane bioreactors treating synthetic greywater. *Water Research* 43, 1711 – 1719.
- Henze, M., 2008. *Biological wastewater treatment: principles, modelling and design*. London.
- Henze, M., Gujer, W., Mino, T., van Loosdrecht, M., 2000. *Activated Sludge Models ASM1, ASM2, ASM2d and ASM3*. London.
- Jiang J.Q., Zhou Z., Sharma V.K., 2013. Occurrence, transportation, monitoring and treatment of emerging micropollutants in waste water —A review from global views. *Microchemical Journal*, 110, 292-300.
- Joss, A., Keller, E., Alder, A.C., Göbel, A., McArdell, C.S., Ternes, T., Siegrist, H., 2005. Removal of pharmaceuticals and fragrances in biological wastewater treatment. *Water Research*, 39, 3139–3152.
- Joss, A., Zabczynski, S., Göbel, A., Hoffmann, B., Löffler, D., McArdell, C.S., Ternes, T., Thomsen, A., Siegrist, H., 2006. Biological degradation of pharmaceuticals in municipal wastewater treatment: Proposing a classification scheme. *Water Research*, 40, 1686–1696.
- Kasprzyk-Hordern, B., Dinsdale, R., Guwy, A.J., 2009. The removal of pharmaceuticals, personal care products, endocrine disruptors and illicit drugs during wastewater treatment and its impact on the quality of receiving waters. *Water Research*, 43, 363–80.

- Kang, A.J., Brown, A.K., Wong, C.S., Yuan, Q., 2018. Removal of antibiotic sulfamethoxazole by anoxic/anaerobic/oxic granular and suspended activated sludge processes. *Bioresource Technology*, 251, 151–157.
- Kårelid, V., Larsson, G., Björleinius, B., 2017. Pilot-Scale removal of pharmaceuticals in municipal wastewater: Comparison of granular and powdered activated carbon treatment at three wastewater treatment plants. *Journal of Environmental Management*, 193, 491–502.
- Kim, M., Guerra, P., Shah, A., Parsa, M., Alaei, M., Smyth, S.A., 2014. Removal of pharmaceuticals and personal care products in a membrane bioreactor wastewater treatment plant. *Water Science and Technology*, 69, 2221–2229.
- Kreuzinger, N., Clara, M., Strenn, B., Kroiss, H., 2004. Relevance of the sludge retention time (SRT) as design criteria for wastewater treatment plants for the removal of endocrine disruptors and pharmaceuticals from wastewater. *Water Science and Technology* 50, 149–156.
- Knopp, G., Prasse, C., Ternes, T.A., Cornel, P., 2016. Elimination of micropollutants and transformation products from a wastewater treatment plant effluent through pilot scale ozonation followed by various activated carbon and biological filters. *Water Research*, 100, 580–92.
- Li, B.; Zhang, T., 2010. Biodegradation and adsorption of antibiotics in the activated sludge process. *Environmental Science & Technology*, 44, 3468–3473.
- Li, B., Zhang, T., 2011. Mass flows and removal of antibiotics in two municipal wastewater treatment plants. *Chemosphere*, 83, 1284–1289.
- Louvet, J.N., Heluin, Y., Attik, G., Dumas, D., Potier, O., Pons, M.N., 2010. Assessment of erythromycin toxicity on activated sludge via batch experiments and microscopic techniques (Epifluorescence and CLSM). *Process Biochemistry* 45, 1787–94.
- Luo, W., Hai, F.I, Kang, J., Price, W.E., Guo, W., Ngo, H.H., Yamamoto, K., Nghiem, L.D., 2015. Effects of salinity build-up on biomass characteristics and trace organic chemical removal: Implications on the development of high retention membrane bioreactors, *Bioresource Technology*, 177, 274–281.
- Luo, Y., Guo, W., Ngo, H.H., Nghiem, D.L., Hai, L.F., Zhang, J., Liang S., Wang, C.X., 2014. A Review on the Occurrence of micropollutants in the aquatic environment and their fate and removal during wastewater treatment. *Science of the Total Environment* 473-474, 619-41.

- Majewsky, M., Gallé, T., Yargeau, V., Fischer, K., 2011. Active heterotrophic biomass and sludge retention time (SRT) as determining factors for biodegradation kinetics of pharmaceuticals in activated sludge. *Bioresource Technology*, 102, 7415–7421.
- Miège, C., Choubert, J.M., Ribeiro, L., Eusèbe, M., Coquery, M., 2009. Fate of pharmaceuticals and Personal Care Products in wastewater treatment plants – conception of a database and first results. *Environmental Pollution* 157, 1721–26.
- Ribeiro, R.P., Kligerman, D.C., Mello, W.Z., Silva, D.P., Correia, R.F., Oliveira, J.L.M., 2018. Effects of different operating conditions on total nitrogen removal routes and nitrous oxide emissions in a lab-scale activated sludge system. *Ambiente & Agua - An Interdisciplinary Journal of Applied Science* 13, 2-15.
- Sahar, E., Ernst, M., Godehardt, M., Hein, A., Herr, J., Kazner, C., Melin, T., 2011. Comparison of two treatments for the removal of selected organic micropollutants and bulk organic matter: conventional activated sludge followed by ultrafiltration versus membrane bioreactor. *Water Science and Technology* 63, 733–40.
- Santos, J.L., Aparicio, I., Callejón, M., Alonso, E., 2009. Occurrence of pharmaceutically active compounds during 1-year period in wastewaters from four wastewater treatment plants in Seville (Spain). *Journal of Hazardous Materials*, 164, 1509–1516.
- Saikaly, P.E., Stroot, P.G., Oerther, D.B., 2005. Use of 16S rRNA gene terminal restriction fragment analysis to assess the Impact of solids retention time on the bacterial diversity of activated sludge. *Applied and Environmental Microbiology*, 71, 5814–5822.
- Singer, H., Jaus, S., Hanke, I., Lück, A., Hollender, J., Alder, A., 2010. Determination of biocides and pesticides by on-Line solid phase extraction coupled with mass spectrometry and their behaviour in Wwastewater and surface water. *Environmental Pollution* 158, 3054–64.
- Sipma, J., Osuna, B., Collado, N., Monclús, H., Ferrero, G., Comas, J., Rodriguez-Roda, I., 2010. Comparison of removal of pharmaceuticals in MBR and activated sludge systems. *Desalination*, 250, 653–659.
- Stasinakis, A.S., Thomaidis, N.S., Arvaniti, O.S., Asimakopoulos, A.G., Samaras, V.G., Ajibola, A., Mamais, D., Lekkas, T.D., 2013. Contribution of primary and secondary treatment on the removal of benzothiazoles, benzotriazoles, endocrine disruptors, pharmaceuticals and perfluorinated compounds in a sewage treatment plant. *Science of The Total Environment*, 463–464, 1067–1075.

- Suárez, S., Reif, R., Lema, J.M., Omil, F., 2012. Mass balance of pharmaceutical and personal care products in a pilot-scale single-sludge system: Influence of T, SRT and recirculation ratio. *Chemosphere*, 89, 164-171.
- Sui, Q., Huang, J., Deng, S., Yu, G., Fan, Q., 2010. Occurrence and removal of pharmaceuticals, caffeine and DEET in wastewater treatment plants of Beijing, China. *Water Resource*, 44, 417–426.
- Tadkaew, N., Hai, F.I., McDonald, J.A., Khan, S.J., Nghiem, L.D., 2011. Removal of trace organics by MBR treatment: The role of molecular properties. *Water Resource*, 45, 2439–2451.
- Tarpani, R.R.Z., Azapagic, A., 2018. A methodology for estimating concentrations of pharmaceuticals and personal care products (PPCPs) in wastewater treatment plants and in freshwaters. *Science of The Total Environment*, 622–623, 1417–1430.
- Tay, K.S., Madehi, N., 2015. Ozonation of ofloxacin in water: By-products, degradation pathway and ecotoxicity assessment. *Science of The Total Environment*, 520, 23–31.
- Tchobanoglous, G., Burton, F.L., Stensel, H.D., 2002. *Wastewater engineering: treatment and reuse*. Boston.
- Ternes, T., Janex-Habibi, M., Knacker, T., Kreuzinger, N., Siegrist, H., 2004. Assessment of technologies for the removal of pharmaceuticals and personal care products in sewage and drinking water facilities to improve the indirect potable water reuse. Contract No. EVK1-CT-2000-00047.
- Tiwari, B., Sellamuthu, B., Ouarda, Y., Drogui, P., Tyagi, R.D., Buelna, G., 2017. Review on fate and mechanism of removal of pharmaceutical pollutants from wastewater using biological approach. *Bioresource Technology*, 224, 1–12.
- Tran, N.H., Urase, T., Ngo, H.H., Hu, J., Ong, S.L., 2013. Insight into metabolic and cometabolic activities of autotrophic and heterotrophic microorganisms in the biodegradation of emerging trace organic contaminants. *Bioresource Technology*, 146, 721–731.
- Vasiliadou, I.A., Molina, R., Martínez, F., Melero, J.A., 2014. Experimental and modelling study on removal of pharmaceutically active compounds in rotating biological contactors. *Journal of Hazardous Materials*, 274, 473–482.
- Verlicchi, P., Al Aukidy, M., Zambello, E., 2012. Occurrence of pharmaceutical compounds in urban wastewater: Removal, mass load and environmental risk after a secondary treatment—A review. *Science of The Total Environment*, 429, 123–155.

- Vieno, N., Sillanpää, M., 2014. Fate of diclofenac in municipal wastewater treatment plant — A review. *Environment International*, 69, 28–39.
- Vuono, D.C., Benecke, J., Henkel, J., Navidi, W.C., Cath, T.Y., Munakata-Marr, J., Spear, J.R., Drewes, J.E., 2015. Disturbance and temporal partitioning of the activated sludge metacommunity. *The ISME Journal*, 9, 425–435.
- Weiss, S., Jakobs, J., Reemtsma, T., 2006. Discharge of Three Benzotriazole Corrosion Inhibitors with Municipal Wastewater and Improvements by Membrane Bioreactor Treatment and Ozonation. *Environmental Science & Technology*, 40, 7193–7199.
- Wick, A., Fink, G., Joss, A., Siegrist, H., Ternes, T., 2009. Fate of beta blockers and psychoactive drugs in conventional wastewater treatment. *Water Research*, 43, 1060–74.
- World Health Organization. Communicable Diseases Cluster (2000). Overcoming antimicrobial resistance. Geneva: World Health Organization.
- Zhang, D., Gersberg, R.M., Ng, W.J., Tan, S.K., 2014. Removal of pharmaceuticals and personal care products in aquatic plant-based systems: a review. *Environmental Pollution*, 184, 620–639.
- Zhang, Y., Sven-Uwe, G., Carmen, G., 2008. Carbamazepine and diclofenac: Removal in wastewater treatment plants and occurrence in water bodies. *Chemosphere*, 73, 1151-61.



**Chapter III. New kinetics law of micropollutants  
removal in activated sludge: non-linear influence of  
biomass concentration**

## Abstract

As the biological treatment of emerging contaminants with activated sludge process relies on the biomass, a proper understanding of the kinetics related to biomass concentration ( $C_{TSS}$ ) is critical in order to well model and evaluate treatment systems. In this chapter, an in-depth analysis of new kinetic constants  $k_{MPs}$  (newly proposed nomenclature) has been carried out, focusing on some physical phenomena that affect its observed value. By structuring the factors influencing the removal rates into advective and diffusional parameters, light has been shed onto the importance of the mixing conditions, which are represented by the order of the reaction  $n$  on the biomass concentration. Particularly, the importance of non-ideal mixing as a source of variability between removal rates for micropollutants (MPs) has been illustrated. Additionally, discussion on the differences existing between diffusion coefficients of MPs that affect their removal rates has been carried out. It has been shown that the molecular weight of MPs reflects diffusional limitations. This diffusional process is also implemented in new kinetics model.

**Keywords:** MPs; floc diffusion; kinetics; activated sludge; power law model; biomass concentration

### III.1. Introduction

In last decades, the occurrence of various micropollutants (MPs) such as pharmaceutical and personal care products (PPCPs) in water bodies, has been widely reported (K'oreje et al. 2018; Sui et al. 2011). Most of the work to date has been aimed to examine the presence of MPs in wastewaters, the elimination efficiency of biological treatment in WWTPs (Zheng et al. 2019; Kosma et al. 2010; Onesios et al. 2009) as well as the identification of factors that can affect the fate of MPs (Ternes et al. 2004; Suarez et al. 2010; Tang et al. 2019). Actually, these studies state significant variations on MPs' removal rates, as well as contradictory results on their fate during the wastewater treatment (Tiwari et al. 2017; Vasiliadou et al. 2013; Deblonde et al. 2011; Stasinakis et al. 2010). Additionally, Banihashemi and Droste (2018) mentioned that the possible fate models for MPs removal in biological processes have not been deeply investigated. Furthermore, most of published models assumed that (i) equilibrium is reached instantaneously between sorbed and dissolved MPs, (ii) sorption equilibria of MPs in water and sludge samples are mostly modelled by Freundlich isotherms, with a Freundlich coefficient close to 1 (Yi et al.



2011), (iii) volatilization is largely ignored in removal modelling compared to sorption and biodegradation pathways. However, all these assumptions are often not experimentally verified.

Many approaches have been reported with different model formulations that have been found to describe biodegradation, including sorption, as a removal pathway in an activated sludge treatment plant. The zero-order and first-order on biomass concentration reported by some authors (Zhao et al. 2008; Helbling et al. 2012), the pseudo-first-order or mixed second-order kinetics (Eq.III-1) emphasized by other groups (Tan et al. 2007; Plosz et al. 2010; Fernandez-Fontaina et al. 2013; Joss et al. 2006; Suárez et al. 2012; Press-Kristensen et al. 2007; Wick et al. 2009; Maurer et al. 2007; Xue et al. 2010; Abegglen et al. 2009; Majewsky et al. 2011; Plosz et al. 2012; Lee et al. 1998) or various types of growth-based Monod formulations (Marfil-Vega et al. 2010; Lee et al. 2012) or Haldane model (Tomei et al. 2008) are some examples. In such an aeration tank, the sludge mainly composed of microorganisms generally ranging from 2 to 5 g L<sup>-1</sup> at solid contents in a conventional activated sludge process (CAS) and > 10 g L<sup>-1</sup> for membrane bioreactors (MBR), was assumed to be constant during the MPs elimination process. This would justify the use of the apparent-first-order linked to the most commonly used expression (Eq.III-2). As a result, this model would implicitly lead to a linear increase in the removal rate, and also a linear increase of the apparent constant  $k'$  with the sludge concentration regardless the concentration range.

$$r_{MPs} = -k C_{TSS} C_{MPs} \Rightarrow r_{MPs} \propto C_{TSS} \quad \text{(III-1)}$$

$$r_{MPs} = -k' C_{MPs} \Rightarrow k' \propto C_{TSS} \quad \text{(III-2)}$$

However, the reactions occurring in a biological reactor are of considerable complexity. The MP concentration profiles between and inside the flocs are influenced by many factors, such as diffusion coefficient, conversions rate, sludge size, biomass spatial distribution, density and mixing mode. For this purpose, it could be interesting to take into account the hydrodynamic of mixing, which mainly depends at high  $C_{TSS}$  on the rheological behavior of activated sludge as well as the diffusion modelling of MPs inter/intraflocs. In the case of non-Newtonian sludge suspensions, such an increase in TSS concentration induces an increase in apparent viscosity of the suspension (Durán et al. 2016; Sanin 2002; Seyssiecq et al. 2008).

In the chapter II, the elimination of pharmaceuticals, such as caffeine (CAF), sulfamethoxazole (SMX), benzotriazole (BZT), roxithromycin (ROX), erythromycin (ERY), diclofenac (DCF)

and carbamazepine (CBZ), using an activated sludge in sequencing batch reactors was experimentally investigated. It was also demonstrated that the kinetics of removal is not proportional to biomass concentration. The removal rate increases by expanding  $C_{TSS}$  from 3 to 8 g L<sup>-1</sup> but with an increase lower than the proportionality. The present chapter aims to develop a new mathematical kinetic model for the elimination of these pharmaceuticals from wastewater for the broad range of biomass concentrations.

### III.2. In-depth analysis of kinetics results at various biomass concentration

The effect of various biomass concentration of activated sludge on MP's removal kinetics was studied in chapter II. It was shown that the increase of biomass concentration ( $C_{TSS}$ ) from 3 to 5 g<sub>TSS</sub> L<sup>-1</sup> significantly increased the removal of the highly and moderately degradable compounds (CAF, SMX, BZT, ROX and ERY), whereas a further increase to 8 g<sub>TSS</sub> L<sup>-1</sup> improved slightly their removal. To our knowledge, these kinds of kinetics performed at high biomass concentration ( $C_{TSS} = 8$  g<sub>TSS</sub> L<sup>-1</sup>) in conventional activated sludge was not employed. Based on the non-linear relation deduced from experimental set operated at various  $C_{TSS}$  in corresponding HRT- 4 h, we can consider a kind of saturation of the system by the presence of the  $C_{TSS}$ . Therefore, a special effort to justify and explain these existing results is conducted in the present chapter.

Bearing in mind the activated sludge binding sites to MPs, it was convenient to assume such saturation phenomena for the number of moles of MPs instead of its mass concentration. The,  $C_{MPs}$  are expressed in  $\mu\text{mol L}^{-1}$ .

In order to determine the removal rate  $r_{MPs}$  (in  $\mu\text{mol L}^{-1} \text{h}^{-1}$ ) at the different biomass concentrations - 3, 5 and 8 g<sub>TSS</sub> L<sup>-1</sup>, the slopes of the tangents at every time  $t$  for the MPs concentration remaining in the reactors were recalculated (Figure III.S1). The resulting  $r_{MPs}$  results were illustrated in Figure III.1 for the first hour of the reaction.

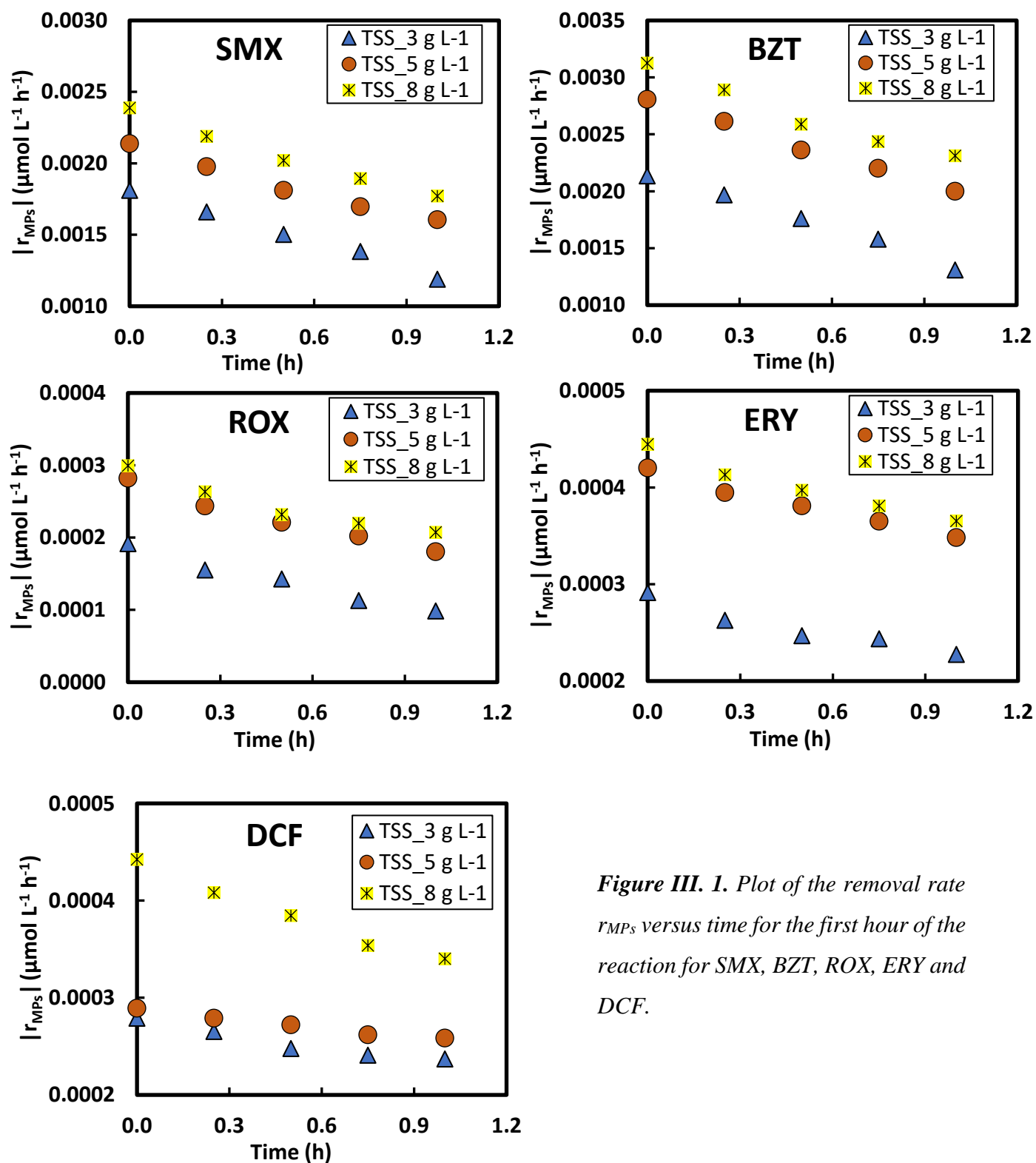


*Figure III. 1.* Plot of the removal rate  $r_{MPs}$  versus time for the first hour of the reaction for SMX, BZT, ROX, ERY and DCF.

The Figure III.1 clearly shows a logical decrease of the removal rates of SMX, BZT, ROX, ERY and DCF with time at 3, 5 and 8  $\text{g}_{\text{TSS}} \text{L}^{-1}$ . Moreover, higher removal rates were recorded at higher biomass concentrations for all investigated micropollutants. However, almost very low change in removal rates was observed with high biomass concentrations (between 5 and 8  $\text{g L}^{-1}$ ) for SMX, BZT, ROX and ERY (almost no change for ROX and ERY). DCF exhibited a different behavior, higher removal rate can be noticed only with a very high biomass concentration, i.e 8  $\text{g}_{\text{TSS}} \text{L}^{-1}$ .

### III.3. The power law kinetics

#### III.3.1. Determination of $n$ coefficient

Based on the results shown in Figure III.1, we can suppose that the kinetics can follow a power law, and then that the removal rate could be proportional to  $(C_{\text{TSS}})^n$  with  $n$  lower than 1. Our new equation was developed in Eq. (III-3) and then linearized in Eq. (III-4).

$$r_{\text{MPs}} = -k_{\text{MPs}} C_{\text{MPs}} (C_{\text{TSS}})^n \quad \text{(III-3)}$$

where  $k_{\text{MPs}}$  is the power law removal rate constant.

$$\log(-r_{\text{MPs}}) = n \log(C_{\text{TSS}}) + \log(k_{\text{MPs}} C_{\text{MPs}}) \quad \text{(III-4)}$$

Subsequently, the removal rate logarithm ( $\log(-r_{\text{MPs}})$ ) vs.  $C_{\text{TSS}}$  logarithm ( $\log(C_{\text{TSS}})$ ) profiles were then represented up to the first hour of the reaction phase for all investigated MPs in Figure III.2.

It is important to note that due to the increase of relative error in the determination of  $r_{\text{MPs}}$  for the lowest concentrations of MPs remaining in the reactor, we limited the study time to 1 hour. For high biodegradable compound such as caffeine, the change of concentration was fast and we realized that our measure of the time was not sufficiently precise. Consequently, due to high relative error, we were not able to treat caffeine.

The Figure III.2 confirmed our hypothesis. Although there was a moderate scatter of the points at different biomass concentration, a straight line of slope  $n$  on the log-log correlates well each micropollutant. The linear regression analysis with respect to SMX (average  $R^2 = 0.9559$ ), BZT (average  $R^2 = 0.9557$ ) and DCF (average  $R^2 = 0.9280$ ) was found to be better than for ROX (average  $R^2 = 0.8840$ ) and ERY (average  $R^2 = 0.8815$ ).

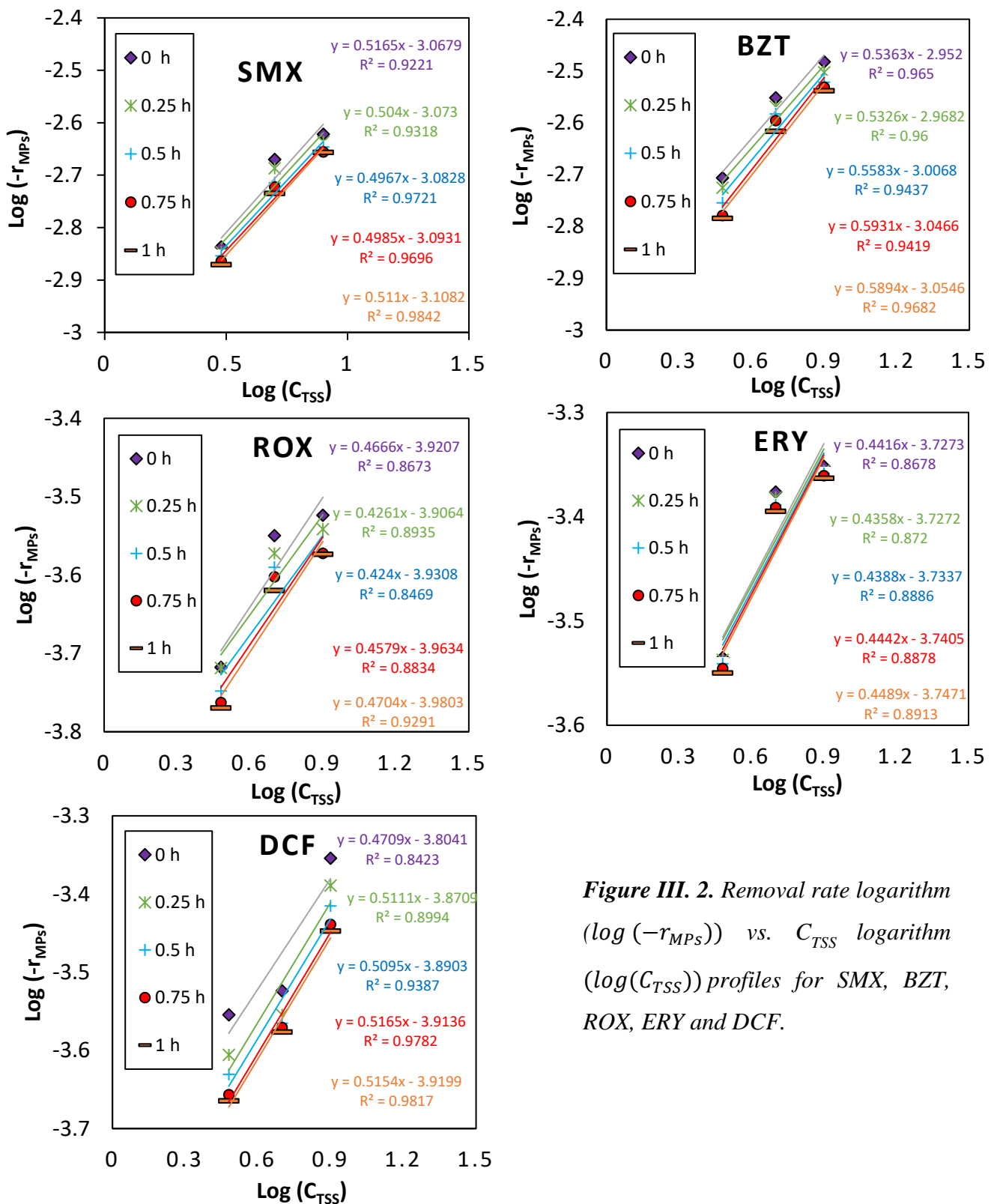


**Figure III. 2.** Removal rate logarithm ( $\log(-r_{MPs})$ ) vs.  $C_{TSS}$  logarithm ( $\log(C_{TSS})$ ) profiles for SMX, BZT, ROX, ERY and DCF.

Results in terms of  $n$  values for each MP are illustrated in Figure III.3. The  $n$  for all MPs are arranged around a horizontal line that represents the average value of  $n$ . It seems obvious that the  $n$  values of all MPs are not significantly different from each other and the average  $n$  of all MPs remains around  $0.5 \pm 0.12$ . However, it seems pertinent to compare the homogenized distribution of  $n$  values of each MP with respect to the horizontal line. The  $n$  of ROX and ERY are slightly below 0.5,  $n$  of SMX and DCF are next to 0.5 while that of BZT are rather above 0.5. According to the Figure III.3, it can be deduced that  $n$  values are less than 1 ( $n < 1$ ) for  $C_{TSS}$  and the new kinetics deviates from the classic apparent-first-order for all micropollutants.

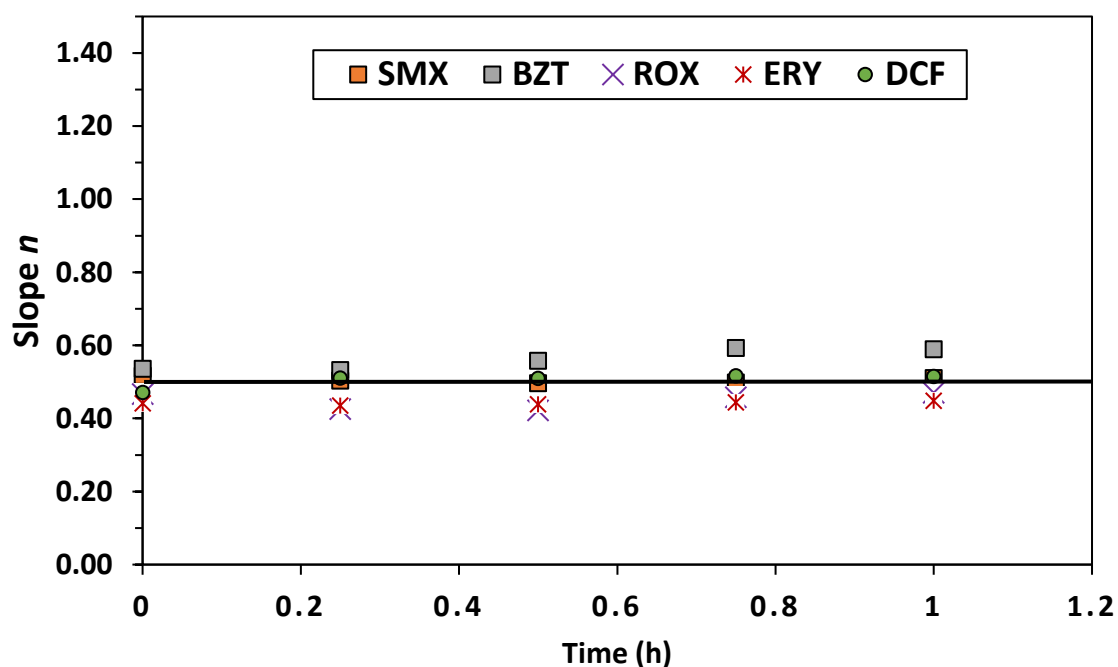


**Figure III. 3.** Plot of the slope  $n$  for the five investigated micropollutants vs. time. The black horizontal line represents the average  $n$  values rounded to 0.5.

### III.3.2. Determination of the new kinetic constants $k_{MPs}$

The new kinetics constant  $k_{MPs}$  values were determined through Eq. (III-4). A real kinetic constants do not depend on time. The second term of the equation groups together the dissolved MP concentration  $C_{MPs}$  ( $\mu\text{mol L}^{-1}$ ) and the new kinetic constant  $k_{MPs}$  ( $\text{L}^n \text{g}^{-n} \text{h}^{-1}$ ). In order to obtain satisfactory results of  $k_{MPs}$  with different biomass concentrations (3, 5 and 8  $\text{g}_{TSS} \text{L}^{-1}$ ) over the appropriate reaction time, a sensitive analysis was required. For more details, Table

III.S1 and Figures III.S2-S5 display the results of the sensitive analysis that have been performed. The new estimated kinetic constants  $k_{MPs}$  were compiled in Table III.1. The  $k_{MPs}$  values could not be compared to literature data because their units depend on the order of the reaction. It is important to note that  $k_{MPs}$  will be used in the following chapter concerning the simulation.

**Table III. 1.** Calculated  $k_{MPs}$  ( $L^n g^{-n} h^{-1}$ ) of each MP for each  $C_{TSS}$  and the average  $k_{MPs}$  ( $\pm$  RSD (%) of +20 % sensitivity test) determined for the three tested biomass concentrations.

$k_{MPs}$ ( $L^n g^{-n} h^{-1}$ )					
	SMX	BZT	ROX	ERY	DCF
$C_{TSS} = 3 g L^{-1}$	0.195	0.121	0.118	0.116	0.032
$C_{TSS} = 5 g L^{-1}$	0.201	0.124	0.114	0.109	0.033
$C_{TSS} = 8 g L^{-1}$	0.207	0.126	0.112	0.111	0.034
<b>Average</b>	$0.201 \pm 0.4$	$0.124 \pm 0.2$	$0.115 \pm 0.3$	$0.112 \pm 0.3$	$0.033 \pm 0.08$
<b><math>k_{MPs} \pm RSD^*</math> (%)</b>					

\*Relative Standard Deviation

### III.3.3. Discussion on the effect of external transport on MPs' kinetics

Our observed kinetics was inconsistent with the apparent-first-order. In current study, the higher biomass concentration increases the active surface and thus the global MPs' removal, but hindered the system and then induces a non-linear kinetics at various biomass concentration. From the equation above, two important conclusions can be drawn in terms of understanding of the  $n$ . Firstly, it is important to note that the so-called  $n$  which constitutes our central results is, in fact, less than 1. Increasing  $C_{TSS}$  increases the mass of reactive biomass but also reduces the mobility of flocs, and then the transport of MPs in the bulk of flocs. Given that the first transport step of MPs in the classical activated sludge system is mainly dominated by advection, factors affecting the MPs' removal will include the mixing energy input, the particular hydraulics in the reactor, and the rheological properties such as density and viscosity of the sludge. It is well known that activated sludge exhibits a pseudoplastic non-Newtonian behavior so that increase of  $C_{TSS}$  leads to radical change in the mixing by a dramatic increase of the apparent viscosity and development of aggregates of flocs. Then, we are facing two opposite processes due to  $C_{TSS}$  increasing: increase of the reactive biomass and decrease of the mobility

of interflocs-water, which lead to a decrease of MPs transport to the flocs where they can be removed. It constitutes the first resistance faced by the MPs.

According to the magnitude of  $n$ , two extreme conditions can be encountered:

- For the classic case where  $n = 1$ , the mixing is efficient and the transport is fast at moderate biomass concentration. So that, the power law model is equal to the biological removal of MPs, which is often described to be governed by apparent-first-order kinetics as following:

$$\Rightarrow r_{MPs} = -k_{MPs}C_{MPs}(C_{TSS})^n = -k_{MPs}C_{MPs}(C_{TSS}) = -k' C_{MPs} \quad (\text{III-5})$$

where  $k'$  is the intrinsic biological removal rate constant which is composed of  $k_{MPs}$  and  $C_{TSS}^n$  ( $k' = k_{MPs} C_{TSS}^n$ ). This configuration occurs with low and moderate  $C_{TSS}$ .

- For lower values of  $n$  ( $n < 1$ ), the apparent-first-order kinetics model cannot be used anymore. The general Eq. (III.3) must be used. Low  $n$  values ( $n < 1$ ) for different MPs could be due to different issues. Generally, the molecule of MP will first have to migrate through the liquid in the reactor until it finds an activated sludge floc. Since this first transport step is mainly dominated by advection, factors affecting the "kinetic constants" will be the mixing and fluid properties such as density and viscosity. Consequently, it could explain the high sensitivity of the new biological kinetics to the physical process through the liquid bulk. Afterwards, MPs have to move in stagnant water between floc aggregates and inside the flocs to reach bacteria.

#### III.3.3.1. Effect of non-ideal mixing

As well as for heterogeneous kinetics or catalysis, the mixing conditions can be the first factor to be investigated in order to explain the new removal rate constants values, since they constitute the first resistance faced by the MP. If mixing issues happen in a real treatment system, there is the risk of calibrating incorrectly the rate constants by using classic kinetics such as first order, apparent-first-order, etc. The kinetic is dependent on the transfer of the MP from the bulk to the biomass activated sludge sites.

Other studies treated similar problems with transfer of substrate or oxygen in activated sludge flocs. In activated sludge systems, maximum dissolved oxygen for biomass growth of  $2 \text{ mg}_{\text{O}_2} \text{ L}^{-1}$  are commonly considered (Henze et al. 2002). It is therefore logical to assume that values



significantly higher than  $2 \text{ mg}_{\text{O}_2} \text{ L}^{-1}$  at higher biomass concentrations ( $4.2 \text{ mg}_{\text{O}_2} \text{ L}^{-1}$  and  $6.1 \text{ mg}_{\text{O}_2} \text{ L}^{-1}$  for reactors operated at  $5 \text{ g}_{\text{TSS}} \text{ L}^{-1}$  and  $8 \text{ g}_{\text{TSS}} \text{ L}^{-1}$ , respectively) are rather due to advection limitations of oxygen in the bulk liquid in their way to the biomass. By analogy, studies were performed on the inconsistencies of the intrinsic half saturation indices ( $K_s$ ) of a substrate. An incompatibility found by Fang et al. (2009) about experimental and theoretical kinetic parameter in nitrifying granules could be attributed to the fact that the bulk concentration that reaches the interface from the bulk solution to the granules is different to the one expected, due to mixing problems. Moreover, Arnaldos et al. (2015) showed that it would be important to first check bulk mixing conditions before attributing different  $K_s$  values to different physical such as diffusion and biological phenomena that affect its observed value.

### *III.3.3.2. Effect of solids concentration of activated sludge on the rheological behavior*

On a structural point of view, it is well known that the biological sludge can be roughly described as concentrated dispersions of structural units, i.e. flocs or aggregates of flocs. The high concentration of solids has been given as the primary reason to break the movement of the bulk liquid carrying the MPs towards aggregates (Table III.2). High viscosity from large solids contents are likely causes of these effects. Considering that the properties of sludge highly depend on solids concentration, it becomes interesting to link the effects of this variable to the rheological properties of activated sludge. A well-mixed activated sludge at low  $C_{\text{TSS}}$  may behave close to water (Newtonian behavior) in terms of rheological properties. However, with increasing biomass concentration, activated sludge exhibits non-Newtonian flow character. It has been identified as a pseudoplastic non-Newtonian fluid (Sanin et al. 2002). This is believed to be due to the increase of the apparent viscosity with solids concentration follows an exponential pattern. Several studies have reported the solids concentration and viscosity relationship in slightly different forms (Seysiecq et al. 2008; Lotito et al. 1997). It indicates that for high  $C_{\text{TSS}}$  (i.e.  $8 \text{ g L}^{-1}$ ) the local mixing become difficult leading to low shear stress, low shear rate and extremely high apparent viscosity. Consequently, this leads to the creation of large aggregates made of flocs and stagnant internal stationary liquid zone.

**Table III. 2.** Physical transport and diffusion limitations of MPs at high biomass concentration.

High biomass concentration		
	Effect	Schema
External transport limitation	<ul style="list-style-type: none"> <li>- Mixing difficulties</li> <li>- Non-Newtonian behaviour</li> <li>- Stationary aggregates area</li> <li>- Almost stationary liquid zone</li> </ul>	
Diffusion	<ul style="list-style-type: none"> <li>- Stagnant film of bulk liquid</li> <li>- Thick boundary layer</li> <li>- Diffusivity inter flocs</li> </ul>	

Additionally, these advection limitations could influence diffusional limitations. Therefore, a comprehensive study of all these starting with the diffusion limitations of MPs existent in the process is represented in the following section.

#### III.3.4. MPs diffusion limitation interflocs

Generally, and for practical reasons the fact of possible limitation of MPs diffusion was of minor importance, since the main focus was on increasing the removal efficiency of recalcitrant compounds. From diffusion point of view, a floc particle can be viewed as a heterogeneous system, where substrates, in this case MPs, diffuses through the matrix and reacts at the surface of the organisms distributed throughout. However, for activated sludge processes, natural diffusion is usually a slow process. Therefore, most of the processing operations depend mainly on the effective mixing for their success.

Based on the above results, the concept of the order of the reaction  $n$  is understood for various MPs in a similar physical manner. However, it is important to note that there is difference in  $n$  values between the investigated MPs (Figure III.3). This observation could mainly be due to the diffusion limitation of each micropollutant between and in the aggregates of flocs due to their molecular weight. Moreover, Mudliar et al. (2008) showed that a region exists near the floc surface where the liquid velocity is very low, giving rise to a near-stagnant film of liquid, which offers maximum resistance to the transfer of substrate to the surface.

To test the hypothesis of MPs' limitation by diffusion, we compared the finding  $n$ -coefficients with diffusion coefficient of each MP. However, going through all available chemical database it was impossible to find diffusion coefficients of investigated MPs neither in CAS water nor in pure water. Subsequently, knowing that in polymer studies, they used correlation between diffusion coefficient and molecular weight ( $D_m \propto 1/M_w$ ), we followed a method inspired by Einstein equation of diffusion. Actually more precise than Einstein equation, models such as the Wilke-Chang and Tyn-Calus allow to obtain a good approximation to the real diffusion coefficient value of component in bulk liquid phase systems from the molecular weight (Wilke and Chang, 1955). It is important to mention that the solvent of our systems is not a pure water (water + sludge) so that, the molecular weight will be useful instead of directly estimation of the MPs diffusion coefficients. The rearrangement of Wilke-Chang equation as a function of the MPs molecular weight ( $M_{MPs}$ ), reveals, a functional dependence of the form  $D_m = f(1/M_{MPs}^{0.6})$ . The complete equation is:

$$D_m = \frac{7.4 \cdot 10^{-8} T \alpha^{0.5} M_{sol}^{0.5} \rho^{0.6}}{\eta M_{MPs}^{0.6}} \quad (\text{III-6})$$

where  $T$  is the absolute temperature,  $M_{MPs}$  is the MPs molecular weight,  $M_{sol}$  is the solvent molecular weight,  $\eta$  is the viscosity of the solvent,  $\rho$  is the density of the solvent and  $\alpha$  is the association parameter which is assumed to be 2.3 for water (Treybal et al. 1980).

We plotted  $n$  versus  $1/M_{MPs}^{0.6}$  (Figure III.4). A very good fit is obtained, showing that there is a relation between the  $n$ -coefficient and the diffusion phenomena. The correlation coefficient ( $R^2$ ) for a linear fit with the respective model was 0.92. This indicates that the decrease of the order of the reaction is attributed to the increasing of the molecular weight of the MP. Then, the expression of  $n$  can be rewritten as:

$$n = k_1 M_{MPs}^{-0.6} + k_2 \quad (\text{III-7})$$

with

$$k_1 = -0.00275 \text{ (mol}^{0.6} \text{ g}^{-0.6}) \text{ and } k_2 = 0.593.$$

Particularly small molecules such as BZT ( $M_{BZT} = 119 \text{ g mol}^{-1}$ ) possess relatively high diffusion coefficient, and reach higher  $n$  values. In the contrary, ROX characterized by the highest molecular weight of  $837 \text{ g mol}^{-1}$  recorded the lowest  $n$  value. Consequently, the MPs with low

diffusion coefficient have a slower transport between the flocs and, the rate of MPs removal in the system is thereby slightly decelerated.

It can be noticed that  $k_1$  and  $k_2$  become then another kind of parameters for characterization of MPs removal. As a first approach, it can be supposed that the values found in the sludge can be used for other sludge for CAS and eventually, SBR and MBR since we used different sludge from two WWTPs in our experiments.

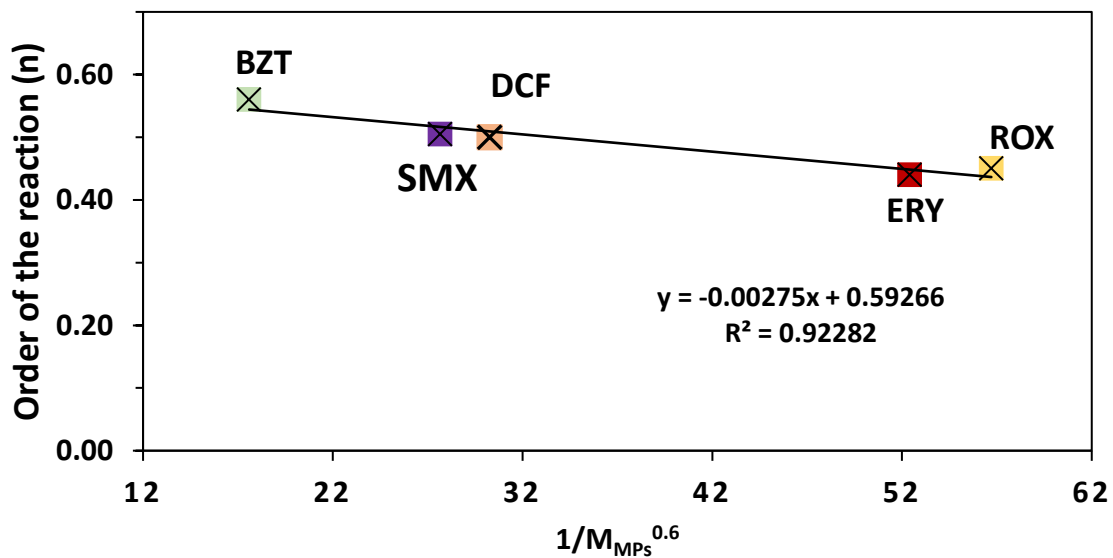


**Figure III. 4.** Plot of the order of the reaction  $n$  for the five investigated micropollutants SMX, BZT, ROX, ERY and DCF vs.  $1/M_{MPs}^{0.6}$ .

Substituting Eq. (III-7) into Eq. (III-3), the new reaction rate takes the form of the following equation:

$$r_{MPs} = -k_{MPs} C_{MPs} C_{TSS} \left( \frac{k_1}{M_{MPs}^{0.6}} + k_2 \right) \quad (\text{III-8})$$

Under these conditions the intrinsic rate is no longer observed since the diffusion of MPs in the bulk liquid affects the rate of MPs' removal and the true kinetics of the reaction (Eq. III-8) must be used. These findings helped to explain the unusual contributions in terms of  $n$  in the overall process of micropollutants removal in previous literature. For activated sludge processes, the diffusion study of micropollutants is often neglected and not considered in the mathematical models. However, LaMotta (1976); Pérez et al. (2005); Benefield and Molz (1983) studied the

kinetic models for biological process by considering both substrates diffusion and reaction in the microbial floc/biofilm. The new current kinetic model seems applicable to all situations, whereas the use of other kinetic relationships would limit the applicability of the model to certain specified conditions (i.e. mixing, sludge properties...).

#### III.4. Conclusion of chapter III

In this chapter, a correlation has been developed to explain the dependence of the kinetic rate of MPs' removal on the biomass concentration raised to the power of  $n$  less than 1 and around 0.5. The power law kinetics allows simple determination of the intrinsic removal rate values and fits to all  $C_{TSS}$  concentrations.

Furthermore, following consequences of the power law kinetics were discussed.

- The removal rate value is directly dependent on mixing conditions.
- The removal rate depends on MPs diffusion.
- The removal rates rely on the rheological properties of the sludge, i.e, biomass concentration. Therefore, further investigations into the rheological properties of sludge would be of high interest.
- Since  $n$  is dependent on local mixing, further research is needed in the reactor design at different scales: local mixing and mixing at the scale of the reactor by using the same experimental data of the current study.
- Moreover, the sensitivity of the simulation of such reaction to the value of  $n$  implies working with care with CFD or systematic simulations.

All of this indicates that still much research is required to gain a better insight into the MPs' removal in biological wastewater treatment.

#### III.5. References of chapter III

- Abegglen, C., Joss, A., McArdell, C.S., Fink, G., Schlüsener, M.P., Ternes, T.A., Siegrist, H., 2009. The Fate of selected micropollutants in a single-house MBR. *Water Research*, 43, 2036–46.
- Arnaldos, M., Amerlinck, Y., Rehman, U., Maere, T., Van Hoey, S., Naessens, W., Ingmar N., I. 2015. From the affinity constant to the half-saturation index: understanding

- conventional modelling concepts in novel wastewater treatment processes. *Water Research* 70, 458–70.
- Banihashemi, B., Droste, R.L., 2018. General fate model for microconstituents in activated sludge system. *Water Environment Research*, 90, 543–53.
- Benfield, L., Molz, F., 1983. A kinetic model for the activated sludge process which considers diffusion and reaction in the microbial floc. *Biotechnology and Bioengineering*, 25, 2591–2615.
- Deblonde, T., Cossu-Leguille, C., Hartemann, P., 2011. Emerging pollutants in wastewater: a review of the literature.” *International Journal of Hygiene and Environmental Health*, 214, 442–48.
- Durán, C., Fayolle, Y., Pechaud, Y., Cockx, A., Gillot, S., 2016. Impact of suspended solids on the activated sludge non-newtonian behaviour and on oxygen transfer in a bubble column. *Chemical Engineering Science*, 141, 154–65.
- Fang, F., Ni, B.J., Li, X.Y., Sheng, G.P., Yu, H.Q., 2009. Kinetic analysis on the two-step processes of AOB and NOB in aerobic nitrifying granules. *Applied Microbiology and Biotechnology*, 83, 1159–69.
- Fernandez, F., Pinho, I., Carballa, M., Omil, F., Lema, J.M., 2013. Biodegradation kinetic constants and sorption coefficients of micropollutants in membrane bioreactors. *Biodegradation*, 24, 165–77.
- Helbling, D.E., Johnson, D.R., Honti, M., Fenner, K., 2012. Micropollutant biotransformation kinetics associate with WWTP process parameters and microbial community characteristics. *Environmental Science & Technology*, 46, 10579–88.
- Henze, M., Gujer, W., Mino, T., Van Loosdrecht, M., 2002. *Activated Sludge Models ASM1, ASM2, ASM2d and ASM3*. London. IWA Publishing.
- Joss, A., Zabczynski, S., Göbel, A., Hoffmann, B., Löffler, D., McArdell, C.S., Ternes, T.A., Thomsen, A., Siegrist, H., 2006. Biological degradation of pharmaceuticals in municipal wastewater treatment: proposing a classification scheme. *Water Research*, 40, 1686–96.
- Kaur, R., Machiraju, R., Nigam, K.D.P., 2007. Agitation effects in a gas-liquid-liquid reactor system: methyl ethyl ketazine production. *International Journal of Chemical Reactor Engineering*, 5, 234-256.
- K’oreje, K.O., Kandie, F.J, Vergeynst, L., Abira, M.A., Van Langenhove, H., Okoth, M., Demeestere, K., 2018. Occurrence, fate and removal of pharmaceuticals, personal care

- products and pesticides in wastewater stabilization ponds and receiving rivers in the Nzoia Basin, Kenya. *Science of The Total Environment*, 637–638, 336–48.
- Kosma, C.I., Lambropoulou, D.A., Albanis, T.A., 2010. Occurrence and removal of PPCPs in municipal and hospital wastewaters in Greece. *Journal of Hazardous Materials*, 179, 804–17.
- LaMotta, E.J., 1976. Internal diffusion and reaction in biological films. *Environmental Science & Technology*, 10, 765–69.
- Lee, D.G., Zhao, F., Rezenom, Y.H., Russell, D.H., Chu, K.H., 2012. Biodegradation of triclosan by a wastewater microorganism. *Water Research*, 46, 4226–34.
- Lee, K.C, Rittmann, B.E., Shi, J., McAvoy, D., 1998. Advanced steady-state model for the fate of hydrophobic and volatile compounds in activated sludge. *Water Environment Research*, 70, 1118–31.
- Lotito, V., Spinosa, L., Mininni, G., Antonacci, R., 1997. The rheology of sewage sludge at different steps of treatment. *Water Science and Technology*, 36, 79–85.
- Majewsky, M., Gallé, T., Yargeau, V., Fischer, K., 2011. Active heterotrophic biomass and sludge retention time (SRT) as determining factors for biodegradation kinetics of pharmaceuticals in activated sludge. *Bioresource Technology*, 102, 7415–21.
- Marfil-Vega, R., Suidan, M.T., Mills, M.A., 2010. Abiotic transformation of estrogens in synthetic municipal wastewater: an alternative for treatment? *Environmental Pollution*, 158, 3372–77.
- Maurer, M., Escher, B.I., Richle, P., Schaffner, C., Alder, A. C., 2007. Elimination of  $\beta$ -Blockers in sewage treatment plants. *Water Research*, 41, 1614–1622.
- Mudliar, S., Banerjee, S., Vaidya, A., Devotta, S., 2008. Steady state model for evaluation of external and internal mass transfer effects in an immobilized biofilm. *Bioresource Technology*, 99, 3468–74.
- Onesios, K.M., Yu, J.T., Bouwer, E.J., 2009. Biodegradation and removal of pharmaceuticals and personal care products in treatment systems: a review. *Biodegradation*, 20, 441–66.
- Pérez, J., Picioreanu, C., Van Loosdrecht, M., 2005. Modelling biofilm and floc diffusion processes based on analytical solution of reaction-diffusion equations. *Water Research*, 39, 1311–23.
- Plosz, B.G., Langford, K.H., Thomas, K.V., 2012. An activated sludge modelling framework for xenobiotic trace chemicals (ASM-X): assessment of diclofenac and carbamazepine. *Biotechnology and Bioengineering*, 109, 2757–69.

- Plosz, B.G., Leknes, H, Thomas, K.V., 2010. Impacts of competitive inhibition, parent compound formation and partitioning behavior on the removal of antibiotics in municipal wastewater treatment. *Environmental Science & Technology*, 44, 734–42.
- Press-Kristensen, K., Lindblom, E., Henze, M., 2007. Modelling as a tool when interpreting biodegradation of micro pollutants in activated sludge systems. *Water Science and Technology*, 56, 11–16.
- Sanin, D.F., 2002. Effect of aolution physical chemistry on the rheological properties of activated Sludge. *Water SA*, 28, 207–12.
- Seyssiecq, I., Marrot, B., Djerroud, D., Roche, N. 2008. In situ triphasic rheological characterisation of activated sludge, in an aerated bioreactor. *Chemical Engineering Journal*, 142, 40–47.
- Stasinakis, A.S., Thomaidis, N.S., Arvaniti, O.S., Asimakopoulos, A, Samaras, V.G., 2010. Fate and Biotransformation of Metal and Metalloid Species in Biological Wastewater Treatment Processes. *Critical Reviews in Environmental Science and Technology*, 40, 307–64.
- Suarez, S., Lema, J.M., Omil, F., 2010. Removal of pharmaceutical and personal care products (PPCPs) under nitrifying and denitrifying conditions. *Water Research*, 44, 3214–3224.
- Suárez, S., Reif, R., Lema, J.M., Omil, F., 2012. Mass balance of pharmaceutical and personal care products in a pilot-scale single-sludge system: influence of T, SRT and recirculation ratio. *Chemosphere*, 89, 164–71.
- Sui, Q., Huang, J., Deng, S., Chen, W., Yu, G., 2011. Seasonal variation in the occurrence and removal of pharmaceuticals and personal care Products in different biological wastewater treatment processes. *Environmental Science & Technology*, 45, 3341–48.
- Tan, B.L.L., Hawker, D.W., Müller, J.F., Leusch, F.D.L., Tremblay, L.A., Chapman, H.F., 2007. Modelling of the fate of selected endocrine disruptors in a municipal wastewater treatment plant in South East Queensland, Australia. *Chemosphere*, 69, 644–54.
- Tang, Y., Guo, L.L., Hong, C.H., Bing, Y.X., Xu, Z.C., 2019. Seasonal occurrence, removal and risk assessment of 10 pharmaceuticals in 2 sewage treatment plants of Guangdong, China. *Environmental Technology*, 40, 458–69.
- Ternes, T.A., Joss, A., Siegrist, H., 2004. Peer Reviewed: scrutinizing pharmaceuticals and personal care products in wastewater treatment. ACS Publications.
- Tiwari, B., Sellamuthu, B., Ouarda, Y., Drogui, P., Tyagi, R.D., Buelna, G., 2017. Review on fate and mechanism of removal of pharmaceutical pollutants from wastewater using biological approach. *Bioresource Technology*, 224, 1–12.



- Tomei, M.C., Annesini, M.C., Rita, S., Daugulis, A.J., 2008. Biodegradation of 4-Nitrophenol in a two-phase sequencing batch reactor: concept demonstration, kinetics and modelling. *Applied Microbiology and Biotechnology*, 80, 1105–12.
- Vasiliadou, I.A., Molina, R., Martínez, F., Melero, J.A., 2013. Biological removal of pharmaceutical and personal care products by a mixed microbial culture: sorption, desorption and biodegradation. *Biochemical Engineering Journal*, 81, 108–19.
- Wick, A., Fink, G., Joss, A., Siegrist, H., Ternes, T.A., 2009. Fate of beta blockers and psychoactive drugs in conventional wastewater treatment. *Water Research*, 43, 1060–74.
- Wilke, C.R., Chang, P., 1955. Correlation of diffusion coefficients in dilute solutions. *AIChE Journal*, 1, 264–70.
- Xue, W., Wu, C., Xiao, K., Huang, X., Zhou, H., Tsuno, H., Tanaka, H., 2010. Elimination and fate of selected micro-organic pollutants in a full-scale anaerobic/anoxic/aerobic process combined with membrane bioreactor for municipal wastewater reclamation. *Water Research*, 44, 5999–6010.
- Yi, T., Mackintosh, S., Aga, D.S., Harper, W.F., 2011. Exploring 17 $\alpha$ -ethinylestradiol removal, mineralization, and bioincorporation in engineered bioreactors. *Water Research*, 45, 1369–77.
- Zhao, J., Li, Y., Zhang, C., Zeng, Q., Zhou, Q., 2008. Sorption and degradation of bisphenol A by aerobic activated sludge. *Journal of Hazardous Materials*, 155, 305–11.
- Zheng, W., Wen, X., Zhang, B., Qiu, Y., 2019. Selective effect and elimination of antibiotics in membrane bioreactor of urban wastewater treatment plant. *Science of The Total Environment*, 646, 1293–1303.



**Chapter IV. Simulation of the micropollutants  
removal in batch and continuous systems**

*In the first part, this chapter introduced the Activated Sludge Model 1 (ASM1), a biological model used for simulation of the evolution of macropollutant concentrations, with attention for the simplifications and parameter optimization behind the model during biological experiments performed in batch mode. Moreover, the modelling of micropollutants (MPs) removal was added to ASM1. This modelling of MPs integrated in the activated sludge process was based on the data presented in chapter II in order to estimate accurate concentrations at the end of the reaction phase of the SBR. Two sets of simulations were performed by testing the apparent-first order in batch system. The first set included the combinations of SRT and HRT experiments and the second the experiments performed with various biomass concentrations. In the second part, this chapter goes to validate numerically the new power law kinetics model in batch experiments and to predict the biomass concentration and the local mixing effects on the kinetics. It also presents the new appropriate kinetics on continuous system by testing different hydrodynamic conditions such as local mixing and reactor configurations in order to enhance the removal of the contaminants of water bodies.*

## IV.1. Introduction

Modelling and simulation are very important tools to design new wastewater treatment plants, optimize and increase the efficiency of the existing ones (Laurent et al. 2014; Nopens et al. 2017; Samstag et al. 2016; Wicklein et al. 2015). Gernaey et al. (2004) showed that modelling makes it possible to better understand the operation of the wastewater treatment plant (WWTP) and the consequences of modifying the operating parameters (residence time, aeration time, organic load, sludge age, etc.). During the last decades, design, modelling, optimization and control of biological wastewater treatment systems, i.e. activated sludge system, has gained a lot of importance due to the fact that not all existing WWTPs comply with the effluent norms. Many WWTPs require modifications to reduce the potential environmental risk of effluents. Typically, model-based assessment is used to generate predicted environmental concentrations for recipient water bodies. Several studies showed that modelling a treatment plant actually requires the use of several models such as a hydrodynamic model (representing the hydraulic behavior of the installation), an aeration and mixing models, models for physicochemical processes (variation of pH and alkalinity, flocculation, precipitation, decantation ...), a biokinetic model (biological processes), a fractionation model (converting the measurements made on the tributary, i.e. chemical oxygen demand, COD, and Kjeldal nitrogen, NTK, into state variables of the biokinetic models such as fractions of substrate slowly and rapidly biodegradable) and the MPs kinetics studied in new frameworks of activated sludge modelling (Bellandi 2014; Fenu et al. 2010; Gillot et al. 2006; Plosz et al. 2010; Pomies et al. 2013; Rehman et al. 2014; Tan et al. 2007; Kristenten et al 2013; Couzot et al. 2013).

The first goal of this chapter is to model the biokinetics of activated sludges represented by ASM1 coupled with the kinetic model of micropollutant removal. A preliminary simulation was performed in order to reproduce the experimental time evolution of the ASM1 state variables (macropollutants and biomass) measured in chapter II. In a second step the micropollutants removal kinetics was added to the ASM1 model. Two kinetics model were considered, the classical apparent-first-order model and a power law kinetics, in order to (i) verify the experimental results of previous chapters and (ii) predict the effect of local mixing for a wide range of biomass concentrations on MPs' removal in the batch system.

The second goal of the chapter is the extrapolation of the new kinetics defined in chapter III to continuous systems in order to predict the effect of the local mixing but also of the hydrodynamic configurations on the MPs removal. The predictions of concentrations evolution

between the inlet and the outlet of the systems were performed with MATLAB/Simulink software.

## **IV.2. Modelling of activated sludge biological treatment**

Henze et al. (1987; 2002) proposed a mathematical modelling of wastewater treatment process using the activated sludge biological treatment. The most widely accepted and used model from this set of models is the activated sludge model no.1 (ASM1) (Hauduc et al. 2013). The ASM1 model incorporates the basic biotransformation processes of an activated sludge wastewater treatment plant for the prediction of biological phenomena in the reactor: it represents phenomena such as carbon oxidation, nitrification and denitrification within an activated sludge system by quantifying the kinetics and stoichiometry of each reaction. This is why the ASM1 model was chosen in the present chapter to describe the evolution of macropollutants during the activated sludge process in the SBR systems studied experimentally in chapter II.

The equations of this semi-deterministic model describe the growth and death of heterotrophic and autotrophic biomasses during the biological conversion of COD and  $\text{NH}_4$ . The system of equations consists of first-order differential equations with respect to time, describing the phenomena of growth, death, hydrolysis and ammonification. Although this model is commonly used, it suffers from following disadvantages: (i) the calibration of all the kinetic parameters can be hazardous task and (ii) the model is highly nonlinear due to the appearance of Monod like kinetics in the material balance equations (Smetz et al. 2003). Many simplified ASM1 were proposed through linearization.

### **IV.2.1. State variables and biological phenomena of ASM1**

Often not ASM1 state variables and/or not all processes are considered. The most straightforward simplification consists in assuming only oxic conditions, which is the case of our experiments.

The compounds involved in ASM1 are represented by twelve state variables described in Table IV.1.

**Table IV. 1.** Variables of the ASM1 model.

Type of compound	Notation	Description
Biomass	$X_{B,H}$	Heterotrophic biomass
	$X_{B,A}$	Autotrophic biomass
	$X_P$	Inert biomass
Organic substrate	$S_S$	Substrate rapidly biodegradable
	$X_S$	Substrate slowly biodegradable
Nitrogen compound	$S_{NO}$	Nitrates and nitrites
	$S_{NH}$	Ammonium and ammonia
	$S_{ND}$	Organic nitrogen substrate rapidly biodegradable
	$X_{ND}$	Organic nitrogen substrate slowly biodegradable
Non-biodegradable compound	$S_I$	Carbon and nitrogen substrate soluble and non-biodegradable
	$X_I$	Carbon and nitrogen substrate non-soluble and non-biodegradable
Oxygen	$S_O$	Dissolved oxygen

The letter  $X$  is proposed for particulate compounds and the letter  $S$  for soluble compounds. These state variables can be divided into 5 groups:

- substrates: the readily biodegradable substrate  $S_S$  ( $\text{mg}_{\text{O}_2} \text{L}^{-1}$ ) and the slowly biodegradable substrate  $X_S$  ( $\text{mg}_{\text{O}_2} \text{L}^{-1}$ ). The latter is considered particulate by the model ASM1 although soluble and colloidal fractions are also present in reality;
- biomasses: the heterotrophic biomass  $X_{B,H}$  ( $\text{mg}_{\text{O}_2} \text{L}^{-1}$ ), responsible for the oxidation of organic matter and denitrification, and the autotrophic biomass  $X_{B,A}$  ( $\text{mg}_{\text{O}_2} \text{L}^{-1}$ ), responsible for nitrification. Biomass growth is described by Monod's law. A third state variable, noted  $X_P$  ( $\text{mg}_{\text{O}_2} \text{L}^{-1}$ ), represents the products of dead biomass;
- nitrogen compounds: particulate biodegradable organic nitrogen  $X_{ND}$  ( $\text{mg}_N \text{L}^{-1}$ ), nitrogen organic soluble biodegradable  $S_{ND}$  ( $\text{mg}_N \cdot \text{L}^{-1}$ ), ammoniacal nitrogen  $S_{NH}$  ( $\text{mg}_N \text{L}^{-1}$ ), and nitrate-nitrite  $S_{NO}$  ( $\text{mg}_N \text{L}^{-1}$ );
- dissolved oxygen  $S_O$  ( $\text{mg}_{\text{O}_2} \text{L}^{-1}$ );
- biologically inert states: the inert soluble organic compounds  $S_I$  ( $\text{mg}_{\text{O}_2} \text{L}^{-1}$ ) and particulate  $X_I$  ( $\text{mg}_{\text{O}_2} \text{L}^{-1}$ ).

The four major biological processes that take place are schematized as follows:

- biological growth of heterotrophic and autotrophic biomass:  
Substrate + Biomass  $\longrightarrow$  Biomass + Products
- endogenous respiration of heterotrophic and autotrophic biomass (mortality):  
Biomass  $\longrightarrow$  Products
- ammonification by heterotrophic biomass, organic nitrogen converts to ammonium;  
hydrolysis of slowly biodegradable compounds, non-soluble carbon and non-soluble  
nitrogen:  
Substrate  $\longrightarrow$  Products

#### IV.2.2. ASM1 model description

Each biological reaction is characterized by the concentrations of the compounds (substrate, biomass and products), the reaction kinetics ( $\rho_u$ ) and the conversion rates (Y). The conversion rate represents the theoretical amount of product formed from a given amount of reactant. It therefore depends on the nature of the compounds involved in the reaction. There is a conversion rate  $Y_{i,u}$  for each biological reaction and compound (i) involved.

For each biological process, the consumption and production rates of the compound (i) involved are given by the product  $Y_{i,u} \times \rho_u$ , preceded respectively by the sign - and the sign +. The set of rates acting on compound (i) of ASM1 model is called the overall biological rate, denoted  $r_i$ . It is represented by the following expression:

$$r_i = \sum Y_{i,u} \rho_u \quad (\text{IV- 1})$$

The reaction kinetics for the different processes ( $\rho_u$ ) are an important part of the dynamics of the system. However, the way in which each compound influences reaction kinetics is sometimes difficult to evaluate. The writing of these kinetics in the form of an equation is generally based on empirical considerations and formulations is therefore often approximate relations. The reaction kinetics of each process is expressed by the following equation:

$$\rho_u = \mu_u C_{TSS} \quad (\text{IV- 2})$$

where  $C_{TSS}$  represents the concentration of the total biomass and  $\mu_u$  represents a parameter that can be expressed by a constant or a parameter varying in time or a product of other system state



variables. For example, in the case of biomass mortality,  $\mu_d$  equals a constant coefficient of biomass mortality "b", which is not usually the case for kinetic parameters.

However, Eq. (IV-2) is not sufficient to describe complex kinetics (oxidation of biodegradable organic matter, nitrification, denitrification, hydrolysis) since it does not allow the representation of saturation or inhibition phenomena. Therefore, the equation of complex kinetics requires determining whether a compound, according to its concentration in the reaction medium, inhibits, activates or limits the reaction and in what proportion. The biomass growth reaction is considered as a complex reaction of the treatment process. The empirical model of Monod provides a solution to this problem (Monod 1941). For example, Monod equation translates the exponential growth phase corresponding to the saturation of the specific growth of heterotrophic biomass in aerobic condition as follows:

$$\mu_1 = \mu_H \left( \frac{S_S}{K_S + S_S} \right) \left( \frac{S_O}{K_{O,H} + S_O} \right) \quad (\text{IV-3})$$

where  $\mu_1$  is the specific growth rate of  $X_{B,H}$  ( $d^{-1}$ ),  $\mu_H$  is the maximum growth rate ( $d^{-1}$ ),  $K_S$  is the substrate half-saturation constant ( $mg_{O_2} L^{-1}$ ) that represents the substrate concentration when the growth rate is equal to half of its maximum value ( $\mu_H$ ),  $K_{O,H}$  is the dissolved oxygen half-saturation coefficient for heterotrophic biomass and  $S_O$  is the dissolved oxygen.

Table IV.2 summarizes the equations of the biological processes involved and their reaction rates.

Although they are different in nature, the biological phenomena present in the anoxic and aerobic phases are simulated under a single model. This is possible thanks to the use of switching functions:

- the kinetics taking place only in the anoxic phase will include the term  $\left( \frac{K_{O,H}}{K_{O,H} + S_O} \right)$  inhibiting the aerobic phase reaction;
- the kinetics taking place only in the aerobic phase will include the following terms of  $\left( \frac{S_O}{K_{O,H} + S_O} \right)$  or  $\left( \frac{S_O}{K_{O,A} + S_O} \right)$  inhibiting the reaction in the anoxic phase.

Table IV. 2. Biological processes of the ASMI model and their reaction rates.

Process		Reaction	Reaction rate	
Biological growth of biomass	Heterotrophic	$\frac{1}{Y_H} S_S + \frac{1 - Y_H}{Y_H} S_O + i_{XB} S_{NH}$ $\rightarrow X_{B,H}$	$\rho_1 = \mu_H \left( \frac{S_S}{K_S + S_S} \right) \left( \frac{S_O}{K_{O,H} + S_O} \right) X_{B,H}$	(IV-4)
		$\frac{1}{Y_H} S_S + \frac{1 - Y_H}{2.86 Y_H} S_{NO} + i_{XB} S_{NH}$ $\rightarrow X_{B,H}$	$\rho_2 = \mu_H \eta_g \left( \frac{S_S}{K_S + S_S} \right) \left( \frac{K_{O,H}}{K_{O,H} + S_O} \right) \left( \frac{S_{NO}}{K_{NO} + S_{NO}} \right) X_{B,H}$	(IV-5)
	Autotrophic	$\left( i_{XB} + \frac{1}{Y_A} \right) S_{NH} + \frac{4.57 - Y_H}{Y_H} S_O$ $\rightarrow X_{B,A} + \frac{1}{Y_A} S_{NO}$	$\rho_3 = \mu_A \left( \frac{S_{NH}}{K_{NH} + S_{NH}} \right) \left( \frac{S_O}{K_{O,A} + S_O} \right) X_{B,A}$	(IV-6)
Mortality of biomass	Heterotrophic	$X_{B,H} \rightarrow (1 - f_P) X_S + f_P \cdot X_P + (i_{XB} - f_P \cdot i_{XP}) X_{ND}$	$\rho_4 = b_H X_{B,H}$	(IV-7)
	Autotrophic	$X_{B,A} \rightarrow (1 - f_P) X_S + f_P \cdot X_P + (i_{XB} - f_P \cdot i_{XP}) X_{ND}$	$\rho_5 = b_A X_{B,A}$	(IV-8)
Ammonification of the soluble nitrogen compound		$S_{ND} \rightarrow S_{NH}$	$\rho_6 = k_a S_{ND} X_{B,H}$	(IV-9)
Hydrolysis of slowly biodegradable compound	Carbon compound	$X_S \rightarrow S_S$	$\rho_7 = k_h \left( \frac{X_S / X_{B,H}}{K_X + X_S / X_{B,H}} \right) \left[ \left( \frac{S_O}{K_{O,H} + S_O} \right) + \eta_h \left( \frac{K_{O,H}}{K_{O,H} + S_O} \right) \left( \frac{S_{NO}}{K_{NO} + S_{NO}} \right) \right] X_{B,H}$	(IV-10)
	Nitrogen compound	$X_{ND} \rightarrow S_{ND}$	$\rho_8 = \frac{X_{ND}}{X_S} \rho_7$	(IV-11)

However, our experimental results in batch mode will be exclusively simulated during the aerobic phase and thus inhibiting the reactions in the anoxic phase.

The production rates of each compound are:

$$X_{B,H} \quad r_1 = \rho_1 + \rho_2 - \rho_4 \quad (\text{IV - 12})$$

$$X_{B,A} \quad r_2 = \rho_3 - \rho_5 \quad (\text{IV - 13})$$

$$X_P \quad r_3 = f_P(\rho_4 + \rho_5) \quad (\text{IV - 14})$$

$$S_S \quad r_4 = -\frac{1}{Y_H}(\rho_1 + \rho_2) + \rho_7 \quad (\text{IV - 15})$$

$$X_S \quad r_5 = (1 - f_P)(\rho_4 + \rho_5) - \rho_7 \quad (\text{IV - 16})$$

$$S_{NO} \quad r_6 = -\frac{1 - Y_H}{2.86Y_H}\rho_2 + \frac{1}{Y_A}\rho_3 \quad (\text{IV - 17})$$

$$S_{NH} \quad r_7 = -i_{XB}(\rho_1 + \rho_2) - \left(i_{XB} + \frac{1}{Y_A}\right)\rho_3 + \rho_6 \quad (\text{IV - 18})$$

$$S_{ND} \quad r_8 = \rho_8 - \rho_6 \quad (\text{IV - 19})$$

$$X_{ND} \quad r_9 = (i_{XB} - f_P i_{XP}) \times (\rho_4 + \rho_5) - \rho_8 \quad (\text{IV - 20})$$

$$S_I \quad r_{10} = 0 \quad (\text{IV - 21})$$

$$X_I \quad r_{11} = 0 \quad (\text{IV - 22})$$

$$S_O \quad r_{12} = -\frac{1 - Y_H}{Y_H}\rho_1 - \frac{4.57 - Y_A}{Y_A}\rho_3 \quad (\text{IV - 23})$$

The values of the stoichiometric parameters of the ASM1 model as well as their units are presented in Table IV.3. The kinetic parameters values were taken either from the Benchmark Simulation Model no. 1 (BSM1, Alex et al., 2008), or in the range of variation reported by the study of (Henze et al. 2002). The values are summarized in Table IV.4.

Table IV. 3. Values of the stoichiometric parameters of the ASM1 model.

Coefficient	Value of Benchmark	Unit	Description
$Y_A$	0.24	$\text{g } X_{B,A\text{COD}} \text{ formed } (\text{g}_N \text{ oxidized})^{-1}$	Conversion rate of the substrate into autotrophic biomass
$Y_H$	0.67	$\text{g } X_{B,H\text{COD}} \text{ formed } (\text{g}_{\text{COD}} \text{ oxidized})^{-1}$	Conversion rate of the substrate into heterotrophic biomass
$f_P$	0.08	without dimension	Inert COD fraction generated by dead biomass
$i_{XB}$	0.086	$\text{g}_N (\text{g}_{\text{COD}})^{-1}$ in biomass ( $X_{B,A}$ and $X_{B,H}$ )	Fraction of nitrogen assimilated by heterotrophic biomass
$i_{XP}$	0.06	$\text{g}_N (\text{g}_{\text{COD}})^{-1}$ in $X_P$	Nitrogen fraction assimilated by inert biomass

Table IV. 4. Kinetic parameter values of the ASM1 model.

Parameter	Value of Benchmark	Henze (2002) at 20°C	Unit	Description
$\mu_H$	4	0.6-13.2	$\text{day}^{-1}$	Maximum growth rate of heterotrophic biomass
$\mu_A$	0.5	0.2-1	$\text{day}^{-1}$	Maximum growth rate of autotrophic biomass
$\eta_g$	0.8	0.6-1	without dimensions	Comparative efficacy of anoxic growth versus aerobic growth
$\eta_h$	0.8	-	$\text{g}_{\text{COD}} \text{ m}^{-3}$	Effectiveness of the anoxic pathway compared to the aerobic pathway
$K_S$	10	2-225	$\text{g}_{\text{O}_2} \text{ m}^{-3}$	Readily biodegradable substrate half-saturation coefficient
$K_{O,H}$	0.2	0.01-0.5	$\text{g}_{\text{NO}_3\text{-N}} \text{ m}^{-3}$	Dissolved oxygen half-saturation coefficient for heterotrophic biomass
$K_{NO}$	0.5	0.01-0.5	$\text{g}_{\text{NH}_3\text{-N}} \text{ m}^{-3}$	Nitrate-nitrite half-saturation coefficient
$K_{NH}$	1	-	$\text{g}_{\text{O}_2} \text{ m}^{-3}$	Coefficient of half-saturation of ammoniacal nitrogen
$K_{O,A}$	0.4	0.4-2	$\text{g}_{\text{COD}} \text{ g}_{X_{B,H\text{COD}}}^{-1}$	Dissolved oxygen half-saturation constant for autotrophic biomass
$K_X$	0.1	0.03	$\text{g}_{\text{COD}} \text{ g}_{X_{B,H}} \text{ COD} \text{ day}^{-1}$	Semi-saturation constant of the proportion of substrate to be hydrolyzed with respect to the heterotrophic biomass
$k_h$	3	-	$\text{day}^{-1}$	Hydrolysis rate constant of slowly biodegradable substrates
$b_H$	0.3	0.04-1.6	$\text{day}^{-1}$	Coefficient of mortality of heterotrophic biomass
$b_A$	0.05	0.04-0.2	$\text{m}^{-3} \text{COD g} \text{ day}^{-1}$	Coefficient of mortality of autotrophic biomass
$k_a$	0.05	-	$\text{g}_{\text{COD}} \text{ m}^{-3}$	Ammonification rate constant

### IV.2.3. Relations between ASM1 model & usual experimental analyses and some ASM1 limitations

As commonly known, the operation of the sequencing batch reactor (SBR) process consists of a filling, a reacting, a settling, a decanting (effluent emptying), and an idling stage (pause) in sequence. In the present study, only the reacting stage (aerobic phase) in the batch mode was modeled in order to simulate the experimental configuration.

The composition of wastewater influents varies during the day in WWTP and so the choice of a typical influent composition is difficult and raises a reproducibility question for laboratory studies. This is why synthetic influents with properties close to average wastewater are often used. As mentioned before in Table II.7, our synthetic influent was composed of sugars (sodium acetate) for the biodegradable carbon substrate, ammonium bicarbonate for ammonia nitrogen, potassium dihydrogen phosphate for phosphorus and various mineral compounds ( $\text{MgSO}_4$ ,  $\text{FeSO}_4$ ,  $\text{CaCl}_2$ ,  $\text{NaHCO}_3$ ). However, the literature is rich with other examples of sugars such as ethanol, molasses, and Viadox for biodegradable carbon substrate. In our study, a substrate was made of only readily biodegradable substance ( $S_S$ ) and no slowly biodegradable substrate was added ( $X_S$ ). By definition, slowly biodegradable substances need to be hydrolyzed before being metabolized, while readily biodegradable substances can be metabolized without prior hydrolysis. The sodium acetate was the only carbon source chosen as the basis for the initial composition of the three different SBRs. The composition of the mixtures used experimentally is detailed in chapter II. In particular:

- The concentrations of acetate, expressed in COD, were calculated for a volume exchange ratio (VER) of 50 %. The volumetric exchange ratio is defined as the ratio between the volumes treated per cycle to the maximum reactor volume. It is equal to  $600 \text{ mg}_{\text{O}_2} \text{ L}^{-1}$  of COD,  $250 \text{ mg}_{\text{O}_2} \text{ L}^{-1}$  of COD, and  $50 \text{ mg}_{\text{O}_2} \text{ L}^{-1}$  of COD in SBR-3 d, SBR-10 d, and SBR-20 d, respectively.
- The ammonia nitrogen concentration equals  $37.5 \text{ mg}_{\text{N-NH}_4^+} \text{ L}^{-1}$ , with a VER of 50 %, in the three above-mentioned SBRs.

In order to use the experimental data in the simulated ASM1 model, many equivalence relationships can be found in the literature between experimentally measured parameters in wastewater treatment plants and ASM1 variables. The following relationships were proposed by Copp et al. (2002). They read as follows.

$$[COD] = S_I + S_S + X_I + X_S + X_{B,H} + X_{B,A} + X_P \quad (IV - 24)$$

and

$$[COD_{filtered}] = S_I + S_S + 0.25 (X_I + X_S + X_{B,H} + X_{B,A} + X_P) \quad (IV - 25)$$

$$C_{TSS} = 0.75 (X_I + X_S + X_{B,H} + X_{B,A} + X_P) \quad (IV - 26)$$

$$[NO_3^- + NO_2^-] = S_{NO} \quad (IV - 27)$$

In the batch mode study, we assumed that no non-biodegradable non-soluble ( $X_I$ ) nor any non-biodegradable soluble substrates ( $S_I$ ) were present and that the 0.45  $\mu\text{m}$  filtration process made it possible to eliminate all the biomass. Consequently, we reach  $[COD_{filtered}] = S_S$ . The  $S_{NO}$  represents the sum of nitrites and nitrates, but in all classical situations the nitrites are considered to be negligible.

Dionisi et al (2017) assumed that endogenous metabolism converts the biomass to carbon dioxide, with very small generation of inert ( $X_P$ ). Hence, the sum of  $X_{B,H} + X_{B,A}$  represents the active biomass. Generally, in CAS systems, authors assumed that most of bacteria that biodegrade pollutants are heterotrophic bacteria (Le Moullec, 2008). Hence, the following relations for biomass concentration will be used:

$$C_{TSS} = 0.75 (X_{B,H} + X_{B,A}) \quad (IV - 28)$$

$$X_{B,A} = 0.05 X_{B,H} \quad (IV - 29)$$

$$X_{B,H} = \beta C_{TSS} \quad (IV - 30)$$

where  $\beta$  is the ratio of the volatile suspended solids ( $C_{VSS}$ ) to the total suspended solids ( $C_{TSS}$ ).

- ASM1 limitations

The assumptions and limitations of the ASM1 model are numerous. It is important to keep some of them in mind during our simulation:

- The hydrolysis of the nitrogen and carbon compounds take place simultaneously with equal rates.
- The parameters for nitrification are assumed to be constant.
- Only the rapidly biodegradable part of the biodegradable organic matter can be used by the biomass.

- The mortality of the bacteria is not affected by the absence of oxygen during the whole cycle of SBR (settling and drawing phases).

### IV.3. Kinetics of MPs removal

Two types of kinetics of MPs removal are tested in the following sections: the common apparent-first order kinetics described in chapter II, and the new power law kinetics investigated in chapter III. In order to simulate the removal of micropollutants concentration ( $C_{MPs}$ ), additional biological processes must be taken into account:

- Growth of bacteria that biodegrade micropollutants
- Mortality of bacteria that biodegrade micropollutants

The bacteria that biodegrade pollutants were assumed to be heterotrophic ( $X_{B,H}$ ). Moreover, we considered no biomass growth due to micropollutants since at very low concentration of micropollutants, the removal of MPs has negligible on biomass.

For low substrate concentrations, much lower than the half-saturation coefficient, e.g. the case of micropollutants in this study, the Monod kinetics can be simplified into the common pseudo-first order kinetics (Eq. IV-31).

$$r_{MPs} = -k C_{MPs} C_{TSS} \quad (IV-31)$$

However, as explained in previous chapters, Eq. (IV-31 and II-3) is often simplified; people assuming that the fluctuations of  $C_{TSS}$  are negligible. Further simulations were carried out by testing the apparent-first-order described in Eq. (IV-32 and II-4) for the different experimental  $C_{TSS}$  of 3, 5 and 8  $g_{TSS} L^{-1}$ .

$$r_{MPs} = -k' C_{MPs} \quad (IV-32)$$

Accordingly, the substituted kinetics called power law model for MPs' removal derived as the following equation (Eq. IV-33 and III-3) from chapter III, was also put to a test.

$$r_{MPs} = -k_{MPs} C_{MPs} (C_{TSS})^n \quad (IV-33)$$

Both kinetics were tested in batch systems to simulate the experimental setups. But only the new kinetics of Eq. IV-33 was applied later on the continuous system.

#### IV.4. Sequencing Batch Reactor simulations

The first modelling approach has been especially developed to simulate the macropollutants during the reaction phase of the SBR system. The ASM1 model was coded with MATLAB version R2018b (the language of technical computing). Two sets of simulation were performed on the batch system as following:

- series 1 groups the seven experimental setups of SBR(s) performed at low  $C_{TSS}$  ( $\sim 3 \text{ g L}^{-1}$ ) presented in chapter II.
- series 2 encompasses a set of experiments carried out only for the SBR-10 d, operated at HRT of 4 h with various biomass concentrations of 3, 5 and  $8 \text{ g}_{TSS} \text{ L}^{-1}$  in chapter II.

From the 12 compounds of ASM1 only 5 compounds are evaluated experimentally:  $S_S$ ,  $S_{NH}$ ,  $S_{NO}$ ,  $S_O$  and biomass concentration expressed by  $X_{B,H}$ . Their measured initial concentrations are summarized in Tables IV S.1 and IV S.2 for series 1 and 2, respectively.

The general characteristics of the batch reactor with activated sludge for the default case are shown in Figure IV.1.

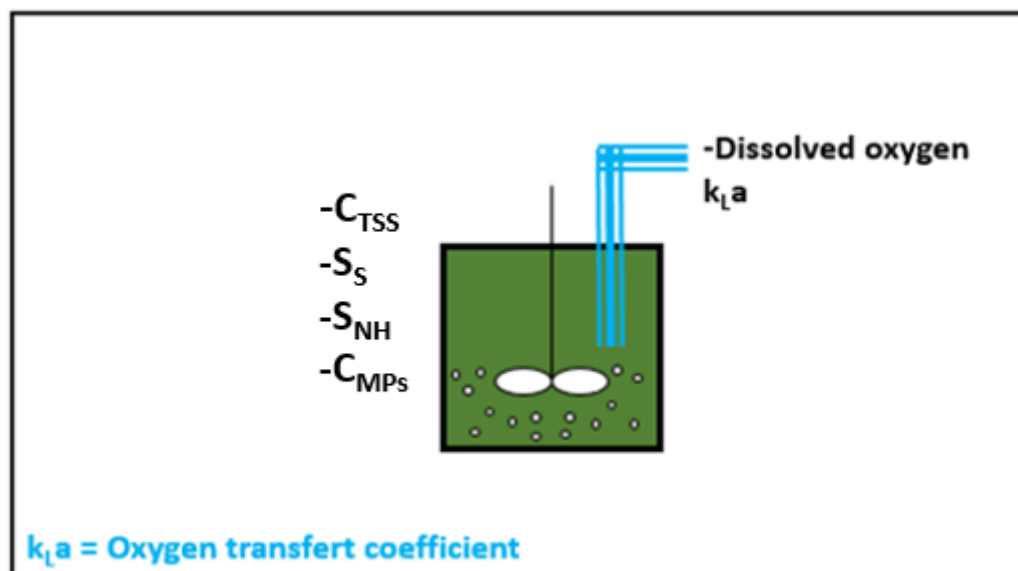


**Figure IV. 1.** General characteristics of the batch reactor with activated sludge for modelling.

During the aeration phase of the SBR systems, no continuous flow enters the system or leaves the system while the reaction takes place. For oxygen, the material balance is expressed by Eq. (IV-34). For both aforementioned series, the material balance for any compound  $i$  in the reactor



was presented by the following Eq. (IV-35) for soluble compounds and Eq. (IV-36) for non-soluble compounds:

$$V r_o + V k_{L,a}(S_{O,sat} - S_O) = V \frac{dS_O}{dt} \quad (\text{IV-34})$$

$$V r_i = V \frac{dS_i}{dt} \quad (\text{IV-35})$$

$$V r_i = V \frac{dX_i}{dt} \quad (\text{IV-36})$$

where  $V$  denotes the volume of the reactor and  $r_i$  denotes the rate of production of the soluble compound ( $S_i$ ) and the non-soluble compound ( $X_i$ ) in the reactor, while  $k_{L,a}(S_{O,sat} - S_O)$  reflects the oxygen supply when the reactor is aerated.

The programs used for simulations consisted of:

- a main program which reads the external files that contain the ASM1 model data (parameters, initial concentrations,  $k_{L,a}$ ...) as well as the experimental data as function of time. The differential equations describing the material balances were solved with ode23s Matlab function which uses an order 2 modified Rosenbrock method.
- a function containing the material balances
- a function which makes it possible to calculate the reaction rates of each compound, i.e. ASM1 compounds or MPs (which are discussed in detail in the following section).

Figure IV.2 described in more details how the program works. After initialization of the vector "y" that groups the concentration of all compounds in the batch reactor, an interval of time is defined to do the integration.

The function defining the differential equations for the SBR system i.e. Eqs. (IV-34, 35 and 36), was called "Balance\_SBR". All the parameters that have been defined or imported into the main program (time,  $k_{L,a}$ , and stoichiometric data) as well as the compound concentrations are the input of the "Balance\_SBR" function. At the output, the derivative of the concentrations are returned.

Following equations IV-12 to IV-23, and IV-32 or IV-33, the reaction rates of the compounds ASM1 state variables and micropollutants are established, respectively. For this reason, the function "rate" which calculates the reaction rates of each compound is created.

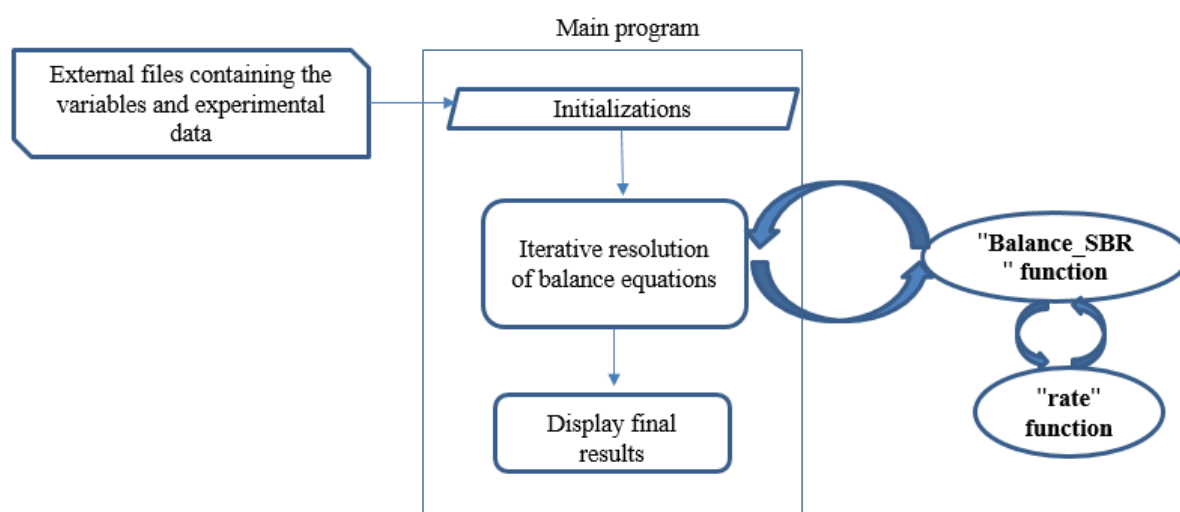


**Figure IV. 2.** Description of the different steps of the simulation of the batch system.

Finally, the concentrations of each micropollutant during the reaction and especially at time  $T_f$  were recorded. It is important to mention that these programs were run for each experimental setup.

#### IV.4.1. Numerical resolution

In the present section, the different Matlab programs used to model the batch system are detailed as follows:

##### a- "Main Program SBR"

As indicated by his name, "Main Program SBR" is the main program of the SBR simulations. It reads the external files containing the parameters necessary to the simulation and performs the integration of the function containing the material balance on the reactor. The following files attributed to one example, the first setup operated at SRT-3 d and HRT-4 h were compiled in Texts IV.S1 and IV.S2 of the supplementary information. Moreover, the script of the Matlab code for the same setup 1 was presented in Text IV.S3.

##### a- External files read by the mainProgramSBR:

'Stoichiometric\_data.txt': contains the stoichiometric data of the ASM1 model, and the kinetic constant values for MPs already calculated in chapter II.

'Conc\_ini.txt': contains the initial concentrations of ASM1 compounds and those of MPs

'Reactors.txt': contains the calibrated values of the transfer coefficients  $k_{La}$ .

In the program, it was also necessary to initialize vector [y] where the concentrations of all compounds were stored, and define the integration interval. The concentrations in the reactors are calculated at each time step within the time integration interval  $[T_0, T_f]$ . The time step was chosen around  $10^{-3}$  days.

#### b- "Balance\_SBR" function

In this matlab function we defined the balance equations of ASM1 model which govern the evolution of the concentrations of the different compounds in time (Eqs. IV-34-36). The input arguments of Balance\_SBR function are the following: time t, vector [y] containing the compounds concentrations at time t, ncomp which gives the number of compounds, don which is a vector containing kinetic and stoichiometric data, and  $k_{La}$  which gives the reactor transfer coefficients.

The function returns as an output the vector [dydt] containing the derivatives of the concentrations, that is to say the derivatives of the vector [y] (see more details in Text IV.S2a).

In batch reactors, the derivative of each compound is equal to the compound production rate due to all reactions involving the compound (see more details in Text IV.S2b). In aerobic conditions however, term  $k_{La} (S_{(O,sat)} - S_{(O,SBR)})$  is added to the production rate.

#### IV.4.2. Parameter optimization of ASM1 model

In order to reproduce the variations of the (i) dissolved oxygen, (ii) the macropollutants as well as (iii) the biomass concentrations in the SBR systems, a pre-simulation step was realized and two types of calibration were suggested as following:

- Optimization of the  $k_{La}$  parameter to reproduce the experimental oxygen concentration evolution;

- Optimization of parameters ( $K_S$ ,  $\mu_H$ ,  $\mu_A$ ,  $b_H$ ,  $b_A$ , and  $K_{O,H}$ ), starting with the Benchmark values and remaining within the ranges defined by Henze 2002 (Table IV.4), in order to reproduce the experimental variation of  $S_S$ ,  $S_{NH}$  and the biomass concentrations.

To this aim, the methodology described in Figure IV.3 was applied.

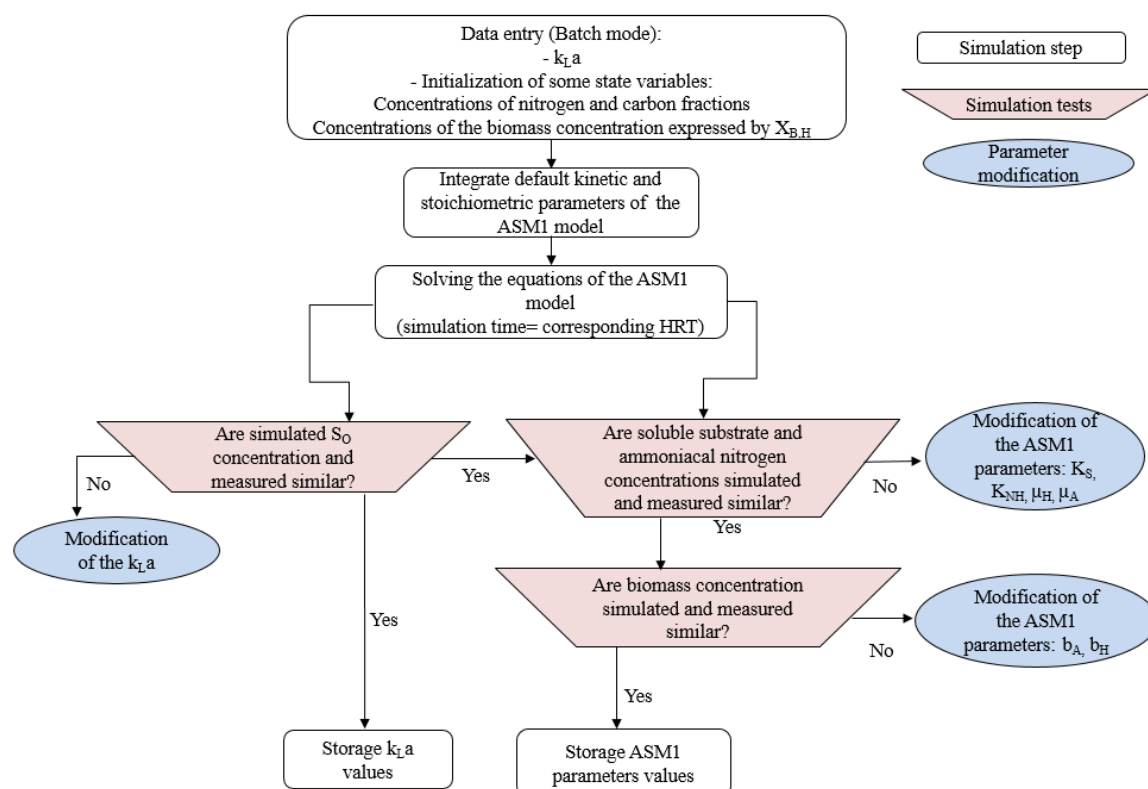


**Figure IV. 3.** Methodology of parameter optimization procedure in ASM1 model.

The default values proposed by the Benchmark are in majority used, except for parameters  $K_S$ ,  $\mu_H$ ,  $\mu_A$ ,  $b_H$ ,  $b_A$ ,  $K_{O,H}$  and  $k_{L,A}$ , which were optimized. Table IV.5 displayed the experimental and simulated values of  $k_{L,A}$  as well as the optimized ASM1 parameters. The  $k_{L,A}$  allows to estimate directly the biodegradability of organic matter ( $S_S$ ) by knowing its [COD]. It is therefore regarded as one of the critical inputs for system optimization. By comparing the experimental and simulated  $S_O$  profiles, if deviation occurs, we can restart simulation by optimizing  $k_{L,A}$ . The simulated  $k_{L,A}$  recorded in the presence of activated sludge were  $12.1 \text{ h}^{-1}$ ,  $12.5 \text{ h}^{-1}$  and  $13.6 \text{ h}^{-1}$  for SBR-3 d, SBR-10 d and SBR-20 d, respectively. Subsequently, the experimental  $k_{L,A}$  values, measured in chapter II, only in clear water seem useful in order to unify the  $k_{L,A}$  values for different setups. For this reason, a term  $\gamma$  designed the ratio of experimental  $k_{L,A}$  in clear water

and simulated  $k_{LA}$  in bulk liquid ( $\gamma = k_{LA} \text{ (clear water)} / k_{LA} \text{ (bulk)}$ ). The calculated  $\gamma$  values are almost identical. Consequently, in order to unify the aeration operation, the average  $k_{LA}$  around  $12.1 \text{ h}^{-1}$  can be interpreted as an optimized reactor transfer coefficient used in both series.

Subsequently, both  $S_S$  and  $S_{NH}$  showed faster elimination in simulation compared to the experimental variation. The rate  $\rho_1$  only depends on the  $K_S$  and  $\mu_H$ . Hence, the increase of  $K_S$  up to 120, 150 and 225  $\text{g}_{\text{COD}} \text{ m}^{-3}$  in setups 1, 2 – 6, and 7, respectively, decreased the biomass growth and so the consumption of  $S_S$  becomes slower in simulation. Moreover, the decrease of  $\mu_H$  from 4 to  $2.5 \text{ day}^{-1}$  diminished the consumption of  $S_S$  in all studied setups. The parameter  $\rho_2$  only depends on the  $K_{NH}$  and  $\mu_A$ . A slightly decrease of  $\mu_A$  from 0.5 to  $0.2 \text{ day}^{-1}$  was enough to reduce the biomass growth and so the consumption of  $S_{NH}$ . However, the heterotrophic and autotrophic biomasses were lower in simulation compared to experimental results in SBR operated at high SRT of 20 d. According to Eqs. (IV-7) and (IV-8), a decrease of the mortality coefficients ( $b_H$  and  $b_A$ ) adjusted the heterotrophic and autotrophic biomasses growth, respectively. The optimized values were compiled in Table IV.5 (the non-calibrated parameters are the default values according to Benchmark).

**Table IV. 5.** Experimental  $k_{LA}$  ( $\text{h}^{-1}$ ) in water, optimized  $k_{LA}$  in the presence of sludge and optimized ASM1 parameters in three SBRs operated at different SRT and HRT.

Series 1	Setup 1	Setup 2	Setup 3	Setup 4	Setup 5	Setup 6	Setup 7
SRT	3 d			10 d			20 d
HRT	4 h	8 h	12 h	4 h	8 h	12 h	4 h
Experimental $k_{LA}$	9.3			9.9			10.1
Optimized $k_{LA}$	12.1			12.5			13.6
$\gamma^*$	0.76			0.79			0.74
Uniform $k_{LA}$	12.1			12.1			12.1
Optimized $K_S$	120	150	150	150	150	150	225
Optimized $\mu_H$	2.5	2.5	2.5	2.5	2.5	2.5	2.5
Optimized $\mu_A$	0.2	0.2	0.2	0.2	0.2	0.2	0.2
Optimized $b_H$	-	-	-	-	-	-	0.01
Optimized $b_A$	-	-	-	-	-	-	0.01
Optimized $K_{O,H}$	0.5	0.5	0.5	0.3	0.3	0.3	-

-: default value of the Benchmark without calibration.

$$*\gamma = k_{LA} \text{ (clear water)} / k_{LA} \text{ (bulk)}$$

Similar steps were performed for series 2 of SBRs operated with three various biomass concentrations of 3, 5 and 8  $\text{g}_{\text{TSS}} \text{L}^{-1}$ . The optimized parameters were compiled in Table IV.6.

**Table IV. 6.** Optimized  $k_{La}$  and ASM1 parameters in the SBRs operated at three different biomass concentrations of 3, 5 and 8  $\text{g}_{\text{TSS}} \text{L}^{-1}$ .

Series 2	Setup 1	Setup 2	Setup 3
	TSS_3 $\text{g L}^{-1}$	TSS_5 $\text{g L}^{-1}$	TSS_8 $\text{g L}^{-1}$
SRT/HRT	10 d/4 h	10 d/4 h	10 d/4 h
Uniform $k_{La}$	12.1	12.1	12.1
Optimized $K_S$	50	50	50
Optimized $\mu_H$	2.5	2.5	2.5
Optimized $K_{O,H}$	0.5	0.5	0.5
Optimized $\mu_A$	0.2	1	1

Figure IV.4 depicts one example of results obtained with series 1. Other detailed graphical results on Matlab are included in Figures IV. S1-S6 and Figures IV. S7-S8 for the SBRs operated at (i) three different SRT and (ii) at various biomass concentrations, respectively. The shape of parameters variations obtained for all setups were qualitatively similar to the trends observed in Figure IV. 4. It must be noted that the setup 4 of series 1 is experimentally the same as setup 1 of series 2.

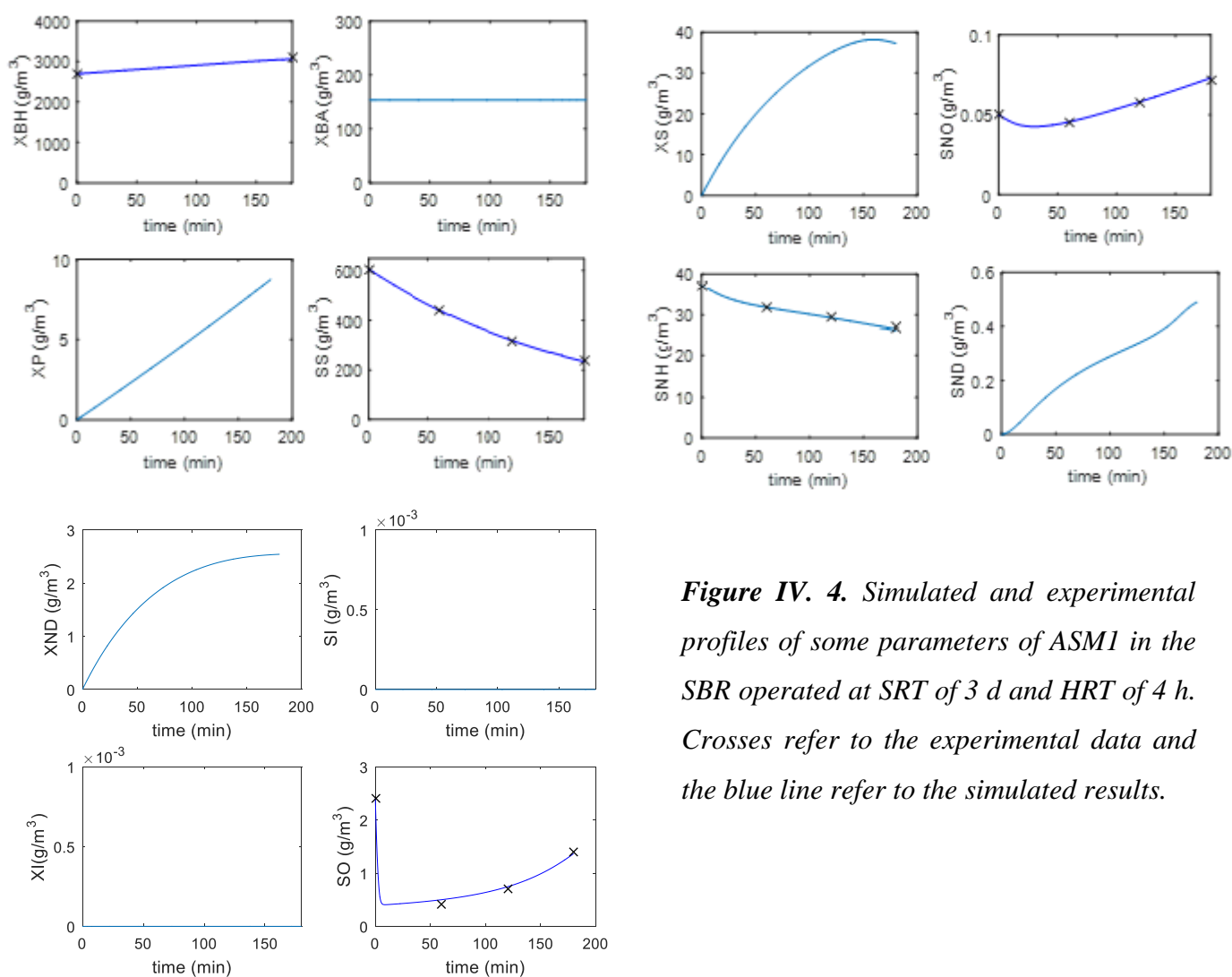


**Figure IV. 4.** Simulated and experimental profiles of some parameters of ASM1 in the SBR operated at SRT of 3 d and HRT of 4 h. Crosses refer to the experimental data and the blue line refer to the simulated results.

From the point of view of the macropollutants' concentrations along the reactor, there is a marked [COD] decay (from 606 to 250 g m<sup>-3</sup>) in 3 hours. At the beginning of the reaction, oxygen value is high, greater than 2 g m<sup>-3</sup>, which implies no limitation due to lack of oxygen. The evolution is also notably pronounced from 2.5 to 0.01 g m<sup>-3</sup> due to the gradually consumption of the substrate quantity. In other setups operated at longer HRTs, the drop of dissolved oxygen concentrations is followed by a regain of oxygen. This can be explained by the exhaustion of soluble carbon source at longer reaction time for the same SRT (see Figures IV S1 and S2). At the same time, the concentration of active biomass in the reactor has slightly increased by 13 % after an aeration phase of 3 hours (HRT- 4 h). Biomass consumes almost 55% of the [COD] of the synthetic wastewater after 3 hours of the reaction. Jing et al (2013)

showed that [COD] removal in form of acetate achieved above 80 % at HRT of 6 hours. Similar numerical results were obtained in current setups operated at higher HRTs. The [COD] removal increased up to 89 % and 90 %, in SBR-3 d and SBR-10 d, respectively, with an increase of HRT up to 12 h. It should be recalled that Figure II.5 showed experimentally the increase of COD up to 89 % and 91 % at HRT of 8 h and 12 h, respectively. Moreover, Figures IV. S1-S2, S4-S5 verified numerically the aforementioned results by drawing their profiles variation as function of the reaction time. As shown for current setup, the evolution of the concentrations of ammonium is slightly decreasing from  $37.1 \text{ g m}^{-3}$  to  $29 \text{ g m}^{-3}$ . This translated into a fairly strong variability in nitrate ion measurements at low SRT. These results confirmed the low nitrification capacities ( $\text{NC} = 28 \%$ ) by autotrophic bacteria at low SRT less than 5 days, i.e. SRT of 3 days. Also, the high nitrification capacity of 55 % and 96 % recorded at high SRTs of 10 and 20 d was numerically verified comparing to the experimental data at low HRT of 4 h (see Figure IV.S3 and S6). As stated above, slowly biodegradable  $X_S$  is not added to the system. Thus, producing  $X_S$  from 0 to an almost stable value of  $38 \text{ g m}^{-3}$  at the end of the reaction was explained by the mortality of the bacteria. Similarly, the same reason explains the increase of  $X_{ND}$ .  $X_{ND}$  and  $X_S$ , which can be subsequently hydrolyzed to  $S_{ND}$  and  $S_S$ , respectively. When the bacteria are "destroyed", they produce  $X_P$  unused by the bacteria.  $X_P$  increases in batch system. Figure IV.4 showed that the profiles for  $X_{BH}$ ,  $S_S$ ,  $S_{NH}$ ,  $S_{NO}$  and  $S_O$  are approximated almost perfectly after calibration.

#### IV.4.3. Predictive accuracy of simulation: statistical calculation

To assess the predictive accuracy of simulation model structure, the percentage error (%) for macropollutants as well as for micropollutants in the further sections was calculated according to the Eq. (IV-37):

$$\% \text{error} = \left| \frac{C_{\text{measured}} - C_{\text{simulated}}}{C_{\text{measured}}} \right| 100 \quad (\text{IV-37})$$

where  $C_{\text{measured}}$  and  $C_{\text{simulated}}$  denote liquid concentration at final time point ( $T_f$ ) of measurements.

Table IV.7 and IV.8 showed the verification of the ASM1 modelling based on experimental/simulated data generated with the ASM1 model in series 1 and 2, respectively. The numerical application matches very well with the experimental results with %error by around 0-5 % for the series 1 and 1-5 % for the series 2. The small discrepancies between



experiments and simulations were also shown graphically in Figures IV.S1-S8. This seemed in good agreement with the above tabulated data. Therefore, the macropollutants profiles verified the good operation of the biological reactors performed at different operating conditions. In this section, we have focused on the macropollutants and the simulation of their evolution by optimizing ASM1 parameters. In the following sections we will focus on the micropollutants by testing different kinetics: the apparent-first-order kinetics and the power law kinetics.

**Table IV. 7.** Percentage error (%) for some parameters of ASM1 between measured and simulated values for series 1 of batch experiments.

%error of ASM1 parameters in series 1 of SBRs							
SRT	3 d			10 d			20 d
HRT	4 h	8 h	12 h	4 h	8 h	12 h	4 h
$X_{B,H}(\text{g m}^{-3})$	1%	2%	3%	1%	2%	2%	1%
$SS(\text{g m}^{-3})$	0%	2%	5%	1%	1%	5%	2%
$S_O(\text{g m}^{-3})$	5%	1%	1%	1%	1%	5%	4%
$S_{NH}(\text{g m}^{-3})$	0%	2%	5%	1%	2%	5%	2%
$S_{NO}(\text{g m}^{-3})$	5%	1%	1%	1%	1%	5%	4%

**Table IV. 8.** Percentage error (%) for some parameters of ASM1 between measured and simulated values for series 2 of batch experiments.

%error of ASM1 parameters in series 2 of SBRs			
SRT/HRT	10 d/4 h		
$C_{TSS}$	3 g L <sup>-1</sup>	5 g L <sup>-1</sup>	8 g L <sup>-1</sup>
$X_{B,H}$ (g m <sup>-3</sup> )	1%	2%	3%
$SS$ (g m <sup>-3</sup> )	1%	1%	5%
$S_O$ (g m <sup>-3</sup> )	1%	5%	5%
$S_{NH}$ (g m <sup>-3</sup> )	1%	1%	1%
$S_{NO}$ (g m <sup>-3</sup> )	1%	3%	5%

#### IV.4.4. Simulation of MPs removal

##### IV.4.4.1. Simulation of the apparent-first-order kinetics

In order to test the models of MPs' removal kinetics, the most common apparent-first-order kinetics in literature was successively performed for the study of the MPs' removal in both series 1 and 2 of SBRs.

Starting with series 1 ( $C_{TSS} = 3 \text{ g L}^{-1}$ ), one example of graphical results showing the experimental and simulated profiles of aqueous MPs' concentrations was illustrated in Figure IV.5. The agreement between the simulated and the experimental data is high, considered with respect to the investigated MPs' concentration. The apparent-first order kinetics reproduces all the experimental setups for series 1 with good agreement, within the simulated scatter. Other graphical variations of MPs' concentrations during the aeration phase of different setups of series 1 were reproduced in the Figures IV. S9-S14 of the supplementary information. These results show a similar agreement between experimental data and the numerical simulations. It can be seen that application of apparent-first order approach is greatly recommended in systems operated with biomass concentration up to  $3 \text{ g}_{TSS} \text{ L}^{-1}$  at different combinations of SRT and HRT. Several studies performed at biomass concentrations lower than or equal to  $3 \text{ g}_{TSS} \text{ L}^{-1}$  and operated at various operational conditions used successfully the apparent-first order (Kang et al. 2018; Majewsky et al. 2011; Massot et al. 2012). For these setups, similar conclusions have been obtained. Therefore, the apparent-first-order model was able to predict the aqueous MPs' concentrations.

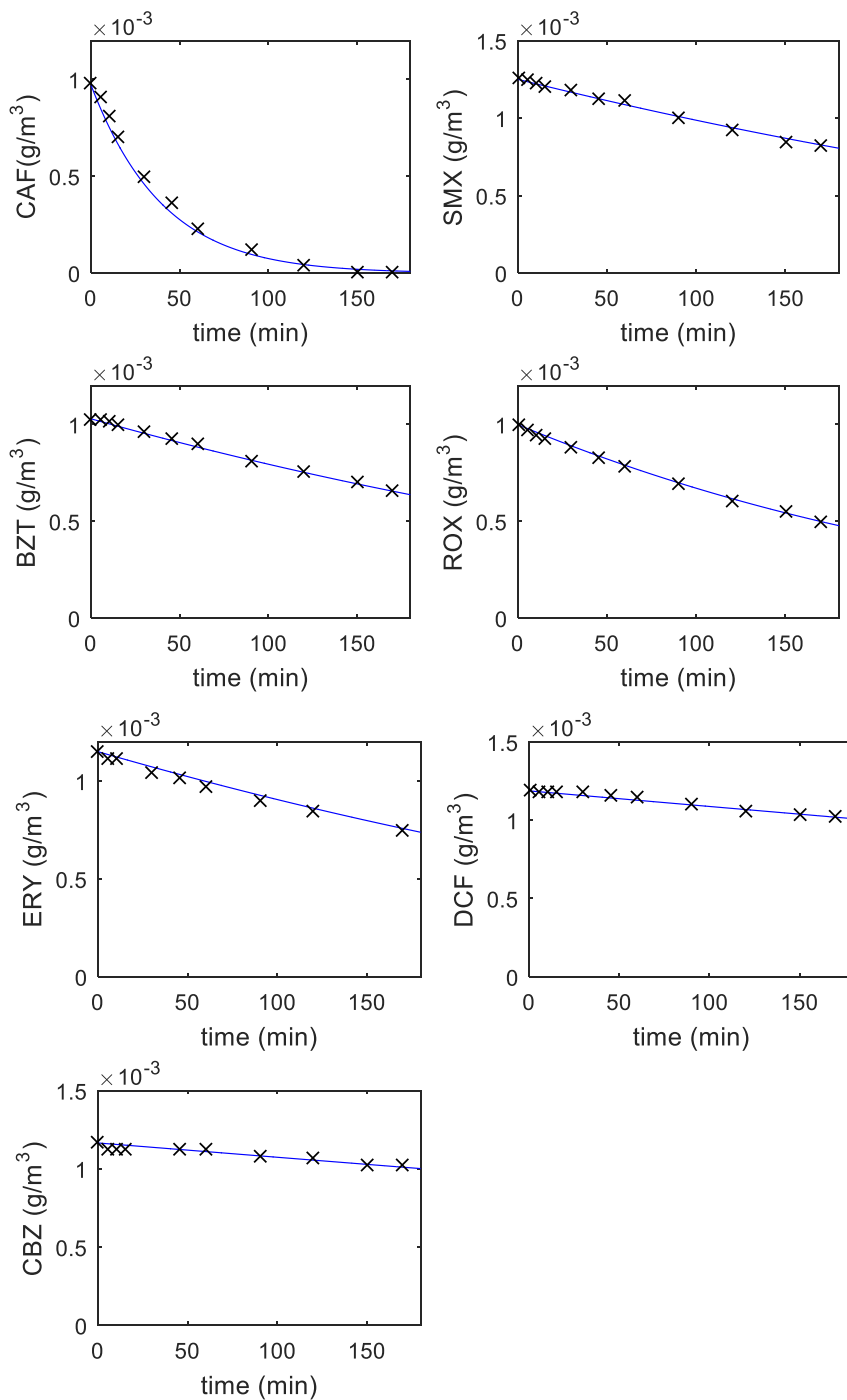


**Figure IV. 5.** Simulated and experimental profiles of MPs' concentrations by applying the apparent-first approach to the SBR operated at SRT of 3 d and HRT of 4 h. Crosses refer to the experimental data and the blue line refer to the simulated results.

In order to evaluate the accuracy of the current simulation, the variation between the experimental and simulated results of MPs' concentrations were presented in terms of %error. The results are given in Tables IV.9 and IV.10 for series 1 and series 2, respectively. For low HRT of 4 h, the %error is very low, lower than 5 % regardless of the SRT (Table IV.9). Conversely, large HRT (8 h, 12 h) increases the deviation between the experimental and simulated values for some compounds. The highest deviation, of 14 %, was recorded for CAF in different type of sludge, i.e. SRT- 3 d and SRT of 10 d. This can be attributed to the fact that the analytical measurements of CAF become less accurate with increasing reaction time, since CAF concentration become very low. In general, these calculated values prove the relevancy of apparent-first-order kinetics for a given value of  $C_{TSS}$  (here  $3 \text{ g L}^{-1}$ ).

**Table IV. 9.** Percentage error (%) between experimentally measured and simulated values of micropollutants by apparent-first-order approach for series 1 of batch experiments.

% error of MPs' removal by applying apparent-first-order kinetic to series 1 of SBRs							
SRT	3 d			10 d			20 d
HRT	4 h	8 h	12 h	4 h	8 h	12 h	4 h
CAF	2%	10%	12%	3%	12%	14%	0%
SMX	4%	0%	2%	2%	10%	1%	3%
BZT	5%	1%	10%	1%	9%	12%	5%
ROX	5%	3%	3%	0%	3%	3%	5%
ERY	5%	7%	5%	4%	0%	7%	5%
DCF	3%	4%	10%	4%	3%	2%	2%
CBZ	5%	2%	10%	2%	2%	2%	4%

The Figures IV.6 and IV.7 were joined in order to compare graphically the experimental and simulated profiles of series 2 during the aeration phase of different biomass concentrations of 5 and 8 g L<sup>-1</sup>, respectively. By applying apparent-first-order, a deviation of all predicted values of MPs with respect to experimental data can be observed, mainly at higher biomass concentration (8 g<sub>TSS</sub> L<sup>-1</sup>). The SMX recorded the highest value of 93 % of deviation with biomass concentration increasing up to 8 g<sub>TSS</sub> L<sup>-1</sup>. These results highlighted the fact that the experiments of series 2 did not obey the common kinetics of apparent-first-order. Therefore, it was interesting to implement in the simulation the new kinetics model deduced from chapter III in order to predict the new MPs' removal in such conditions of high biomass concentrations.

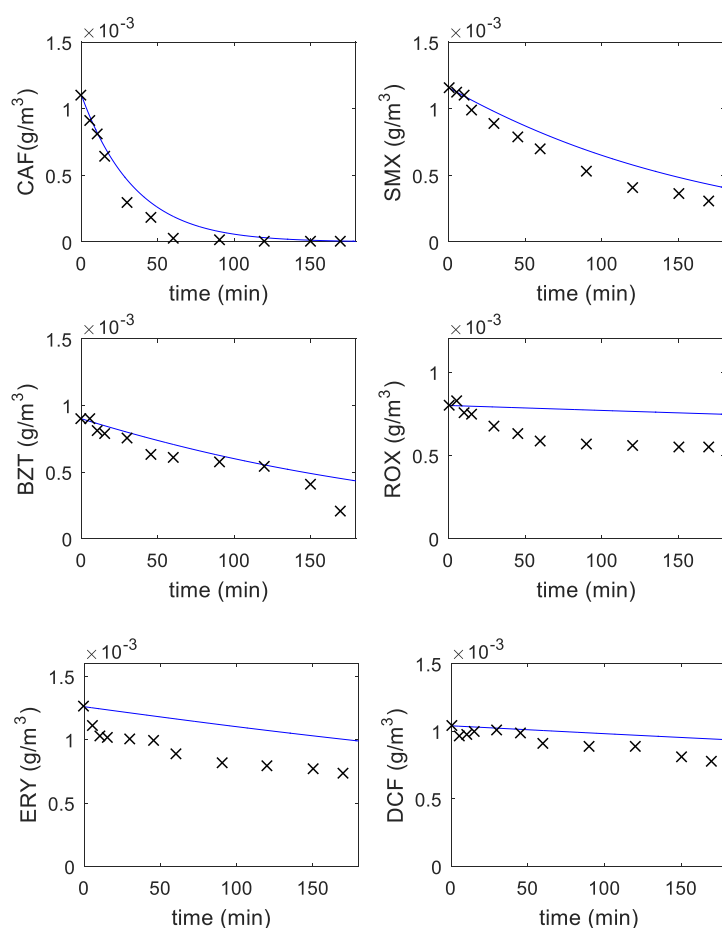


**Figure IV. 6.** Simulated and experimental profiles of MPs' concentrations by applying the apparent-first order approach to the SBR operated at  $C_{TSS}$  of 5 g L<sup>-1</sup>. Carbamazepine has not been detected during biological experiments of series 2.

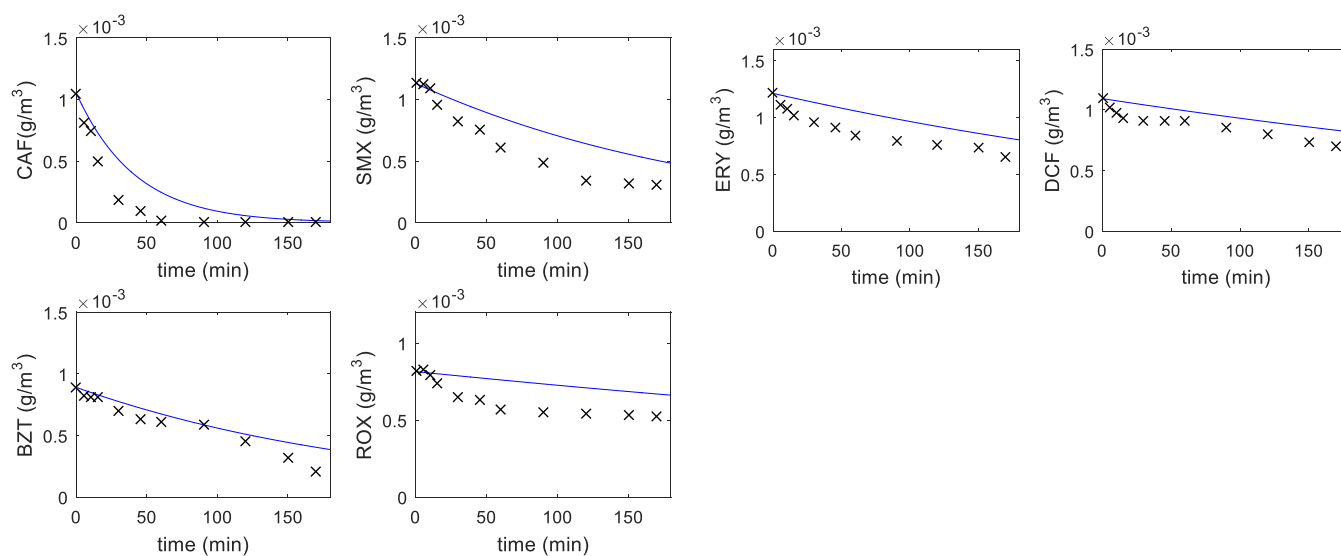


**Figure IV. 7.** Simulated and experimental profiles of MPs' concentrations by applying the apparent-first order approach to the SBR operated at  $C_{TSS}$  of  $8 \text{ g L}^{-1}$ .

To study the accuracy of the apparent-first-order on series 2, similar calculations were carried out. The %error of series 2 are compiled in Table IV.10.

**Table IV. 10.** Percentage error (%) between experimentally measured and simulated values of micropollutants by apparent-first-order approach for series 2 of batch experiments.

%error of MPs' removal by applying apparent-first-order kinetic to series 2 of SBRs			
Biomass concentration- $C_{TSS}$	$3 \text{ g L}^{-1}$	$5 \text{ g L}^{-1}$	$8 \text{ g L}^{-1}$
CAF	7%	41%	67%
SMX	2%	49%	93%
BZT	1%	36%	28%
ROX	0%	36%	27%
ERY	4%	21%	19%
DCF	4%	19%	21%

*IV.4.4.2. Modelling of series 2 with the power law kinetics*

For the current kinetic study, we started with the same Matlab code as the one used for series 1 in SBR performed at SRT of 10 d and HRT of 4 h. The apparent-first-order kinetics of MPs' removal previously modelled was replaced by the power law kinetics (Eq. IV-33) with the order of reaction  $n$ . The code returned the value of the MPs' concentrations at the end of the reaction phase and compared it with experimental measurements at various biomass concentrations. The Text IV. S4 in the supplementary information explained the code for one example of MPs removal by using the power law kinetics performed at  $3 \text{ g}_{\text{TSS}} \text{ L}^{-1}$ . A similar code was used for the other tested  $C_{\text{TSS}}$ . The user may change the biomass concentration expressed by  $X_{B,H}$  as well as the initial concentration of each MP according to each setup of biomass concentration in the external file "Conc-Ini". It is important to remind that the calculated average of the initial MPs concentrations for each  $C_{\text{TSS}}$  was distinguished for current kinetics and presented in ( $\mu\text{mol L}^{-1}$ ) as seen in chapter III.

Three consecutive simulations were applied in order to evaluate the effect of the power law kinetics that was investigated in chapter III on the MPs removal in batch mode at different  $C_{\text{TSS}}$ . Recall that Eq. IV-33 including the  $n$ -coefficient constitutes our central result about the kinetics of MPs' removal deduced from previous chapter. In order to run the simulations, the following input parameters were needed: the MPs' initial concentration in the dissolved phase, the biomass concentration as well as the kinetic constant, and  $n$ -coefficient that have been calculated for each studied MP. The parameter values, obtained from the experiments, were compiled in Table IV.11.

**Table IV. 11.** Average initial  $C_{MPs}$  calculated at various biomass concentration setup (number of replicates=3) and averages of  $n$ -coefficient of each MP and new constants  $k_{MPs}$  used in computer simulation.

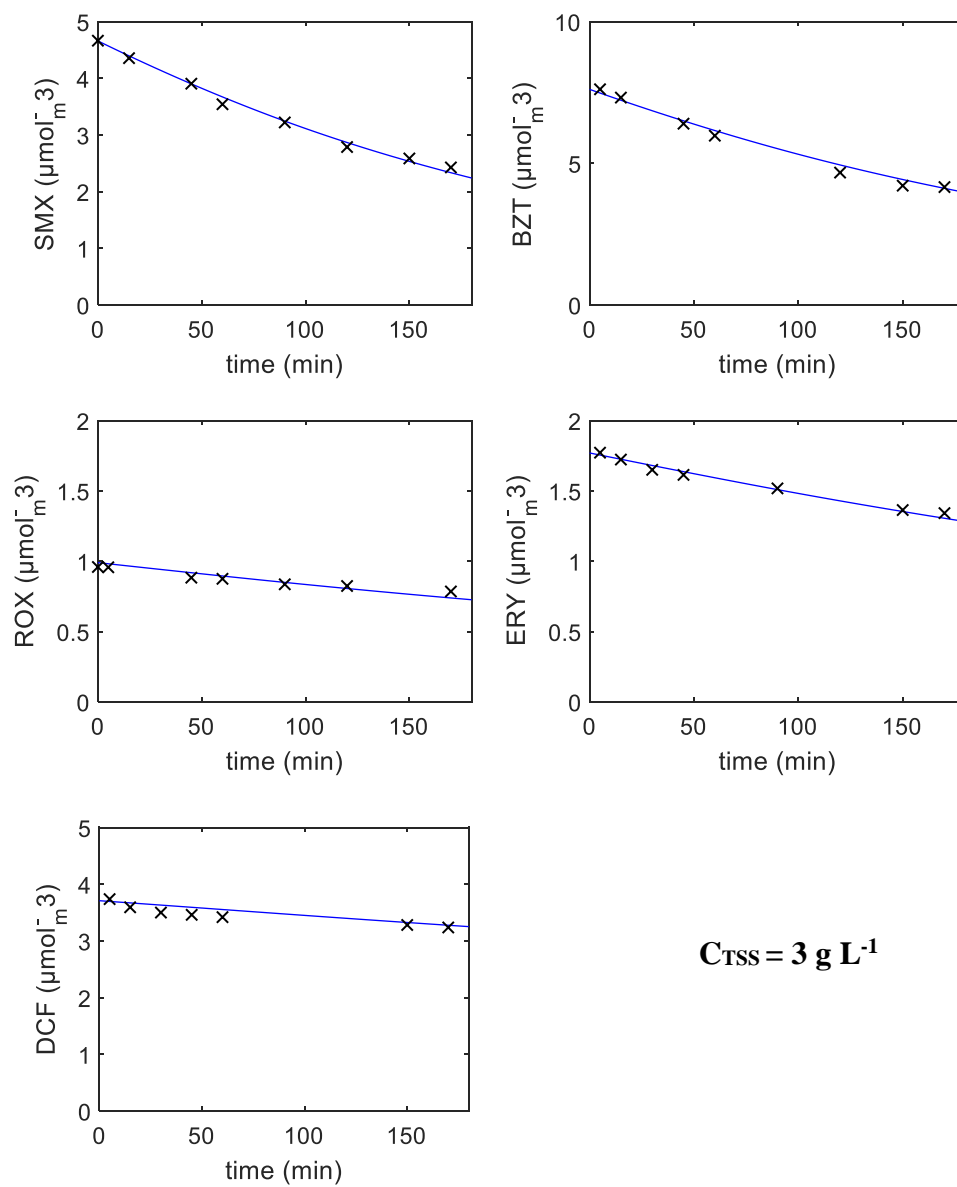
Biomass concentration ( $g_{TSS} L^{-1}$ )	Initial $C_{MPs} 10^{-3} (\mu mol L^{-1})$			Average $n$ -coefficient	Average $k_{MPs} (L^n g^{-n} h^{-1})$	Average initial $C_{MPs} 10^{-3} (\mu mol L^{-1})$ from batch experiments*
	3	5	8	3,5 and 8	3,5 and 8	3,5 and 8
SMX	4.66	4.58	4.46	0.51	0.201	4.56
BZT	7.61	7.64	7.47	0.56	0.123	7.57
ROX	0.96	0.96	0.98	0.45	0.115	0.97
ERY	1.77	1.71	1.65	0.44	0.112	1.71
DCF	3.73	3.73	3.71	0.50	0.033	3.72

\*Used as inlet for continuous simulations in section IV.4.4.3.

Simulated curves testing the power law kinetics were compared to the experimental results in Figures IV.8 (a), (b) and (c) for SBRs operated at 3, 5 and  $8g_{TSS} L^{-1}$ , respectively. For every considered biomass concentration, the theoretical values fit well the experimental curves. These results confirmed that the power law kinetic model is more adapted to describe the MPs' removal at different biomass concentrations than the apparent-first order kinetics model. A similar behaviour was noted for SMX, BZT, ROX and ERY. Their concentrations obviously decreased only during the first increase of  $C_{TSS}$  from 3 to  $5g_{TSS} L^{-1}$ . However, when the  $C_{TSS}$  reaches  $8g L^{-1}$ , the trends of residual MPs concentrations do not vary that much at the corresponding  $n$ -coefficients are around 0.5. Further simulations with various biomass concentrations for MPs modelling will be carry out in the next section to investigate the predictions of wide range of  $C_{TSS}$  with various  $n$ -coefficients in order to characterize different local mixing levels.



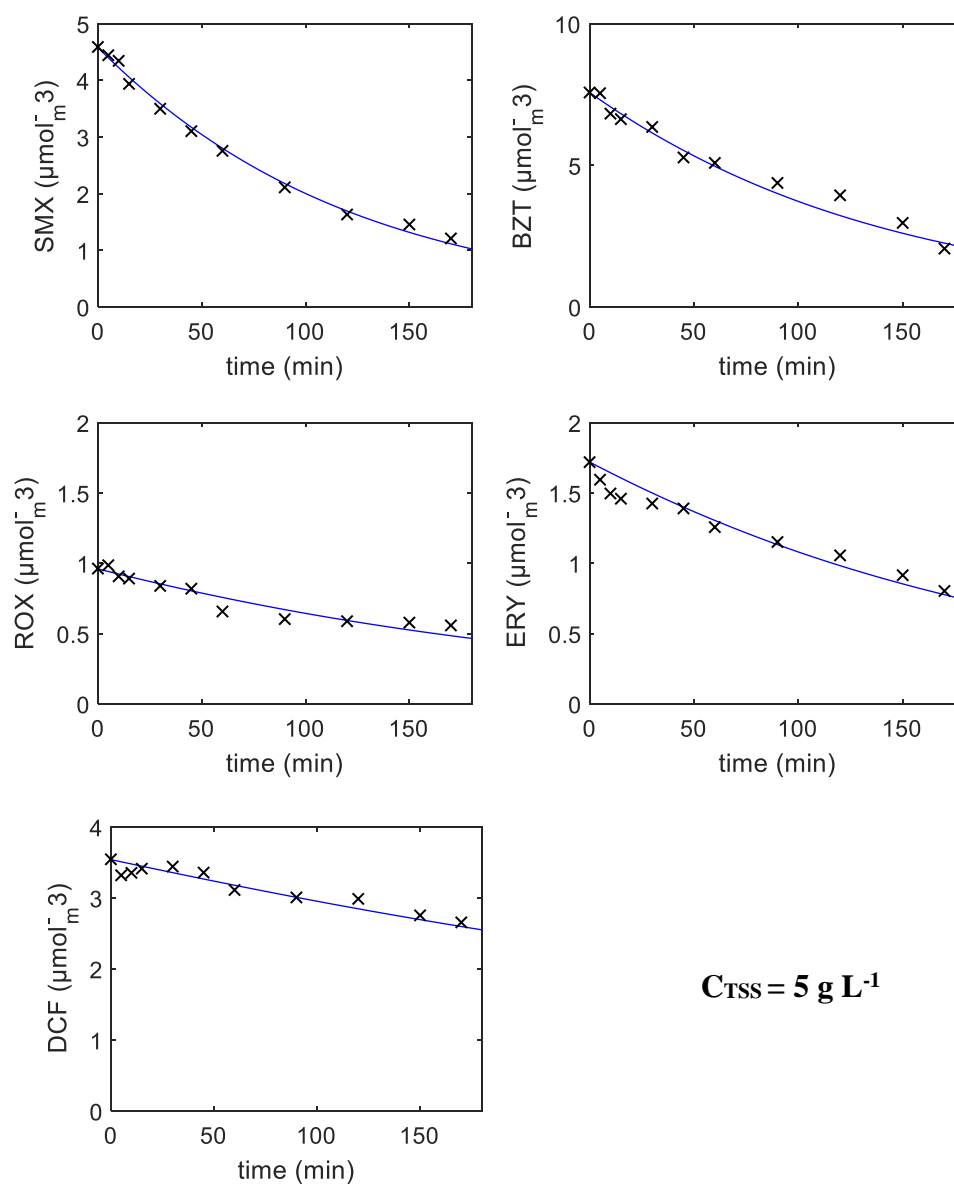
(a)



(Continued on next page)

Figure IV. 8. Continued

(b)



(Continued on next page)

Figure IV. 8. Continued

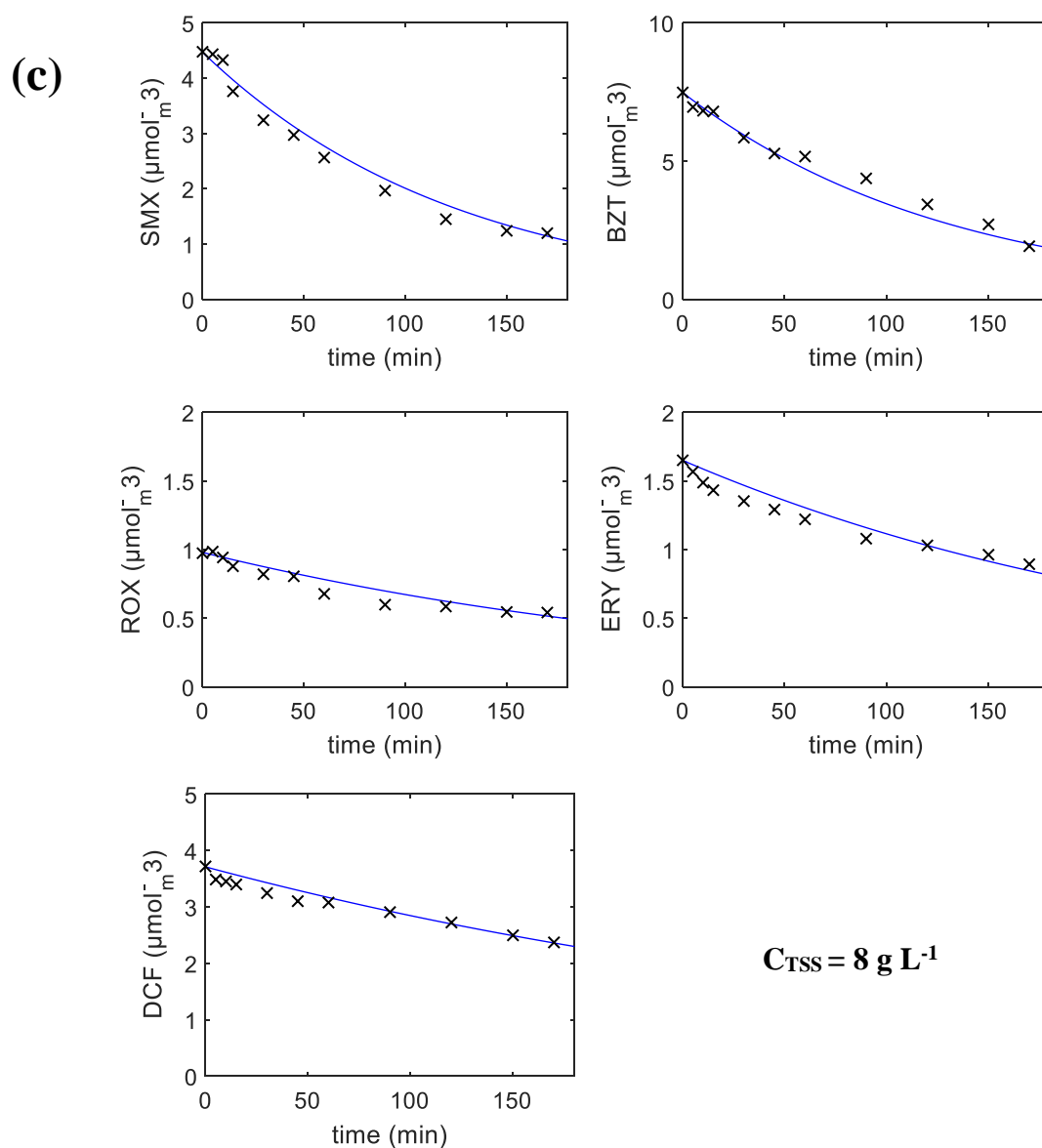


**Figure IV. 8.** Simulated and experimental profiles of MPs' concentrations by applying the power law approach to the SBR operated at SRT of 10 d and HRT of 4 h operated at  $C_{TSS}$  of 3  $\text{g L}^{-1}$  (a), 5  $\text{g L}^{-1}$  (b) and 8  $\text{g L}^{-1}$  (c).

#### IV.4.4.3. Predictions by applying power law kinetics

As seen in previous section, it is of particular importance to use the new kinetic law in order to model MPs removal at different  $C_{TSS}$ . Moreover, it is important to mention that the order of reaction  $n$  directly depends on the mixing quality. Therefore, the objective of this section is to

give a concise overview of the effect of the mixing quality beside the biomass concentration, on MPs removal efficiency. To this aim, another Matlab code was developed. For all aforementioned files described in Text IV. S4, the "nvect" vector was simply replaced by a scalar. For every simulation, the user defines one value of  $n$  for all investigated MPs and the biomass concentration is input in the external file (Conc\_Ini). Twelve different biomass concentrations were tested in the range 1.5 to 12  $\text{g}_{\text{TSS}} \text{L}^{-1}$  and 10 values of  $n$  in the range 0.1 to 1. The averages of the experimental initial concentrations of each micropollutant for 3, 5 and 8  $\text{g}_{\text{TSS}} \text{L}^{-1}$  were used to initialize the MPs concentration in the simulations. They can be found in the last column of Table IV.11. Similarly, the average of the experimental  $k_{\text{MPs}}$  were injected in the numerical model. The computer simulation was performed for the following different cases. The first set (i) was performed with different mixing levels at the same biomass concentration for each MP, including the calculated  $n$  of Chapter III, section III.3.1. The second set (ii) was realized with low to high biomass concentrations up to 12  $\text{g}_{\text{TSS}} \text{L}^{-1}$  (including the tested biomass of 3, 5 and 8  $\text{g}_{\text{TSS}} \text{L}^{-1}$ ) by using the same  $n$  level for all MPs. As a result, the removal efficiency (RE) was computed by comparing the numerical value of the remaining  $C_{\text{MPs}}$  to the experimental average initial  $C_{\text{MPs}}$  (last column of Table IV.11) and plotted in Figure IV.9.

As reported in Table IV.11, the order of magnitude for new kinetic constants  $k_{\text{MPs}}$  of investigated MPs is correct. It decreases according to their degree of biodegradability i.e. (from moderately biodegradable compound SMX to persistent compound DCF). Therefore, the variation of the removal efficiency differs from one micropollutant to another. As shown in Figure IV.9, the removal efficiency of all MPs increases considerably when the  $n$  coefficient increases, especially for  $n > 0.3$ . For low values of  $n$ , lower than 0.5, increasing the biomass generally does not improve the removal efficiency. For  $n$  values higher than 0.5, the biomass concentration has a significant effect on the removal efficiency. It is useless to increase the biomass concentration if the local mixing is bad. These results confirm the sensitivity of the system to the mixing level and alert on the need for good mixing conditions in order to provide higher removal of MPs. It is reminded here that the parameter  $n$  describes both the macromixing and the local diffusion, which is related to the molecular mass of each MP.

All MPs showed significant increase of removal for  $n$  values greater than the corresponding  $n$  of each MP up to 1 and high biomass concentration, above 8  $\text{g}_{\text{TSS}} \text{L}^{-1}$ , resulting in an almost

total disappearance of all SMX, BZT, ROX and ERY (RE > 95 %). For DCF, the highest achievable removal is lower than for the other MPs (RE up to 70 %).

The simulated removal efficiencies at 3, 5 and 8  $\text{g}_{\text{TSS}} \text{L}^{-1}$  of each MP for the experimental values of  $n$  are close to the experimental removals (white boxes in Figure IV.9). For the values of  $n$  determined experimentally, we observe again that micropollutants SMX and BZT are more efficiently removed (74 % and 70 % for 8  $\text{g}_{\text{TSS}} \text{L}^{-1}$ ) than ROX, ERY and DCF (36 %, 45 % and 35 % for 8  $\text{g}_{\text{TSS}} \text{L}^{-1}$ ). The values of  $n$  obtained from the experiments, compiled in Table IV.11 for all investigated MPs, do not exceed 0.6. In order to improve further the removal, it is recommended to increase  $n$  towards 1.

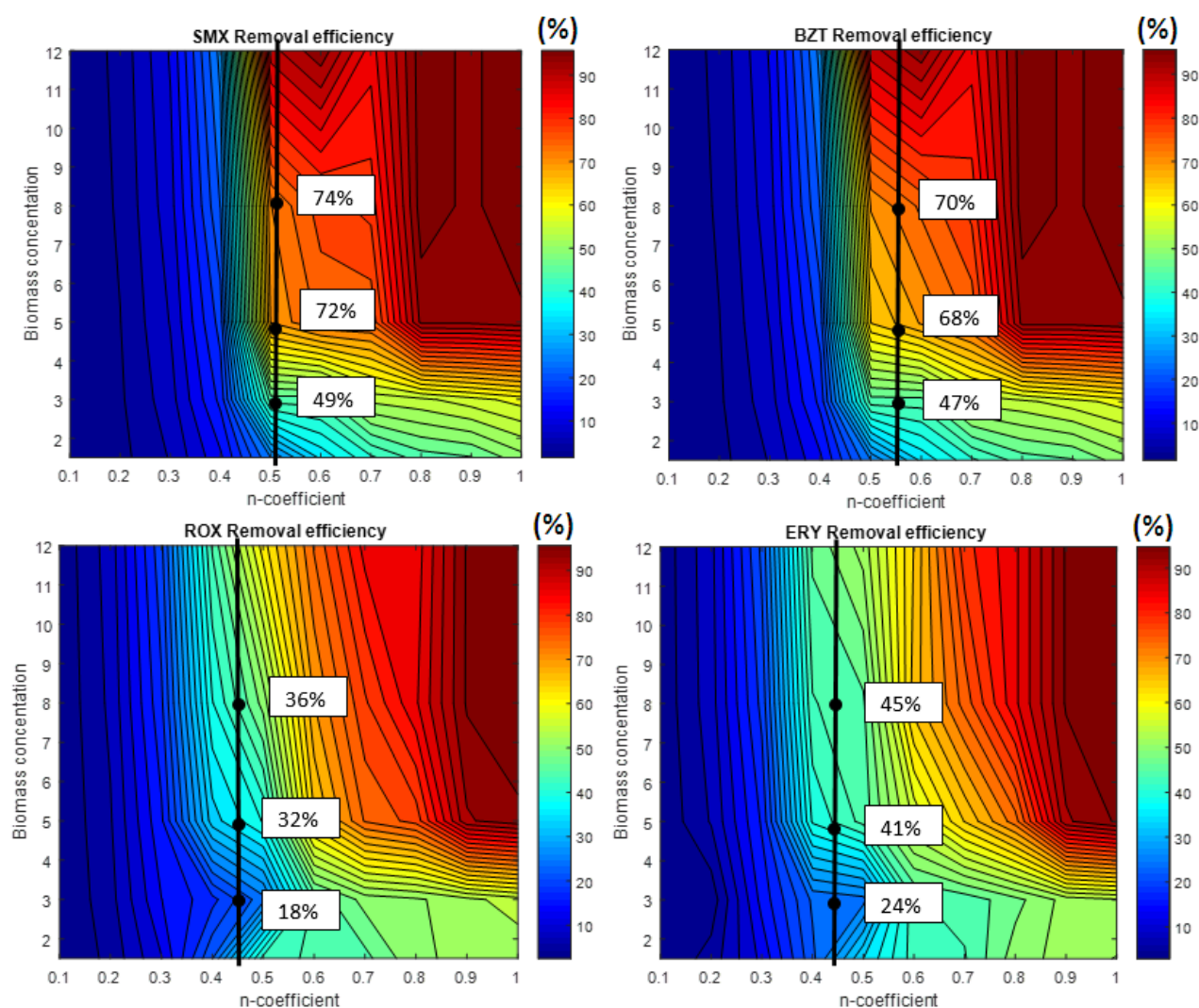
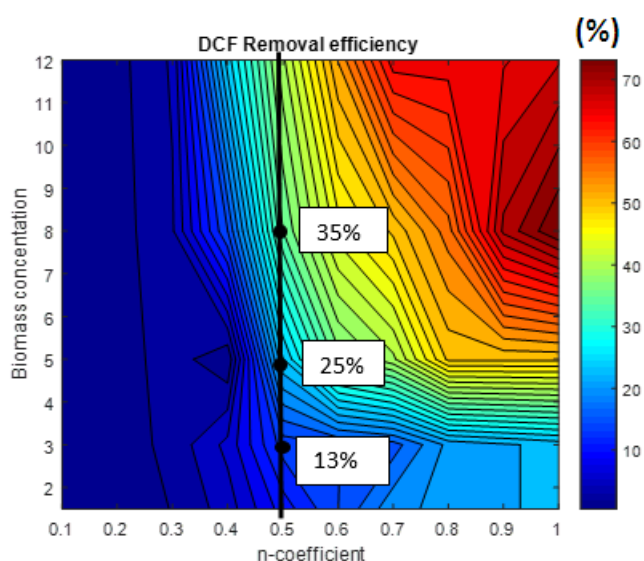


Figure IV. 9. Continued



**Figure IV. 9.** Contours of the removal efficiency (%) of SMX, BZT, ROX, ERY and DCF micropollutants as a function of the sludge biomass concentration and the  $n$ -coefficient. Red color means the highest removal efficiency of each MP. The black line and the percentages on each figure correspond to the experimental  $n$  value and the removal efficiency of each MP at 3, 5 and 8  $\text{g}_{\text{TSS}} \text{L}^{-1}$ , respectively.

#### IV.4.4.4. Partial conclusion

Simulations have been performed using the Matlab software to represent the batch system conditions of two sets of experiments. The first set was performed at different SRT and HRT but keeping the biomass concentration almost constant around 3  $\text{g}_{\text{TSS}} \text{L}^{-1}$ . The second set of simulations was realized at SRT of 10 d and HRT of 4 h at various biomass concentrations of 3, 5 and 8  $\text{g}_{\text{TSS}} \text{L}^{-1}$ . The simulations with two different kinetics of MPs' removal in batch systems showed that the apparent-first order fits well the experiments performed at various SRT and HRT with  $C_{\text{TSS}}$  around 3  $\text{g}_{\text{TSS}} \text{L}^{-1}$ . However, the apparent-first-order kinetics fails for the other biomass concentrations. Alternatively, the power law kinetics has been tested and compared to the experimental concentration profiles. This new kinetics succeeds in predicting the removal of all investigated MPs at all tested  $C_{\text{TSS}}$ .

Simulations of the MPs removal for different values of  $n$  and different values of biomass concentration were then performed. In favorable conditions (high  $n$ , high  $C_{\text{TSS}}$ ), a very high

removal of all MPs occurs in the first 3 hours of the reaction. Conversely, for unfavorable conditions (low  $n$ , low  $C_{TSS}$ ), less than 50 % of removal of the different types of MPs were reached.

## IV.5. Extrapolation to continuous system

### IV.5.1. Validation by comparison with Benchmark Simulation Model no.1 (BSM1)

The basic diagram of continuous system considered in this section is presented in Figure IV.10. The whole system structure is the one of the Benchmark, except for the clarifier. Experiments performed by researchers of our laboratory (Bendounan 1995; Roche et al. 1994) about clarifier hydrodynamics showed results very different from the Benchmark clarifier model. This system consists of a cascade of 2 anoxic tanks followed by 3 aerated tanks, and a clarifier. In our study, we use a simple clarifier model. The goal is to obtain a representative residence time in the clarifier, so that the flow in the reactor model be realistic. Then, we build a clarifier model resulting from residence time distribution realized by Bendounan (1995) and Roche et al. (1994). The separation of sludge is supposed perfect; the whole biomass is recycled. The 1<sup>st</sup> anoxic tank is fed with the global inlet flow  $Q_e$ , the recycled mixed liquor flow  $Q_L$  and the sludge recycling flow  $Q_S$ . The flow at the exit of the 3<sup>rd</sup> aerated tank is split into  $Q_L$  (which is recycled towards the system inlet) and  $Q_{IC}$  which enters into the clarifier. At the clarifier inlet the flow divides into an upper flow  $Q_{out}$ , made of a monophasic aqueous solution, which travels towards the clarifier upper outlet, and a bottom flow  $Q_{BOC}$ , which contains the sludge carrying soluble and non-soluble compounds travelling to the bottom outlet. At the bottom, the great part of flow  $Q_{BOC}$  is recycled to the global inlet ( $Q_S$ ) and the other part is withdrawn from the system ( $Q_w$ ). The sludge recycling rate is constant and equal to the inlet flow rate ( $Q_e$ ). The recycling flow rate of the mixed liquor ( $Q_L$ ) is 3 times the inlet flow rate ( $Q_e$ ).

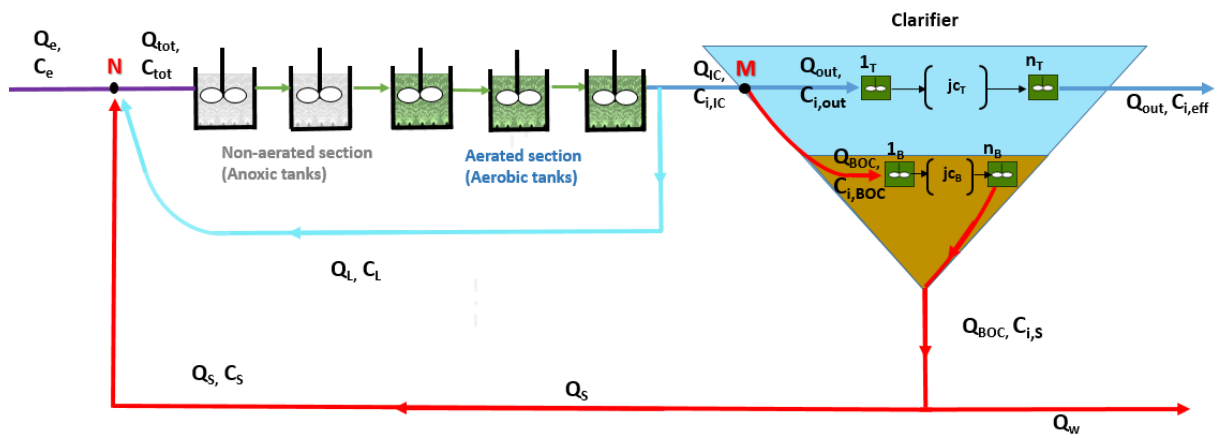


**Figure IV. 10.** Schematic of the Benchmark plant layout.

The operation mode is relatively simple. It combines oxidation of organic compounds as well as nitrification coupled to denitrification. The latest couple is most commonly used for N-removal. The aerobic tanks are used to remove the biological oxygen demand (BOD) or COD, and to oxidize organic nitrogen and ammonia (mainly from the wastewater) to nitrates. 3/5<sup>th</sup> of the nitrate and nitrite nitrogen return from the exit of the last aerobic reactor by the internal loop to the 1<sup>st</sup> reactor which operates in anoxia. The nitrogen pollution is treated first by denitrification which takes place under anoxic conditions. At that point nitrates are transformed into gaseous nitrogen. In the aerobic phase, ammonia nitrogen is oxidized into nitrates. The user guide for the five reactors configuration of the continuous system describing the following sections was presented in Text IV.S5 (A, B, C, D and E).

#### IV.5.1.1. Material balance in the cascade

Each reactor  $j$  is considered as a continuous stirred tank reactor (CSTR) of volume  $V_j$  crossed by a constant flow rate  $Q_{tot}$ . Being a CSTR, the reactor is perfectly mixed at all times. Then the concentration of each substance (substrate or biomass) is homogeneous in the whole reactor at each time. The overall mass balance for the whole WWTP reads as:

$$Q_e = Q_{out} + Q_w \quad (\text{IV-38})$$

and the mass balance material for the anoxic reactor:

$$Q_{tot} = Q_e + Q_L + Q_S \quad (\text{IV-39})$$



The concentrations at the inlet of the anoxic reactor are computed from the balance at node (N) located before the reactor:

$$C_{tot} = \frac{Q_e C_e + Q_S C_S + Q_L C_L}{Q_{tot}} \quad (\text{IV-40})$$

Material balance is written for every compound  $i$  in each reactor  $j$ . The variation of the mass compound ( $m_{i,j} = C_{i,j} V_j$ ) is equal to the difference between inward ( $F_{in,i,j} = C_{in,i,j} Q_{tot}$ ) and outward flux ( $F_{out,i,j} = C_{out,i,j} Q_{tot}$ ) plus the net production due to the chemical reactions (production minus consumption,  $V_j r_{i,j}$ ):

$$\frac{dC_{i,j}}{dt} V_j = (F_{in,i,j} - F_{out,i,j}) + V_j r_{i,j} \quad (\text{IV-41})$$

**Remark:**  $F_{in,i,j} = F_{out,i,j-1}$

The material balance for oxygen in an aerated reactor  $j$  is written as follows:

$$\frac{dC_{O,j}}{dt} V_j = (F_{in,O,j} - F_{out,O,j}) + V_j r_{O,j} + V_j k_l a (S_{O,sat} - S_{O,j}) \quad (\text{IV-42})$$

**Remark:**  $F_{in,O,j} = F_{out,O,j-1}$

- The material balance on the compound  $i$  in the reactor 1 thus reads:

$$\frac{dC_{i,1}}{dt} = \frac{1}{V_1} Q_{tot} (C_{i,tot} - C_{i,1}) + r_{i,1} \quad (\text{IV-43})$$

- The material balance on the compound  $i$  (except for oxygen) in the other reactor of the cascade ( $2 \leq j \leq j_{max-1}$ ) is written as following:

$$\frac{dC_{i,j}}{dt} = \frac{1}{V_j} Q_{tot} (C_{i,j-1} - C_{i,j}) + r_{i,j} \quad (\text{IV-44})$$

- The material balance on the compound  $i$  (except for oxygen) on the last reactor  $j_{max}$  is written as following:

$$\frac{dC_{i,jmax}}{dt} = \frac{1}{V_{jmax}} Q_{tot} (C_{i,jmax-1} - C_{i,IC}) + r_{i,jmax} \quad (\text{IV-45})$$

with  $C_{i,IC} = C_{i,jmax}$

#### IV.5.1.2. Material balance in the clarifier

A typical WWTP model consists of biological reactor(s) coupled with a clarifier. The sedimentation in the settling tank is a complex process. Indeed, biological models typically consist of ordinary differential equations, whereas a sedimentation model involves both time and space dependence, leading to partial differential equation. The simulation models developed for the Benchmark do not fully represent the physical and mathematical properties of sedimentation. In our study, a complete separation of the compounds, without reaction, is assumed. In other words, the clarifier is 100 % effective and so, all non-soluble compounds fall into the sludge (at the bottom) while soluble compounds travel both up and down. In this study, we used a realistic residence time distribution. It was inspired from the studies performed by Bendouan (1995) and Roche et al. (1994) about residence time distribution in clarifiers. The clarifier is divided into an upper part and a lower part of volumes  $V_T$  and  $V_B$ , respectively.  $V_T$  and  $V_B$  are modelled by a cascade of interconnected well-mixed cells of  $n_T$  and  $n_B$  cells, respectively. In the simplest case,  $V_T = V_B$  and  $n_T = n_B$ . Thus, the volume of each elementary cell of both parts of the clarifier is calculated as follows:

$$V_{jc_T} = \frac{V_T}{n_T} \quad (\text{IV-46})$$

$$V_{jc_B} = \frac{V_B}{n_B} \quad (\text{IV-47})$$

A global mass balance on the clarifier leads to:

$$Q_{IC} = Q_{out} + Q_{BOC} \quad (\text{IV-48})$$

Material balance is then written for each compound  $i$  of each elementary cell  $jc$  of the clarifier. We need to distinguish at this stage the soluble and the non-soluble compounds. It is important to mention here that the micropollutants are considered as soluble compounds. The non-soluble compounds settle down to the bottom of the clarifier. The soluble compounds leave the clarifier by both the bottom and the overflow. Furthermore, it is assumed that the compounds are not involved in any reaction in the clarifier. They leave the clarifier at the same concentration as they enter, but with a delay due to the residence distribution time in the clarifier.

- Clarifier upper volume:

Even if in real clarifier the settling process happens progressively, in this simple model, there are only soluble compounds in the upper volume.

- First cell ( $j_{cT} = 1_T$ )

$$Q_{out}C_{i,out} + V_{1_T} \cancel{r_{i,1_T}^0} - Q_{out}C_{i,1_T} + V_{1_T} \frac{dC_{i,1_T}}{dt}$$

Then,

$$\frac{dC_{i,1_T}}{dt} = \frac{1}{V_{1_T}} Q_{out} (C_{i,out} - C_{i,1_T}) \quad (\text{IV-49})$$

- For  $2 \leq j_{cT} \leq n_T$

$$Q_{out}C_{i,j_{cT}-1} + V_{j_{cT}} \cancel{r_{i,j_{cT}}^0} - Q_{out}C_{i,j_{cT}} + V_{j_{cT}} \frac{dC_{i,j_{cT}}}{dt}$$

Then,

$$\frac{dC_{i,j_{cT}}}{dt} = \frac{1}{V_{j_{cT}}} Q_{out} (C_{i,j_{cT}-1} - C_{i,j_{cT}}) \quad (\text{IV-50})$$

- Clarifier lower volume:

There are both soluble and non-soluble compounds in this volume. At the volume inlet, the concentrations of soluble compounds are equal to that at the output of the cells cascade. But the concentrations of non-soluble compounds are different. They are computed with a mass balance at node (M) which separates the upper and lower clarifier volumes.

- For soluble compounds:

$$Q_{IC}C_{i,IC} = Q_{out}C_{i,out} + Q_{BOC}C_{i,BOC} \quad (\text{IV-51})$$

- For non-soluble compounds:

$$Q_{IC}C_{i,IC} = Q_{BOC}C_{i,BOC} \quad (\text{IV-52})$$

It is important to remind here that  $C_{i,out}$  of non-soluble compound is equal to zero in the present model in which a perfect clarifier was considered. The following coefficient "coef" compares the flow rate at the overflow of the clarifier to the total flow rate entering the clarifier:

$$coef = \frac{Q_{out}}{Q_{IC}} \quad (\text{IV-53})$$

and

$$\frac{Q_{BOC}}{Q_{IC}} = (1 - coef) \quad (IV-54)$$

Here, we considered that  $coef = 0.5$ . This case corresponds to equal fluxes of soluble compounds in the upper and lower parts of the clarifier; and to a concentration of non-soluble compounds twice the one in the inlet.

The material balance on the bottom of the clarifier is the following:

- First cell ( $j_{CB} = 1_B$ )

$$Q_{BOC}C_{i,BOC} + \cancel{V_{1B}r_{i,1B}} = Q_{BOC}C_{i,1B} + V_{1B} \frac{dC_{i,1B}}{dt} \quad 0$$

Then,

$$\frac{dC_{i,1B}}{dt} = \frac{1}{V_{1B}} Q_{BOC} (C_{i,BOC} - C_{i,1B}) \quad (IV-55)$$

- For  $2 \leq j_{CB} \leq n_B$

$$Q_{BOC}C_{i,j_{CB}-1} + \cancel{V_{j_{CB}}r_{i,j_{CB}}} = Q_{BOC}C_{i,j_{CB}} + V_{j_{CB}} \frac{dC_{i,j_{CB}}}{dt} \quad 0$$

Then,

$$\frac{dC_{i,j_{CB}}}{dt} = \frac{1}{V_{j_{CB}}} Q_{BOC} (C_{i,j_{CB}-1} - C_{i,j_{CB}}) \quad (IV-56)$$

#### IV.5.1.3. Benchmark parameters

The following parameter values were chosen in the Benchmark study (Alex et al. 2008). The first two reactors of the cascade (anoxic zone) had an individual volume of  $1000 \text{ m}^3$ . The 3 following reactors representing the aerobic zone had an individual volume of  $1333 \text{ m}^3$  (see Table IV.12).

The flow rate of the internal recirculation  $Q_L$  is kept at  $55338 \text{ m}^3 \text{ d}^{-1}$ . The flow rate of the sludge ( $Q_S$ ) recirculation equals the inlet flow rate  $Q_e$  at  $18446 \text{ m}^3 \text{ d}^{-1}$  and the excess sludge is removed from the settler at  $385 \text{ m}^3 \text{ d}^{-1}$  (See Table IV.13).

**Table IV. 12.** Volumes and values of the transfer in the BSM1.

Reactors	Volumes (m <sup>3</sup> )	k <sub>La</sub> (h <sup>-1</sup> )
R1	1000	-
R2	1000	-
R3	1333	10
R4	1333	10
R5	1333	3.5

**Table IV. 13.** Flow rates of the coefficients of the BSM1 reactors.

Flow rates	(m <sup>3</sup> d <sup>-1</sup> )
Q <sub>e</sub>	18446
Q <sub>L</sub>	55338
Q <sub>s</sub>	18446
Q <sub>w</sub>	385

The initial concentrations were not mentioned in the Benchmark. The chosen initial values of ASM1 compounds are given in Table IV.14. The initial concentration of micropollutants is equal to zero. This means that there is no MP in the WWTP before operating the system.

The inlet concentrations were given in the Benchmark study, except for the MPs concentrations. We adopted the same inlet values of ASM1 compounds in our simulations (Table IV.15). The inlet concentrations of MPs were taken equal to the average of the initial C<sub>MPs</sub> measured in the batch reactors.

**Table IV. 14.** The chosen initial concentration of ASM1 compounds. Initial MPs concentration equals zero.

	Initial concentration of ASM1 compounds and MPs
$X_{B,H}$ (g m <sup>-3</sup> )	2500
$X_{B,A}$ (g m <sup>-3</sup> )	190
$X_P$ (g m <sup>-3</sup> )	870
$S_S$ (g m <sup>-3</sup> )	14
$X_S$ (g m <sup>-3</sup> )	200
$S_{NO}$ (g m <sup>-3</sup> )	5
$S_{NH}$ (g m <sup>-3</sup> )	4
$S_{ND}$ (g m <sup>-3</sup> )	1.4
$X_{ND}$ (g m <sup>-3</sup> )	6
$S_I$ (g m <sup>-3</sup> )	18
$X_I$ (g m <sup>-3</sup> )	1150
$S_O$ (g m <sup>-3</sup> )	0.4
$C_{SMX}$ (μmol m <sup>-3</sup> )	0
$C_{BZT}$ (μmol m <sup>-3</sup> )	0
$C_{ROX}$ (μmol m <sup>-3</sup> )	0
$C_{ERY}$ (μmol m <sup>-3</sup> )	0
$C_{DCF}$ (μmol m <sup>-3</sup> )	0

**Table IV. 15.** Inlet concentrations of ASM1 compounds borrowed from the BSM1 except for the MPs concentrations which were equal to the average of the initial  $C_{MPs}$  measured in the batch reactors.

	Inlet concentration of ASM1 compounds and MPs
$X_{B,H}$ (g m <sup>-3</sup> )	28.17
$X_{B,A}$ (g m <sup>-3</sup> )	0
$X_P$ (g m <sup>-3</sup> )	0
$S_S$ (g m <sup>-3</sup> )	69.5
$X_S$ (g m <sup>-3</sup> )	202.32
$S_{NO}$ (g m <sup>-3</sup> )	0
$S_{NH}$ (g m <sup>-3</sup> )	31.56
$S_{ND}$ (g m <sup>-3</sup> )	6.95
$X_{ND}$ (g m <sup>-3</sup> )	10.59
$S_I$ (g m <sup>-3</sup> )	30
$X_I$ (g m <sup>-3</sup> )	51.2
$S_O$ (g m <sup>-3</sup> )	0
$C_{SMX}$ (μmol m <sup>-3</sup> )	4.56
$C_{BZT}$ (μmol m <sup>-3</sup> )	7.57
$C_{ROX}$ (μmol m <sup>-3</sup> )	0.97
$C_{ERY}$ (μmol m <sup>-3</sup> )	1.71
$C_{DCF}$ (μmol m <sup>-3</sup> )	3.72

#### IV.5.1.4. Comparison with the Benchmark results

Figure IV.11 shows the concentration profiles obtained with Matlab compared to the Benchmark values. It can be seen that the duration of simulation of 100 days is sufficient to reach almost similar Benchmark concentrations. For more details, Table IV.S4 shows the numerical results obtained with Matlab in terms of concentrations. For further evaluation of the simulation results, the generated output data compiled in Table IV.16 is compared to the standardized output that is included in the Benchmark description gathered in Table IV.S5. The relative difference between the concentrations is less than 11% for all concentrations in the cascade of reactors as well as at the overflow and the bottom outlets of the clarifier.

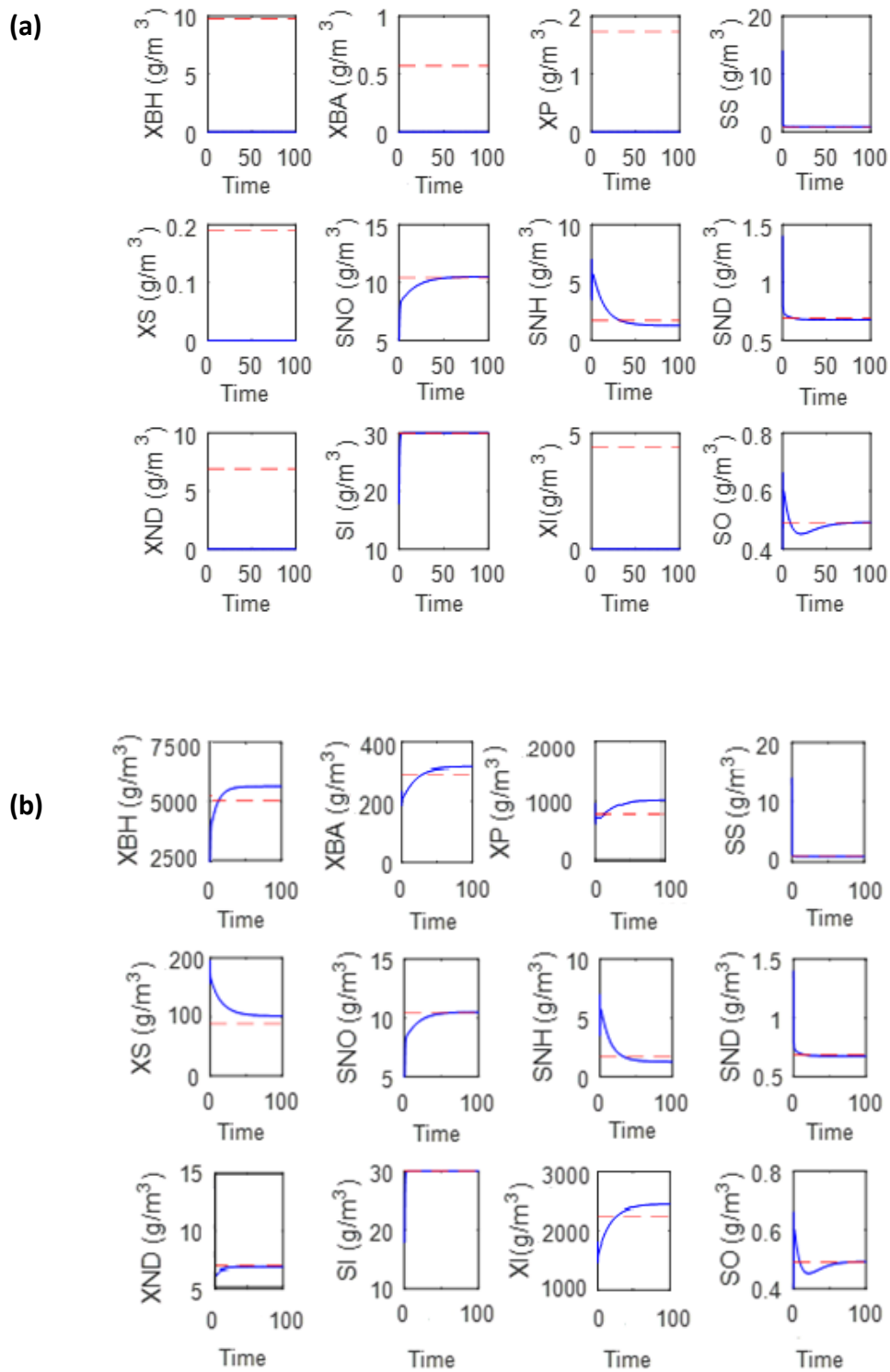


**Figure IV. 11.** Profiles of solubles and non-solubles concentrations obtained from simulation on Matlab (blue line) for  $C_{eff}$  denoted for clear water concentration (a) at the overflow outlet of the clarifier and  $C_s$  denoted to sludge concentration (b) at the bottom outlet of the clarifier, respectively. Concentration obtained at the end of simulation of Benchmark are represented by the red line.

The concentrations in the feed of the cascade (reactor 1) as well as in feed of clarifier (exit of reactor 5), the effluent, and the return sludge are very well predicted by our model. However, the difference observed in the Table IV. 16 could be explained by the performance of the clarifier which is not similar for that used in the Benchmark Simulation Model no. 1 (BSM1). Furthermore, in the case of the Benchmark, the clarifier is not 100 % effective. It does not completely separate the insoluble compounds from the soluble ones. On the contrary, in the present Matlab simulations, a complete separation of the insoluble and soluble compounds is assumed. This is why the %error was not computed for the non-soluble compounds ( $X_{B,H}$ ,  $X_{B,A}$ ,  $X_P$ ,  $X_S$ ,  $X_{ND}$  and  $X_I$ ) in the upper part of the clarifier and were marked N/A in Table IV.16.

**Table IV. 16.** Percentage error (%) of the simulated results compared to the Benchmark results. N/A refers to a large %error for the non-soluble compounds in the upper part of the clarifier.

	%error			
	Reactor 1	Reactor 5	Sludge	Effluent
$X_{B,H}$	2.8	2.7	8.9	N/A
$X_{B,A}$	6.4	5.4	5.5	N/A
$X_P$	10.4	10.3	10.1	N/A
$S_S$	3.8	1.9	0.9	0.9
$X_S$	1.6	0.8	0.8	N/A
$S_{NO}$	0.33	0.86	0.62	0.8
$S_{NH}$	2.3	0.5	0.5	0.5
$S_{ND}$	2.3	0.4	0.3	0.2
$X_{ND}$	2.2	3	3.3	N/A
$S_I$	0.1	0.11	0.2	0.11
$X_I$	0.8	0.8	4.5	N/A
$S_O$	0.6	0	0	0



## IV.5.2. Cascade of an arbitrary number of CSTR operated with power law kinetics

The objective of the current set of simulations is to test the effects of hydrodynamic configurations coupled to the power law kinetics on the MPs removal. In order to do that, the tested plant model is identical to that used for the above Benchmark reference (Section IV.5.1), but with a higher number of CSTR with constant total volume. The whole reactor is always represented by cascades of same total volume, but with different number of tanks in series. For this reason, ten different configurations of total number of 5, 10, 15, 20, 30, 45, 60, 75, 90 and 100 reactors of equal volumes were simulated consecutively with different  $n$  values of the kinetic model from 0.1 to 1 for each configuration. The number of reactors represented by  $j_{max}$  was simply changed each time in the "MainPrgm\_cas" of continuous system described in Text IV.S5A. Additionally, hydrodynamic parameters such as the volume of reactors and  $k_{LA}$  were also reset with respect to the tested number of reactors while keeping the same ratio of anoxic (2/5<sup>th</sup>) and aerobic (3/5<sup>th</sup>) as that used in the Benchmark. Table IV.17 shows the changes that have been performed on different hydrodynamic configurations. Note that the volume of the reactor used in the Benchmark, of around 6000 m<sup>3</sup>, was divided into reactors of equivalent volume in order to compare correctly the effect of different hydrodynamics on MPs' removal. After developing and running the simulation code, we obtained all the MPs effluent data (from the overflow outlet of the clarifier). These results are plotted on 3D surfaces in Figure IV.13 representing the removal efficiency of the 5 investigated MPs, as a function of coefficient  $n$  and as a function of the number of the aerobic reactors (which amounts for 3/5<sup>th</sup> of the total number of reactors). We made the choice to present the removal efficiency as function of aerobic reactors instead of the total number of reactors because only the aerobic zone will be used afterwards in sizing section (IV.6).

**Table IV. 17.** Adjustment of physical parameters according to different hydrodynamic configurations.

Total number of reactors	5	10	15	20	30	45	60	75	90	100
Number of aerobic reactors ( $k_{La}$ per reactor = $10 \text{ h}^{-1}$ )	<b>3</b>	<b>6</b>	<b>9</b>	<b>12</b>	<b>18</b>	<b>27</b>	<b>36</b>	<b>45</b>	<b>54</b>	<b>60</b>
Number of anoxic reactors ( $k_{La}$ per reactor = $0 \text{ h}^{-1}$ )	2	4	6	8	12	18	24	30	36	40
Volume per aerobic reactor ( $\text{m}^3$ )	1200	600	400	300	200	133.33	100	80	66.66	60
Volume per anoxic reactor ( $\text{m}^3$ )	1200	600	400	300	200	133.33	100	80	66.66	60

From Figure IV.12, it appears that the worst removal efficiency is achieved for low  $n$  and low number of reactors. Increasing  $n$  or the number of the reactors tends to enhance the removal of micropollutants. The highest removal, 92 %, is achieved for SMX, followed by BZT, ROX and ERY which reach at best 80 %, 72 % and 69 %, respectively. DCF is the most poorly removed with only 39 % at best.

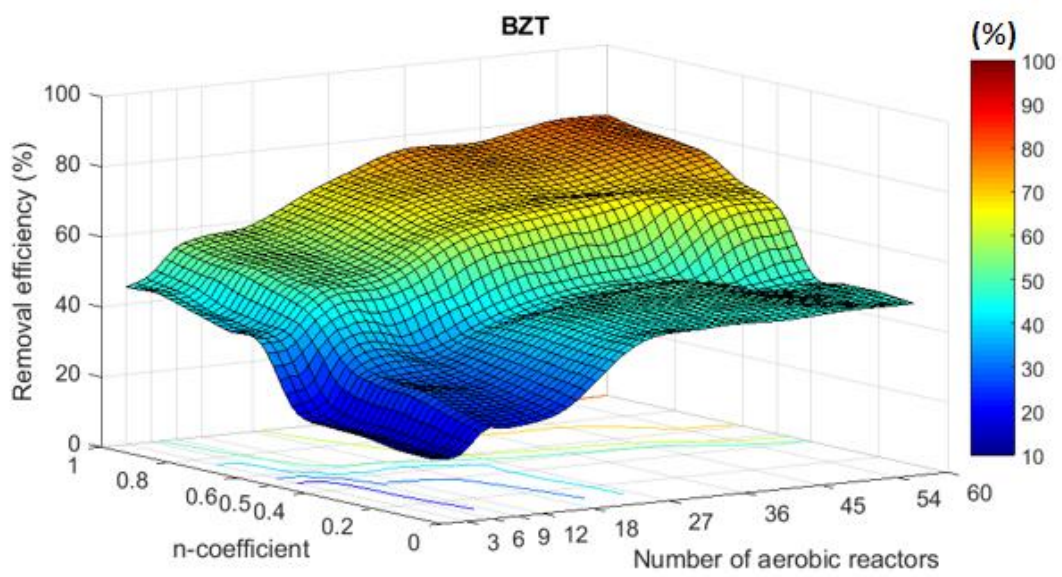
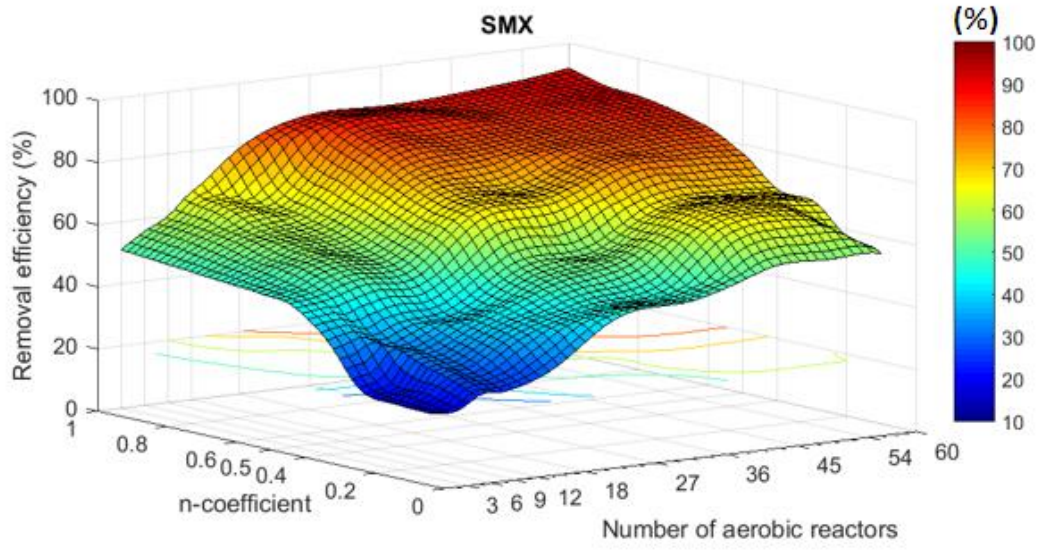
For BZT, ROX and ERY, a plateau is observed at low  $n < 0.4$  and high number of reactors (starting from 27 reactors): it is useless to increase the number of reactors if  $n$  is low.

The moderately biodegradable compounds SMX and BZT show a similar behavior for low hydrodynamics conditions. For low  $n$  (generally,  $n < 0.5$ ) and low number of aerobic reactors (i.e. 3 to 18), SMX and BZT are removed by 20-40 % and 16-34 %, respectively. These results imply that 3 to 18 reactors produce an insufficient removal of the moderately biodegradable compounds if the local mixing is not good enough (i.e. low  $n$ ). The higher  $n$  values, up to 1, reflecting better mixing conditions, improve the removal of SMX and BZT up to 79 % and 59 %, for the same low number of reactors. Additionally, increasing the number of aerobic reactors, up to 60, coupled with a good local mixing (high  $n$ ), significantly increases the removal of SMX and BZT up to 92 % and 80 %, respectively.

Comparable trends were observed for both macrolides ROX and ERY but with lower removal up to 72 % and 69 % respectively, compared to SMX and BZT in most favorable conditions (high  $n$  and 60 aerobic reactors). Indeed, a higher plateau is observed for  $n > 0.45$  and high number of aerobic reactors (starting from 27 reactors) showing the saturation of the system to remove both macrolides.

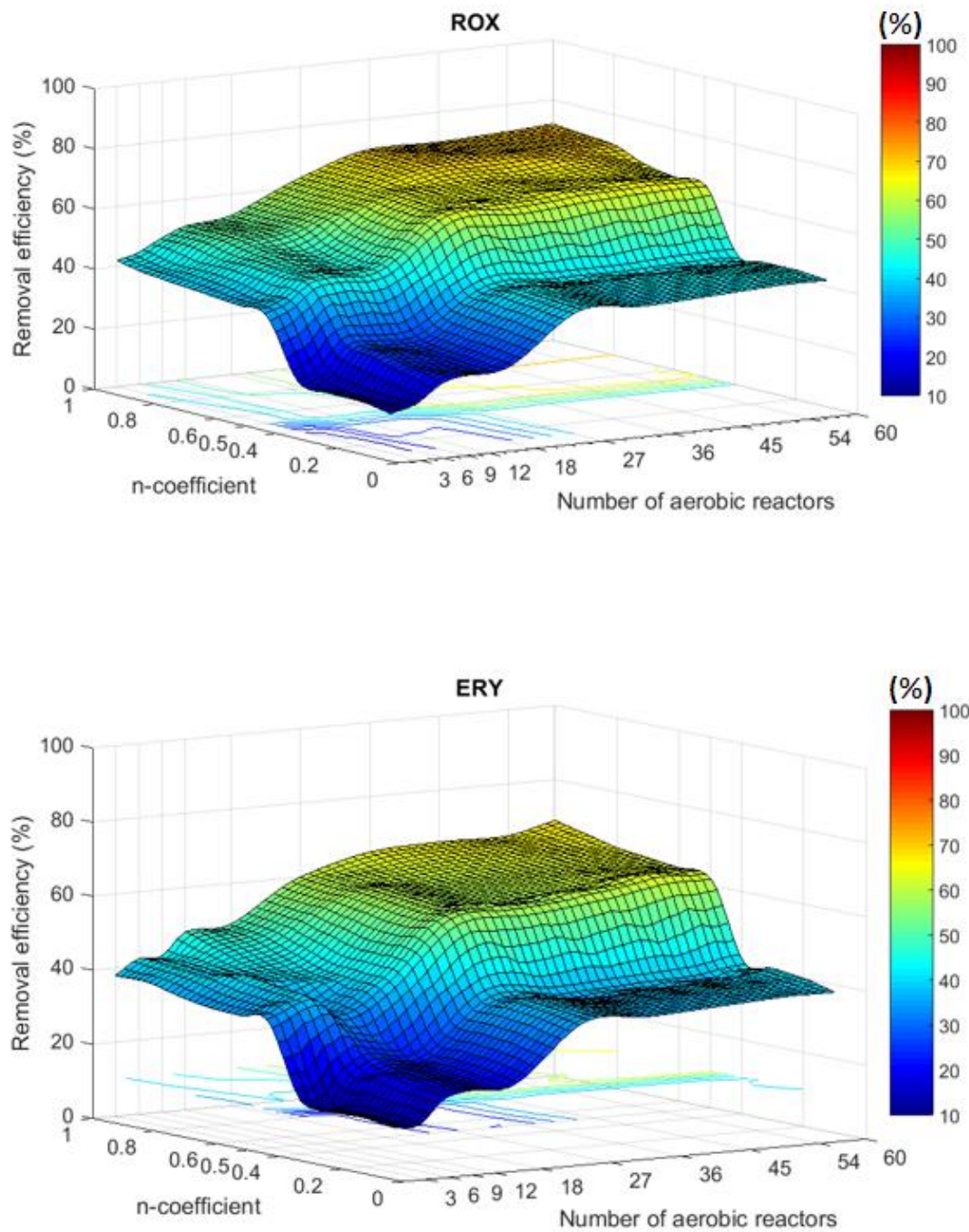
DCF, the persistent compound, showed the lowest removal up to 39 % by applying the most favorable conditions.

Note that we choose to consider at most 60 reactors, since the removal remains almost constant above 45 reactors, coupled with good mixing, for all tested compounds. Joss et al. (2006) showed that dividing of the available reactor volume into reactor cascades (e.g. three tanks in series) can appreciably improve the removal of 25 pharmaceuticals including (ROX and DCF), hormones and fragrances. However, the same authors found that if sorption levels are high ( $K_d > 100 \text{ L kg}_{\text{TSS}}^{-1}$ ), which is the case of none of our compounds, the impact of dividing the reactor volume into cascades becomes less significant. Moreover, Ternes et al. (2005) found that, due to first order kinetics of biological degradation of all compounds with  $k_{\text{biol}} > 0.5 \text{ L gSS}^{-1} \text{ d}^{-1}$  such as SMX and ROX, the removal produced by a single completely stirred reactor is significantly lower as compared to the same total volume subdivided into cascaded compartments. To the best of our knowledge, there exists no other reported works in literature on the experimental effect of dividing the reactor volume into cascades on MP's removal.



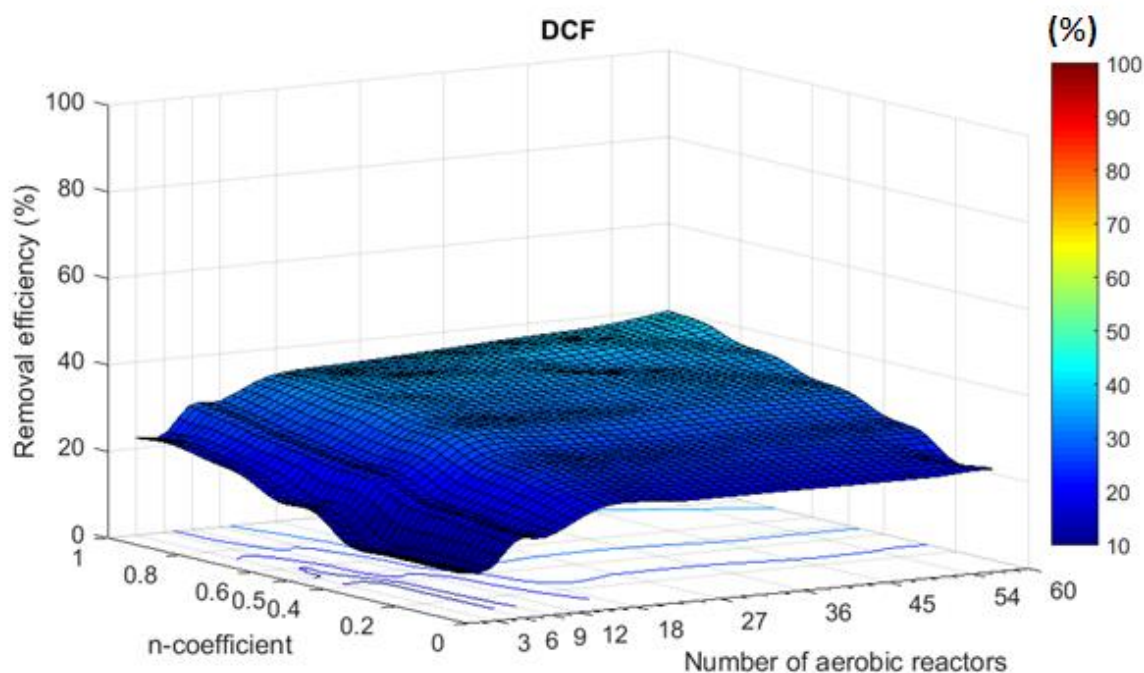
(Continued on next page)

Figure IV. 12. Continued



(Continued on next page)

Figure IV.12. Continued

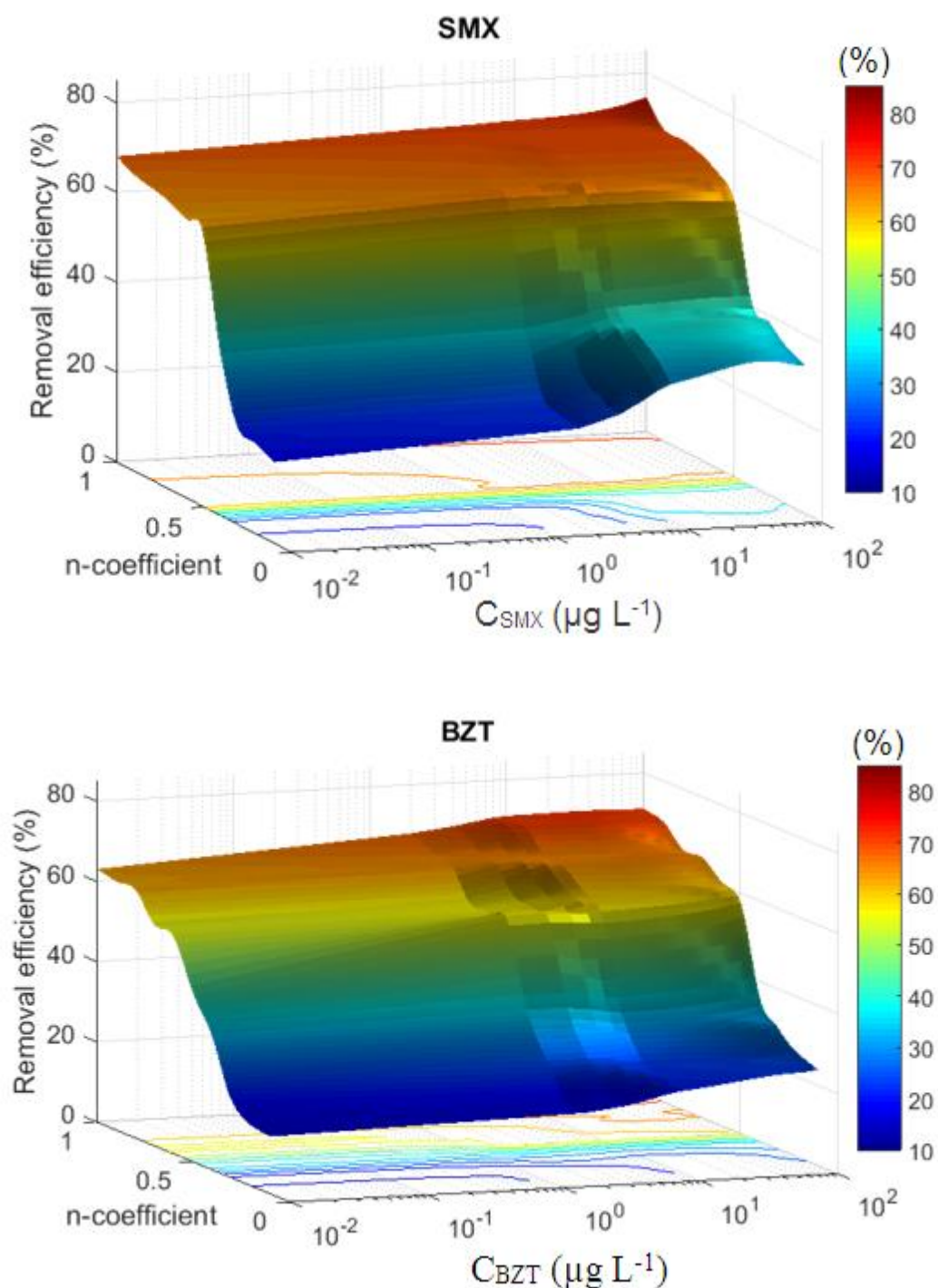


**Figure IV. 12.** 3D plots representing the removal efficiency (%) of SMX, BZT, ROX, ERY and DCF as a function of the order of the reaction  $n$  (varying from 0.1 to 1) and as a function of the number of aerobic reactors (from 3 to 60) for the same inlet concentration  $C_{MPs} = 1 \mu\text{g L}^{-1}$ . Red color means the highest removal efficiency of each MP.

#### IV.5.3. Cascade of 5 reactors tested with wide range of inlet $C_{MPs}$

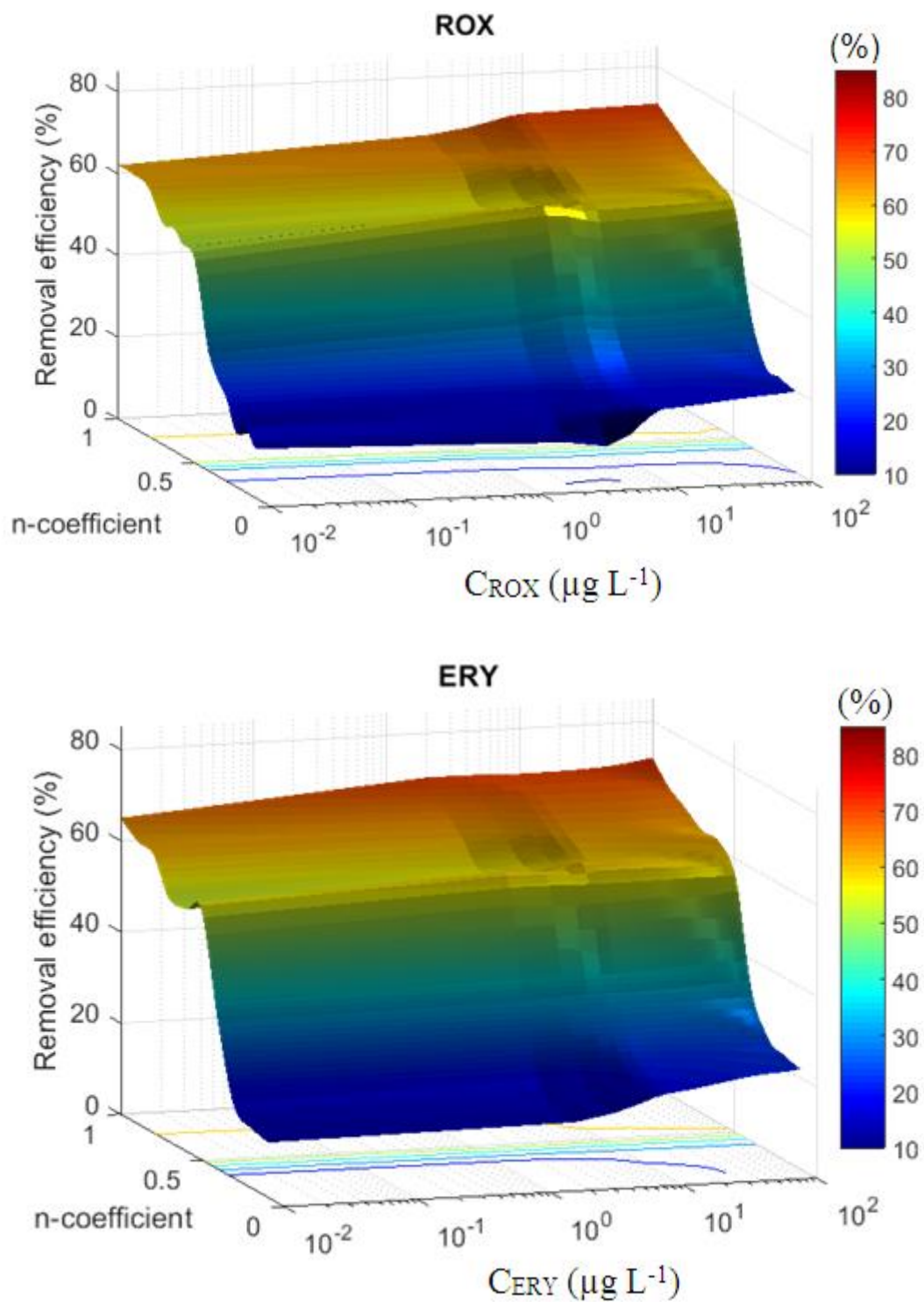
The kinetics of MPs removals is dependent on their inlet concentration feeding the first reactor of the system. Hence, it is of importance to study the effect of a wide range of micropollutants inlet concentration ( $C_{MPs}$ ) on their removal efficiency. The classic values of all studied MPs concentration in the influent of WWTP are in the range of  $10 \text{ ng L}^{-1}$  to  $100 \mu\text{g L}^{-1}$ , as mentioned in Table I.1. Several compounds studied by (Luo et al., 2014), including the 5 MPs investigated in the present study, showed an inlet concentration ranging from  $0.007$  to  $56.7 \mu\text{g L}^{-1}$ . The caffeine entered with the highest concentration,  $56.7 \mu\text{g L}^{-1}$ , and underwent a removal rate of around 97 %. Based on the kinetics of MPs removal, it is well known that a higher inlet concentration of MPs induces an increase of their removal. In order to test whether our model based on the power law kinetic reproduced this fact, several simulations were performed on the

basic configuration of 5 reactors (3 aerobic and 2 anoxic), using the same conditions of  $k_{MPs}$ , and different MPs inlet concentrations. The five consecutive simulations were realized at  $10 \text{ ng L}^{-1}$ ,  $100 \text{ ng L}^{-1}$ ,  $1 \text{ } \mu\text{g L}^{-1}$ ,  $10 \text{ } \mu\text{g L}^{-1}$  and  $100 \text{ } \mu\text{g L}^{-1}$ , respectively. Figure IV.13 describes the removal efficiencies of SMX, BZT, ROX, ERY and DCF for inlet concentrations ranging from  $10^{-2}$ - $10^2 \text{ } \mu\text{g L}^{-1}$  coupled with different mixing conditions ( $n$  varied from 0.1 to 1).



(Continued on next page)

Figure IV. 13. Continued



(Continued on next page)



Figure IV. 13. Continued

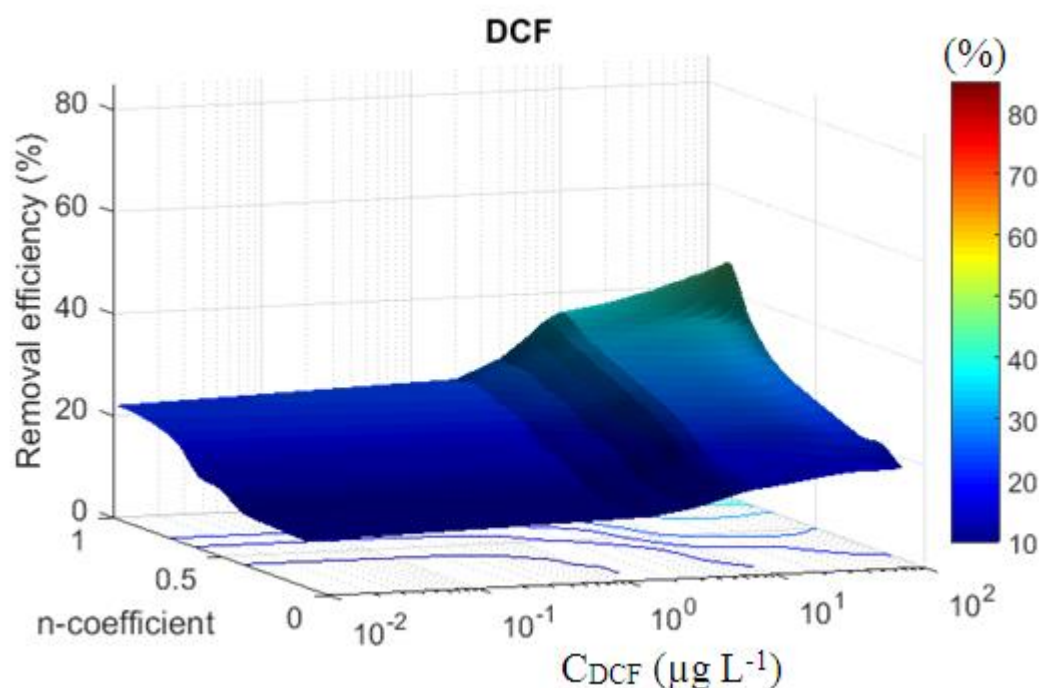


**Figure IV. 13.** 3D plots representing the removal efficiency (%) of SMX, BZT, ROX, ERY and DCF as a function of both the order of the reaction  $n$  (0.1 to 1) and the inlet concentration  $C_{MPs}$  ( $10^{-2}$  to  $10^2$   $\mu\text{g L}^{-1}$ ) in the configuration of 5 tanks in series. Red color indicates the highest removal efficiency of each MP.

As shown in Figure IV.13, all MPs were badly removed ( $< 20\%$  for SMX and BZT and  $< 10\%$  for ROX, ERY and DCF) for poor mixing conditions ( $0.1 < n < 0.5$ ) and low  $C_{MPs} < 1$   $\mu\text{g L}^{-1}$ .

For better mixing conditions ( $0.6 < n < 1$ ), despite low  $C_{MPs}$ , the removal of moderately biodegradable compounds SMX and BZT increased up to 65 % and 45 % respectively and the removal of both antibiotics ROX and ERY increased significantly up to 60%. As opposed to the others DCF was little removed (20 %), due to its poor biodegradability.

Inversely, at high  $C_{MPs}$  i.e, 10 and 100  $\mu\text{g L}^{-1}$ , and bad local mixing conditions (low  $n$ ), the removal efficiencies increased only slightly, of approximately 5 %, for all tested MPs.

Finally, high conditions of mixing coupled with high  $C_{MPs}$  showed the highest removal regardless the type of the compound. The removal of SMX, BZT, ROX, ERY and DCF reached up to 75 %, 55 %, 70 %, 65 % and 45 %, respectively. Limited literature about the effect of increasing MPs inlet concentration, coupled with the mixing conditions, on their removal

behavior was found. The present results obtained at high  $C_{MPs}$  are in good agreement with those reported by the studies of (Gobel et al. 2007 and Gros et al. 2010), while Deblonde et al. (2011) showed lower removal efficiencies at high  $C_{MPs}$ , with a removal rate for antibiotics of about 50 % and 30 % removal rate for analgesics and anti-inflammatories.

## IV.6. Estimation of fundamental dimensions of the continuous reactor configuration

### IV.6.1. Reactor modelling

In previous section, we realized that hydrodynamics is important both at micro and macro scales. The reactor design explained in this section is based on knowhow and modelling developed in our laboratory. It is based, on the one hand, models binding Peclet numbers to the geometry, shape and size of aerated reactors and on the other hand on equivalence of hydrodynamic of cascade of CSTR and plug flow reactor with axial dispersion.

The goal is then to design aerated channel reactors, which hydrodynamics correspond to different cascades of CSTR presented in previous section about simulation. We will first start with an aerated channel reactor corresponding to the one of the Benchmark: volume of 3600 m<sup>3</sup>. Afterwards, we will change its shape proportions to fit higher corresponding number of CSTR. The total volume, horizontal surface, and depth remain constant for all configurations.

- The Peclet number ( $P_e$ ) is one of the main parameters in the classic plug flow reactor with axial dispersion (axial dispersion model or ADM). It is represented as following (Potier et al. 2005):

$$P_e = \frac{uL}{D} \quad (\text{IV-57})$$

with

$$u = \frac{Q_e}{\Omega}; \Omega = HW$$

where  $u$  is the average longitudinal velocity of the liquid phase inside the reactor (m s<sup>-1</sup>),  $D$  is the axial dispersion coefficient (m<sup>2</sup> s<sup>-1</sup>),  $Q_e$  is the volumetric flow rate of the liquid (m<sup>3</sup> s<sup>-1</sup>),  $\Omega$  is the vertical section (m<sup>2</sup>),  $L$  is the reactor length (m),  $H$  is the water depth (m) and  $W$  is the width (m).

$$P_e = \frac{Q_e L}{HWD} \quad (\text{IV-58})$$

Le Moullec and Potier (2008) proposed a correlation giving the axial dispersion coefficient as a function of the geometrical parameters (H, L, W) and the gaz flowrate ( $Q_G$ ) as following:

$$D = \frac{2}{3} \frac{H}{H+W} \sqrt{\frac{Q_G W_d (L+W)}{2L}} \quad (\text{IV-59})$$

$W_d$  is the aeration width. In this modelling, it would be equal to the total width (aeration device covers the whole bottom). For a given geometry of reactor, the volume is simply calculated by  $V = H W L$ . The given total volume is  $3600 \text{ m}^3$ . We proposed a channel with depth ( $H = 7 \text{ m}$ ). For the simplest tested configuration, there are 3 CSTR in series. The constant H means that  $W L$  is constant and equals the horizontal section designed by ( $S_h = 514.3 \text{ m}$ ).

When W decrease, L increase in a way to keep the horizontal surface constant according to Eq. (IV-60):

$$W = \frac{S_h}{L} \quad (\text{IV-60})$$

If  $W = 9.65 \text{ m}$ , L is calculated to be  $53.3 \text{ m}$ .

From Eqs. (IV-58) and (IV-59), the following relation can be deduced:

$$P_e = \frac{3}{\sqrt{2}} \frac{Q_e}{\sqrt{Q_G}} \left(\frac{L}{W}\right)^{\frac{3}{2}} \frac{(H+W)}{H^2 \sqrt{L+W}} \quad (\text{IV-61})$$

With  $Q_G = 0.1 \text{ m}^3 \text{ s}^{-1}$  and  $Q_e = 1.07 \text{ m}^3 \text{ s}^{-1}$  already used in Benchmark (Alex et al. 2008), the reactor can be represented as a plug flow reactor with axial dispersion with  $P_e = 4$ .

- In most cases the following equivalence between the plug flow reactor with axial dispersion and the tanks in series models may be applied (Villermoux, 1982; Potier et al. 2005):

$$(J - 1) \# \frac{P_e}{2}$$

So,

$$(J - 1) \# \frac{P_e}{2} = \frac{Q_e L}{2 H W D} \quad (\text{IV-62})$$

J is the number of tanks in series.

In terms of  $J$ , the geometrical parameters ( $H = 7$  m,  $W = 9.65$  m and  $L = 53.3$  m) correspond to the configuration of  $J = 3$  ( $P_e = 4$ ), that is the number of CSTR used by the Benchmark.

From Eqs. (IV-59) and (IV-62), the following Eq. (IV-63) can be deduced in order to calculate the number of mixing cells ( $J$ ) as following:

$$(J - 1) = \frac{3 L^{3/2} Q_e (H+W)}{2\sqrt{2} W^{3/2} H^2 \sqrt{L+W} \sqrt{Q_G}} \quad (\text{IV-63})$$

From Eqs (IV-60) and (IV-63), the following relation can be deduced:

$$(J - 1) = \frac{3 S_h^{3/2} Q_e (H+W)}{2\sqrt{2} W^{5/2} H^2 \sqrt{S_h+W^2} \sqrt{Q_G}} \quad (\text{IV-64})$$

#### IV.6.2. Proper design of biological reactor

Then, it is possible to build an equation based on initial number of CSTR used in the Benchmark ( $J_i$ ) and the corresponding initial reactor width ( $W_i$ ) in order to calculate the number of CSTR ( $J_{cal}$ ) corresponding to another width ( $W_{cal}$ ). The depth ( $H$ ) and the horizontal surface ( $S_h$ ) remain the same for all calculations. This relation is given by:

$$\frac{(J_{cal}-1)}{(J_i-1)} = \frac{W_i^{5/2} (H+W_{cal}) \sqrt{(S_h+W_i^2)}}{W_{cal}^{5/2} (H+W_i) \sqrt{(S_h+W_{cal}^2)}} \quad (\text{IV-65})$$

So,

$$J_{cal} = 1 + \frac{(J_i-1) W_i^{5/2} (H+W_{cal}) \sqrt{(S_h+W_i^2)}}{W_{cal}^{5/2} (H+W_i) \sqrt{(S_h+W_{cal}^2)}} \quad (\text{IV-66})$$

Remark: as mentioned before, this equation is obtained for  $W_d = W$ .

Based on Eq. (IV-66),  $J_{cal}$  was calculated for the range of the initial  $W_{cal}$  up to 9.65 m.  $J_{cal}$  has been plotted versus  $W_{cal}$  (Figure IV.14). Moreover, the calculated length ( $L_{cal}$ ) was estimated by dividing the surface ( $S_h$ ) of 514.3 m<sup>2</sup> by every  $W_{cal}$  for the same range.  $J_{cal}$  has been plotted versus  $L_{cal}$  (Figure IV.15). For example, for  $J_{cal} = 12$  reactors, the width become 4 m and the

length of 120 m.  $J_{cal}$  almost increases linearly with the ratio of  $L_{cal}/W_{cal}$ , so it depends upon the geometry of the reactor (Figure IV.16).

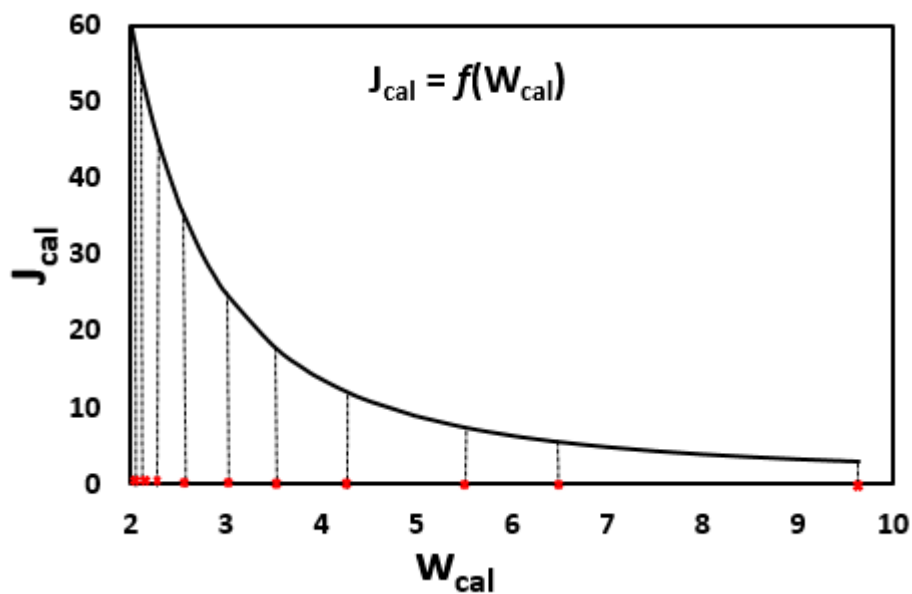


**Figure IV. 14.** Number of CSTR ( $J_{cal}$ ) corresponding to the reactor width ( $W_{cal}$ ). Red crosses refer to the calculated width ( $W_{cal}$ ) by projection for every tested configuration of aerobic reactors: 3, 6, 9, 12, 18, 27, 36, 45, 54 and 60 (by progressive transformation of the reactor of the benchmark:  $J_i=3$ ,  $W_i=9.65$  m and  $S_h$  of 514.3 m<sup>2</sup>).

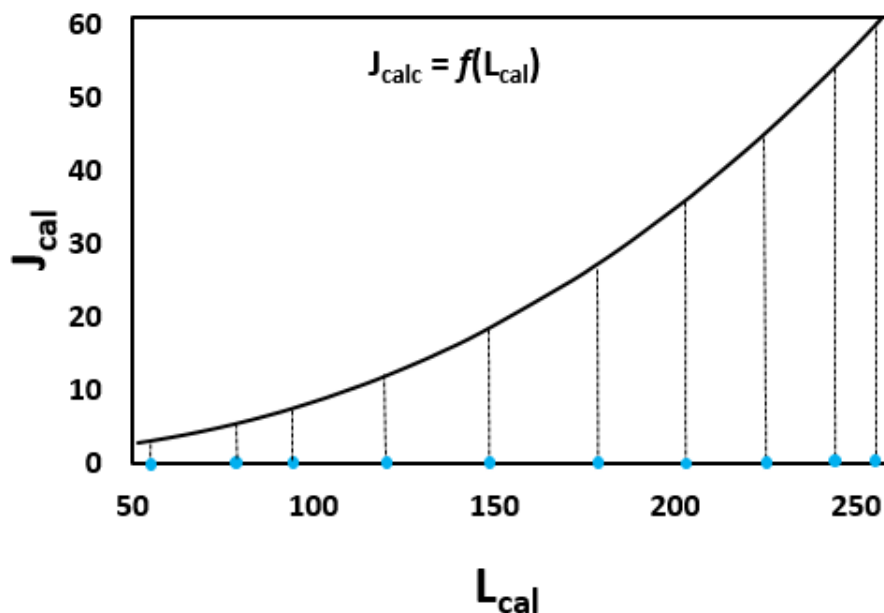


**Figure IV. 15.** Number of CSTR ( $J_{cal}$ ) corresponding to the reactor length ( $L_{cal}$ ). Blue circles refer to the calculated length ( $L_{cal}$ ) by projection for every tested configuration of aerobic

reactors: 3, 6, 9, 12, 18, 27, 36, 45, 54 and 60 (by progressive transformation of the reactor of the benchmark:  $J_i = 3$ ,  $W_i = 9.65$  m and  $S_h$  of 514.3 m<sup>2</sup>).

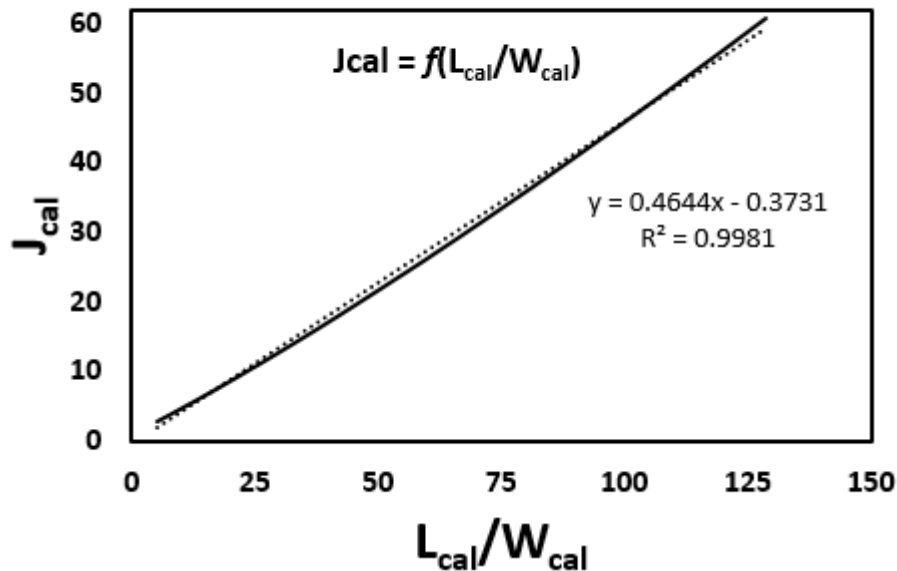


**Figure IV. 16.** Relationship between  $J_{cal}$  and  $L_{cal}/W_{cal}$ . The dashed line represents the linear trend line.

Finally, a width of 2.0 m and a length of 255 are necessary to reach  $J_{cal} = 60$  (Figure IV.17), by respecting the same volume and the same surface of the reactor and compared to the initial reactor, the width is divided by about 5 whereas the length was multiplied by about 5. In order to avoid problem of buildings and the mechanical resistance of the wall structure and to save space, it is possible to build the new reactor with 5 Baffles. The geometry of the building is 51 m x 10 m (very similar to initial reactor) when dimensions of the reactor are 2 m x 255 m.

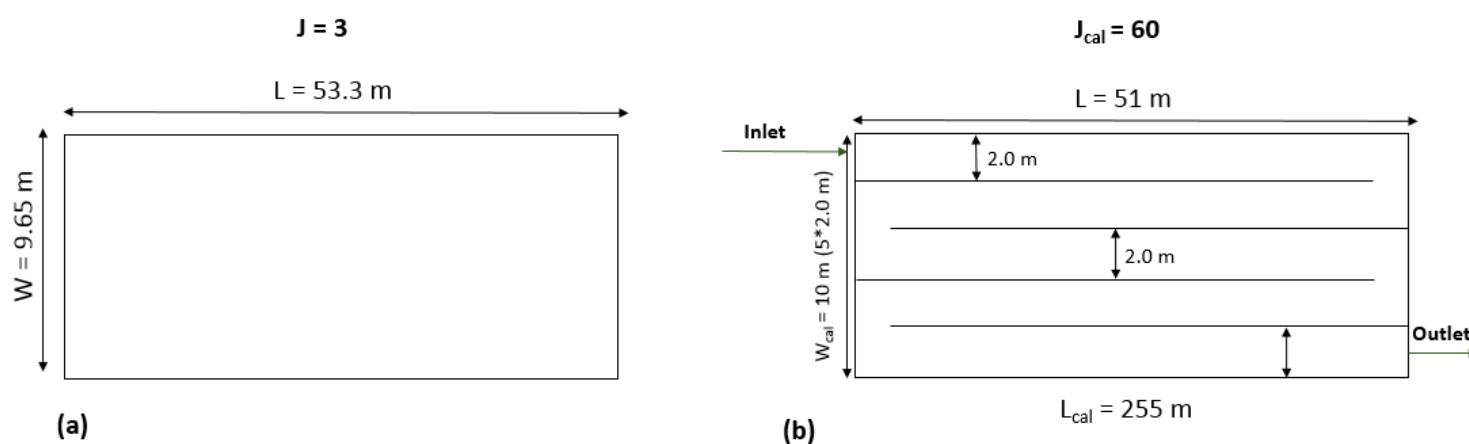


**Figure IV. 17.** Schematic representations of the (a) reactor with  $J = 3$  (initial geometry) and (b) the new geometry with 5 Baffles for the highest  $J = 60$  with inlet and outlet on opposite sides.

For the same  $n$  kinetic coefficient, increasing the length and reducing the width will increase the number of CSTR ( $J$ ) and consequently, could increase the removal of micropollutants. For example, for the case of SMX  $n = 0.51$ , the removal with  $J = 3$  was only 50 %, but, increasing  $J$  up to 60 reactors increases the SMX removal up to 80 %.

#### IV.7. Conclusion of chapter IV

The aim of this chapter was (i) to simulate the experimental data (in batch mode), (ii) to test different kinetics of MPs removal (including the effect of  $n$ ) and (iii) to predict the effect of different hydrodynamic configurations as well as different MPs concentration coupled with mixing conditions on the MPs' removal in continuous systems. The experiments performed in chapter II in batch mode were simulated successfully. The experiments performed at different SRT and HRT follow approximately an apparent-first order kinetics. However, the power law kinetics is only able to describe the MPs removal at all biomass concentrations and especially at high ones, showing the interest of the new kinetic model. Subsequently, several simulations were performed in batch mode by applying the new kinetics to a wide range of  $C_{\text{TSS}}$ . The results showed that high biomass concentration coupled with high local mixing conditions increased the removal of all investigated MPs (SMX, BZT, ROX, ERY and DCF).

Later on, the last kinetics was applied to continuous systems. Different configurations were tested. Increasing the number of aerobic reactors up to 60 together with enforcing good local mixing significantly increases the removal of all studied MPs. However, 45 to 54 reactors were enough to achieve the highest removal efficiency. Similarly, the effect of the inlet concentrations of MPs was tested. High  $C_{MPs}$  coupled with high local mixing produce the highest removal of all MPs. However, high mixing level and low  $C_{MPs}$  also improve significantly the removal of SMX, BZT, ROX and ERY. In the future, the effect of local mixing on the MPs removal should be further investigated. Finally, a first design of aerated reactor showed by reducing its width, but maintaining the same horizontal surface that is possible to increase the number of CSTR that correspond to its hydrodynamic model. Then, changing the dimension proportions of the reactor could help to increase the removal of moderately and slowly biodegradable MPs.

#### **IV.8. References of chapter IV**

- Bassompierre, C., 2007. Procédé à boues activées pour le traitement d'effluents papetiers : de la conception d'un pilote à la validation de modèles.
- Bellandi, G., 2014. Model-based analysis of aeration in lab and full-scale activated sludge systems Belgium: MSc Thesis, Ghent University.
- Bendounan R., 1995. Hydrodynamique et performances d'un décanteur primaire de station d'épuration des eaux usées urbaines : thèse, Université de Lorraine.
- Clouzot, L., Choubert, J.M., Cloutier, F., Goel, R., Love, N.G., Melcer, H., Ort, C., 2013. Perspectives on modelling micropollutants in wastewater treatment plants. *Water Science and Technology*, 68, 448–61.
- Copp, J.B., 2002. The COST Simulation Benchmark: description and simulator manual: A product of COST action 624 and COST action 682. EUR-OP.
- Cruz, N.M., Hooshiar, K., Arellano-Garcia, H., Wozny, G., Lyberatos, G., 2013. Model based optimization of the intermittent aeration profile for SBRs under partial Nitrification. *Water Research*, 47, 3399–3410.
- Deblonde, T., Cossu-Leguille C., and Hartemann P. 2011. Emerging pollutants in wastewater: A review of the literature. *International Journal of Hygiene and Environmental Health* 214 (6): 442–48.



- Dionisi, D., Bornoroni L., Mainelli S., Majone M., Pagnanelli F., Papini, M.P., 2008. Theoretical and experimental analysis of the role of sludge age on the removal of adsorbed micropollutants in activated sludge processes. *Industrial & Engineering Chemistry Research*, 47, 6775–82.
- Fenu, A., Guglielmi, G., Jimenez, J., Spèrandio, M., Saroj, D., Lesjean, B., Brepols, C., Thoeye, C., Nopens, I., 2010. Activated Sludge Model (ASM) based modelling of membrane bioreactor (MBR) processes. *Water Research*, 44, 4272–94.
- Gernaey, K.V., Van Loosdrecht, M.C.M., Henze, M., Lind, M., Jørgensen, S.B., 2004. Activated sludge wastewater treatment plant modelling and simulation: state of the art. *Environmental Modelling & Software, Environmental Sciences and Artificial Intelligence*, 19, 763–83.
- Gillot, S., Capela-Marsal S., Roustan M., Héduit, A., 2005. Predicting oxygen transfer of fine bubble diffused aeration systems—Model issued from dimensional analysis. *Water Research*, 39, 1379–87.
- Gobel, A., Mcardell, C., Joss, A., Siegrist, H., Giger, W., 2007. Fate of sulfonamides, macrolides, and trimethoprim in different wastewater treatment technologies. *Science of The Total Environment*, 372, 361–71.
- Gros, M., Petrović, M., Ginebreda, A., Barceló, D., 2010. Removal of pharmaceuticals during wastewater treatment and environmental risk assessment using hazard indexes. *Environment International*, 36, 15–26.
- Hauduc, H., Rieger L., Oehmen A., van Loosdrecht, M.C.M., Comeau, Y., Héduit, A., Vanrolleghem, P.A., Gillot, S., 2013. Critical review of activated sludge modelling: State of process knowledge, modelling concepts, and limitations. *Biotechnology and Bioengineering*, 110, 24–46.
- Henze, M., 1987. Activated sludge model No. 1. IAWPRC Scientific and Technical Reports 1.
- Henze, M., Gujer W., Mino T., Van Loosdrecht, M., 2002. Activated sludge models ASM1, ASM2, ASM2d and ASM3. London. IWA Publishing.
- Joss, A., Zabczynski, S., Göbel, A., Hoffmann, B., Löffler, D., McArdell, C.S., Ternes, T.A., Thomsen, A., Siegrist, H., 2006. Biological degradation of pharmaceuticals in municipal wastewater treatment: Proposing a classification scheme. *Water Research*, 40, 1686–96.
- Kang, A.J., Brown, A.K., Wong, C.S., Yuan, Q., 2018. Removal of antibiotic sulfamethoxazole by anoxic/anaerobic/oxic granular and suspended activated sludge processes. *Bioresource Technology*, 251, 151–57.

- Kim, Y., Yoo, C., Lee, I., 2008. Optimization of biological nutrient removal in a SBR using simulation-based iterative dynamic programming. *Chemical Engineering Journal*, 139, 11–19.
- Laurent, J., R. Samstag, W., Ducoste, J. M., Griborio, A., Nopens, I., Batstone, D. J., Wicks, J. D., Saunders, S., Potier, O. 2014. A protocol for the use of Computational Fluid Dynamics as a supportive tool for wastewater treatment plant modelling. *Water Science and Technology*, 70, 1575–84.
- Le Moullec, Y., 2008. Comparaison des approches systémique, mécanique des fluides numérique et compartimentale pour la modélisation des réacteurs : application à un réacteur canal à boues activées, thèse de doctorat, Institut National Polytechnique de Lorraine, 207.
- Luo, Y., Guo, W., Ngo, H.H., Nghiem, D.L., Hai, L.F., Zhang, J., Liang, S., Wang, C.X., 2014. A Review on the occurrence of MPs in the aquatic environment and their fate and removal during WW treatment. *Science of the Total Environment*, 473-474, 619-41.
- Majewsky, M., Gallé, T., Yargeau, V., Fischer, K., 2011. Active heterotrophic biomass and sludge retention time (SRT) as determining factors for biodegradation kinetics of pharmaceuticals in activated sludge. *Bioresource Technology*, 102, 7415–21.
- Massot, A., Estève, K., Noilet, P., Méoule, C., Poupot, C., and Mietton-Peuchot, M., 2012. Biodegradation of phytosanitary products in biological wastewater treatment. *Water Research*, 46, 1785–92.
- Monod, J., 1942. *Recherches sur la croissance des cultures bactériennes*. Paris, Hermann, 210.
- Nopens, I., Samtag, R., Wicks J., Laurent, J., Rehman U., Potier o., 2017. To Mix, or Not to Mix, That Is the Question. *Frontiers in Wastewater Treatment and Modelling*, 677-683.
- Plosz, B.G., Leknes, H., Thomas, K.V., 2010. Impacts of competitive inhibition, parent compound formation and partitioning behavior on the removal of antibiotics in municipal wastewater treatment. *Environmental Science & Technology*, 44, 734–42.
- Pomiès, M., Choubert, J.-M., Wisniewski, C., Coquery, M., 2013. Modelling of micropollutant removal in biological wastewater treatments: A review. *Science of The Total Environment*, 443, 733–48.
- Press-Kristensen, K., Lindblom, E., Henze, M., 2007. Modelling as a tool when interpreting biodegradation of micro pollutants in activated sludge systems. *Water Science and Technology*, 56, 11–16.

- Rehman, U., Amerlinck, Y., Arnaldos, M., Nopens, I., 2014. CFD and biokinetic model integration applied to a full scale WWTP. *Proceedings of the Water Environment Federation*, 8, 6894–6905.
- Roche, M., Bendounan, R., Prost, C., 1994. Modélisation de l'hydrodynamique d'un décanteur primaire de station d'épuration. *Revue des sciences de l'eau*, 7, 153.
- Samstag, R. W., Ducoste, J. J., Griborio, A., Nopens, I., Batstone, D. J., Wicks, J. D., Saunders S., Wicklein, E. A., Kenny, G., Laurent, J. 2016. CFD for wastewater treatment: an Overview. *Water Science and Technology*, 74, 549–63.
- Smets, I.Y., Haegebaert, J. V., Carrette, R., Van Impe, J.F., 2003. Linearization of the activated sludge model ASM1 for fast and reliable predictions. *Water Research*, 37, 1831–51.
- Tan, B.L.L., Hawker, D.W., Müller, J.F., Leusch, F.D.L., Tremblay L.A., Chapman, H.F., 2007. Modelling of the fate of selected endocrine disruptors in a municipal wastewater treatment plant in south east Queensland, Australia. *Chemosphere*, 69, 644–54.
- Ternes, T., Joss, A., Kreuzinger, N., Miksch, K., Lema, J.M., von Gunten, U., McArdell, C.S., Siegrist, H., 2005. Removal of pharmaceuticals and personal care products: results of the Poseidon project. *Proceedings of the Water Environment Federation*, 16, 227–43.
- Wicklein, E., Batstone, D.J., Ducoste, J., Laurent, J., Griborio, A., Wicks, J., Saunders, S., Samstag, R., Potier, O., Nopens, I., 2015. Good modelling practice in applying Computational Fluid Dynamics for WWTP modelling. *Water Science and Technology*, 73, 969-982.

## V. Conclusions and perspectives

This last chapter presents the conclusions of this thesis work. In addition, the particular perspectives relating to the study of mixing effect on wastewater treatment reactors and the biological reactor design are also discussed.

### V.1. General conclusion

In this thesis we confirmed that the operational parameters of WWTPs such as SRT, HRT, and  $C_{TSS}$  have a great impact on micropollutants removal efficiency. However, the performance of activated sludge MPs removal is not only dependent on the operational parameters and the nature of the micropollutant, but we highlight that the hydrodynamic conditions such as the reactor configuration and careful mixing promote MPs removal. To reach these conclusions, three main aspects were investigated.

#### *- Experimental study*

Emerging micropollutants detected in wastewater representing various degrees of biodegradability were selected. According to the literature and our own experience, caffeine (CAF), sulfamethoxazole (SMX), benzotriazole (BZT), roxithromycin (ROX), erythromycin (ERY), diclofenac (DCF) and carbamazepine (CBZ) were selected. They range from highly biodegradable to quite persistent MPs. Subsequently, a systematic study of the operational conditions of WWTPs was managed to study the potential effect of each parameter on the MPs removal with activated sludge. To achieve this goal seven experimental setups were applied to sequencing batch reactors (SBRs), which varied in SRT (3 d, 10 d and 20 d) and HRT (4 h, 8 h and 12 h). The effect of biomass concentration was measured for 3, 5 and 8  $g_{TSS} L^{-1}$ . At the beginning of each kinetics experiment, reactors were spiked directly with fresh mix solution of MPs of concentration 1  $\mu g L^{-1}$  and samples were collected in the fixed time points during aeration phase of all tested setups. The micropollutants were successively quantified using the LC-MS/MS analysis. The kinetics of MPs removal was investigated and removal rates were determined. The results indicated that the operational conditions such as SRT and HRT can

influence the MPs removal efficiency to some extent, which depends on the nature of the MPs. Highly biodegradable compounds have in general high removal efficiency. In terms of HRT, better removal with higher HRT of 12 h compared to 8 h and 4 h was reported. In the case of moderately biodegradable compounds, SRT and HRT had larger influence. In general, an increase of SRT caused an improvement of removal efficiency. This aspect was evident for very high SRT except for roxithromycin and erythromycin. Higher HRT also produced larger removal efficiency. However, complete MPs removal was not achieved in any of the studied setups. In terms of application, the improvement of removal obtained with a higher HRT should be compared to the cost of a larger reactor. For persistent compounds, very low removal efficiency in all tested scenarios ( $> 10\%$ ) was reported. HRT produced minor impacts and SRT exhibited a slight effect only if it was very long (e.g. DCF SRT 20 d,  $\sim 25\%$ ). Due to higher energy consumption, such conditions are not often applied in existing WWTP with activated sludge. Furthermore, although the conditions tested in SBRs covered both nitrifying and non-nitrifying conditions, a relation between nitrification capacity and MPs removal was observed.

The influence of the biomass concentration on the pseudo-first order rate constant was discussed. This allowed us to widen our research study. The increase of biomass concentration from 3 to 5  $\text{g}_{\text{TSS}} \text{L}^{-1}$  significantly increased the removal of the highly and moderately degradable compounds (CAF, SMX, BZT, ROX and ERY), whereas a further increase to 8  $\text{g}_{\text{TSS}} \text{L}^{-1}$  had lower effect. These results highlighted that usual kinetics, which consider that the removal rate is directly proportional to the biomass concentration is only valid for low and moderate biomass concentration. This unexpected effect of biomass concentration opens up a new field of research and questioning. We, consequently, worked to develop new kinetics model able to represent it.

#### ***- Development of a new kinetic model***

Our investigations highlighted that the MPs removal is proportional to  $C_{\text{TSS}}$  to the power of  $n$ . Then, the new investigated kinetics was called the power law ( $r_{\text{MPs}} = -k_{\text{MPs}} C_{\text{MPs}} (C_{\text{TSS}})^n$ ). For all the MPs, the power  $n$  appeared less than 1. It is around 0.5 in our study. The power law kinetics allows simple determination of the intrinsic rate removal values ( $k_{\text{MPs}}$ ), which fits to a wide range of  $C_{\text{TSS}}$ . So, we can propose an explanation of that phenomenon. As a result, the removal rate value of MPs was found to be strongly dependent on the transport of MPs based on mixing conditions. High concentration of solids leads to the

creation of both large aggregates made of flocs and stagnant internal liquid zone. Consequently, in this condition, the MPs transport is also due to their diffusion in the aggregates. Subsequently, we used the Wilke-Chang equation, (which is an improvement of Einstein equation of diffusion), which relates the molecular weight of MPs ( $M_{MPs}$ ) to the diffusion coefficient. It reveals a functional dependence of the form  $D_m = f(1/M_{MPs}^{0.6})$ :  $n = \frac{k_1}{M_{MPs}^{0.6}} + k_2$ . Thus, the new kinetics model is:  $r_{MPs} = -k_{MPs} C_{MPs} C_{TSS}^{\left(\frac{k_1}{M_{MPs}^{0.6}} + k_2\right)}$ . It seems applicable to all situations. In addition, it helped to explain the unusual contributions in terms of  $n$ , in the overall process of micropollutants removal previously reported in the literature. Moreover, in accordance with our observation and the model structure,  $n$  is characteristic of both MP diffusion and local mixing. Then,  $n$  values can be very different from a reactor to another. This leads to important consequences in simulation and design: the necessity to know actual value of  $n$  of studied reactor; values coming from literature or pilot plants could lead to error if they do not take into account the actual local mixing.

#### ***- Simulation and hydrodynamic study***

A simulator was created to reproduce the experimental data performed in the batch mode. This simulation highlights the application of the new model on the operation at the full-scale wastewater treatment reactor. The power law kinetics was applied in order to predict the effect of different hydrodynamic configurations as well as different inlet MPs concentration coupled with local mixing conditions on the MPs' removal in continuous systems. The numerical results confirmed that the experimental setups in batch mode were simulated successfully. The experiments performed at low biomass concentration and different SRT and HRT follow approximately an apparent-first-order kinetics. However, a power law kinetics is only able to describe the MPs removal at high biomass concentration. Several simulations in batch mode by applying the new kinetics were subsequently performed at different biomass concentrations. The simulated removal efficiencies at 3, 5 and 8  $g_{TSS} L^{-1}$  of each MP for the experimental values of  $n$  are very close to the experimental removals. Moreover, the simulations predicted that high biomass concentration coupled with efficient local mixing conditions (high values of  $n$ ) enhanced the removal of all investigated MPs (SMX, BZT, ROX, ERY and DCF). Later on, the new kinetics was applied to continuous system modeled as tanks in series. Different

configurations were tested. Increasing the number of reactors increases MPs removal. Moreover, enforcing local mixing (high value of  $n$ ) significantly improves the removal of all studied MPs, too. Similarly, the effect of the input concentrations of MPs at time  $T_0$  was tested. High  $C_{MPs}$  coupled with high local mixing produce the highest removal of all MPs. However, high local mixing level and low  $C_{MPs}$  also improve significantly the removal of SMX, BZT, ROX and ERY. Finally, it was showed that decreasing the width of a reactor, but keeping the same reactor volume and the same horizontal surface is useful to design a reactor whose hydrodynamics is equivalent to a cascade of CSTRs with high number of tanks in series. Then, the sizing approach of a reactor could help to enhance the removal of moderately and slowly biodegradable MPs. It seems also possible to change the already existing built reactors by adding Baffles to increase Peclet number.

## **V.2. Perspectives**

The perspectives relate to three topics:

- better understanding and modelling of micromixing and diffusion
- study of design of new mixing devices
- design of new shapes of reactor

The effect of local mixing and MPs removal could be further investigated. Since  $n$  is dependent on both local mixing and diffusion, and is function of the molecular weight ( $M_{MPs}$ ),  $k_1$  and  $k_2$ . It would be interesting to investigate how local mixing influences  $k_1$  and  $k_2$ . Such study could help to bind together different approaches such as mixing energy, sensors, mixing device design, sludge rheology and properties, simulation, etc. However, we can suppose that  $k_1$  is a constant only related to diffusion, and  $k_2$  is related to the local mixing. Therefore,  $k_2$  could be a function (not necessary a constant) of local mixing. Then,  $k_2$  is probably related to pseudo-plastic rheology properties (apparent viscosity increasing with  $C_{TSS}$  would decrease  $k_2$ ), dissipated mixing energy (higher energy, higher  $k_2$ ), mixing process and characteristics of mixing devices, etc.

This also leads to new studies focusing on best aeration devices. Impellers could be also added in aerated reactors. In chemical reactors, turbulence promoters are sometimes added. Are the turbulence promoters interesting in wastewater reactors? Which size? Which shape?

Systemic modelling is very useful to obtain global trend of reactor design; giving ideas of reactor shape and size. However, to best design reactors, it would be interesting to be able to implement such approach in computational fluid dynamics and multi-scale compartmental modelling.

Another important point, what we can call the paradox of mixing, should be solved: we need a high Peclet number so, a low local mixing; but we also need a high  $n$  so, a large local mixing. Therefore, we should find a technical solution allowing a high local mixing and low global mixing along the length of the reactor.

Remark about adding Baffles in aerated reactor: we can suppose that these Baffles can help to avoid channelling of oxygen bubbles and then would help to also increase local mixing. In this case, Baffles could help to not only increase the global Peclet number but also the value of  $n$ . This hypothesis would be verified, but it requires very large pilot reactor or real full-scale plant.

Finally, the cost of all possible improvements should be estimated and compared to performance refinements and post-treatment costs.



## List of Figures

<b>Figure I. 1.</b> Map showing the percentage of water bodies in Europe's River Basin District (RBD) that are not in good ecological status: second River Basin Management Plans (RBMPs) (EEA, 2018). .....	11
<b>Figure I. 2.</b> Chemical status of (a) surface water bodies (SWBs), with and without ubiquitous, persistent, bioaccumulative and toxic (uPBTs) pollutants and (b) groundwater bodies, by area, reported in first and second River Basin Management Plans (RBMPs) (EEA Report No 7/2018 2018).....	12
<b>Figure I. 3.</b> Sources and possible pathways of water pollution into the environment (adapted from Daughton (2006)). .....	14
<b>Figure I. 4.</b> Basic steps of wastewater treatment process (adapted from Gandiglio et al. (2017)). .....	24
<b>Figure I. 5.</b> Schematic of basic diagram of biological treatment with activated sludge (Duchene, 2005).....	26
<b>Figure I. 6.</b> Reactor configuration according to the composition of the influent (adapted from Lee et al. (2017)). .....	27
<b>Figure I. 7.</b> Schematic of the relation between pH and charge forms partition in aqueous phase. ....	38
<b>Figure I. 8.</b> Scheme of the fate of a micropollutant in a biological reactor: mechanisms occurring between the different compartments (gas, dissolved, solid). Compiled based on studies by (Clouzot et al. 2013; Plosz et al. 2013; Pomiès et al. 2013). .....	41
<b>Figure I. 9.</b> Scheme of a continuous stirred tank reactor (CSTR) (a) and a plug-flow reactor (PFR) (b) (Levenspiel 1999). .....	56
<b>Figure II. 1.</b> Sampling sites located in the Bruchsal and Neureut WWTPs. The notation B refers to sludge collecting point in Bruchsal WWTP and N trickling filter reactor in Neureut WWTP. ....	86
<b>Figure II. 2.</b> Photographs of the lab-scale of the Sequencing Batch Reactors (SBR-3 d, SBR-10 d and SBR-20 d). .....	90
<b>Figure II. 3.</b> Method of determination of $d_{k_{LA}}$ by de-oxygenation re-oxygenation, in absence of biomass. ....	97
<b>Figure II. 4.</b> $\ln(S_{O_{sat}} - S_O)$ curve versus time for $k_{LA}$ estimation in SBRs-3 d, 10 d and 20d. .	99
<b>Figure II. 5.</b> Sorption results of caffeine, sulfamethoxazole, benzotriazole, roxithromycin, erythromycin, tetracycline, ciprofloxacin, diclofenac and carbamazepine on the wall of the reactor at both freeze and fridge conditions. ....	104
<b>Figure II. 6.</b> Removal of (a) CAF, (b) SMX and (c) BZT, (d) ROX, (e) ERY, (f) DCF and (g) CBZ at three different types of sludge age of 3 d, 10 d and 20 d at the HRT of 4 h; $k'$ is the apparent-first order removal rate constant ( $h^{-1}$ ); number of replicates = 3; error bars indicate one standard error.....	106
<b>Figure II. 7.</b> Linear (on the left side) and logarithmic (on the right side) scales of the correlation between the nitrification capacities (%) and the apparent constants $k'$ ( $h^{-1}$ ) of SMX, BZT, ROX,	

ERY, DCF and CBZ estimated at different three different sludge ages (3 d, 10 d and 20 d) at HRT of 4 h. Nitrogen load - $0.08 \text{ g}_N \text{ g}_{TSS}^{-1} \text{ d}^{-1}$ .....	110
<b>Figure II. 8.</b> Removal efficiencies of wastewater parameters (COD, $\text{N-NH}_4^+$ and $\text{P-PO}_4^{3-}$ ) and nitrate-nitrogen production over 4 h, 8 h and 12 h HRT for SRT – 3 d and SRT - 10 d (error bars present standard error). .....	111
<b>Figure II. 9.</b> Removal of (a) CAF, (b) SMX and (c) BZT, (d) ROX and (e) ERY, (f) DCF, (g) CBZ, at both sludge age of 3 d and 10 d at the HRT of 8 h; $k'$ is the apparent-first order removal rate constant ( $\text{h}^{-1}$ ); number of replicates = 3; error bars indicate one standard error. ....	114
<b>Figure II. 10.</b> Removal of (a) CAF, (b) SMX and (c) BZT, (d) ROX, (e) ERY, (f) DCF and (g) CBZ at both sludge age of 3 d and 10 d at the HRT of 12 h; $k'$ is the apparent-first order removal rate constant ( $\text{h}^{-1}$ ); number of replicates = 3; error bars indicate one standard error. ....	116
<b>Figure II. 11.</b> Removal (%) of selected MPs in SBRs - 3, 10 and 20 d over three different HRT 4, 8 and 12 h. $C_{TSS} \sim 3 \text{ g}_{TSS} \text{ L}^{-1}$ and $C_{MPs} \sim 1 \mu\text{g L}^{-1}$ .....	119
<b>Figure II. 12.</b> Change of concentration of (a) CAF, (b) SMX, (c) BZT, (d) ROX, (e) ERY and (f) DCF during biological treatment in reactors inoculated with biomass at concentrations of 3, 5 and $8 \text{ g}_{TSS} \text{ L}^{-1}$ ; $k'$ is the apparent-first-order removal rate constant ( $\text{h}^{-1}$ ) operated at SRT-10 d and HRT- 4 h. ....	122
<b>Figure II. 13.</b> Effect of the $C_{TSS}$ ( $\text{g L}^{-1}$ ) on the apparent-first-order removal rate constant $k'$ ( $\text{h}^{-1}$ ) for CAF, SMX, BZT, ROX, ERY and DCF. The apparent constants $k'$ of SMX, BZT, ROX, ERY and DCF and $k'$ of CAF are shown on the left side and the right side of the graph, respectively. Continuous lines represented the linear expected pseudo-first-order approach (calculated from the first three $C_{TSS}$ of 0, 3 and $5 \text{ g L}^{-1}$ ). ....	123
<b>Figure III. 1.</b> Plot of the removal rate $r_{MPs}$ versus time for the first hour of the reaction for SMX, BZT, ROX, ERY and DCF. ....	139
<b>Figure III. 2.</b> Removal rate logarithm ( $\log(-r_{MPs})$ ) vs. $C_{TSS}$ logarithm ( $\log(C_{TSS})$ ) profiles for SMX, BZT, ROX, ERY and DCF. ....	141
<b>Figure III. 3.</b> Plot of the slope $n$ for the five investigated micropollutants vs. time. The black horizontal line represents the average $n$ values rounded to 0.5. ....	142
<b>Figure III. 4.</b> Plot of the order of the reaction $n$ for the five investigated micropollutants SMX, BZT, ROX, ERY and DCF vs. $1/M_{MPs}^{0.6}$ . ....	148
<b>Figure IV. 1.</b> General characteristics of the batch reactor with activated sludge for modelling. ....	168
<b>Figure IV. 2.</b> Description of the different steps of the simulation of the batch system. ....	170
<b>Figure IV. 3.</b> Methodology of parameter optimization procedure in ASM1 model. ....	172
<b>Figure IV. 4.</b> Simulated and experimental profiles of some parameters of ASM1 in the SBR operated at SRT of 3 d and HRT of 4 h. Crosses refer to the experimental data and the blue line refer to the simulated results. ....	175
<b>Figure IV. 5.</b> Simulated and experimental profiles of MPs' concentrations by applying the apparent-first approach to the SBR operated at SRT of 3 d and HRT of 4 h. Crosses refer to the experimental data and the blue line refer to the simulated results. ....	179

<b>Figure IV. 6.</b> Simulated and experimental profiles of MPs' concentrations by applying the apparent-first order approach to the SBR operated at $C_{TSS}$ of $5 \text{ g L}^{-1}$ . Carbamazepine has not been detected during biological experiments of series 2.....	181
<b>Figure IV. 7.</b> Simulated and experimental profiles of MPs' concentrations by applying the apparent-first order approach to the SBR operated at $C_{TSS}$ of $8 \text{ g L}^{-1}$ .....	182
<b>Figure IV. 8.</b> Simulated and experimental profiles of MPs' concentrations by applying the power law approach to the SBR operated at SRT of 10 d and HRT of 4 h operated at $C_{TSS}$ of $3 \text{ g L}^{-1}$ (a), $5 \text{ g L}^{-1}$ (b) and $8 \text{ g L}^{-1}$ (c).....	187
<b>Figure IV. 9.</b> Contours of the removal efficiency (%) of SMX, BZT, ROX, ERY and DCF micropollutants as a function of the sludge biomass concentration and the $n$ -coefficient. Red color means the highest removal efficiency of each MP. The black line and the percentages on each figure correspond to the experimental $n$ value and the removal efficiency of each MP at 3, 5 and $8 \text{ g}_{TSS} \text{ L}^{-1}$ , respectively.....	190
<b>Figure IV. 10.</b> Schematic of the Benchmark plant layout.....	192
<b>Figure IV. 11.</b> Profiles of solubles and non-solubles concentrations obtained from simulation on Matlab (blue line) for $C_{eff}$ denoted for clear water concentration (a) at the overflow outlet of the clarifier and $C_s$ denoted to sludge concentration (b) at the bottom outlet of the clarifier, respectively. Concentration obtained at the end of simulation of Benchmark are represented by the red line.....	199
<b>Figure IV. 12.</b> 3D plots representing the removal efficiency (%) of SMX, BZT, ROX, ERY and DCF as a function of the order of the reaction $n$ (varying from 0.1 to 1) and as a function of the number of aerobic reactors (from 3 to 60) for the same inlet concentration $C_{MPs} = 1 \text{ } \mu\text{g L}^{-1}$ . Red color means the highest removal efficiency of each MP.....	206
<b>Figure IV. 13.</b> 3D plots representing the removal efficiency (%) of SMX, BZT, ROX, ERY and DCF as a function of both the order of the reaction $n$ (0.1 to 1) and the inlet concentration $C_{MPs}$ ( $10^{-2}$ to $10^2 \text{ } \mu\text{g L}^{-1}$ ) in the configuration of 5 tanks in series. Red color indicates the highest removal efficiency of each MP. ....	209
<b>Figure IV. 14.</b> Number of CSTR ( $J_{cal}$ ) corresponding to the reactor width ( $W_{cal}$ ). Red crosses refer to the calculated width ( $W_{cal}$ ) by projection for every tested configuration of aerobic reactors: 3, 6, 9, 12, 18, 27, 36, 45, 54 and 60 (by progressive transformation of the reactor of the benchmark: $J_i = 3$ , $W_i = 9.65 \text{ m}$ and $S_h$ of $514.3 \text{ m}^2$ ).....	213
<b>Figure IV. 15.</b> Number of CSTR ( $J_{cal}$ ) corresponding to the reactor length ( $L_{cal}$ ). Blue circles refer to the calculated length ( $L_{cal}$ ) by projection for every tested configuration of aerobic reactors: 3, 6, 9, 12, 18, 27, 36, 45, 54 and 60 (by progressive transformation of the reactor of the benchmark: $J_i = 3$ , $W_i = 9.65 \text{ m}$ and $S_h$ of $514.3 \text{ m}^2$ ).....	213
<b>Figure IV. 16.</b> Relationship between $J_{cal}$ and $L_{cal}/W_{cal}$ . The dashed line represents the linear trend line.....	214
<b>Figure IV. 17.</b> Schematic representations of the (a) reactor with $J = 3$ (initial geometry) and (b) the new geometry with 5 Baffles for the highest $J = 60$ with inlet and outlet on opposite sides.....	215

## List of Tables

<b>Table I. 1.</b> The concentrations and removals of several micropollutants present in the WWTPs of different countries. ....	18
<b>Table I. 2.</b> Physical-chemical properties and chemical structure of the target compounds which are studied in this thesis. ....	30
<b>Table I. 3.</b> Comparison of the average removal efficiency of a pharmaceuticals in conventional activated sludge process and in MBR and their removal mechanisms (Tiwari et al. 2017). ...	34
<b>Table I. 4.</b> $K_d$ values of some pharmaceuticals in activated sludge found in the literature.....	45
<b>Table I. 5.</b> Different models for biological degradation/and sorption of micropollutants found in the literature. ....	48
<b>Table I. 6.</b> Values of biodegradation rates $k_{\text{biol}}$ and $k'$ of some pharmaceuticals in activated sludge found in the literature.....	51
<b>Table I. 7.</b> Summary of the characteristics of different modelling approaches by Le Moullec (2008). ....	54
<b>Table II. 1.</b> Overview of the removal efficiency of some MPs in published studies according to some operational conditions in activated sludge.....	84
<b>Table II. 2.</b> The concentrations and removals of investigated micropollutants present in the WWTPs of different countries. ....	88
<b>Table II. 3.</b> Application and physico-chemical properties of the target micropollutants (industrial chemical and PPCPs). ....	89
<b>Table II. 4.</b> Sequencing Batch Reactor setups operated at different SRTs during kinetics experiments. ....	92
<b>Table II. 5.</b> Operating schedule of SBRs.....	94
<b>Table II. 6.</b> Mean values of biomass concentration ( $\pm$ standard error), ratio of $C_{\text{VSS}}$ to $C_{\text{TSS}}$ ( $\beta$ ), dissolved oxygen (DO), pH and T ( $^{\circ}\text{C}$ ) in the three SBRs during seven experimental setups.	95
<b>Table II. 7.</b> Composition of the synthetic wastewater and supplementary solutions I and II.	96
<b>Table II. 8.</b> Apparent removal rate constant $k'$ ( $\pm$ standard error) of investigated compounds at different types of sludge age*, and changes of $k'$ from: SRT- 3 d to SRT-20 d, 10 d to 20 d and 3 d to 20 d. $C_{\text{TSS}} \sim 3 \text{ g}_{\text{TSS}} \text{ L}^{-1}$ . ....	107
<b>Table II. 9.</b> An overview of calculated apparent-first order rate constants of all investigated MPs at all tested HRT- 4 h, 8 h, and 12 h for both sludge ages of 3 d and 10 d as well as change of $k'$ from 4 h to 8 h, 8 h to 12 h and 4 h to 12 h. ....	117
<b>Table II. 10.</b> Experimental and expected apparent-first-order rate constants estimated at $C_{\text{TSS}} = 8 \text{ g}_{\text{TSS}} \text{ L}^{-1}$ as well as the experimental and expected $C_{\text{MPs}}$ of SMX, BZT, ROX, ERY and DCF at HRT of 4 h (Time of reaction = 170 min) and their removal efficiency (%). ....	125
<b>Table III. 1.</b> Calculated $k\text{MPs}$ ( $\text{L}^n \text{ g}^{-n} \text{ h}^{-1}$ ) of each MP for each $C_{\text{TSS}}$ and the average $k\text{MPs}$ ( $\pm$ RSD (%)) of +20 % sensitivity test) determined for the three tested biomass concentrations. ....	143

<b>Table III. 2.</b> Physical transport and diffusion limitations of MPs at high biomass concentration. .....	146
<b>Table IV. 1.</b> Variables of the ASM1 model. ....	159
<b>Table IV. 2.</b> Biological processes of the ASM1 model and their reaction rates. ....	162
<b>Table IV. 3.</b> Values of the stoichiometric parameters of the ASM1 model. ....	164
<b>Table IV. 4.</b> Kinetic parameter values of the ASM1 model. ....	164
<b>Table IV. 5.</b> Experimental $k_{LA}$ ( $h^{-1}$ ) in water, optimized $k_{LA}$ in the presence of sludge and optimized ASM1 parameters in three SBRs operated at different SRT and HRT. ....	173
<b>Table IV. 6.</b> Optimized $k_{LA}$ and ASM1 parameters in the SBRs operated at three different biomass concentrations of 3, 5 and 8 $g_{TSS} L^{-1}$ . ....	174
<b>Table IV. 7.</b> Percentage error (%) for some parameters of ASM1 between measured and simulated values for series 1 of batch experiments. ....	177
<b>Table IV. 8.</b> Percentage error (%) for some parameters of ASM1 between measured and simulated values for series 2 of batch experiments. ....	178
<b>Table IV. 9.</b> Percentage error (%) between experimentally measured and simulated values of micropollutants by apparent-first-order approach for series 1 of batch experiments. ....	180
<b>Table IV. 10.</b> Percentage error (%) between experimentally measured and simulated values of micropollutants by apparent-first-order approach for series 2 of batch experiments. ....	182
<b>Table IV. 11.</b> Average initial $C_{MPs}$ calculated at various biomass concentration setup (number of replicates=3) and averages of n-coefficient of each MP and new constants $k_{MPs}$ used in computer simulation. ....	184
<b>Table IV. 12.</b> Volumes and values of the transfer in the BSM1. ....	197
<b>Table IV. 13.</b> Flow rates of the coefficients of the BSM1 reactors. ....	197
<b>Table IV. 14.</b> The chosen initial concentration of ASM1 compounds. Initial MPs concentration equals zero. ....	198
<b>Table IV. 15.</b> Inlet concentrations of ASM1 compounds borrowed from the BSM1 except for the MPs concentrations which were equal to the average of the initial $C_{MPs}$ measured in the batch reactors. ....	198
<b>Table IV. 16.</b> Percentage error (%) of the simulated results compared to the Benchmark results. N/A refers to a large %error for the non-soluble compounds in the upper part of the clarifier. ....	200
<b>Table IV. 17.</b> Adjustment of physical parameters according to different hydrodynamic configurations. ....	202

## Supplementary Information

### Supplementary Information of chapter II

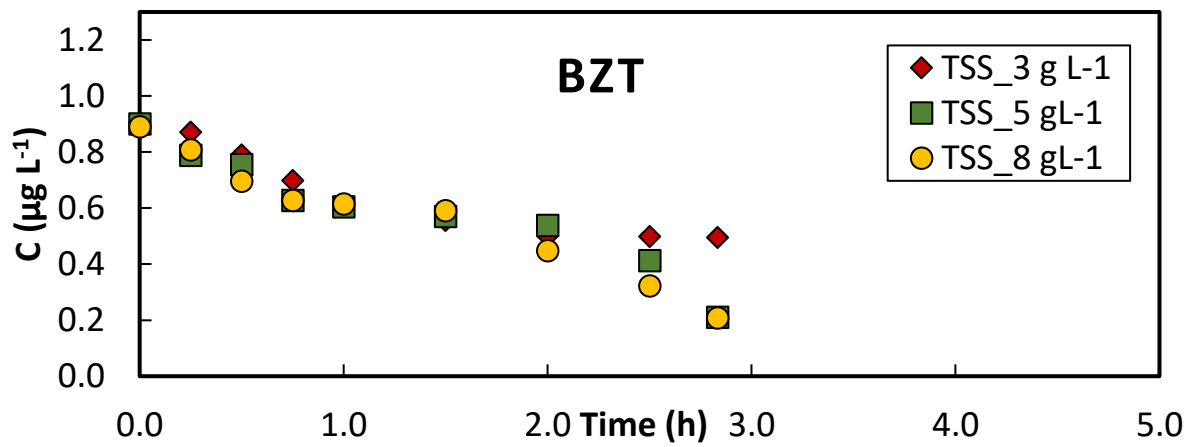
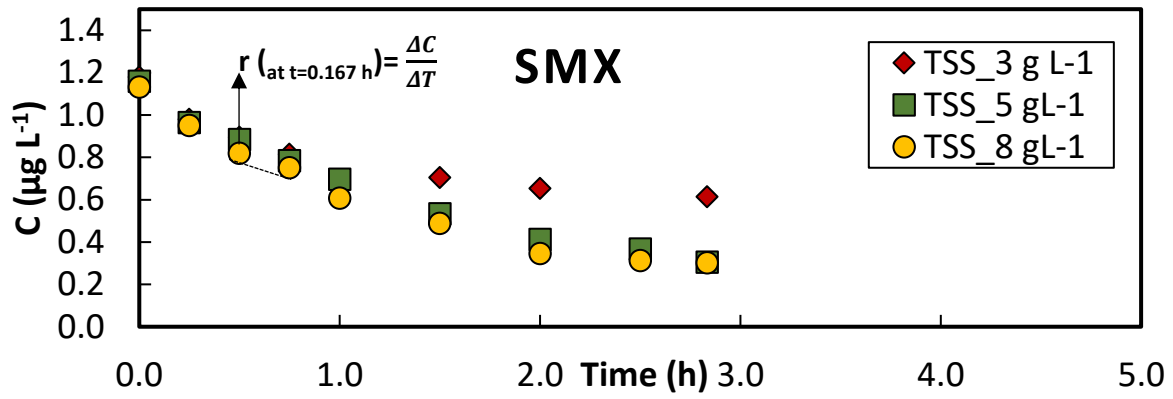
*Table II.S1. Source parameters applied during sample measurements.*

Source parameters	
Gas Temperature	200 °C
Gas Flow	8 L min <sup>-1</sup>
Nebulizer	40 psi
Sheath Gas Temperature	300 °C
Sheath Gas Flow	12 L min <sup>-1</sup>
Capillary	Positive: 4500 V Negative 3500 V
Nozzle Voltage	Positive 500 V Negative 300 V

*Table II.S2. Mass spectrometric parameters for detection.*

Compound	RT min	Polarity	Precursor Ion	Quantifier	CE	Qualifier	CE
Benzotriazole	3.3	Positive	120.1	65.0	24	92.1	20
Benzotriazole-d <sub>4</sub>	3.3	Positive	124.1	41.4	48	96.0	20
Caffeine	3.0	Positive	195.1	137.9	20	110.0	24
Caffeine- <sup>13</sup> C <sub>3</sub>	3.0	Positive	198.2	140.0	20	43.5	44
Carbamazepine	5.8	Positive	237.1	193.4	28	178.9	40
Carbamazepine-d <sub>8</sub>	5.8	Positive	245.2	202.1	24	200.6	40
Diclofenac	8.0	Positive	296.0	213.9	40	250.0	12
Diclofenac-d <sub>4</sub>	8.0	Positive	300.1	218.0	36	-	-
		Negative	298.0	-	-	254.0	8
Erythromycin	3.6	Positive	734.5	158.0	32	576.0	20
Erythromycin-d <sub>3</sub>	3.6	Positive	737.5	161.0	32	579.4	20
Roxithromycin	3.9	Positive	837.5	158.0	36	679.4	20
Roxithromycin-d <sub>7</sub>	3.9	Positive	844.6	158.0	36	686.5	20
Sulfamethoxazole	4.4	Positive	254.1	155.9	12	92.0	28
Sulfamethoxazole-d <sub>4</sub>	4.4	Positive	258.1	159.9	36	151.1	12

Supplementary Information (chapter III)



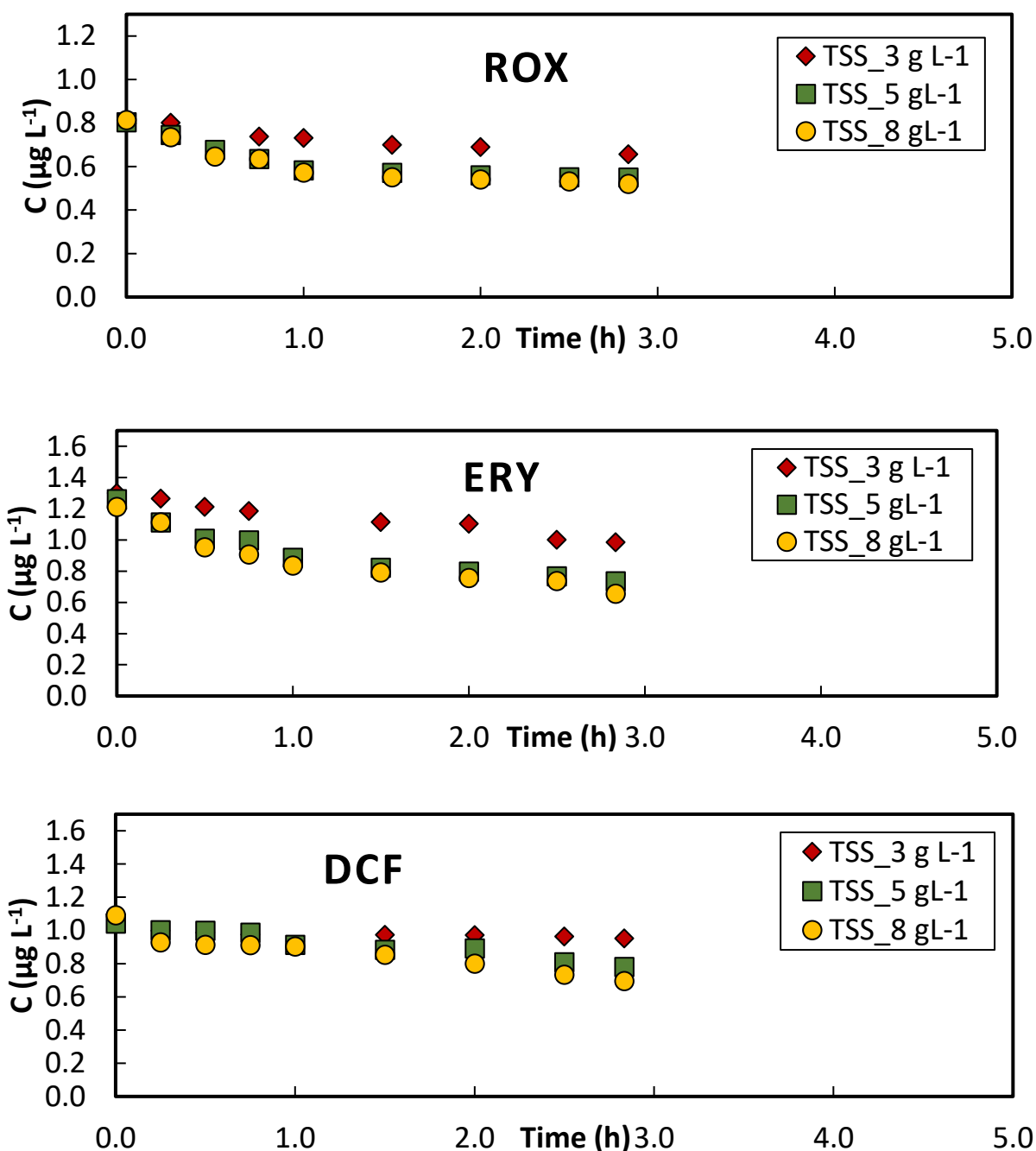


Figure III. S1. Plot of the removal rate  $C_{MPs}$  ( $\mu\text{mol L}^{-1}$ ) versus time (h) over HRT of 4 h for SMX, BZT, ROX, ERY and DCF and an example of drawing the tangents at different time  $t$  for various biomass concentration in order to calculate the  $r_{MPs}$  ( $\mu\text{mol L}^{-1} \text{h}^{-1}$ ) of SMX.

- The tests of the  $k_{MPs}$  values on the molar residual concentration of all MPs was performed changing all over a  $\pm 20\%$  range. Reproducibility was presented as relative standard deviation (RSD, %) in Table III.S1.



**Table III.S1.** Relative standard deviation (RSD, %) of different sensitive analysis of  $k_{MPs}$  values in  $L^n g^{-n} h^{-1}$ .

Relatif standard deviation					
Micropollutants	-20 %	-10 %	+10 %	-15 %	20 %
SMX	1.8	1.2	0.8	0.7	0.4
BZT	0.8	0.5	0.3	0.4	0.2
ROX	2.4	2.3	1.5	1.2	0.3
ERY	2.1	1.9	1.2	0.8	0.3
DCF	0.2	0.2	0.1	0.1	0.08

Reproducibility was assessed from calculating average  $k_{MPs}$  for each  $C_{TSS}$  over 1 hour. The lowest RSD was obtained with +20 % on  $C_{MPs}$  for the five investigated MPs. The results of all sensitive analysis over the range -20% to + 20 % were plotted in Figures III.S2-S5.

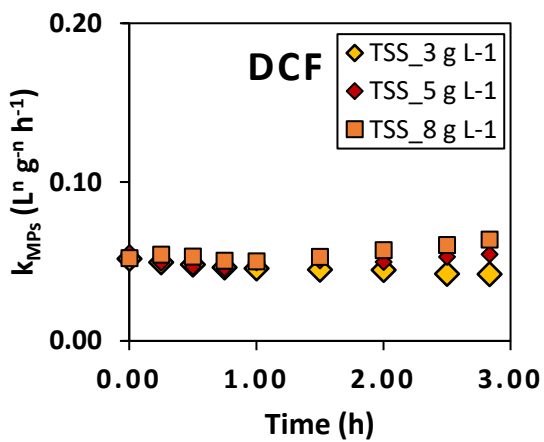
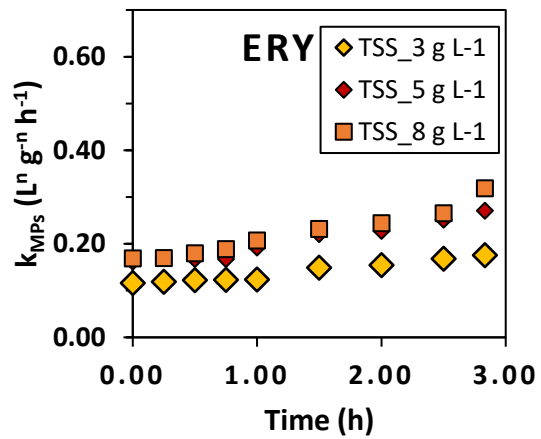
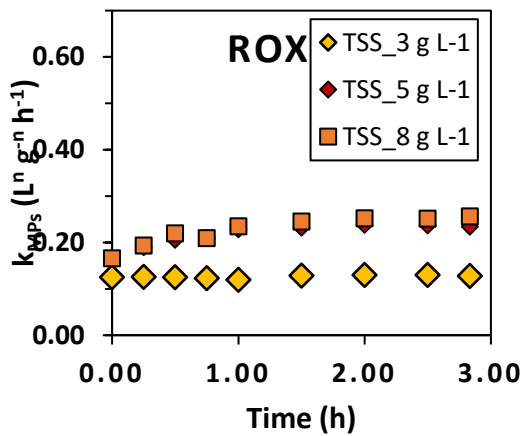
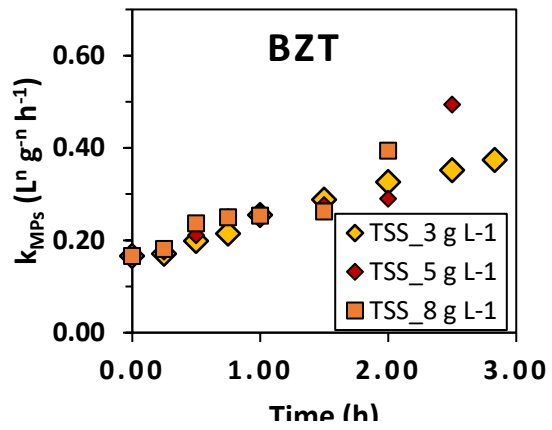
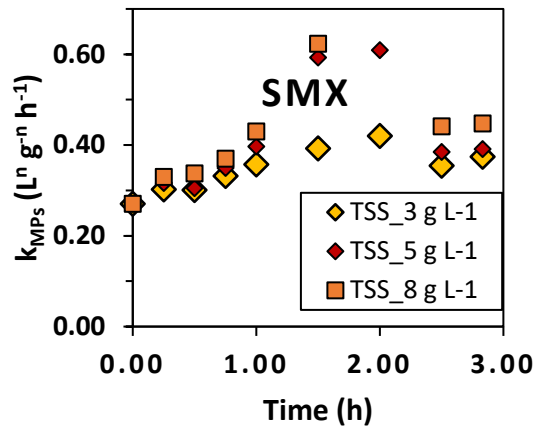


*Figure III. S2. Plot of the new removal rate constants  $k_{MPs}$  ( $L^n g^{-n} h^{-1}$ ) versus time (h) with sensitivity analysis on  $C_{MPs}$  of -20 % for SMX, BZT, ROX, ERY and DCF.*

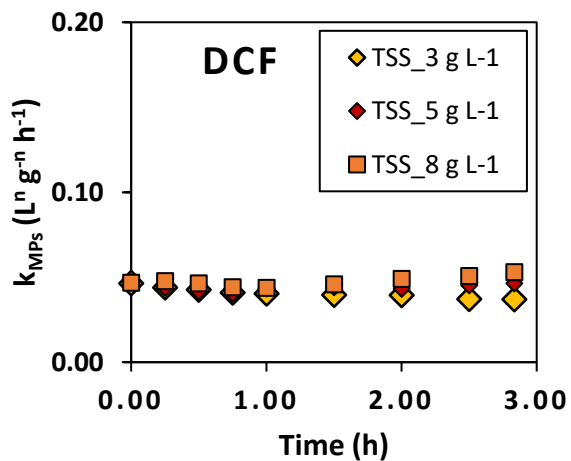
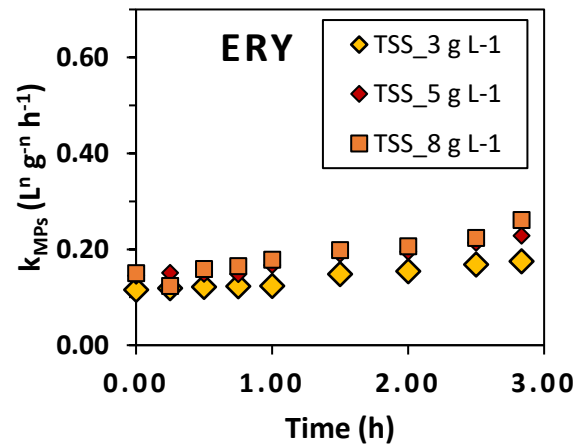
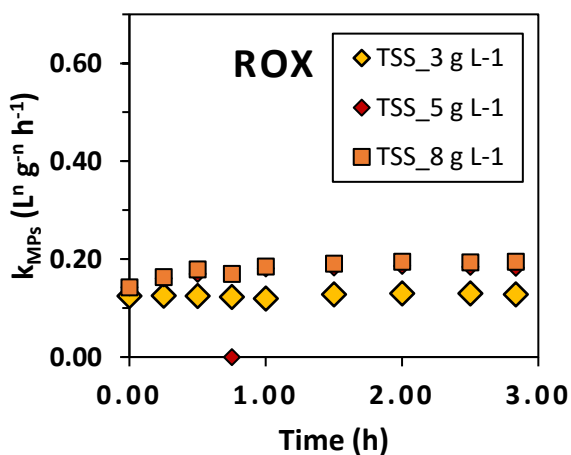
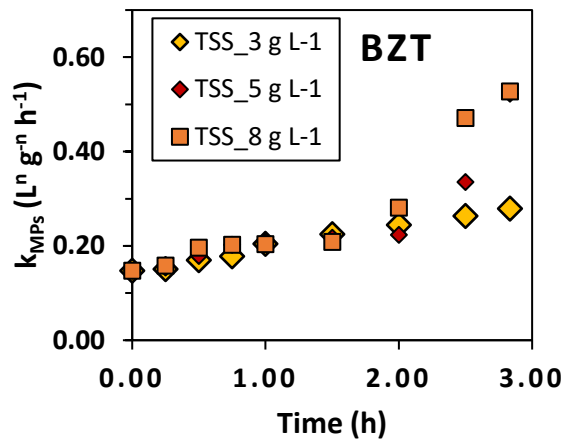
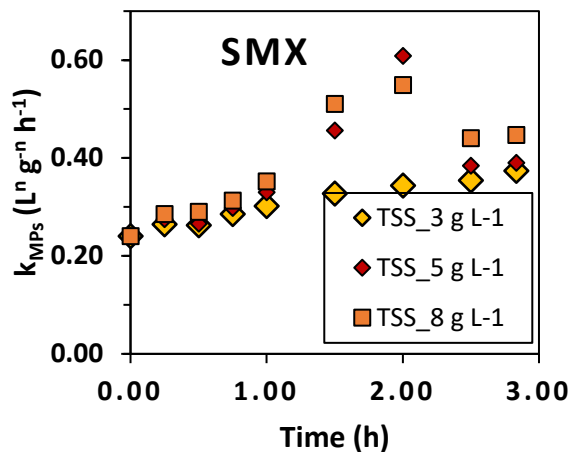


*Figure III. S3. Plot of the new removal rate constants  $k_{MPs}$  ( $L^n g^{-n} h^{-1}$ ) versus time (h) with sensitivity analysis on  $C_{MPs}$  of -10 % for SMX, BZT, ROX, ERY and DCF.*

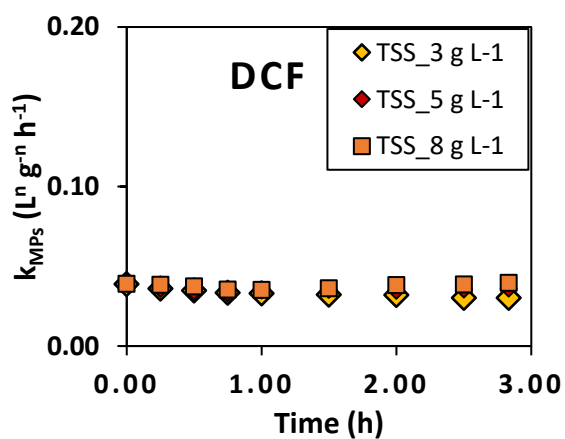
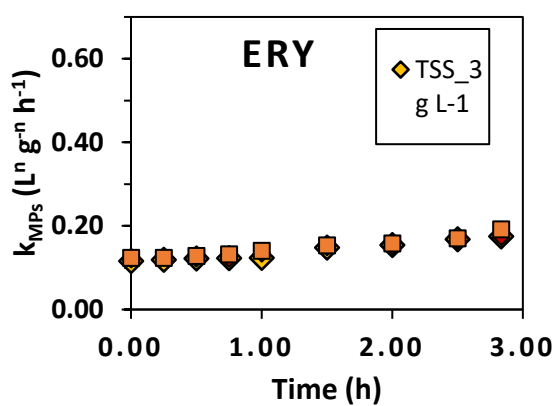
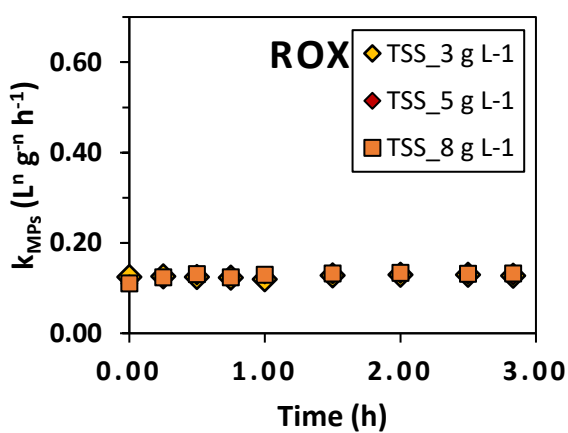
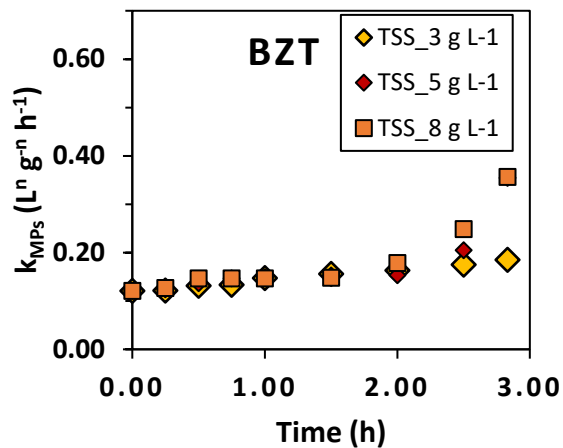
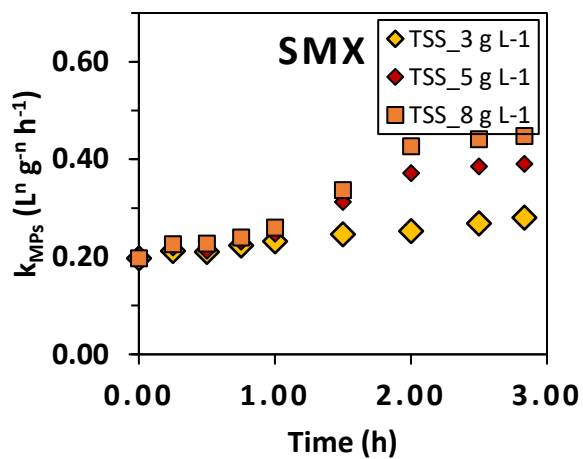


*Figure III. S4. Plot of the new removal rate constants  $k_{MPs}$  ( $L^n g^{-n} h^{-1}$ ) versus time (h) with sensitivity analysis on  $C_{MPs}$  of +10 % for SMX, BZT, ROX, ERY and DCF.*

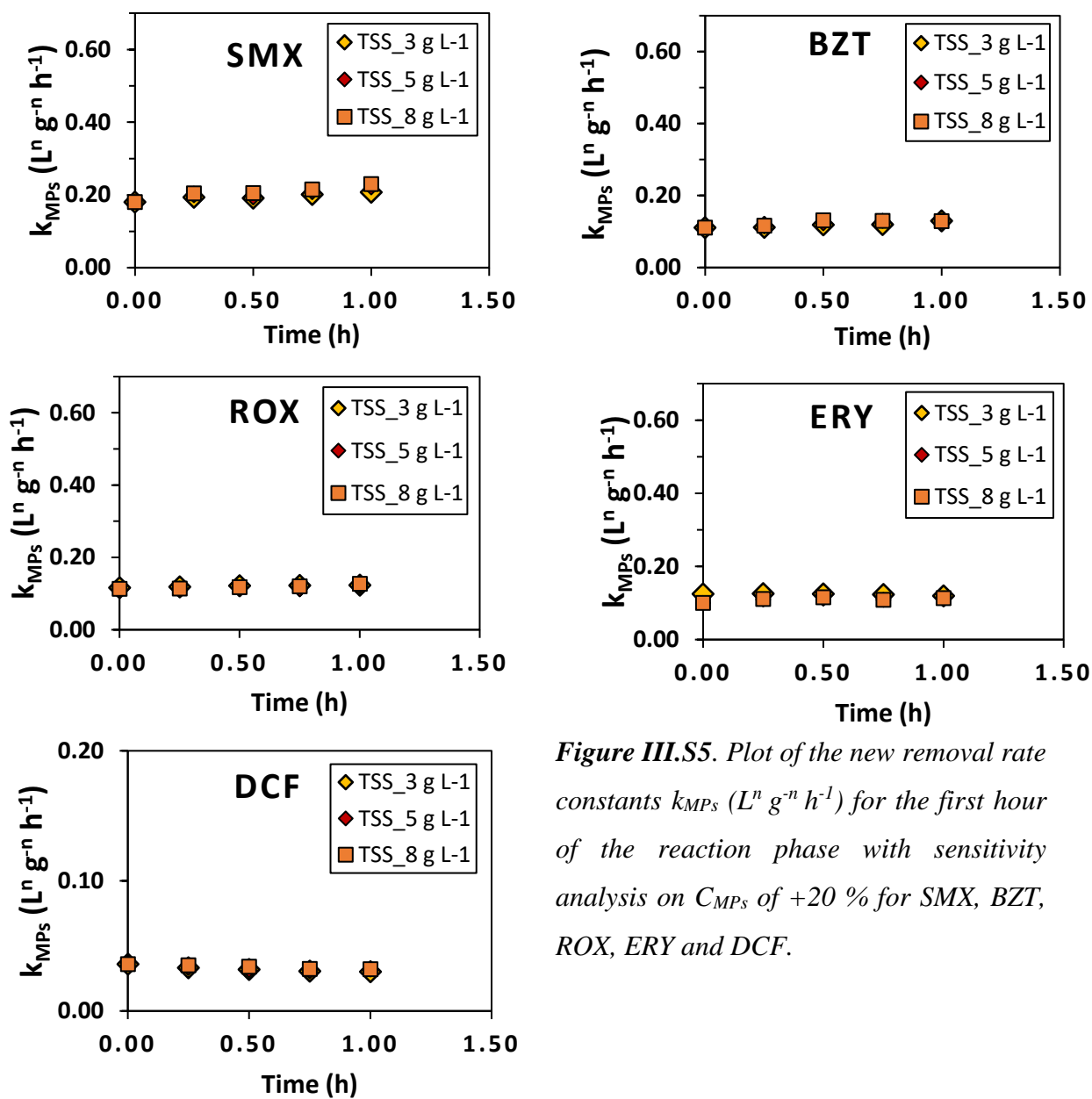


*Figure III.S5. Plot of the new removal rate constants  $k_{MPs}$  ( $L^n g^{-n} h^{-1}$ ) for the first hour of the reaction phase with sensitivity analysis on  $C_{MPs}$  of +20 % for SMX, BZT, ROX, ERY and DCF.*

## Supplementary Information of chapter IV

**Table IV. S1.** Mean values of the experimental analysis at  $t_0$  of biomass concentrations represented by  $X_{B,H}$ , soluble substrate ( $S_S$ ), dissolved oxygen ( $S_O$ ), ammonia nitrogen ( $S_{NH}$ ) and soluble organic nitrogen substrate ( $S_{NO}$ ) for the series 1 of experiments performed at different SRT and HRT; number of replicates = 3 per setup.

Series 1	Setup 1	Setup 2	Setup 3	Setup 4	Setup 5	Setup 6	Setup 7
SRT	3 d			10 d			20 d
HRT	4 h	8 h	12 h	4 h	8 h	12 h	4 h
$X_{B,H}$ (g m <sup>-3</sup> )	2690	2380	2272	2371	2541	2449	2835
$S_S$ (g m <sup>-3</sup> )	606	655	630	301	247	261	157
$S_O$ (g m <sup>-3</sup> )	2.5	2.4	2.2	4.3	4.3	4.2	4.4
$S_{NH}$ (g m <sup>-3</sup> )	37.2	37.3	37.0	27.5	37.1	37.5	37.2
$S_{NO}$ (g m <sup>-3</sup> )	0.05	0.5	1.5	1.3	1.2	0.9	0.12

**Table IV.2.** Mean values of the experimental analysis at  $t_0$  of biomass concentrations represented by  $X_{B,H}$ , soluble substrate ( $S_S$ ), dissolved oxygen ( $S_O$ ), ammonia nitrogen ( $S_{NH}$ ) and soluble organic nitrogen substrate ( $S_{NO}$ ) for the series 2 of experiments performed at various biomass concentration; number of replicates = 3 per setup.

Series 2	Setup 1	Setup 2	Setup 3
	$TSS_{3} \text{ g L}^{-1}$	$TSS_{5} \text{ g L}^{-1}$	$TSS_{8} \text{ g L}^{-1}$
SRT/HRT	10 d/4 h		
$X_{B,H}$ (g m <sup>-3</sup> )	2371	3521	5623
$S_S$ (g m <sup>-3</sup> )	301	321	332
$S_O$ (g m <sup>-3</sup> )	4.3	4.2	4
$S_{NH}$ (g m <sup>-3</sup> )	27.5	37.7	30.1
$S_{NO}$ (g m <sup>-3</sup> )	1.3	0.04	0.9

**Text IV. SI.** Matlab script main program "MainPrgm\_SBR" for the first setup of experiments performed at SRT of 3 d and HRT of 4 hours.

- External text (.txt) files for batch setups

For the files "Stoichiometric\_Data.txt", and "Conc\_Ini", the first column corresponds to the names of the variables and their units (in parentheses), the second column represents the values. Leave a space between the two columns, but no space between the name of the variable and its unit. As for the "Reactors" file, it contains three columns, the first corresponds to the name of the reactor, the second corresponds to volumes and the third to  $k_{La}$  ( $h^{-1}$ ). Similarly, make sure to leave a space between each column.

- "Stoichiometric\_data"

```

1- muH(day^-1) 2.5 %Henze
2- muA(day^-1) 0.2 %Henze
3- ng(dimensionless) 0.8 %Benchmark
4- nh(dimensionless) 0.8 %Benchmark
5- KS(g_COD_m^-3) 120 %Henze
6- KOH(g_O2_m^-3) 0.5 %Henze
7- KNO(g_NO3-N_m^-3) 0.5 %Benchmark
8- KNH(g_NH3-N_m^-3) 1 %Benchmark
9- KOA(g_O2_m^-3) 0.4 %Benchmark
10- KX(gXS/(g_XBH_COD)^-1) 0.1 %Benchmark
11- KH(gXS/(g_XBH_COD_day)^-1) 3 %Benchmark
12- bh(day^-1) 0.3 %0.3%Benchmark
13- ba(day^-1) 0.05 %Benchmark
14- ka(m^3/(g_COD_day)^-1) 0.05 %Benchmark
15- kcaffeine(m^3_(gSSday)^-1) 0.0132
16- ksulfametoxazole(m^3_(gSSday)^-1) 0.00154%from_Setup_1
17- kbenzotriazole(m^3_(gSSday)^-1) 0.00175%from_Setup_1
18- kroxithromycin(m^3_(gSSday)^-1) 0.00241%from_Setup_1
19- kerythromycin(m^3_(gSSday)^-1) 0.00192%from_Setup_1
20- kdiclofenac(m^3_(gSSday)^-1) 0.00045%from_Setup_1
21- kcarbamazepine(m^3_(gSSday)^-1) 0.00042%from_Setup_1

```

The values ranging from  $\mu_H$  to  $k_a$  (line 1 to 14) are fixed for the ASM1 model either by optimization or default Benchmark value. The values of experimental kinetic constants (*k*caffeine, *k*sulfametoxazole, etc...) depend on the studied setup.

- "Conc\_Ini"

This is the file where are stored the initial concentrations of biomass inoculated into the reactor, the organic matter and the MPs concentrations spiked directly during the reaction phase of each reaction phase.

```
XBH(g_COD_m^-3) 2.69e3
XBA(g_COD_m^-3) 153.3
XP(g_COD_m^-3) 0
SS(g_COD_m^-3) 606
XS(g_COD_m^-3) 0.001
SNO(g_N_m^-3) 0.05
SNH(g_N_m^-3) 37.1
SND(g_N_m^-3) 0
XND(g_N_m^-3) 0
SI(g_COD_m^-3) 0
XI(g_COD_m^-3) 0
SO(g_O2_m^-3) 2.5
Ccaffeine(g_m^-3) 0.97e-3
Csulfametoxazole(g_m^-3) 1.25e-3
Cbenzotriazole(g_m^-3) 1.029e-3
Croxithromycin(g_m^-3) 0.999e-3
Cerythromycin(g_m^-3) 1.15e-3
Cdiclofenac(g_m^-3) 1.187e-3
Ccarbamazepine(g_m^-3) 1.165e-3
```

- "Reactors"

This is the file that contains the reactor volumes (useful only in the continuous system) and the values of the oxygen transfer coefficients. The first column corresponds to the name of the reactor, the second to volume (in m<sup>3</sup>) and the third to k<sub>La</sub> (in h<sup>-1</sup>).

```
SBR 1e-2 12.1 % Volume of SBR in m^3; kLa in h-1
```

All external files can be modified. In the further case of continuous system, when the number of reactors and / or their volumes and transfer coefficient values are modified, the Reactors.txt file must be modified. If there are more/less than 7 micropollutants the used can add additional lines to the files Conc\_Init.txt and Stoichiometric\_data.txt. It is necessary to add the initial concentrations of the micropollutants for the batch mode and the inlet C<sub>MPs</sub> in the continuous program as well as the values of the appropriate kinetic constants of MPs elimination.



## Text IV. S2. Functions "rate" and "balance\_SBR" of the batch systems

### A. "Balance\_SBR"

```
function [ dydt ] = balanceSBR(t,y,ncomp,don,vol,kla)

Sosat=8.45; %gO2.m-3
var=ncomp-12;%number of micropolluants

dydt=zeros(ncomp,1);

%%%%%%%%%%%%%%%%%%%%%%%%%%%%%%%%%%%%%%%%%%%%%%%%%%%%%%%%%%%%%%%%%%%%%%%%%
r=rate(y,don,var);
for i=1:ncomp
    if i==12
        oxy=1;
    else
        oxy=0;
    end
    dydt(i)=r(i)+oxy*kla*(Sosat-y(12));
end

end
```

### B. Function "rate"

Rate function denoted "rate" is a function that calculates the production rates of each compound in the given reactor of each setup.

Input:

- conc is a vector of size ncomp containing the concentrations of the compounds in the given reactor
- don: vector where the stoichiometric data are stored
- Var: number of micropollutants

Output:

- r is a vector of size ncomp containing the production/removal rate of all ASM1 compounds and MPs.

```
function [ry] = rate(conc,don,var)
%Input:
%rate are the rates of the reactions of the ASM1 model+ MPs
%conc is the vector of size (ncomp, 1) containing the concentrations of the
compounds in a given reactor
%don is the stoichiometric data of ASM1 model
```

```

%stoechiometriques du modèle ASM1
%var is the number of micropollutants
%Output:
%ry is a vector of size ncomp containing the production rates of each
compound

muh=don(1); mua=don(2);
etah=don(3); etah=don(4);
KS=don(5); KOH=don(6);
KNO=don(7); KNH=don(8);
KOA=don(9); KX=don(10);
kh=don(11); bh=don(12);
ba=don(13); ka=don(14);
kbiol=zeros(1,var);
if var ~=0
    for i=1:var
        kbiol(1,i)=don(14+i);
    end
end

muh
bh

Ya=0.24; %(g_XBACOD/gN_utilised) %Benchmark
Yh=0.67;%(g_XBHCOD/gCOD_utilised) %Benchmark
fp=0.08;%(dimensionless) %Benchmark
iXB=0.08;%(gN/gCOD_in_biomass) %Benchmark
iXP=0.06;%(gN/gCOD_in_XP) %Benchmark

% XBH=y(1,j); % XBA=y(2,j); % XP=y(3,j);
% SS=y(4,j); % XS=y(5,j);
% SNO=y(6,j); % SNH=y(7,j);
% SND=y(8,j); % XND=y(9,j);
% SI=y(10,j); % XI=y(11,j);
% SO=y(12,j);

        %ASM1 model

%Aerobic growth of heterotrophic biomass
rate(1,1)=muh*(conc(4)/(KS+conc(4)))*(conc(12)/(KOH+conc(12)))*conc(1);
%Anoxic growth of heterotrophic biomass
rate(2,1)=muh*etah*(conc(4)/(KS+conc(4)))*(KOH/(KOH+conc(12)))*(conc(6)/(KNO+conc(6)))*conc(1);
%Growth of autotrophic biomass
rate(3,1)=mua*(conc(7)/(KNH+conc(7)))*(conc(12)/(KOA+conc(12)))*conc(2);
%Mortality of heterotrophic biomass
rate(4,1)=bh*conc(1)
%Mortality of autotrophic biomass
rate(5,1)=ba*conc(2);
%Ammonification of the soluble nitrogen compound
rate(6,1)=ka*conc(8)*conc(1);
%Hydrolysis of slowly biodegradable carbon compounds
rate(7,1)=kh*((conc(5)/conc(1))/(KX+(conc(5)/conc(1))))*((conc(12)/(KOH+conc(12)))+etah*(KOH/(KOH+conc(12)))*(conc(6)/(KNO+conc(6))))*conc(1);
%Hydrolysis of slowly biodegradable nitrogen compounds
rate(8,1)=rate(7)*conc(9)/conc(5);

%rate of each compound of ASM1
ry(1,1)=rate(1)+rate(2)-rate(4);
ry(2,1)=rate(3)-rate(5);

```

```

ry(3,1)=fp*(rate(4)+rate(5));
ry(4,1)=(-rate(1)-rate(2))/Yh+rate(7);
ry(5,1)=(1-fp)*(rate(4)+rate(5))-rate(7);
ry(6,1)=-((1-Yh)/(2.86*Yh))*rate(2)+rate(3)/Ya;
ry(7,1)=-iXB*(rate(1)+rate(2))-(iXB+(1/Ya))*rate(3)+rate(6);
ry(8,1)=rate(8)-rate(6);
ry(9,1)=(iXB-fp*iXP)*(rate(4)+rate(5))-rate(8);
ry(10,1)=0;
ry(11,1)=0;
ry(12,1)=-((1-Yh)/Yh)*rate(1)-((4.57-Ya)/Ya)*rate(3);

%rate of MP removal/ Apparent-first order kinetic
if var~=0
    for i=1:var
        ry(12+i,1)=-kbiol(1,i)*conc(12+i)*conc(1);
    end
end
end
end

```

**Text IV. S3.** Matlab script main program "MainPrgm\_SBR" for the first setup of experiments performed at SRT of 3 d and HRT of 4 hours / apparent -first order kinetic.

- Matlab script main program "MainPrgm\_SBR"

```

clear
clc
close all
format long
%Reading files

fid=fopen('Stoichiometric_data.txt','r'); data1=textscan(fid,'%s %f %s');
fclose(fid); don=data1{2};
size(don)

fid=fopen('Conc_Ini.txt','r'); data2=textscan(fid,'%s %f');
fclose(fid); Cini=data2{2};

fid=fopen('Reactors.txt','r'); data4=textscan(fid,'%s %f %f');
fclose(fid);
vol=data4{2}; kla=data4{3}*24;% kla in d-1

tic

%Usre settings
var=7;%number of micropolluants
ncomp=var+12; %number of compounds (ASM1+micropolluants)

%Integration interval
to=0;
tf=0.125;% in days

% INITIALISATION OF CALCULATION
yo=Cini;%vector initial concentrations

options=odeset('RelTol',1e-8,'NonNegative',[]);

[tout,yout]=ode23tb(@balanceSBR,[to tf],yo,options,ncomp,don,vol,kla);

```

```

% DISPLAY RESULTS

toutmin=tout*24*60;
figure;
tXBH=[0
180
];

CXBH=[2690
3102
];
subplot(2,2,1),plot(toutmin,yout(:,1),'b-',tXBH,CXBH,'kx');
xlabel('time (min)'),ylabel('XBH (g/m^3)'),axis([0 180 0 4000])
subplot(2,2,2),plot(toutmin,yout(:,2));
xlabel('time (min)'),ylabel('XBA (g/m^3)'),axis([0 180 0 300])
subplot(2,2,3),plot(toutmin,yout(:,3));
xlabel('time (min)'),ylabel('XP (g/m^3)'),
tSS=[0
60
120
180
];

CSS=[606
442.2
315.5
250.5
];
subplot(2,2,4),plot(toutmin,yout(:,4),'b-',tSS,CSS,'kx');xlabel('time
(min)'),ylabel('SS (g/m^3)'),axis([0 180 0 650])

figure;
subplot(2,2,1),plot(toutmin,yout(:,5));
xlabel('time (min)'),ylabel('XS (g/m^3)'),
tSNO=[0
60
120
180
];

CSNO=[0.05
0.045
0.058
0.072
]
subplot(2,2,2),plot(toutmin,yout(:,6),'b-',tSNO,CSNO,'kx');xlabel('time
(min)'),ylabel('SNO (g/m^3)'),axis([0 180 0 0.1])
tSNH=[0
60
120
180
];

CSNH=[37.1
32.3
30.5
29
];
subplot(2,2,3),plot(toutmin,yout(:,7),tSNH,CSNH,'kx');xlabel('time
(min)'),ylabel('SNH (g/m^3)'),axis([0 200 0 40])

```

```

subplot(2,2,4),plot(toutmin,yout(:,8));
xlabel('time (min)'),ylabel('SND (g/m^3)'),

figure;
subplot(2,2,1),plot(toutmin,yout(:,9));
xlabel('time (min)'),ylabel('XND (g/m^3)'),
subplot(2,2,2),plot(toutmin,yout(:,10));
xlabel('time (min)'),ylabel('SI (g/m^3)'),axis([0 180 0 0.001])
subplot(2,2,3),plot(toutmin,yout(:,11));
xlabel('time (min)'),ylabel('XI(g/m^3)'),axis([0 180 0 0.001]),
tSO=[0
60
120
180
];

CSO=[2.41
0.415
0.712
1.4
];
subplot(2,2,4),plot(toutmin,yout(:,12),'b-',tSO,CSO,'kx');xlabel('time
(min)'),ylabel('SO (g/m^3)')

%% WITH EXPERIMENTAL POINTS

txp=[0
5
10
15
30
45
60
90
120
150
170
];

CCAF=1e-3*[0.978
0.908
0.806
0.706
0.500
0.359
0.232
0.119
0.0382
0.03612
0.0282
];

tsmx=[0
5
10
15
30
45
60

```

```
90
120
150
170
];
CSMX=1e-3*[1.258
1.249
1.228
1.214
1.241
1.193
1.167
1.090
0.992
0.922
0.876
];
```

```
tbzt=[0
5
10
15
30
45
60
90
120
150
170
];
CBZT=1e-3*[1.029
1.021
1.015
0.997
0.965
0.923
0.898
0.832
0.798
0.740
0.704
];
```

```
trox=[0
5
10
15
30
45
60
90
120
150
170
];
CROX=1e-3*[0.999
0.974
0.946
0.928
0.886
0.831
```

```
0.786
0.726
0.652
0.579
0.500
];
```

```
tery=[0
5
10
30
45
60
90
120
170
];
```

```
CERY=1e-3*[1.15
1.113
1.112
1.042
1.014
0.974
0.902
0.843
0.791
];
```

```
tdcf=[0
5
10
15
30
45
60
90
120
150
170
];
```

```
CDCF=1e-3*[1.187
1.184
1.182
1.181
1.176
1.156
1.145
1.103
1.093
1.061
1.056
];
```

```
tcbz=[0
5
10
15
45
60
90
120
```

```

150
170
];
CCBZ=1e-3*[1.165
1.128
1.125
1.123
1.121
1.125
1.085
1.065
1.065
1.065
];

figure;
subplot(2,2,1),plot(toutmin,yout(:,13),'b-',txp,CCAF,'kx');
xlabel('time (min)'),ylabel('CAF (g/m^3)'),axis([0 180 0 1.2e-3])
subplot(2,2,2),plot(toutmin,yout(:,14),'b-',tsmx,CSMX,'kx');
xlabel('time (min)'),ylabel('SMX (g/m^3)'),axis([0 180 0 1.5e-3])
subplot(2,2,3),plot(toutmin,yout(:,15),'b-',tbzt,CBZT,'kx');
xlabel('time (min)'),ylabel('BZT (g/m^3)'),axis([0 180 0 1.2e-3])
subplot(2,2,4),plot(toutmin,yout(:,16),'b-',trox,CROX,'kx');
xlabel('time (min)'),ylabel('ROX (g/m^3)'),axis([0 180 0 1.2e-3])

figure;
subplot(2,2,1),plot(toutmin,yout(:,17),'b-',tery,CERY,'kx');
xlabel('time (min)'),ylabel('ERY (g/m^3)'),axis([0 180 0 1.2e-3])
subplot(2,2,2),plot(toutmin,yout(:,18),'b-',tdcf,CDCF,'kx');
xlabel('time (min)'),ylabel('DCF (g/m^3)'),axis([0 180 0 1.5e-3])
subplot(2,2,3),plot(toutmin,yout(:,19),'b-',tcbz,CCBZ,'kx');
xlabel('time (min)'),ylabel('CBZ (g/m^3)'),axis([0 180 0 1.5e-3])

vectvalfinalesNum=[
spline(toutmin,yout(:,1),170);
spline(toutmin,yout(:,4),170);
spline(toutmin,yout(:,6),170);
spline(toutmin,yout(:,7),170);
spline(toutmin,yout(:,12),170);
spline(toutmin,yout(:,13),170);
spline(toutmin,yout(:,14),170);
spline(toutmin,yout(:,15),170);
spline(toutmin,yout(:,16),170);
spline(toutmin,yout(:,17),170);
spline(toutmin,yout(:,18),170);
spline(toutmin,yout(:,19),170);
]

vectvalfinalesExp=[CXBH(end),CSS(end),CSNO(end),CSNH(end),CSO(end),CCAF(end),
),CSMX(end),CBZT(end),CROX(end),CERY(end),CDCF(end),CCBZ(end)]'

RelativestandarddeviationValFinalNumExp=[abs(vectvalfinalesNum-
vectvalfinalesExp)./vectvalfinalesExp]

MatResult=[vectvalfinalesExp,vectvalfinalesNum,RelativestandarddeviationVal
FinalNumExp];

save SRT10dHRT4h.txt MatResult -ASCII

```



toc

```
% save tf50Dt0P1Reactors50.mat
```

- *Setups of series 1 of experiments (ASMI parameters)*

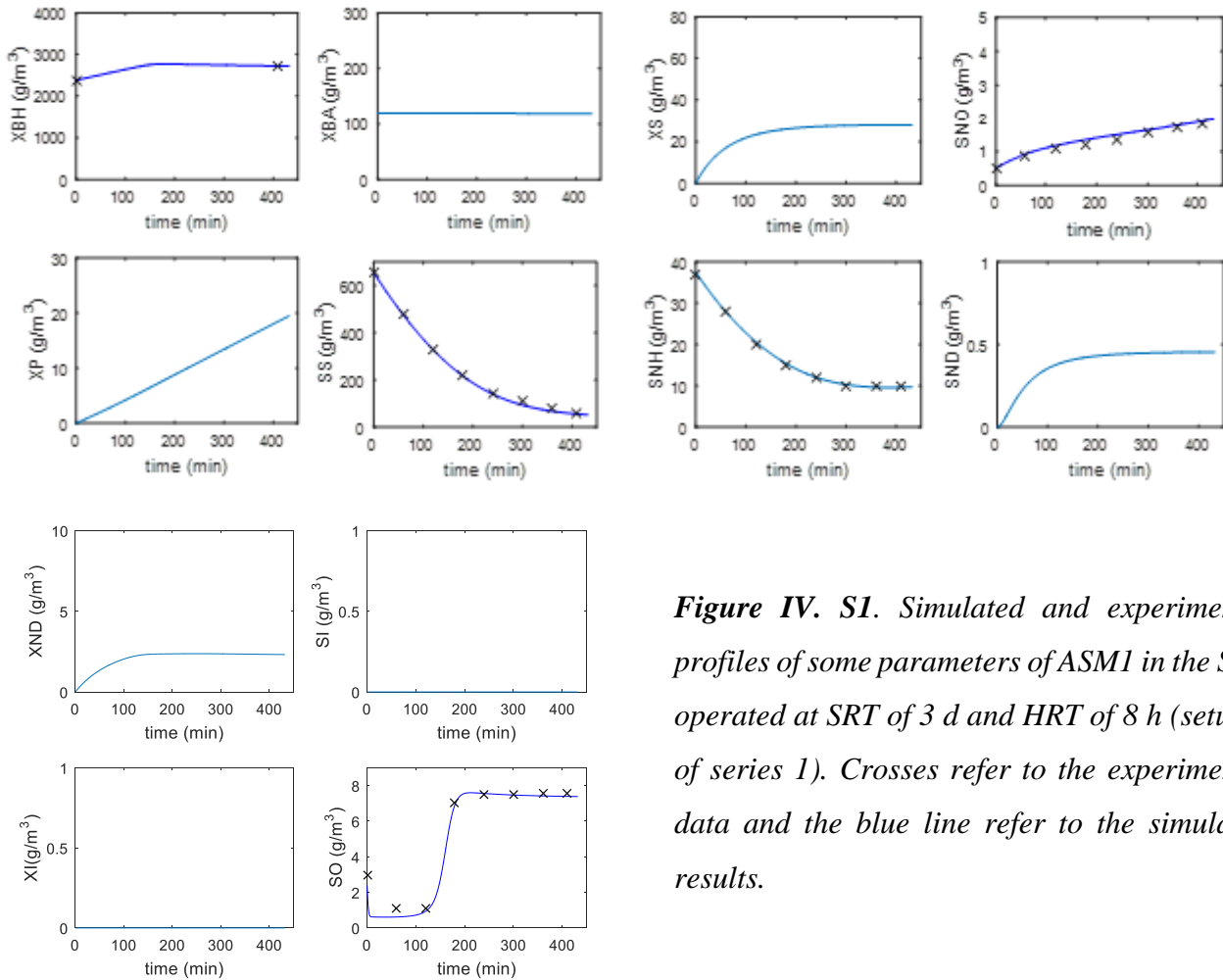


**Figure IV. S1.** Simulated and experimental profiles of some parameters of ASMI in the SBR operated at SRT of 3 d and HRT of 8 h (setup 2 of series 1). Crosses refer to the experimental data and the blue line refer to the simulated results.

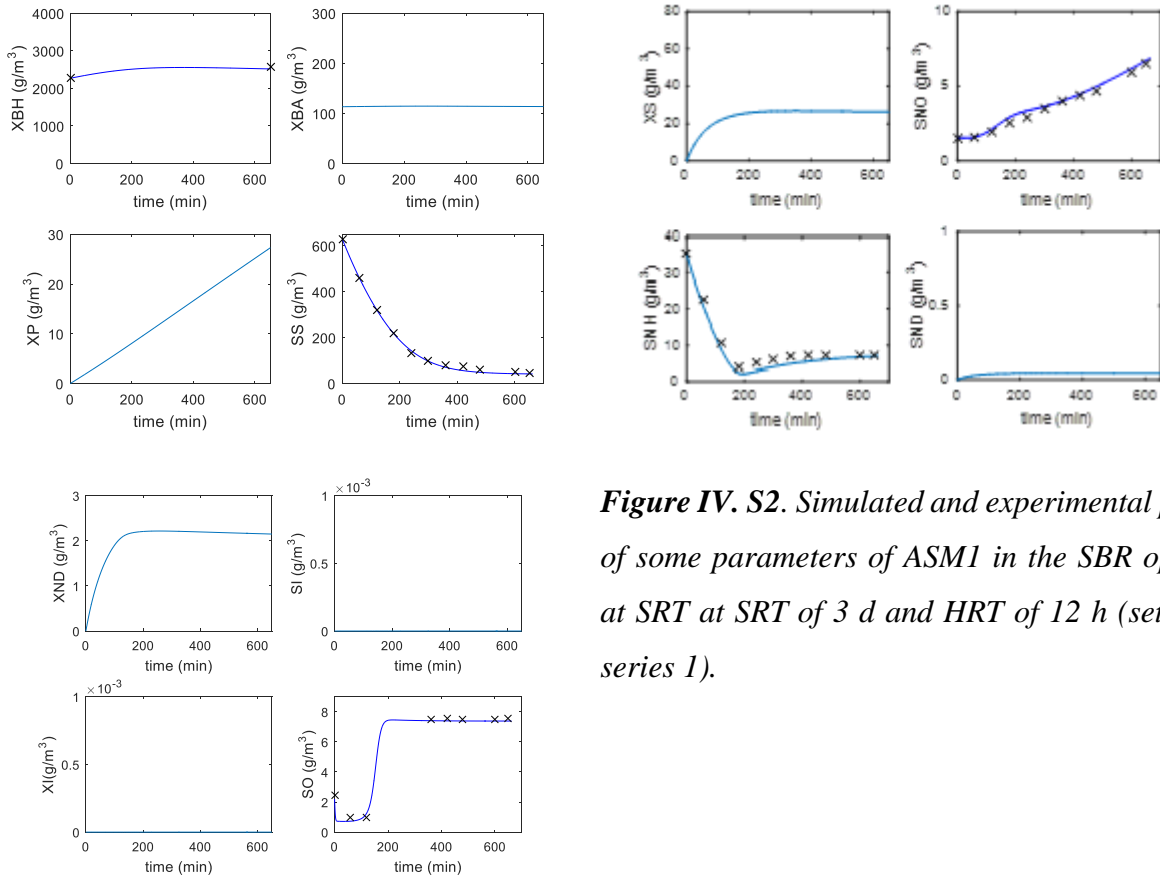


**Figure IV. S2.** Simulated and experimental profiles of some parameters of ASM1 in the SBR operated at SRT of 3 d and HRT of 12 h (setup 3 of series 1).

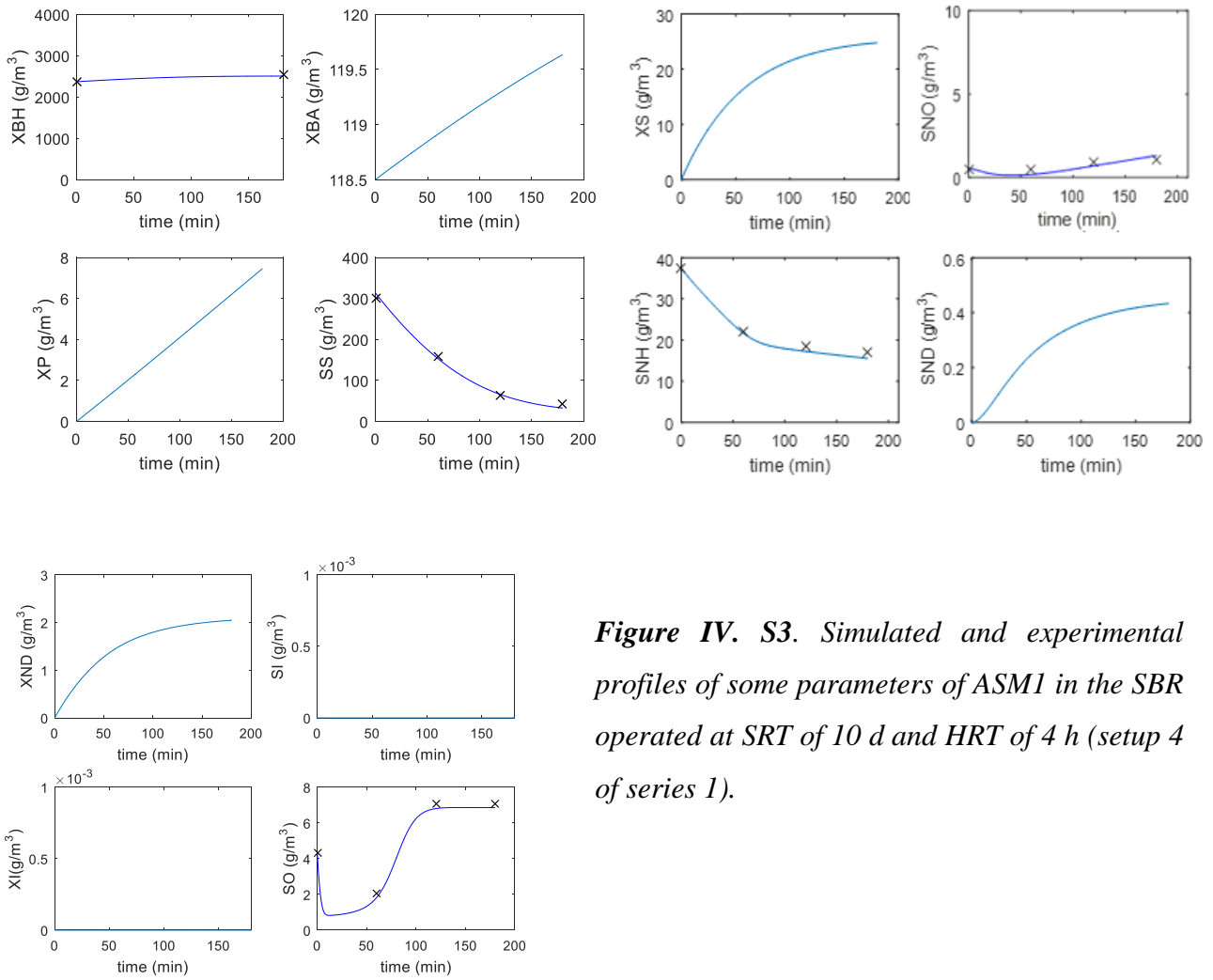


**Figure IV. S3.** Simulated and experimental profiles of some parameters of ASM1 in the SBR operated at SRT of 10 d and HRT of 4 h (setup 4 of series 1).

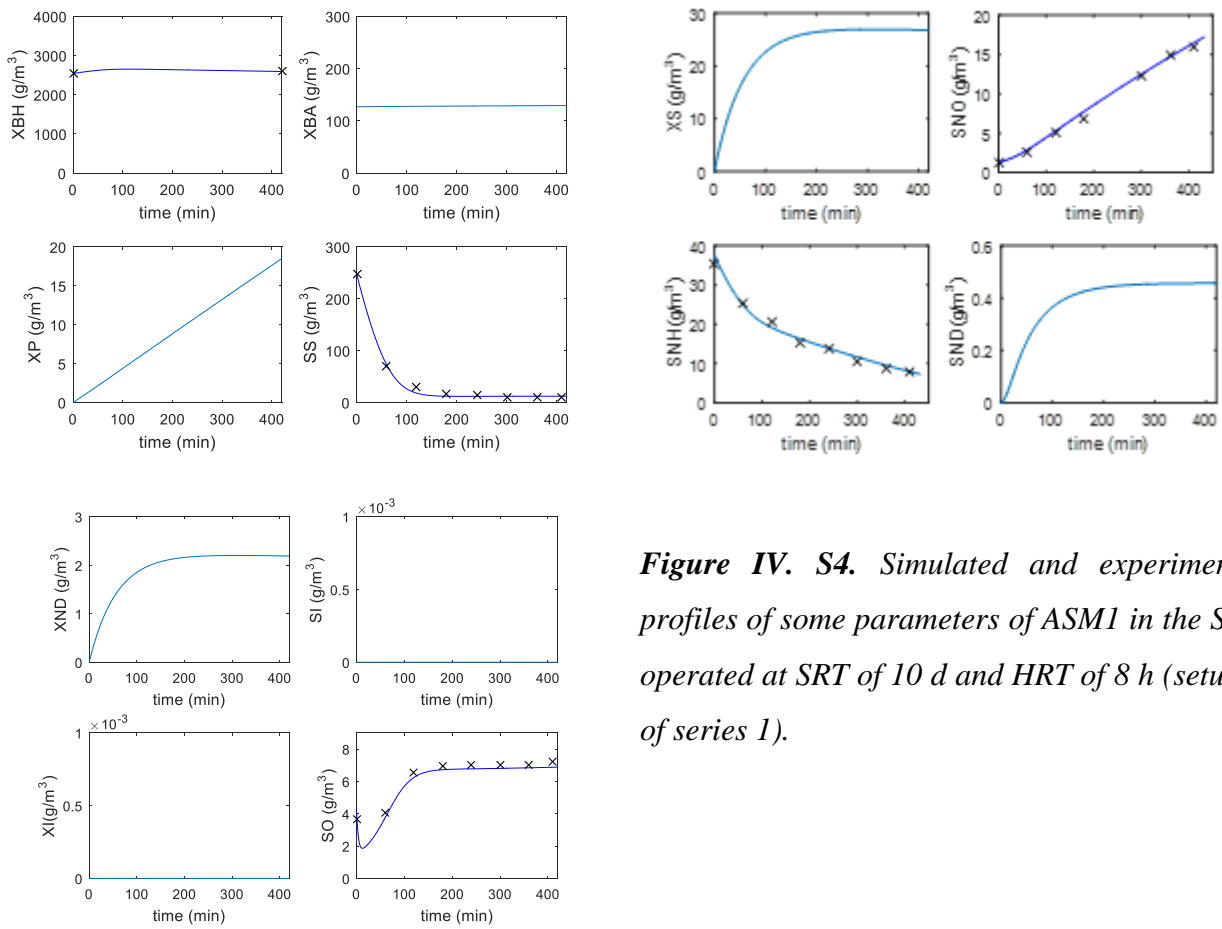


**Figure IV. S4.** Simulated and experimental profiles of some parameters of ASM1 in the SBR operated at SRT of 10 d and HRT of 8 h (setup 5 of series 1).

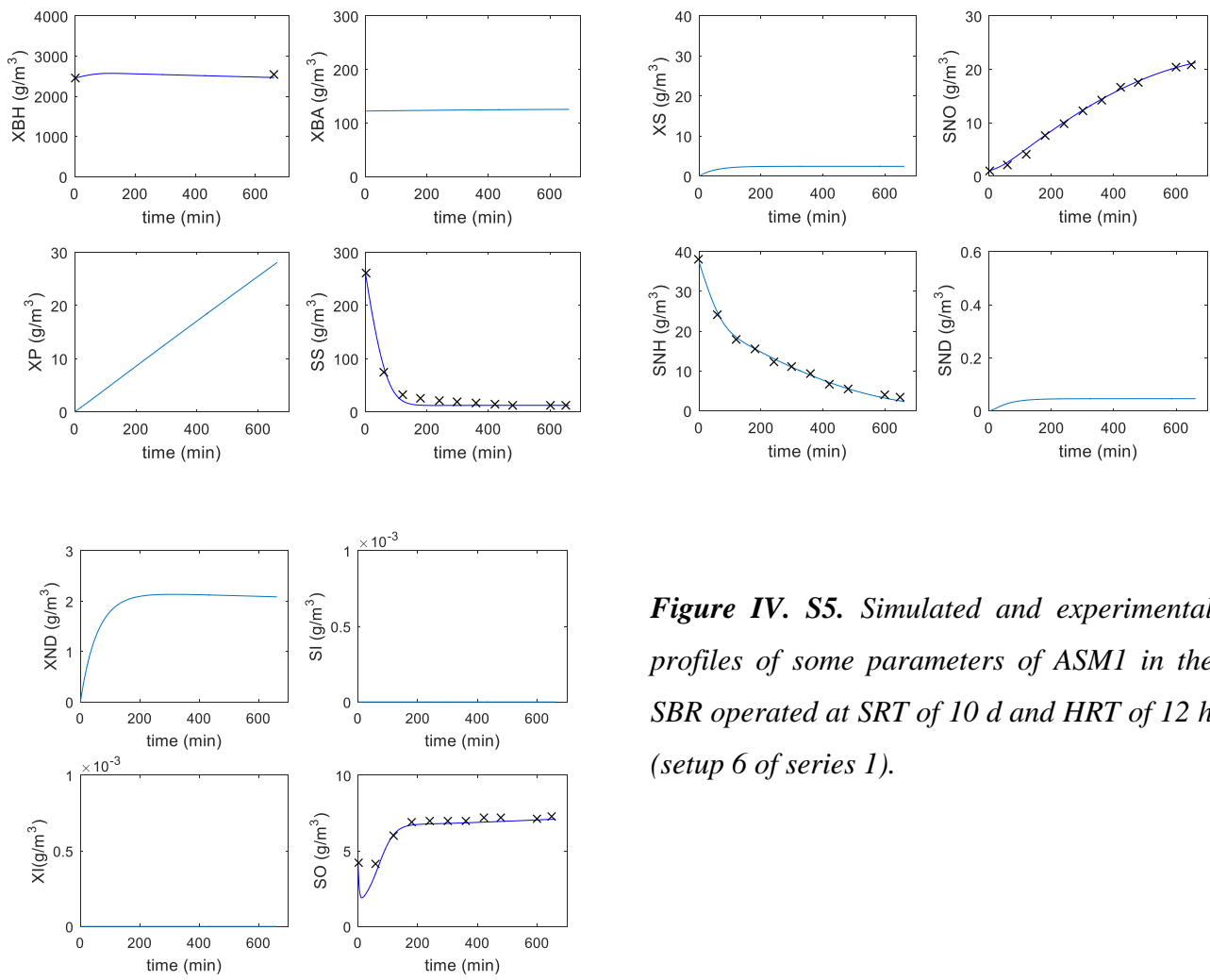


**Figure IV. S5.** Simulated and experimental profiles of some parameters of ASM1 in the SBR operated at SRT of 10 d and HRT of 12 h (setup 6 of series 1).

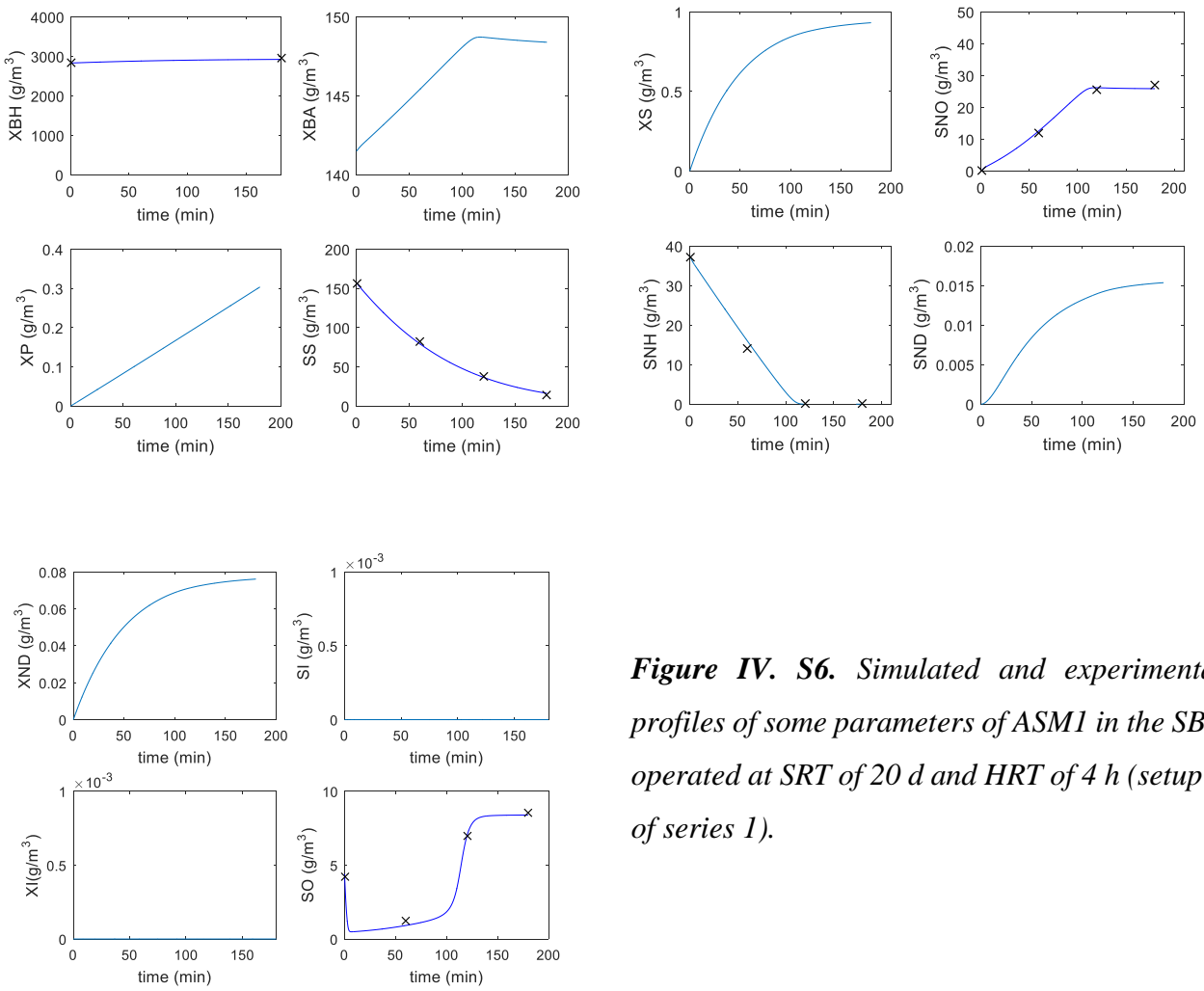


**Figure IV. S6.** Simulated and experimental profiles of some parameters of ASM1 in the SBR operated at SRT of 20 d and HRT of 4 h (setup 7 of series 1).

- *Setups of series 2 of experiments (ASMI parameters)*

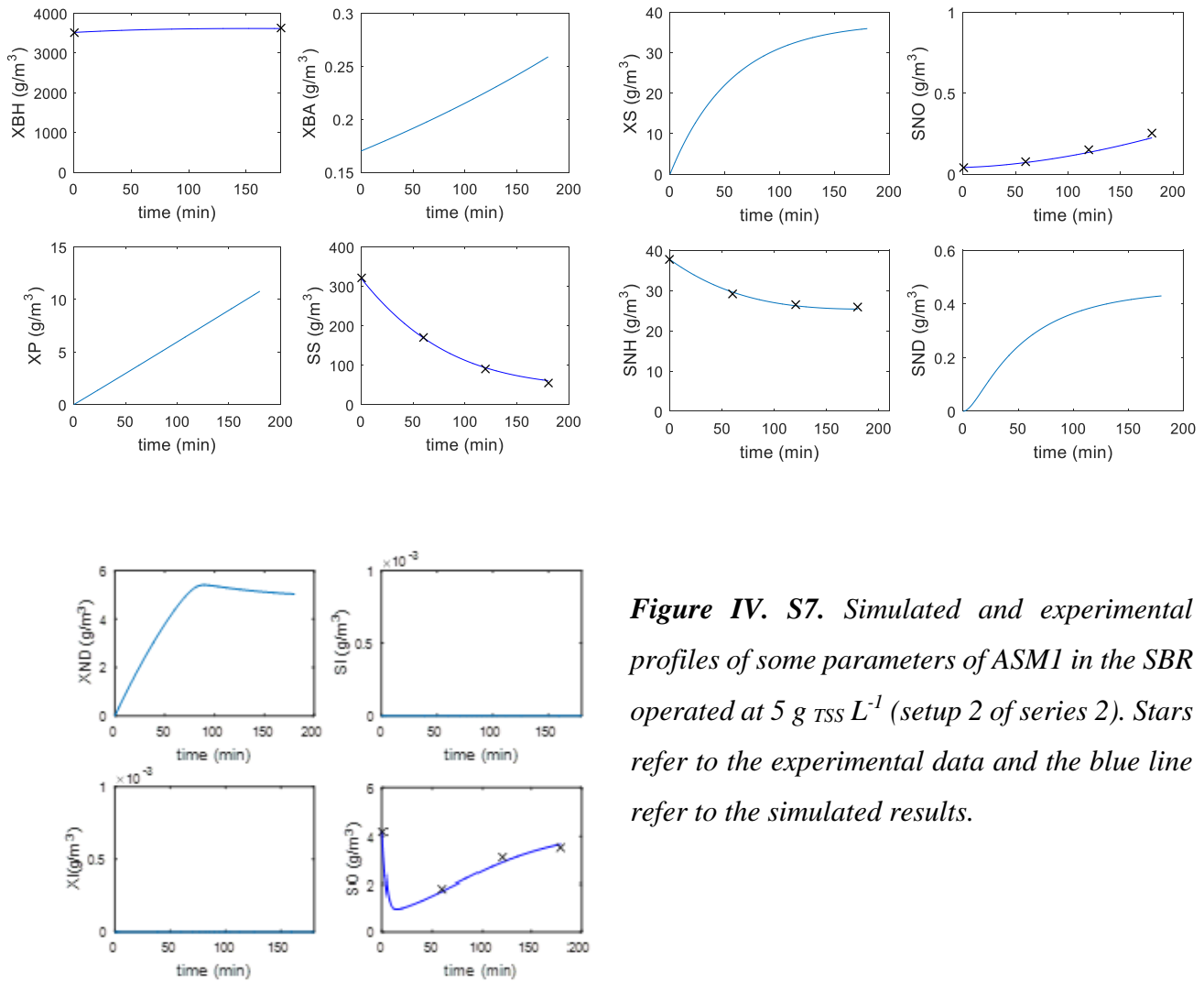


**Figure IV. S7.** Simulated and experimental profiles of some parameters of ASMI in the SBR operated at  $5 \text{ g TSS L}^{-1}$  (setup 2 of series 2). Stars refer to the experimental data and the blue line refer to the simulated results.

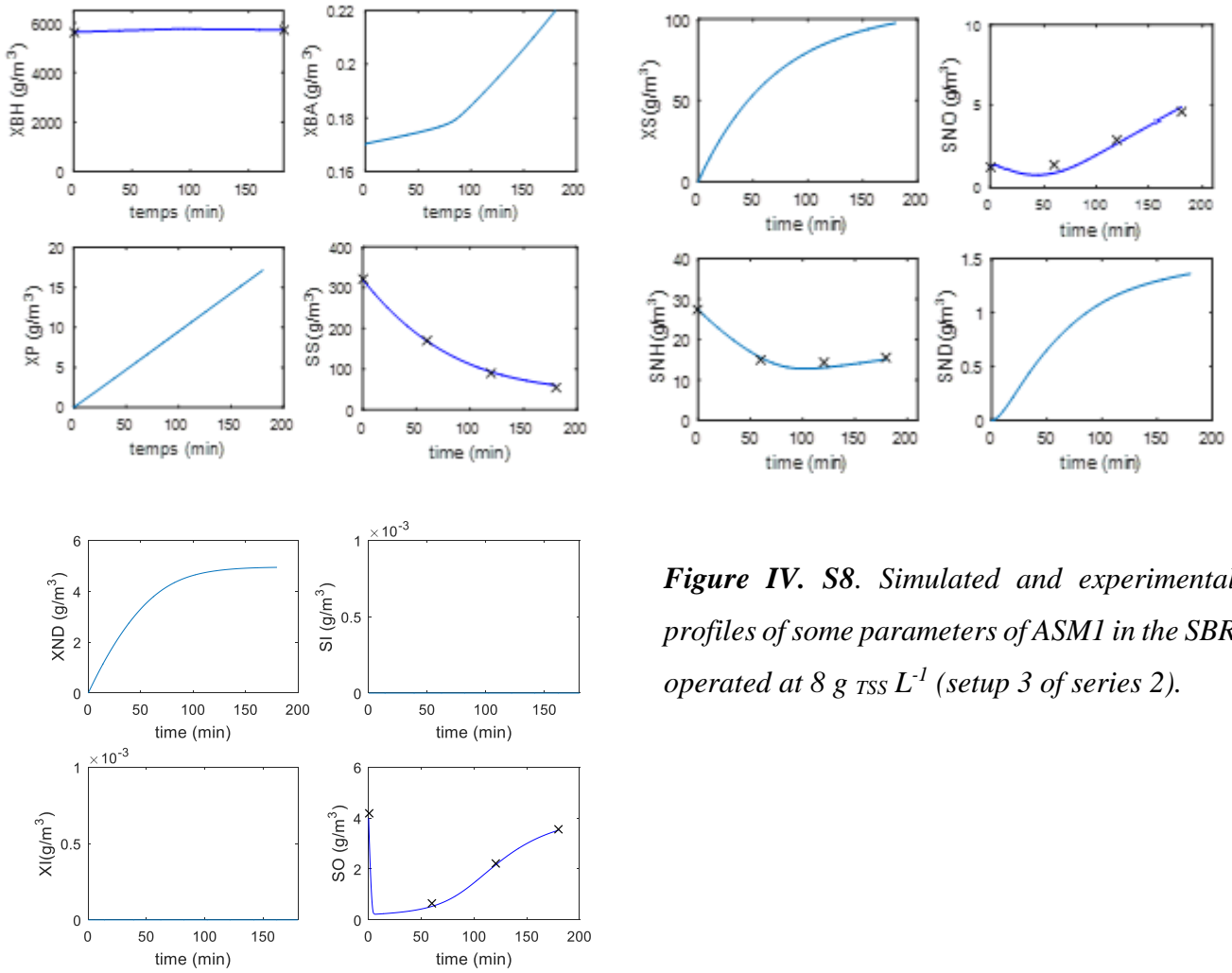


**Figure IV. S8.** Simulated and experimental profiles of some parameters of ASM1 in the SBR operated at  $8 \text{ g rss L}^{-1}$  (setup 3 of series 2).



- *Setups of series 1 by applying apparent -first order approach*

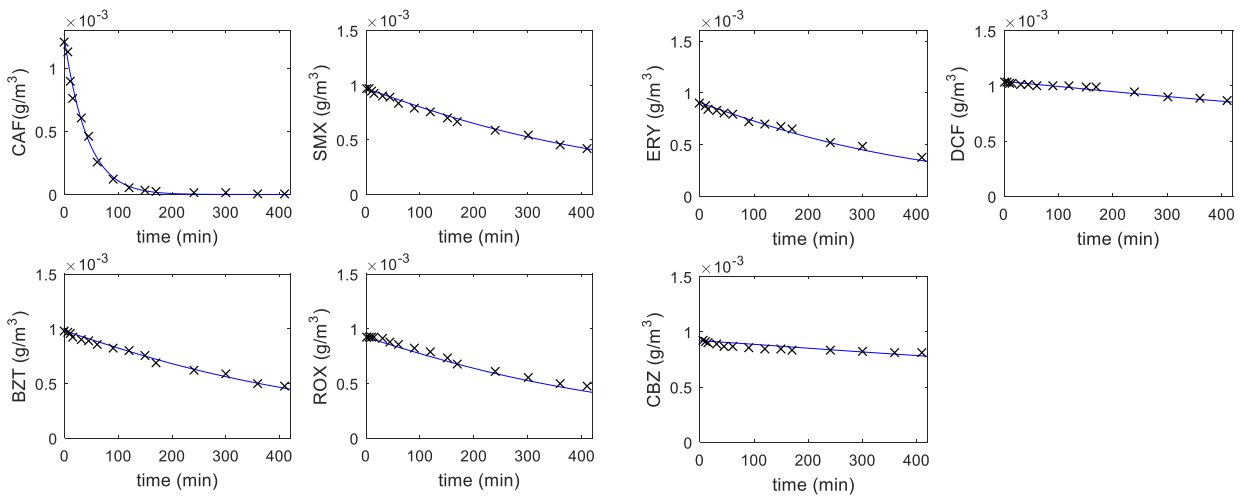


**Figure IV. S9.** Simulated and experimental profiles of MPs' concentrations by applying the apparent -first approach to the SBR operated at SRT of 3 d and HRT of 8 h. Crosses refer to the experimental data and the blue line refer to the simulated results.

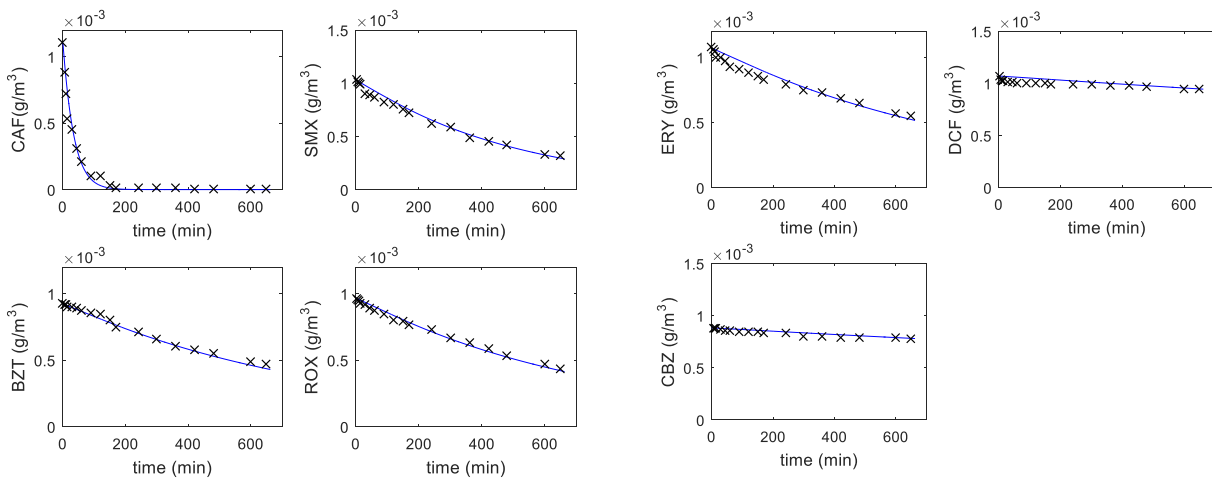


**Figure IV. S10.** Simulated and experimental profiles of MPs' concentrations by applying the apparent -first approach to the SBR operated at SRT of 3 d and HRT of 12 h.

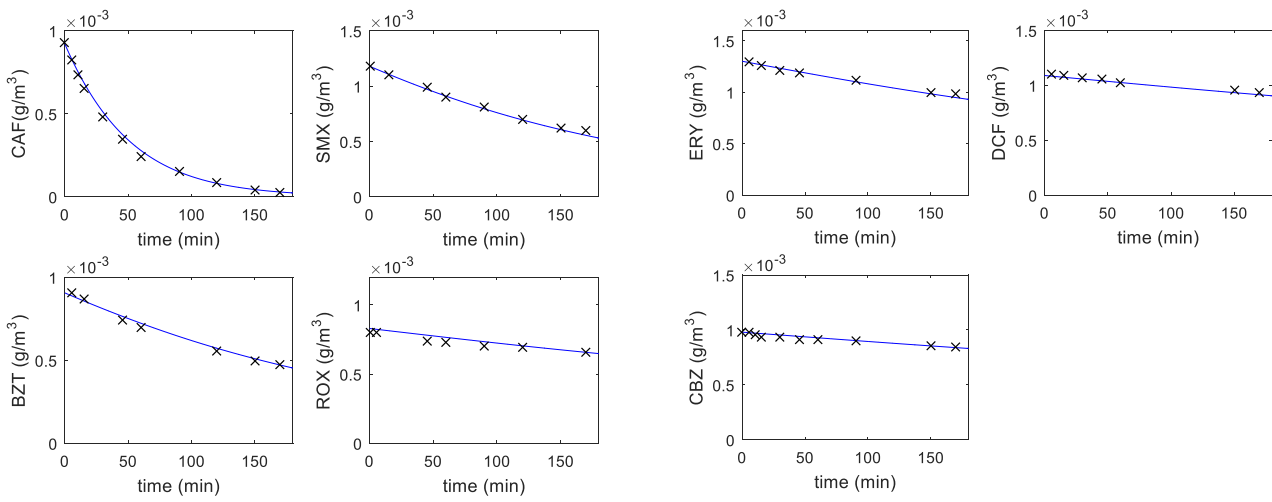


**Figure IV. S11.** Simulated and experimental profiles of MPs' concentrations by applying the apparent -first approach to the SBR operated at SRT of 10 d and HRT of 4 h.

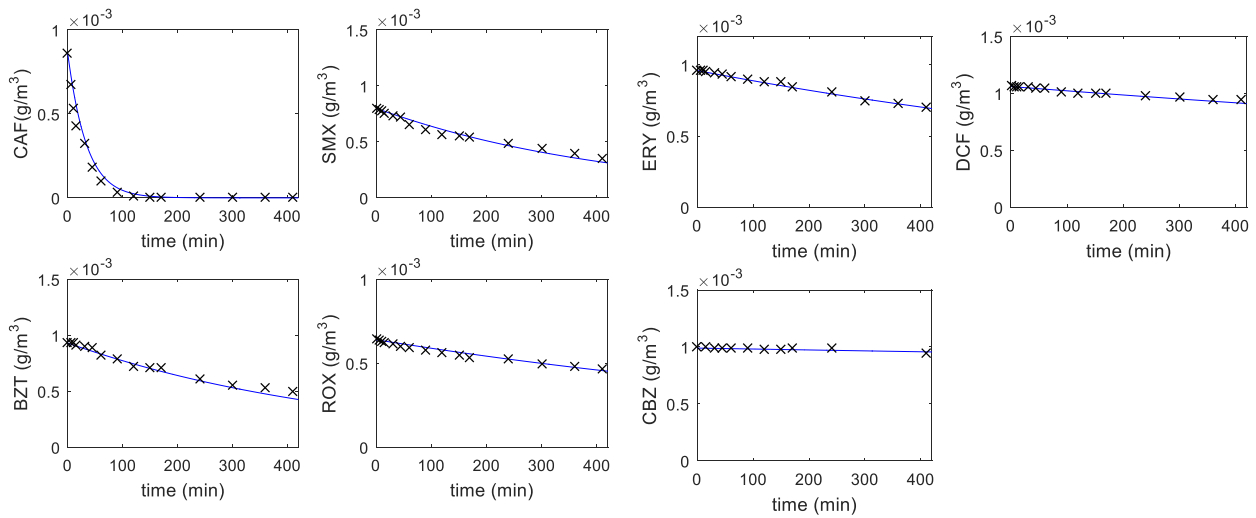


**Figure IV. S12.** Simulated and experimental profiles of MPs' concentrations by applying the apparent -first approach to the SBR operated at SRT of 10 d and HRT of 8 h.

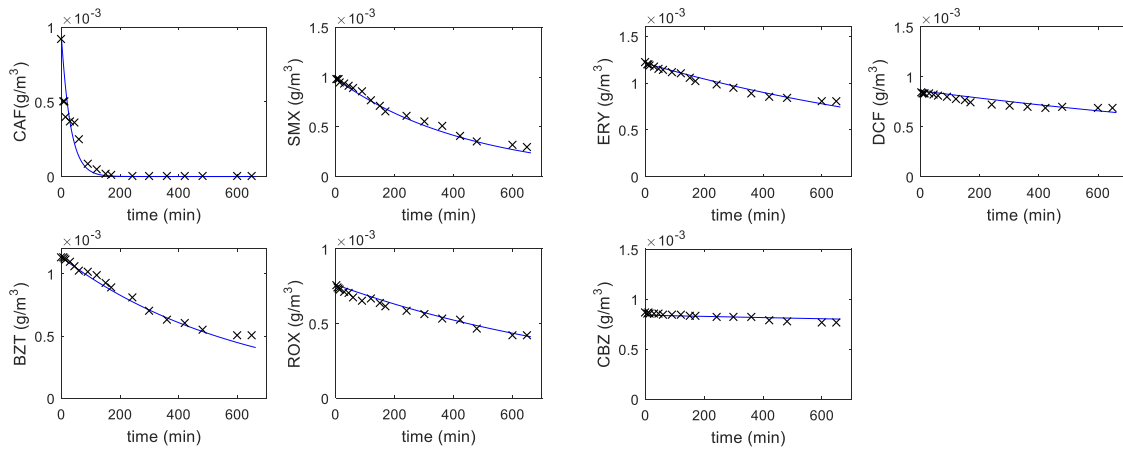


**Figure IV. S13.** Simulated and experimental profiles of MPs' concentrations by applying the apparent -first approach to the SBR operated at SRT of 10 d and HRT of 12 h.

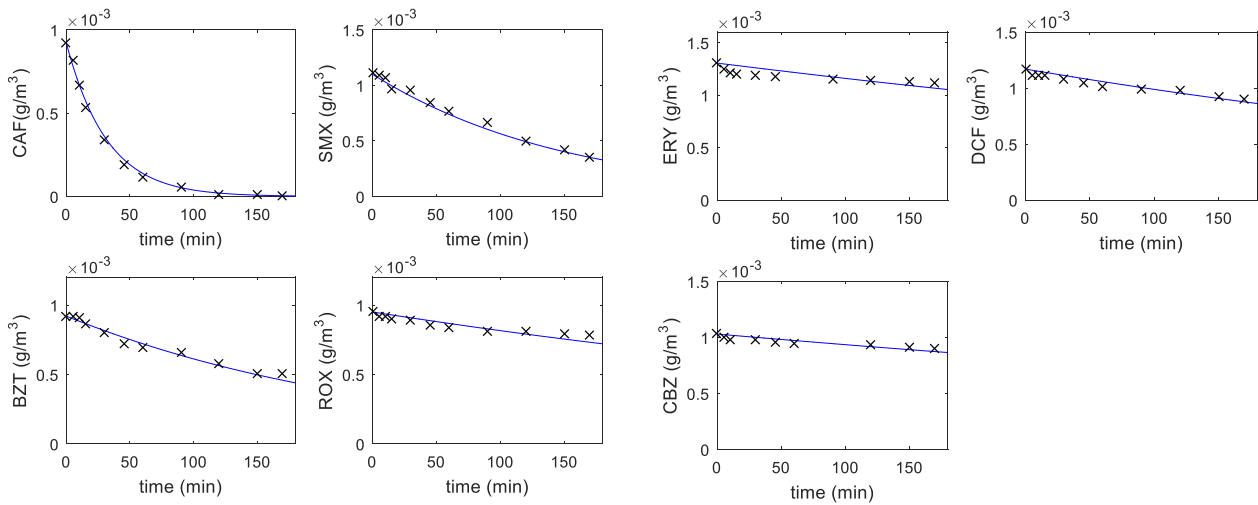


**Figure IV. S14.** Simulated and experimental profiles of MPs' concentrations by applying the apparent -first-order approach to the SBR operated at SRT of 20 d and HRT of 4 h.

**Text IV. S4.** Adapted files for power law kinetics simulation of series 2 setups. The difference comparing to the previous files of series 1 was marked in red color.

- Function rate

```
function [ry] = rate(conc,don,var,nvect)
%Input:
%rate are the rates of the reactions of the ASM1 model+ MPs
%conc is the vector of size (ncomp, 1) containing the concentrations of the
compounds in a given reactor
%don is the stoichiometric data of ASM1 model
%stoichiometriques du modèle ASM1
%var is the number of micropollutants
%Output:
%ry is a vector of size ncomp containing the production rates of each
compound

muh=don(1); mua=don(2);
etah=don(3); etah=don(4);
KS=don(5); KOH=don(6);
KNO=don(7); KNH=don(8);
KOA=don(9); KX=don(10);
kh=don(11); bh=don(12);
ba=don(13); ka=don(14);
kbiol=zeros(1,var);
if var ~=0
    for i=1:var
        kbiol(1,i)=don(14+i)*24/(1000)^nvect(i);
    end
end

Ya=0.24; %(g_XBACOD/gN_utilised) %Benchmark
Yh=0.67;%(g_XBHCOD/gCOD_utilised) %Benchmark
fp=0.08;%(dimensionless) %Benchmark
iXB=0.08;%(gN/gCOD_in_biomass) %Benchmark
iXP=0.06;%(gN/gCOD_in_XP) %Benchmark

% XBH=y(1,j); % XBA=y(2,j); % XP=y(3,j);
% SS=y(4,j); % XS=y(5,j);
% SNO=y(6,j); % SNH=y(7,j);
% SND=y(8,j); % XND=y(9,j);
% SI=y(10,j); % XI=y(11,j);
% SO=y(12,j);

%ASM1 model

%Aerobic growth of heterotrophic biomass
rate(1,1)=muh*(conc(4)/(KS+conc(4)))*(conc(12)/(KOH+conc(12)))*conc(1);
%Anoxic growth of heterotrophic biomass
rate(2,1)=muh*etah*(conc(4)/(KS+conc(4)))*(KOH/(KOH+conc(12)))*(conc(6)/(KN
O+conc(6)))*conc(1);
%Growth of autotrophic biomass
rate(3,1)=mua*(conc(7)/(KNH+conc(7)))*(conc(12)/(KOA+conc(12)))*conc(2);
%Mortality of heterotrophic biomass
rate(4,1)=bh*conc(1)
%Mortality of autotrophic biomass
rate(5,1)=ba*conc(2);
%Ammonification of the soluble nitrogen compound
```

```

rate(6,1)=ka*conc(8)*conc(1);
%Hydrolysis of slowly biodegradable carbon compounds
rate(7,1)=kh*((conc(5)/conc(1))/(KX+(conc(5)/conc(1))))*((conc(12)/(KOH+conc(12)))+etah*(KOH/(KOH+conc(12)))*(conc(6)/(KNO+conc(6))))*conc(1);
%Hydrolysis of slowly biodegradable nitrogen compounds
rate(8,1)=rate(7)*conc(9)/conc(5);

%rate of each compound of ASM1
ry(1,1)=rate(1)+rate(2)-rate(4);
ry(2,1)=rate(3)-rate(5);
ry(3,1)=fp*(rate(4)+rate(5));
ry(4,1)=(-rate(1)-rate(2))/Yh+rate(7);
ry(5,1)=(1-fp)*(rate(4)+rate(5))-rate(7);
ry(6,1)=-((1-Yh)/(2.86*Yh))*rate(2)+rate(3)/Ya;
ry(7,1)=-iXB*(rate(1)+rate(2))-(iXB+(1/Ya))*rate(3)+rate(6);
ry(8,1)=rate(8)-rate(6);
ry(9,1)=(iXB-fp*iXP)*(rate(4)+rate(5))-rate(8);
ry(10,1)=0;
ry(11,1)=0;
ry(12,1)=-((1-Yh)/Yh)*rate(1)-((4.57-Ya)/Ya)*rate(3);

%rate of MP removal
if var~=0
    for i=1:var
        ry(12+i,1)=-kbiol(1,i)*conc(12+i)*(conc(1)^nvect(i));
    end
end
end
end

```

- "Balance\_SBR"

```
function [ dydt ] = BalanceSBR(t,y,ncomp,don,vol,kla,nvect)
```

```

Sosat=8.45; %gO2.m-3
var=ncomp-12;%number of micropollutants

```

```
dydt=zeros(ncomp,1);
```

```
%////////////////////////////////Balance SBR //////////////////////////////////
```

```

r=rate(y,don,var,nvect);
for i=1:ncomp
    if i==12
        oxy=1;
    else
        oxy=0;
    end
    dydt(i)=r(i)+oxy*kla*(Sosat-y(12));
end
end

```

- Script main program "MainPrgm\_SBR" for series 2 performed at SRT of 10 d and HRT of 4 hours /power law kinetic

```
clear
```

```

clc
close all
format long
%Reading files

fid=fopen('Stoichiometric_data.txt','r'); data1=textscan(fid,'%s %f %s');
fclose(fid); don=data1{2};
size(don)

fid=fopen('Conc_Ini.txt','r');data2=textscan(fid,'%s %f');
fclose(fid);Cini=data2{2};

fid=fopen('Reactors.txt','r');data4=textscan(fid,'%s %f %f');
fclose(fid);
vol=data4{2}; kla=data4{3}*24;% kla in d-1

tic

%User settings
var=5;%number of micropolluants
ncomp=var+12; %number of compounds (ASM1+micropolluants)

%Integration interval
to=0;
tf=0.125;% in days

% INITIALISATION OF CALCULATION
yo=Cini;%vector initial concentrations

options=odeset('RelTol',1e-8,'NonNegative',[]);

nvect=[0.51
0.56
0.45
0.44
0.50
];
[tout,yout]=ode23tb(@BalanceSBR,[to
tf],yo,options,ncomp,don,vol,kla,nvect);

%% Experimental points of MPs ( $\mu\text{mol}_m^{-3}$ )

tsmx=[0
15
45
60
90
120
150
170
];
CSMX=[4.664
4.356
3.905
3.542
3.221
2.787
2.585

```

```
2.427  
];
```

```
tbzt=[5  
15  
45  
60  
120  
150  
170  
];  
CBZT=[7.613  
7.319  
6.398  
5.974  
4.672  
4.210  
4.160  
];
```

```
trox=[0  
5  
45  
60  
90  
120  
170  
];  
CROX=[0.959  
0.957  
0.883  
0.875  
0.836  
0.824  
0.785  
];
```

```
tery=[5  
15  
30  
45  
90  
150  
170  
];  
CERY=[1.772  
1.723  
1.650  
1.614  
1.518  
1.364  
1.342  
];
```

```
tdcf=[5  
15  
30  
45  
60  
150
```

```

170
];
CDCF=[3.738
3.594
3.501
3.461
3.420
3.282
3.238
];

figure;
subplot(2,2,1),plot(toutmin,yout(:,13),'b-',tsmx,CSMX,'kx');
xlabel('time (min)'),ylabel('SMX (µmol_m^-3)'),axis([0 180 0 5])
subplot(2,2,2),plot(toutmin,yout(:,14),'b-',tbzt,CBZT,'kx');
xlabel('time (min)'),ylabel('BZT (µmol_m^-3)'),axis([0 180 0 10])
subplot(2,2,3),plot(toutmin,yout(:,15),'b-',trox,CROX,'kx');
xlabel('time (min)'),ylabel('ROX (µmol_m^-3)'),axis([0 180 0 2])

figure;
subplot(2,1,1),plot(toutmin,yout(:,16),'b-',tery,CERY,'kx');
xlabel('time (min)'),ylabel('ERY (µmol_m^-3)'),axis([0 180 0 2])
subplot(2,1,2),plot(toutmin,yout(:,17),'b-',tdcf,CDCF,'kx');
xlabel('time (min)'),ylabel('DCF (µmol_m^-3)'),axis([0 180 0 4])

vectvalfinalesNum=[
spline(toutmin,yout(:,13),170);
spline(toutmin,yout(:,14),170);
spline(toutmin,yout(:,15),170);
spline(toutmin,yout(:,16),170);
spline(toutmin,yout(:,17),170);
]

MatResult=[vectvalfinalesNum];

save SRT10joursHRT4h.txt MatResult -ASCII

toc

% save tf50Dt0P1Reacteurs50.mat

```



*Text IV. S5. User guide for a general configuration of the continuous system.*

**A. "MainPrgm\_cas":**

The main program of the cascade configuration (starting from 1 reactor) is similar to the batch system. The main program reads external files already shown in section 4.1 and supplementary files detailed in section 5.3.2.

The balances on the clarifier are in the main program and not in the same function as the other balance sheets because there is a lag in time. In fact, it is important to know the concentrations at the outlet of the last reactor at a given time  $t$  to calculate the sludge concentration and the outlet concentration of the clarifier. The balance sheets are thus made on the reactor (s) in the cascade. The concentration at the outlet of the last reactor found at time ( $T_f$ ) allows to calculate the sludge concentration and the concentration of the outlet flow after  $\tau_T$  and  $\tau_B$  by writing a balance on the clarifier named "balance\_clarifier ". The steady state solution was achieved by running the system for 5 days.

In general, the values requested from the user by the program "MainPrgm\_cas" could be:

- Number of reactors in the cascade
- Recirculation rate ( $0 < \alpha < 1$ )
- Number in cascade in parallel

The script of the "MainPrgm\_cas" performed on continuous system is presented in the following Text IV. S5a.

- *Text IV. S5a. Matlab script main program "MainPrgm\_cas" of continuous system.*

```
clear
clc
close all
format long e
%Reading files

fid=fopen('Data_stoichiometric.txt','r'); data1=textscan(fid,'%s %f');
fclose(fid); don=data1{2};
```

```

fid=fopen('Conc_entrance.txt','r');data2=textscan(fid,'%s %f');
fclose(fid);Ce=data2{2};

fid=fopen('Data_react.txt','r');data3=textscan(fid,'%s %f');
fclose(fid);para=data3{2};

fid=fopen('Reactors.txt','r');data4=textscan(fid,'%s %f %f');
fclose(fid);
vol=data4{2}; kla=data4{3}*24;% kLa in days

fid=fopen('Conc_initial.txt','r');data5=textscan(fid,'%s %f');
fclose(fid);Conc_initial=data5{2};

tic

prompt='Value of n, order of the reaction? ';
n=input(prompt);

%User settings
var=5;%number of micropolluants
ncomp=var+12;%number of compounds (ASM1+micropolluants)
jmax=5 %input(prompt); %nombre of CSTR reactors
prompt='Recirculation rate';
alpha=input(prompt);

jtot=jmax+1;%jmax reactors + large upstream reactor

%//////////////////////Integration interval
to=1e-3;
tf=100;

%//////////////////////initialisations
Ceff=zeros(ncomp,1);% concentrations of the top of the clarifier (clear
water)
CS=zeros(ncomp,1);%concentrations of the bottom of the reactor (sludge)
resu3=zeros(ncomp*jtot,1);
ResultsFin=zeros(ncomp,jtot);

%//////////////////////Flow rates
Deb(1)=para(1); %Qe=18446
Deb(2)=para(2); %QS=18446
Deb(3)=3*Deb(2);%QL=55338
Deb(4)=Deb(1)+Deb(2)+Deb(3);%Qtot=92230
Deb(5)=para(3);%QW=385
Deb(6)=Deb(1)-Deb(5);%Qout=18061
Deb(7)=Deb(4)-Deb(3);%QIC=36892
Deb(8)=Deb(2)+Deb(5);%QBOC=18831
coef=Deb(6)/Deb(7); %outlet coefficient flow rate comparing of the inlet
flowrate entering the clarifier

% Qe=Deb(1);%Inlet flowrate into the system
% QS=Deb(2);%Sludge recycling flowrate equal to Qe max
% QL=Deb(3); %recycling rate of mixed liquor
Qtot=Deb(4);% total flowrate
% QW=Deb(5);%withdrawal flowrate (excess of sludge)
Qout=Deb(6);% output of clear water flowrate (Top of the clarifier)
QIC=Deb(7);% Clarifier inlet flowrate

```

```

QBOC=Deb(8);% Bottom output flowrate of the clarifier
% Q=Deb(9); % Flowrate circulating in the cascade
Q=Qtot;

%Volumes of reactors
% V=zeros(jmax,1);
% VRA=vol(1);
% VGR=vol(2);
Vdec=vol(2);
VT=vol(3);
Vb=Vdec-VT;

options=odeset('RelTol',1e-8);%,'NonNegative',[,]);

nT=12; % number of cells in cascade representing the upper part of the
clarifier
nB=12; % number of cells in cascade representing the bottom part of the
clarifier

%%% INITIALISATION in the cascade of reactors
for i=1:ncomp
    for j=1:jtot
        yo(j+jtot*(i-1))=Conc_initial(i);
    end
end

%%% INITIALISATION IN THE CLARIFIER
yodec=ones(ncomp*nT+ncomp*nB,1);%vector initial concentrations in the
clarifier
for jc=1:nT
    for ic=1:ncomp
        if ic==1 ||ic==2 ||ic==3 || ic==5 || ic== 9 || ic==11 %Non-soluble
compounds
            yodec((jc-1)*ncomp+ic)=0; % insolubles have concentration equal
to zero on the top of the clarifier
        else
            yodec((jc-1)*ncomp+ic)=Conc_initial(ic); %initial
concentrations in the last reactor
        end
    end
end

for jc=1:nB
    for ic=1:ncomp
        if ic==1 ||ic==2 ||ic==3 ||ic==5||ic==9||ic==11%Solubles compounds

            yodec(ncomp*nT+(jc-1)*ncomp+ic)=(QIC*Conc_initial(ic)-
Qout*yodec((jc-1)*ncomp+ic))/QBOC;

        else

            yodec(ncomp*nT+(jc-1)*ncomp+ic)=Conc_initial(ic);% initial
concentrations in the last reactor
        end
    end
end

```

```

        end
    end
end

ydeckP1=yodec;
ykP1=yo;

Dt=0.001 % Time step (d-1)
tvect=[to:Dt:tf];
resu3tps=zeros(jtot*ncomp,length(tvect));
resu3tps(:,1)=yo;

for it=1:(length(tvect)-1)%t=tvect
%     k=k+1
    it
    tk=tvect(it);
    tkP1=tvect(it+1)
    tps=[tk tkP1];
    yk=ykP1;
    [tout,yout]=ode15s(@ (t,y)
balance_cas(t,y,ncomp,jmax,alpha,Deb,Ce,don,CS,vol,kla,n),tps,yk,options);
    ykP1=yout(end,:);
    resu3tps(:,it+1)=ykP1;
% ykP1 column vector that contains compound 1 in the jmax reactors, then
the
% compound 2 in the jmax reactors .... up to ncomp in the jmax reactors
% resu3tps is a matrix that contains in its columns the ykpl at different
times

% concentrations at the outlet of the cascade and thus at the inlet of
% the clarifier
for i=1:ncomp
    CenterC(i)=yk(i*jtot);
    CenterCtps(i,it)=CenterC(i);
end

tpsdec=[tk tkP1];
ydeck=ydeckP1;

[toutdec,youtdec]=ode15s(@ (t,ydec)
balance_clarifier(t,ydec,ncomp,nT,nB,coef,VT,Vb,QIC,
CenterC,tk),tpsdec,ydeck,options);
    ydeckP1=youtdec(end,:);

for i=1:ncomp
    Ceff(i)=ydeckP1((nT-1)*ncomp+i);
    CS(i)=ydeckP1(ncomp*nT+(nB-1)*ncomp+i);
    Cefftps(i,it)=Ceff(i);
    CStps(i,it)=CS(i);
end
end
end

```

```

Resultstps=zeros(ncomp,jtot,length(tvect));
for k=1:ncomp*jtot
    div=k/jtot;
    if round(div)==div
        i=floor(k/jtot);
    else
        i=floor(k/jtot)+1;
    end
    j=k-jtot*(i-1);
    ResultsEnd(i,j)=resu3tps(k,end); % matrix of the concentrations ranked
by reactor with tf
    Resultstps(i,j,:)=resu3tps(k,:); % 3D matrix that contains the equivalent
of ResultsFin (i, j) at every such time
end

    ResultstpsLastReactor=zeros(ncomp,length(tvect))
for it=1:ncomp,

    ResultstpsLastReactor(it,:)=Resultstps(it,end,:);
% matrix that contains all the compounds in the last reactor as a function
of time
end

figure(1); % MACROPOLLUENTS OVER TIME IN THE LAST REACTOR OF THE CASCADE
subplot(3,3,1),plot(tvect,ResultstpsLastReactor(1,:));
xlabel('Time'),ylabel('XBH (g/m^3)'),
subplot(3,3,2),plot(tvect,ResultstpsLastReactor(2,:));
xlabel('Time'),ylabel('XBA (g/m^3)'),
subplot(3,3,3),plot(tvect,ResultstpsLastReactor(3,:));
xlabel('Time'),ylabel('XP (g/m^3)'),
subplot(3,3,4),plot(tvect,ResultstpsLastReactor(4,:));
xlabel('Time'),ylabel('SS (g/m^3)'),
subplot(3,3,5),plot(tvect,ResultstpsLastReactor(5,:));
xlabel('Time'),ylabel('XS (g/m^3)'),
subplot(3,3,6),plot(tvect,ResultstpsLastReactor(6,:));
xlabel('Time'),ylabel('SNO (g/m^3)'),
subplot(3,3,7),plot(tvect,ResultstpsLastReactor(7,:));
xlabel('Time'),ylabel('SNH (g/m^3)'),
subplot(3,3,8),plot(tvect,ResultstpsLastReactor(8,:));
xlabel('Time'),ylabel('SND (g/m^3)'),

figure(2); % MACROPOLLUTANTS AND MICROPOLLUTANTS OVER TIME IN THE LAST
REACTOR OF THE CASCADE
subplot(3,3,1),plot(tvect,ResultstpsLastReactor(9,:));xlabel('Time'),ylabel
('XND (g/m^3)'),
subplot(3,3,2),plot(tvect,ResultstpsLastReactor(10,:));xlabel('Time'),ylabe
l('SI (g/m^3)'),
subplot(3,3,3),plot(tvect,ResultstpsLastReactor(11,:));xlabel('Time'),ylabe
l('XI (g/m^3)'),
subplot(3,3,4),plot(tvect,ResultstpsLastReactor(12,:));xlabel('Time'),ylabe
l('SO (g/m^3)'),
subplot(3,3,5),plot(tvect,ResultstpsLastReactor(13,:),tvect,Ce(13)*ones(siz
e(tvect)), 'g--');xlabel('temps'),ylabel('SMX (µmol_m^-3)'),
subplot(3,3,6),plot(tvect,ResultstpsLastReactor(14,:),tvect,Ce(14)*ones(siz
e(tvect)), 'g--');xlabel('temps'),ylabel('BZT (µmol_m^-3)'),
subplot(3,3,7),plot(tvect,ResultstpsLastReactor(15,:),tvect,Ce(15)*ones(siz
e(tvect)), 'g--');xlabel('temps'),ylabel('ROX (µmol_m^-3)'),

```

```

subplot(3,3,8),plot(tvect,ResultstpsLastReactor(16,:),tvect,Ce(16)*ones(size(tvect)), 'g--');xlabel('temps'),ylabel('ERY (µmol_m^-3)'),
subplot(3,3,9),plot(tvect,ResultstpsLastReactor(17,:),tvect,Ce(17)*ones(size(tvect)), 'g--');xlabel('temps'),ylabel('DCF (µmol_m^-3)'),

```

```

figure(3);
subplot(3,3,1),plot((1:jmax),ResultsEnd(1,2:jtot));
xlabel('reactor'),ylabel('XBH (g/m^3)'),
subplot(3,3,2),plot((1:jmax),ResultsEnd(2,2:jtot));
xlabel('reactor'),ylabel('XBA (g/m^3)'),
subplot(3,3,3),plot((1:jmax),ResultsEnd(3,2:jtot));
xlabel('reactor'),ylabel('XP (g/m^3)'),
subplot(3,3,4),plot((1:jmax),ResultsEnd(4,2:jtot));
xlabel('reactor'),ylabel('SS (g/m^3)'),
subplot(3,3,5),plot((1:jmax),ResultsEnd(5,2:jtot));
xlabel('reactor'),ylabel('XS (g/m^3)'),
subplot(3,3,6),plot((1:jmax),ResultsEnd(6,2:jtot));
xlabel('reactor'),ylabel('SNO (g/m^3)'),
subplot(3,3,7),plot((1:jmax),ResultsEnd(7,2:jtot));
xlabel('reactor'),ylabel('SNH (g/m^3)'),
subplot(3,3,8),plot((1:jmax),ResultsEnd(8,2:jtot));
xlabel('reactor'),ylabel('SND (g/m^3)'),

```

```

figure(4);
subplot(3,3,1),plot((1:jmax),ResultsEnd(9,2:jtot));xlabel('reactor'),ylabel('XND (g/m^3)'),
subplot(3,3,2),plot((1:jmax),ResultsEnd(10,2:jtot));xlabel('reactor'),ylabel('SI (g/m^3)'),
subplot(3,3,3),plot((1:jmax),ResultsEnd(11,2:jtot));xlabel('reactor'),ylabel('XI (g/m^3)'),
subplot(3,3,4),plot((1:jmax),ResultsEnd(12,2:jtot));xlabel('reactor'),ylabel('SO (g/m^3)'),
subplot(3,3,5),plot((1:jmax),ResultsEnd(13,2:jtot));xlabel('reactor'),ylabel('SMX (µmol_m^-3)'),
subplot(3,3,6),plot((1:jmax),ResultsEnd(14,2:jtot));xlabel('reactor'),ylabel('BZT (µmol_m^-3)'),
subplot(3,3,7),plot((1:jmax),ResultsEnd(15,2:jtot));xlabel('reactor'),ylabel('ROX (µmol_m^-3)'),
subplot(3,3,8),plot((1:jmax),ResultsEnd(16,2:jtot));xlabel('reactor'),ylabel('ERY (µmol_m^-3)'),
subplot(3,3,9),plot((1:jmax),ResultsEnd(17,2:jtot));xlabel('reactor'),ylabel('DCF (µmol_m^-3)'),

```

```

disp('Concentrations at the final time Tf in the last reactor')
ResultstpsLastReactor(:,end)

```

```

CSBench=[5007.7,292.9,884.3,0.89,96.42,10.42,1.73,0.69,6.9,30,2247.1,0.49]';
RelativeDeviationCS=(CS(1:12)-CSBench)./CSBench
CeffBench=[9.78,0.57,1.73,0.89,0.19,10.42,1.73,0.69,6.9,30,4.39,0.49]';
RelativeDeviationCeff=(Ceff(1:12)-CeffBench)./CeffBench

```

```

disp('CS and Ceff MACROPOLLUANTS at Tf')
[CS(1:12) Ceff(1:12)]

```

```

disp('CS and Ceff MICROPOLLUANTS at Tf')
[CS(13:17) Ceff(13:17)]
% [CStps(13:17,end) Cefftps(13:17,end)]

```

```

figure(5); subplot(3,4,1),title('CS Macropolluants');
subplot(3,4,1),plot(tvect(2:end),CStps(1,:), 'b-', [tvect(1)
tvect(end)], [CSBench(1) CSBench(1)], 'r--'); xlabel('Time'),ylabel('XBH
(g/m^3)'),
subplot(3,4,2),plot(tvect(2:end),CStps(2,:), 'b-', [tvect(1)
tvect(end)], [CSBench(2) CSBench(2)], 'r--'); xlabel('Time'),ylabel('XBA
(g/m^3)'),
subplot(3,4,3),plot(tvect(2:end),CStps(3,:), 'b-', [tvect(1)
tvect(end)], [CSBench(3) CSBench(3)], 'r--'); xlabel('Time'),ylabel('XP
(g/m^3)'),
subplot(3,4,4),plot(tvect(2:end),CStps(4,:), 'b-', [tvect(1)
tvect(end)], [CSBench(4) CSBench(4)], 'r--'); xlabel('Time'),ylabel('SS
(g/m^3)'),
subplot(3,4,5),plot(tvect(2:end),CStps(5,:), 'b-', [tvect(1)
tvect(end)], [CSBench(5) CSBench(5)], 'r--'); xlabel('Time'),ylabel('XS
(g/m^3)'),
subplot(3,4,6),plot(tvect(2:end),CStps(6,:), 'b-', [tvect(1)
tvect(end)], [CSBench(6) CSBench(6)], 'r--'); xlabel('Time'),ylabel('SNO
(g/m^3)'),
subplot(3,4,7),plot(tvect(2:end),CStps(7,:), 'b-', [tvect(1)
tvect(end)], [CSBench(7) CSBench(7)], 'r--'); xlabel('Time'),ylabel('SNH
(g/m^3)'),
subplot(3,4,8),plot(tvect(2:end),CStps(8,:), 'b-', [tvect(1)
tvect(end)], [CSBench(8) CSBench(8)], 'r--'); xlabel('Time'),ylabel('SND
(g/m^3)'),
subplot(3,4,9),plot(tvect(2:end),CStps(9,:), 'b-', [tvect(1)
tvect(end)], [CSBench(9) CSBench(9)], 'r--'); xlabel('Time'),ylabel('XND
(g/m^3)'),
subplot(3,4,10),plot(tvect(2:end),CStps(10,:), 'b-', [tvect(1)
tvect(end)], [CSBench(10) CSBench(10)], 'r--'); xlabel('Time'),ylabel('SI
(g/m^3)'),
subplot(3,4,11),plot(tvect(2:end),CStps(11,:), 'b-', [tvect(1)
tvect(end)], [CSBench(11) CSBench(11)], 'r--');
xlabel('Time'),ylabel('XI(g/m^3)'),
subplot(3,4,12),plot(tvect(2:end),CStps(12,:), 'b-', [tvect(1)
tvect(end)], [CSBench(12) CSBench(12)], 'r--'); xlabel('Time'),ylabel('SO
(g/m^3)'),

```

```

figure(6); subplot(3,2,1),title('CS Micropolluants');
subplot(3,2,1),plot(tvect(2:end),CStps(13,:), 'b-');
xlabel('Time'),ylabel('SMX (μmol_m^-3)'),
subplot(3,2,2),plot(tvect(2:end),CStps(14,:), 'b-');
xlabel('Time'),ylabel('BZT (μmol_m^-3)'),
subplot(3,2,3),plot(tvect(2:end),CStps(15,:), 'b-');
xlabel('Time'),ylabel('ROX (μmol_m^-3)'),
subplot(3,2,4),plot(tvect(2:end),CStps(16,:), 'b-');
xlabel('Time'),ylabel('ERY (μmol_m^-3)'),
subplot(3,2,5),plot(tvect(2:end),CStps(17,:), 'b-');
xlabel('Time'),ylabel('DCF (μmol_m^-3)'),

```

```

figure(7); subplot(3,4,1), title('Ceff Macropolluants');
subplot(3,4,1),plot(tvect(2:end),Cefftps(1,:), 'b-', [tvect(1)
tvect(end)], [CeffBench(1) CeffBench(1)], 'r--'); xlabel('Time'),ylabel('XBH
(g/m^3)'),
subplot(3,4,2),plot(tvect(2:end),Cefftps(2,:), 'b-', [tvect(1)
tvect(end)], [CeffBench(2) CeffBench(2)], 'r--'); xlabel('Time'),ylabel('XBA
(g/m^3)'),

```

```

subplot(3,4,3),plot(tvect(2:end),Ceffftps(3,:), 'b-', [tvect(1)
tvect(end)], [CeffBench(3) CeffBench(3)], 'r--'); xlabel('Time'),ylabel('XP
(g/m^3)'),
subplot(3,4,4),plot(tvect(2:end),Ceffftps(4,:), 'b-', [tvect(1)
tvect(end)], [CeffBench(4) CeffBench(4)], 'r--'); xlabel('Time'),ylabel('SS
(g/m^3)'),
subplot(3,4,5),plot(tvect(2:end),Ceffftps(5,:), 'b-', [tvect(1)
tvect(end)], [CeffBench(5) CeffBench(5)], 'r--'); xlabel('Time'),ylabel('XS
(g/m^3)'),
subplot(3,4,6),plot(tvect(2:end),Ceffftps(6,:), 'b-', [tvect(1)
tvect(end)], [CeffBench(6) CeffBench(6)], 'r--'); xlabel('Time'),ylabel('SNO
(g/m^3)'),
subplot(3,4,7),plot(tvect(2:end),Ceffftps(7,:), 'b-', [tvect(1)
tvect(end)], [CeffBench(7) CeffBench(7)], 'r--'); xlabel('Time'),ylabel('SNH
(g/m^3)'),
subplot(3,4,8),plot(tvect(2:end),Ceffftps(8,:), 'b-', [tvect(1)
tvect(end)], [CeffBench(8) CeffBench(8)], 'r--'); xlabel('Time'),ylabel('SND
(g/m^3)'),
subplot(3,4,9),plot(tvect(2:end),Ceffftps(9,:), 'b-', [tvect(1)
tvect(end)], [CeffBench(9) CeffBench(9)], 'r--'); xlabel('Time'),ylabel('XND
(g/m^3)'),
subplot(3,4,10),plot(tvect(2:end),Ceffftps(10,:), 'b-', [tvect(1)
tvect(end)], [CeffBench(10) CeffBench(10)], 'r--'); xlabel('Time'),ylabel('SI
(g/m^3)'),
subplot(3,4,11),plot(tvect(2:end),Ceffftps(11,:), 'b-', [tvect(1)
tvect(end)], [CeffBench(11) CeffBench(11)], 'r--');
xlabel('Time'),ylabel('XI (g/m^3)'),
subplot(3,4,12),plot(tvect(2:end),Ceffftps(12,:), 'b-', [tvect(1)
tvect(end)], [CeffBench(12) CeffBench(12)], 'r--'); xlabel('Time'),ylabel('SO
(g/m^3)'),

```

```

figure(8); title('Ceff Micropolluants');
subplot(3,2,1),plot(tvect(2:end),Ceffftps(13,:), 'b-');
xlabel('Time'),ylabel('SMX (μmol_m^-3)'),
subplot(3,2,2),plot(tvect(2:end),Ceffftps(14,:), 'b-');
xlabel('Time'),ylabel('BZT (μmol_m^-3)'),
subplot(3,2,3),plot(tvect(2:end),Ceffftps(15,:), 'b-');
xlabel('Time'),ylabel('ROX (μmol_m^-3)'),
subplot(3,2,4),plot(tvect(2:end),Ceffftps(16,:), 'b-');
xlabel('Time'),ylabel('ERY (μmol_m^-3)'),
subplot(3,2,5),plot(tvect(2:end),Ceffftps(17,:), 'b-');
xlabel('Time'),ylabel('DCF (μmol_m^-3)'),

```

```

figure(9); title('Micropollutant concentration at the inlet of the
clarifier')

```

```

subplot(3,2,1),plot(tvect(2:end), CenterCtps(13,:), 'b-');
xlabel('Time'),ylabel('SMX (μmol_m^-3)'),
subplot(3,2,2),plot(tvect(2:end), CenterCtps(14,:), 'b-');
xlabel('Time'),ylabel('BZT (μmol_m^-3)'),
subplot(3,2,3),plot(tvect(2:end), CenterCtps(15,:), 'b-');
xlabel('Time'),ylabel('ROX (μmol_m^-3)'),
subplot(3,2,4),plot(tvect(2:end), CenterCtps(16,:), 'b-');
xlabel('Time'),ylabel('ERY (μmol_m^-3)'),
subplot(3,2,5),plot(tvect(2:end), CenterCtps(17,:), 'b-');
xlabel('Time'),ylabel('DCF (μmol_m^-3)'),

```

toc



```

% save tf50Dt0P1Reactors50.mat

% RelativeStandardDeviation ./ . BENCHMARK
% Benchmark values
ValBench=[
%R1      R2      R3      R4      R5
2551.8    2553    2557    2259    2559.4    %XB,H
148.4     148     149     150     149.8    %XB,A
448.9     450     450     451     452.2    %XP
2.81      1.46    1.15    0.995   0.89     %SS
82.14    76.4    64.9    55.7    49.31    %XS
5.37      3.66    6.54    9.30    10.42    %SNO
7.92      8.34    5.55    2.97    1.73     %SNH
1.22      0.882   0.829   0.767   0.69     %SND
5.28      5.03    4.39    3.88    3.53     %XND
30         30      30      30      30       %SI
1149.2    1149    1149    1149    1149.2   %XI
0.00430   0.0000631  1.72    2.43    0.49     %SO
];

RelativeDeviation=(ResultsEnd(1:12,2:end)-ValBench) ./ValBench

```

## B. "balance\_clarifier"

Function that contain the material balances on the top and bottom part of the clarifier for soluble and non-soluble compounds. Since the Matlab functions integrate vectors, a vector "y<sub>dec</sub>" containing the concentrations has been defined divided into two main parts: Top part and bottom part. The indices  $i_c$  and  $j_c$  respectively denote the compound  $i$  and the cell  $j_c$  of the clarifier ( $1 < i < n_{comp}$  and  $1_T < j_{cT} < n_T$  for the top cascade of reactors of the clarifier and  $1 < j_{cB} < n_B$  for the bottom cascade of reactors of the clarifier). Thus  $C(i, j_c)$  denotes the concentration of compound  $i$  in cell  $j_c$ . The vector  $y_{dec}$  is defined as follows:

$$\begin{array}{c}
 \begin{array}{c}
 C_{1,1T} \\
 C_{2,1T} \\
 C_{3,1T} \\
 C_{4,1T} \\
 \vdots \\
 \vdots \\
 C_{ncomp,1T} \\
 C_{1,nreact} \\
 C_{2,nreact} \\
 C_{3,nreact} \\
 C_{ncomp,nreact}
 \end{array} \\
 \text{Top of the clarifier} \\
 \dots\dots\dots \\
 \begin{array}{c}
 C_{1,1B} \\
 C_{2,1B} \\
 C_{3,1B} \\
 C_{4,1B} \\
 \vdots \\
 \vdots \\
 \vdots \\
 C_{ncomp,1B} \\
 \vdots \\
 \vdots \\
 C_{ncomp,nreactB}
 \end{array} \\
 \text{Bottom of the clarifier}
 \end{array}$$

The script of the "balance\_ clarifier " performed on continuous system is detailed in the following Text IV. S5b.

- Text IV. S5b. "balance\_ clarifier " file of continuous system.

```

function [dydtdec]= balance_ clarifier (t,ydec,ncomp,nT,nB,coef,VT,Vb,QIC,
CenterC,tk)

viT=VT/nT;
viB=Vb/nB;
Qout=coef*QIC;% In real WWTPSs, coef is very close to half up and half down
(coef = 0.5)
QBOC=(1-coef)*QIC;

CenterCT= CenterC;
for ic= 1:ncomp
    if ic==1 ||ic==2 ||ic==3 || ic==5 || ic== 9 || ic==11 %Non-soluble (MPs
are considered as soluble compounds)
        CenterCT(ic)=0; %Concentrations of insoluble are assumed to be
zero at the entrance of the upper part (the insolubles go only in the lower
part)
    end
end

CenterCB= CenterC; % the concentration of soluble and non-soluble
compounds at the bottom of the clarifier
%is equal to that of the output of the cascade
for ic= 1:ncomp

```

```

    if ic==1 ||ic==2 ||ic==3 ||ic==5||ic==9||ic==11% Non-soluble compounds
        CenterCB(ic)=(QIC* CenterC(ic)-Qout* CenterCT(ic))/QBOC;
    end
end

%%% the vector ydec contains in its first part the concentrations in the
% high part of the clarifier as following:
% the 1st solute in the 1st reactorT,
% then the 2nd solute in the 1st reactorT,
% then the ncomp-th solute in the 1st reactorT
% ...
% then from 1st to ncomp-th solute in 2nd reactorT
% then from 1st to ncomp-th solute in n reaction
%%% and in its 2nd part the concentration in the
% lower part of the clarifier as following:
% the first solute in the first reactorB,
% then the 2nd solute in the first reactorB,
% then the ncomp-th solute in the first reactorB
% ...
% then from the 1st to the ncomp-th solute in the nB
% then from 1st to ncomp-th solute in n reactorB
%%% Its size is therefore ncomp * nT + ncomp * nB

% Balance at node 2 before entering the clarifier for all compounds since
% the soluble go up and down, (CBOC=Cout)
% For all compounds, the balance is written as following:
QIC*CBIC=QBOC*CBOC + QOUT*Cout
% However, this balance was used to calculate CBOC of non soluble noted by
CenterB
% Be careful, you can express the loss of biomass that does not decant
% (i.e, Benchmark case)
% or and if you wanted to express different flow rates in each branch
% with respect to that entering the clarifier with 0 <coef <1;

% Balance on the top of the clarifier
for ic= 1:ncomp
    jc=1; % distinguish first reactor
    dydtdec((jc-1)*ncomp+ic)= Qout/viT*( CenterCT(ic)-ydec((jc-
1)*ncomp+ic));

    for jc= 2:nT
        dydtdec((jc-1)*ncomp+ic)= Qout/viT*(ydec((jc-2)*ncomp+ic)-ydec((jc-
1)*ncomp+ic));
    end
end

% Balance on the bottom part of the clarifier
for ic= 1:ncomp
    jc=1; % distinguish first reactor
    dydtdec(ncomp*nT+(jc-1)*ncomp+ic)= QBOC/viB*( CenterCB(ic)-
ydec(ncomp*nT+(jc-1)*ncomp+ic));

    for jc= 2:nB
        dydtdec(ncomp*nT+(jc-1)*ncomp+ic)= QBOC/viB*(ydec(ncomp*nT+(jc-
2)*ncomp+ic)-ydec(ncomp*nT+(jc-1)*ncomp+ic));
    end
end

dydtdec=dydtdec';

```

### C. "balance\_cas"

Function that contain the derivatives of the concentrations defined from the material balances of each compound in the reactor (s) of the cascade (s). This is the file that will be changed at the material balance according to the further studied hydrodynamics in order to verify the kinetics of micropollutants in the following sections. However, the vector " $y_{cas}$ " still remain of the same general configuration as follows:

$$y_{cas} = \begin{bmatrix} C_{1,UR} \\ C_{1,1} \\ C_{1,2} \\ C_{1,3} \\ \cdot \\ \cdot \\ C_{1,jmax} \\ C_{2,UR} \\ C_{2,1} \\ C_{2,2} \\ C_{2,3} \\ \cdot \\ \cdot \\ C_{2,jmax} \\ \cdot \\ \cdot \\ C_{ncomp,UR} \\ \cdot \\ \cdot \\ C_{ncomp,jmax} \end{bmatrix}$$

The variables of inputs of the function "balance\_cas" are the following:

- Time t
- Vector [y]
- ncomp: the number of compounds
- alpha: recirculation rate
- jmax: the number of reactors in the cascades
- Deb: vector containing the input flowrates

- $C_e$ : inlet concentrations
- don: vector where kinetic and stoichiometric data are stored
- $C_s$ : concentrations in sludge
- vol: reactor volumes
- $k_{LA}$ : reactor transfer coefficients
- conc\_initial: concentrations in mixed liquor at time  $t_0$ .

Exit:

[dydt]: vector containing the derivatives of the concentrations, that is to say the derivatives of the vector  $y$ .

To reduce the time taken by the program, and to facilitate understanding of the code, the matrix  $A$  of concentrations arranged by reactors has been defined:

$$A = \begin{bmatrix} C_{1,UR} & C_{1,1} & C_{1,2} & C_{1,3} & \dots & \dots & C_{1,jmax} \\ C_{2,UR} & C_{2,1} & C_{2,2} & C_{2,3} & \dots & \dots & C_{2,jmax} \\ \cdot & \cdot & \cdot & \cdot & \dots & \dots & \cdot \\ \cdot & \cdot & \cdot & \cdot & \dots & \dots & \cdot \\ \cdot & \cdot & \cdot & \cdot & \dots & \dots & \cdot \\ C_{ncomp,UR} & C_{ncomp,1} & C_{ncomp,2} & C_{ncomp,3} & \dots & \dots & C_{ncomp,jmax} \end{bmatrix}$$

The matrix  $A$  was used in the "balance\_cas". In the same way, a matrix  $B$  containing the derivatives of the concentrations was defined. Further details on the script of the "balance\_cas" in continuous system were provided in Text IV. S5c.

- Text IV. S5c. "balance\_cas" file of continuous system.

```
function [dydt] = balance_cas % Material balances for the cascade of
reactors
(t,y,ncomp,jmax,alpha,Deb,Ce,don,CS,vol,kla,n)
% eqvect: material balance of ASM1 + micropollutants
% output: derived from concentrations of dydt compounds (ncomp * jtot)

%%% the vector contains
% 1st solute in all reactors up to the jmax reactor,
% then the 2nd solute in the jmax reactors,
% then the 3rd solute in the jmax reactors
```

```

% ...
% then the ncomp-th solute in the jmax reactors

%%%%%%%%%%%%%%%%%%%%%%%%%%%%%%%%%%%%%%%%%%%%%%%%%%%%%%%%%%%%%%%%%%%%%%%%Flow rates
Qe=Deb(1);
QS=Deb(2);
QL=Deb(3);
Qtot=Deb(4);
Q=Qtot;
Sosat=8; %gO2.m-3
var=ncomp-12;%number of micropolluants
jtot=jmax+1;

%%%%%%%%%%%%%%%%%%%%%%%%%%%%%%%%%%%%%%%%%%%%%%%%%%%%%%%%%%%%%%%%%%%%%%%%volume of reactors%%%%%%%%%%%%%%%%%%%%%%%%%%%%%%%%%%%%%%%%%%%%%%%%%%%%%%%%%%%%%%%%%%%%%%%%
V=zeros(jtot,1);

V(1)=vol(1); %large upsetram reactor
Vdec=vol(2); %clarifier
VT=vol(3);
Vb=Vdec-VT;

for j=2:jtot
    V(j)=vol(2+j);%volume of the reactors in the cascade
end

%%%%%%%%%%%%%%%%%%%%%%%%%%%%%%%%%%%%%%%%%%%%%%%%%%%%%%%%%%%%%%%%%%%%%%%%values of kla%%%%%%%%%%%%%%%%%%%%%%%%%%%%%%%%%%%%%%%%%%%%%%%%%%%%%%%%%%%%%%%%%%%%%%%%
klar=zeros(jtot,1);
klar(1)=kla(1);
for j=2:jtot
    klar(j)=kla(2+j);
end

%initialisations
A=zeros(ncomp,jtot);
B=zeros(ncomp,jtot);
vit=zeros(ncomp,jtot);
ctot=zeros(ncomp,1); %Inlet concentration of the first reactor of the
cascade
dydt=zeros(ncomp*jtot,1);
ycor=zeros(ncomp*jtot,1);

for i=1:ncomp*(jtot)
    if y(i)<0
        ycor(i)=0;
    else
        ycor(i)=y(i);
    end
end

for k=1:ncomp*jtot
    div=k/jtot;
    if round(div)==div
        i=floor(k/jtot);
    else

```

```

        i=floor(k/jtot)+1;
    end
    j=k-jtot*(i-1);
    vit(i,j)=ycor(k);
    A(i,j)=y(k); %matrix of concentrations arranged per reactor
end
% Each line of A corresponds to a different compound i
% each column of A corresponds to a different reactor
% first contains the compound 1 in the jmax reactors, then the
% compound 2 in the jmax reactors .... up to ncomp in the jmax
% reactors

% Balance at node 1 before the big upstream reactor
% to calculate Ctot
for i=1:ncomp
ctot(i)=(Qe*Ce(i)+QS*CS(i)+QL*A(i,jtot))/Qtot;%((Qe+QS)*A(i,1)+QL*A(i,jtot)
)/Qtot;
end

%% Balance in the large reactor upstream
r=Rate(vit(:,1),don,var,n);
for i=1:ncomp
    if i==12
        oxy=1;
    else
        oxy=0;
    end
    B(i,1)=(Qtot/V(1))*(ctot(i)-A(i,1))+r(i)+oxy*klar(1)*(Sosat-A(12,1));
end

%%%%%%%%%%%%%%%%%%%%%%%%%%%%%%%%%%%%%%%%%%%%%%%%%%%%%%%%%%%%%%%%%%%%%%%%%%%%%%réacteur 1
r=Rate(vit(:,2),don,var,n);
for i=1:ncomp
    if i==12
        oxy=1;
    else
        oxy=0;
    end
    B(i,2)=Q/V(2)*(A(i,1)+alpha*A(i,3)-
(1+alpha)*A(i,2))+r(i)+oxy*klar(2)*(Sosat-A(12,2));
end

%%%%%%%%%%%%%%%%%%%%%%%%%%%%%%%%%%%%%%%%%%%%%%%%%%%%%%%%%%%%%%%%%%%%%%%%%%%%%%reactors 2 to 4
for j=3:jtot-1
    ry=Rate(vit(:,j),don,var,n);
    for i=1:ncomp
        if i==12
            oxy=1;
        else
            oxy=0;
        end
        B(i,j)=Q/V(j)*((1+alpha)*A(i,j-1)+alpha*A(i,j+1)-
(1+2*alpha)*A(i,j))+ry(i)+oxy*klar(j)*(Sosat-A(12,j));
    end
end

%%%%%%%%%%%%%%%%%%%%%%%%%%%%%%%%%%%%%%%%%%%%%%%%%%%%%%%%%%%%%%%%%%%%%%%%%%%%%%last reactor
ryl=Rate(vit(:,jtot),don,var,n);

```

```

for i=1:ncomp
    if i==12
        oxy=1;
    else
        oxy=0;
    end
    B(i,jtot)=Q/V(jtot)*((1+alpha)*A(i,jtot-1)-
(1+alpha)*A(i,jtot))+ryl(i)+oxy*klar(jtot)*(Sosat-A(12,jtot));
end

%///// Convert the matrix A into a vector y ///////////
for k=1:ncomp*jtot
    div=k/jtot;
    if round(div)==div
        i=floor(k/jtot);
    else
        i=floor(k/jtot)+1;
    end
    j=k-jtot*(i-1);
%   y(k)=A(i,j); %Matrix of concentrations per reactor
    dydt(k)=B(i,j);
% Each line of B corresponds to a different compound i
% each column of B corresponds to a different reactor
% dydt first contains compound 1 in the jmax reactors, then the
% compound 2 in the jmax reactors .... up to ncomp in the jmax
% reactors
end
end

```

#### D. "Rate"

"Rate" is the function that calculates the rates of each compound in all the reactors and "vit" is a matrix defined from the matrix A. This matrix has been defined to avoid that the concentrations become negative, which is not possible physically but can be mathematically. Thus, the matrix "vit" takes the values of the concentrations of the matrix A, but set to zero as soon as a concentration is negative. Therefore, we do not take into account the production of a compound whose rate has become negative. The Function "Rate" of continuous system is presented in the following Text IV. S5d.

- *Text IV. S5d. Function "Rate" of continuous system.*

```

function [ry] = Rate(conc,don,var,n)
%Input:
%rate are the rates of the reactions of the ASM1 model+ MPs
%conc is the vector of size (ncomp, 1) containing the concentrations of the
compounds in a given reactor
%don is the stoichiometric data of ASM1 model
%stoechiometriques du modèle ASM1

```



```

%var is the number of micropollutants
%Output:
%ry is a vector of size ncomp containing the production rates of each
compound

muh=don(1); mua=don(2);
etah=don(3); etah=don(4);
KS=don(5); KOH=don(6);
KNO=don(7); KNH=don(8);
KOA=don(9); KX=don(10);
kh=don(11); bh=don(12);
ba=don(13); ka=don(14);
kbiol=zeros(1,var);
if var ~=0
    for i=1:var
        kbiol(1,i)=don(14+i)*24/(1000)^n; %convert in (m^3)^n/(gSS^n*d)
    end
end

Ya=0.24; %(g_XBACOD/gN_utilised)
Yh=0.67;%(g_XBHCOD/gCOD_utilised)
fp=0.08;%(dimensionless)
iXB=0.08;%(gN/gCOD_in_biomass)
iXP=0.06;%(gN/gCOD_in_XP)

% XBH=y(1,j); % XBA=y(2,j); % XP=y(3,j);
% SS=y(4,j); % XS=y(5,j);
% SNO=y(6,j); % SNH=y(7,j);
% SND=y(8,j); % XND=y(9,j);
% SI=y(10,j); % XI=y(11,j);
% SO=y(12,j);

                                %ASM1 model

%Aerobic growth of heterotrophic biomass
rate(1,1)=muh*(conc(4)/(KS+conc(4)))*(conc(12)/(KOH+conc(12)))*conc(1);
%Anoxic growth of heterotrophic biomass
rate(2,1)=muh*etah*(conc(4)/(KS+conc(4)))*(KOH/(KOH+conc(12)))*(conc(6)/(KNO+conc(6)))*conc(1);
%Growth of autotrophic biomass
rate(3,1)=mua*(conc(7)/(KNH+conc(7)))*(conc(12)/(KOA+conc(12)))*conc(2);
%Mortality of heterotrophic biomass
rate(4,1)=bh*conc(1)
%Mortality of autotrophic biomass
rate(5,1)=ba*conc(2);
%Ammonification of the soluble nitrogen compound
rate(6,1)=ka*conc(8)*conc(1);
%Hydrolysis of slowly biodegradable carbon compounds
rate(7,1)=kh*((conc(5)/conc(1))/(KX+(conc(5)/conc(1))))*((conc(12)/(KOH+conc(12)))+etah*(KOH/(KOH+conc(12)))*(conc(6)/(KNO+conc(6))))*conc(1);
%Hydrolysis of slowly biodegradable nitrogen compounds
rate(8,1)=rate(7)*conc(9)/conc(5);

%rate of each compound of ASM1
ry(1,1)=rate(1)+rate(2)-rate(4);
ry(2,1)=rate(3)-rate(5);
ry(3,1)=fp*(rate(4)+rate(5));
ry(4,1)=(-rate(1)-rate(2))/Yh+rate(7);
ry(5,1)=(1-fp)*(rate(4)+rate(5))-rate(7);
ry(6,1)=-((1-Yh)/(2.86*Yh))*rate(2)+rate(3)/Ya;

```

```

ry(7,1)=-iXB*(rate(1)+rate(2))-(iXB+(1/Ya))*rate(3)+rate(6);
ry(8,1)=rate(8)-rate(6);
ry(9,1)=(iXB-fp*iXP)*(rate(4)+rate(5))-rate(8);
ry(10,1)=0;
ry(11,1)=0;
ry(12,1)=-((1-Yh)/Yh)*rate(1)-((4.57-Ya)/Ya)*rate(3);

if var~=0
    for i=1:var
        ry(12+i,1)=-kbiol(1,i)*conc(12+i)*(conc(1)^n);
    end
end
end

```

All the following files are common for the continuous system. Moreover, the user has an open access to edit the external files according to the adapted configurations.

#### E. External files read by the mainProgram\_continuous system:

- 'Stoichiometric\_data.txt' is the same file used for batch system
- 'Conc\_initial.txt': the initial concentrations for all state variables of the system are presented

as following:

```

1  XBH(g_COD_m^-3) 2500
2  XBA(g_COD_m^-3) 190
3  XP(g_COD_m^-3) 870
4  SS(g_COD_m^-3) 14
5  XS(g_COD_m^-3) 200
6  SNO(g_N_m^-3) 5
7  SNH(g_N_m^-3) 4
8  SND(g_N_m^-3) 1.4
9  XND(g_N_m^-3) 6
10 SI(g_COD_m^-3) 18
11 XI(g_COD_m^-3) 1150
12 SO(g_O2_m-3) 0.4
13 Csulfametoxazole(μmol_m^-3) 0
14 Cbenzotriazole(μmol_m^-3) 0
15 Croxithromycin(μmol_m^-3) 0
16 Cerythromycin(μmol_m^-3) 0
17 Cdiclofenac(μmol_m^-3) 0

```

- 'Conc\_entrance.txt': is the file where are stored the inlet concentrations to the cascade, it corresponds to the concentrations of flow  $Q_e$ . Lines 1 to 12 below are the concentrations used for the simulation of the benchmark model. The average experimental concentrations

of the MPs (lines 13 to 19) will be useful in the following section regarding MPs' kinetic predictions on continuous system.

```
1 XBH(g_COD_m^-3) 28.17
2 XBA(g_COD_m^-3) 0
3 XP(g_COD_m^-3) 0
4 SS(g_COD_m^-3) 69.5
5 XS(g_COD_m^-3) 202.32
6 SNO(g_N_m^-3) 0
7 SNH(g_N_m^-3) 31.56
8 SND(g_N_m^-3) 6.95
9 XND(g_N_m^-3) 10.59
10 SI(g_COD_m^-3) 30
11 XI(g_COD_m^-3) 51.20
12 SO(g_O2_m-3) 0
13 Csulfametoxazole(μmol_m^-3) 4.56
14 Cbenzotriazole(μmol_m^-3) 7.57
15 Croxithromycin(μmol_m^-3) 0.97
16 Cerythromycin(μmol_m^-3) 1.71
17 Cdiclofenac(μmol_m^-3) 3.72
```

- 'data\_react.txt': contains the value of the inlet flow rate  $Q_e$ , the value of the sludge recycling  $Q_s$  and the sludge waste  $Q_w$ .

- 'Reactors.txt': is the same file as described for batch system. The data used for the simulation of the benchmark model is present below

```
1 U.R.upstream 0.0001 0
2 Decanter 6000 0
3 Volum_Top 3000 0
4 R1 1000 0
5 R2 1000 0
6 R3 1333 10
7 R4 1333 10
8 R5 1333 3.5
```

*Table IV. S4. Results obtained with Matlab.*

	Concentrations (g m <sup>-3</sup> )			
	First reactor	Last reactor	Bottom outlet of the clarifier	Top outlet of the clarifier
	XBH	2625.3	2630.4	5493.6
XBA	158.5	158.4	309.9	0.0
XP	506.7	509.8	983.6	0.0
SS	2.9	0.9	0.90	0.9
XS	84.3	49.7	97.2	0.0
SNO	5.4	10.5	10.5	10.3
SNH	8.1	1.7	1.7	1.7
SND	1.2	0.7	0.7	0.7
XND	5.3	3.5	6.9	0.0
SI	30.0	30.0	30.1	30.0
XI	1182.3	1178.7	2353	0.0
SO	0.45	0.5	0.5	0.5

*Table IV. S5. Inlet concentration and results of the benchmark model.*

	Concentrations (g m <sup>-3</sup> )				
	Inlet	First reactor	Last reactor	Bottom outlet of the clarifier	Top outlet of the clarifier
XBH	28.17	2551.8	2559.4	5004.7	9.78
XBA	0	148.4	149.8	292.9	0.57
XP	0	448.9	452.2	884.3	1.73
SS	69.5	2.81	0.89	0.89	0.89
XS	202.32	82.14	49.31	96.42	0.19
SNO	0	5.37	10.42	10.42	10.42
SNH	31.56	7.92	1.73	1.73	1.73
SND	6.95	1.22	0.69	0.69	0.69
XND	10.59	5.28	3.53	6.9	6.9
SI	30	30	30	30	30
XI	51.2	1149.2	1149.2	2247.1	4.39
SO	0	0	0.49	0.49	0.49

## Abstract

One of the main challenges currently facing environmental conservation is to reduce the discharge of micropollutants (MPs) from wastewater treatment plants outflows (WWTPs). Biological aerobic processes are the most commonly used treatment, but conventional systems were not conceived with the objective of eliminating micropollutants (MPs). In this work, the removal enhancement of seven micropollutants compounds (pharmaceuticals and industrial chemical) which cover various degree of biodegradability was studied using activated sludge process. To achieve this goal, an experimental methodology followed by a simulation strategy were developed. The systematic study of the impact of WWTPs operational parameters, such as sludge retention time (SRT), hydraulic retention time (HRT) and biomass concentration ( $C_{TSS}$ ), on the MPs removal was experimentally quantified in nine Sequencing Batch Reactor (SBR) setups. The enhancement of the SRT increased the removal of all the MPs except for two macrolides antibiotics. Application of a higher HRT did also improve MPs removal as could be expected from the measured removal rate constants. More interestingly, our results indicated that, contrary to what is postulated, the removal rate of micropollutants is not proportional to biomass concentration, especially for high ones. Compared to removal rates at 3 to 5  $g_{TSS} L^{-1}$  of biomass, an additional increase at 8  $g_{TSS} L^{-1}$  produced only an unexpected moderate effect. New kinetics of the power law have been studied to cover the full range of biomass concentration conditions in activated sludge systems. It takes into account the limitation of the transport of micropollutants to biomass when its concentration is high. In this case, it has also been shown that the transport of micropollutants is based on molecular diffusion. This process has been added to the proposed kinetic equation. A simulation program of a wastewater treatment plant (SBR and continuous) has been developed. The numerical results using the new kinetics corresponded well to the experimental results. The simulations showed that, on the one hand, the improvement of the local mixing of the mixture greatly favors the elimination, on the other hand, the tiering of the reactor configuration by giving it a hydrodynamic close to a very large cascade of reactors also contributes to greatly improve the elimination of MPs. This can be achieved by building baffle reactors with a width of 2 m and an extended length of more than 200 m. Finally, the combination of these two local and global processes makes it possible to considerably increase the elimination of moderately and slowly biodegradable MPs.

**Keywords:** Micropollutants, wastewater treatment, kinetics, activated sludge, new kinetic model, hydrodynamic, simulation, reactor configuration, local mixing.

## Résumé

L'un des défis auxquels la conservation de l'environnement est actuellement confrontée est la réduction des rejets de micropolluants par les effluents des stations d'épuration des eaux usées. Les procédés biologiques sont les traitements les plus couramment utilisés, mais ces techniques classiques n'ont pas été conçues dans le but d'éliminer les micropolluants (MPs). Dans ce travail, l'amélioration de l'élimination de sept composés de micropolluants (des produits pharmaceutiques et un produit chimique industriel) qui couvrent divers degrés de biodégradabilité est étudiée à l'aide du procédé de traitement par boues activées. Pour atteindre cet objectif, une méthodologie expérimentale suivie d'une stratégie de simulation a été développée. L'étude systématique de l'impact des paramètres opérationnels des stations d'épuration sur les MPs, tels que l'âge des boues (SRT), le temps de passage (HRT) et la concentration de biomasse ( $C_{TSS}$ ), sur les MPs a été quantifiée expérimentalement dans neuf installations de réacteur discontinu (SBR). L'augmentation de SRT a amélioré l'élimination des MPs, à l'exception de deux antibiotiques macrolides. L'application d'un HRT plus élevé a quant à elle conduit aussi à une amélioration. De manière plus intéressante, nos résultats ont indiqué que, contrairement à ce qui est postulé, le taux d'élimination des micropolluants n'est pas proportionnel à la concentration en biomasse, en particulier pour celles élevées. Comparé aux taux d'élimination à 3 et 5  $g L^{-1}$  de biomasse, une augmentation supplémentaire à 8  $g_{TSS} L^{-1}$  n'a produit qu'un effet modéré inattendu. Une nouvelle cinétique de la loi de puissance a été étudiée afin de couvrir toute la gamme des conditions de concentration de biomasse dans les systèmes à boues activées. Elle prend en compte la limitation du transport des micropolluants vers la biomasse quand sa concentration est élevée. Dans ce cas, il a été aussi montré que le transport des micropolluants repose sur la diffusion moléculaire. Ce processus a été ajouté à l'équation cinétique proposée. Un programme de simulation de station d'épuration (SBR et continu) a été développé. Les résultats numériques utilisant la nouvelle cinétique correspondent bien aux résultats expérimentaux. Les simulations montrent que d'une part, l'amélioration de l'agitation locale du mélange favorise grandement l'élimination, d'autre part, l'étagement du réacteur en lui conférant une hydrodynamique proche d'une très grande cascade de réacteurs contribue aussi à améliorer fortement l'élimination des MPs. Ceci peut être obtenu en construisant des réacteurs en chicanes d'une largeur de 2 m et d'une longueur déployée de plus de 200 m. Finalement, l'association de ces deux processus locale et globale permet de considérablement augmenter l'élimination des MPs moyennement et lentement biodégradables.

**Mots clés:** Micropolluants, traitement des eaux usées, boues activées, nouveau modèle cinétique, hydrodynamique, simulation, configuration du réacteur, agitation locale.